departement
Mobiliteit en
Openbare Werken

Vervolgstudie inventarisatie en historische analyse van slikken en schorren langs de Zeeschelde

KALIBRATIE EN VALIDATIE VAN HET HYDRODYNAMISCH 2 DIMENSIONAAL NUMERIEK MODEL: PILOOTSTUDIE NOTELAER EN BALLOOI

713_21 WL Rapporten

waterbouwkundig LABORATORIUM

Vlaamse overheid

flanders
HYDRAULICS RESEARCH

Vervolgstudie inventarisatie en historische analyse van slikken en schorren langs de Zeeschelde

Kalibratie en validatie van het hydrodynamisch 2 dimensionaal numeriek model: pilootstudie Notelaer en Ballooi

Maximova, T.; Plancke, Y.; Vanlede, J.; Mostaert, F.

September 2010

WL2010R713_21_6rev2_0

This publication must be cited as follows:

Maximova, T.; Plancke, Y.; Vanlede, J.; Mostaert, F. (2010). Vervolgstudie inventarisatie en historische analyse van slikken en schorren langs de Zeeschelde: Kalibratie en validatie van het hydrodynamisch 2 dimensionaal numeriek model: pilootstudie Notelaer en Ballooi. Version 2_0. WL Rapporten, 713_21. Flanders Hydraulics Research: Antwerp, Belgium

Waterbouwkundig Laboratorium

Flanders Hydraulics Research

Berchemlei 115
B-2140 Antwerp
Tel. +32 (0)3 224 60 35
Fax +32 (0)3 224 60 36
E-mail: waterbouwkundiglabo@vlaanderen.be
www.watlab.be

Document identification

Title:	Vervolgstudie inventarisatie en historische analyse van slikken en schorren langs de Zeeschelde: Kalibratie en validatie van het hydrodynamisch 2 dimensionaal numeriek model: pilootstudie Notelaer en Ballooi		
Customer:	afdeling Maritieme Toegang	Ref.:	WL2010R713_21_6rev2_0
Keywords (3-5):	Scheldt estuary, 2D modeling, hydrodynamics, intertidal area		
Text (p.):	33	Tables (p.):	15
Appendices (p.):	1	Figures (p.):	102
Confidentiality:	☐ Yes	Exceptions:	☐ Customer ☐ Internal ☐ Flemish government
		Released as from	
	☒ No		☒ Available online

Approval

Author	Reviser	Project leader	Division Head
Tatiana Maximova Yves Plancke	Joris Vanlede	Yves Plancke	Frank Mostaert

Revisions

Nr.	Datum	Omschrijving	Auteur
1_0	01/04/2010	Concept version	Tatiana Maximova
1_1	29/04/2010	Substantive revision	Yves Plancke
1_2	07/05/2010	Adapted concept version	Tatiana Maximova
1_3	02/06/2010	Addition Dutch summary	Yves Plancke
1_4	13/09/2010	Internal revision	Joris Vanlede
1_5	15/09/2010	Adapted version	Tatiana Maximova
1_6	24/09/2010	Revision customer	Chantal Martens
2_0	30/09/2010	Final version	Tatiana Maximova

Abstract

The shallow waters, intertidal mudflats and marshes along the Sea Scheldt have an important ecological value. They form a habitat for the development of ecosystems. A good understanding of the impact of human interventions on the estuarine ecosystem is required to manage the river in a sustainable way.

A calibration of the NEVLA model of the Scheldt estuary – including all tributaries which are tidally influenced – was executed in (*Maximova et al*., 2009). The water movement on the intertidal areas was not analyzed during the calibration because it is has a limited effect on the general water movement in the estuary. However, a good reproduction of the velocity in the littoral zone is necessary to answer ecological questions. The intertidal areas Notelaer and Ballooi were chosen as a pilot study in the framework of the project “Vervolgstudie inventarisatie en historische analyse van slikken en schorren in de Zeeschelde”. These areas are located between Rupelmonde and Temse. Both zones are ecologically valuable areas of the Upper Sea Scheldt.

Since the grid resolution of the calibrated NEVLA model is too rough to represent the water movement in the intertidal areas correctly, it was necessary to refine the model grid. Delft3D model with the domain decomposition was used for the analysis. The input files from the calibrated NEVLA model were adapted for the use in the Delft 3D software.

This report describes the sensitivity analysis, model calibration and validation. The calibration and validation were based on comparison with ADCP and GPS float measurements of 10 and 11 June 2009.

Contents

List of tables

List of figures

Nederlandse samenvatting

In het kader van het project “Vervolgstudie inventarisatie en historische analyse van slikken en schorren langs de Zeeschelde” werd een detailstudie uitgevoerd rond het kalibreren en valideren van het 2-dimensionaal hydrodynamisch numeriek model voor de slik- en schorgebieden Notelaer en Ballooi in de Zeeschelde. Deze gebieden zijn gelegen in de Boven-Zeeschelde in de zone Rupelmonde-Temse. De Notelaer wordt gekenmerkt door een uitgestrekt slikgebied met laagdynamische slibrijke zones. De Ballooi is gelegen in de binnenbocht waardoor een hoogdynamische zandplaat aanwezig is voor het slikgebied.

Voor deze studie is gebruik gemaakt van een 2-dimensionaal hydrodynamisch numeriek model vertrekkende van het bestaande NEVLA model. Uit een gevoeligheidsanalyse [*Maximova et al, 2009*] bleek dat het rekenrooster verfijnd diende te worden om de topo-bathymetrie voldoende goed te kunnen representeren in het model en alzo de waterbeweging goed te reproduceren. Gelet op het interessegebied, werd geopteerd op een lokale verfijning (via domein-decompositie) toe te passen om de rekentijd beperkt te houden. Daarnaast bleek uit het gevoeligheidsonderzoek dat met name de stromingsweerstand en de viscositeit een grote invloed hadden op het ruimtelijk beeld van de waterbeweging. Deze parameters werden dan ook gevarieerd tijdens de kalibratie.

Waar in het verleden de modellen hoofdzakelijk gekalibreerd werden op waterstanden en debieten, werd de kalibratie en validatie voor deze studie gefocust op de stroming ter hoogte van het intergetijdengebied. Hiervoor werden bijkomende metingen uitgevoerd:

- ADCP-dwarsraai over de volledige sectie ter hoogte van Notelaer (11/06/2009) en Ballooi (10/06/2009)
- ADCP-langsraai over het intergetijdengebied ter hoogte van Notelaer (10/06/2009) en Ballooi (11/06/2009)
- GPS-vlottermetingen in het ondiepwater- en intergetijdengebied

De ADCP-metingen werden gerapporteerd in [*Aquavision, 2010*] en de vlottermetingen in [*Plancke et al, 2009*].

Bij de kalibratie werd gebruik gemaakt van de ADCP-meetgegevens van 10/06/2010. Voor de verschillende parameterinstellingen (voornamelijk variatie in ruwheid en viscositeit) werden de afwijkingen tussen het model en de metingen geanalyseerd. Hierbij werd zowel in tijd (verschillende fases van het getij, i.e. eerste fase eb, tweede fase eb, kentering LW, eerste fase vloed, maximum vloed en kentering HW) als in ruimte (horizontaal: Notelaer en Ballooi, verticaal: diep, ondiep, intergetijden) een opdeling gemaakt. Naast deze gedetailleerde analyse, werd op een geaggregeerd niveau een uitspraak gedaan over de overeenstemming tussen het model en de metingen. Er werden 14 simulaties uitgevoerd tijdens de kalibratie om uiteindelijk als beste instellingen een viscositeit van 2 m²/s en een lage stromingsweerstand in het intergetijdengebied te bekomen. De gemiddelde afwijking (RMSE) over de volledige getijcyclus en de verschillende diepteklassen bedraagt hierbij 10,5 cm/s. Hierbij is de afwijking in het intergetijdengebied, het interessegebied voor deze studie, beperkt kleiner dan voor de geul. Daarnaast varieert de afwijking over de getijcyclus slechts minimaal, waarbij de overeenstemming het best is tijdens de vloed (eerder beperkte (< 10 cm/s) overschatting) en iets minder tijdens de eb (eerder beperkte (< 15 cm/s) onderschatting).

Bij de validatie werd gebruik gemaakt van de ADCP-meetgegevens van de dwarsraai van 11/06/2010 en de GPS-vlottermetingen. De gemiddelde afwijking (RMSE) over de volledige getijcyclus en de verschillende diepteklassen bedraagt 12 cm/s voor de ADCP-metingen en 16 cm/s voor de GPS-vlottermetingen. Hierbij dient opgemerkt te worden dat de vlottermetingen (vlotter op 1m diepte) een overschatting geven van de diepte-gemiddelde stroming, waardoor de afwijking dus groter is. Bij de validatie is de afwijking in het intergetijdengebied, het interessegebied voor deze studie, beperkt groter dan voor de geul. Daarnaast varieert de afwijking over de getijcyclus slechts minimaal, waarbij de overeenstemming het best is tijdens de eb (eerder beperkte (< 10 cm/s) onderschatting) en iets minder tijdens de vloed (eerder beperkte (< 15 cm/s) onderschatting). Dit verschilt met het beeld van de kalibratie. Een mogelijke oorzaak is de beperktere hoeveelheid meetgegevens in het intergetijdengebied door het ontbreken (probleem GPS-ADCP-koppeling in verwerking) van de ADCP-meetgegevens van

de langsraai die tijdens 11/06/2009 werd bemeten.

De uitgevoerde kalibratie en validatie voor het slikken- en schorrengebied van de Notelaer en Ballooi geeft aan dat een goede overeenstemming kan bekomen worden voor de stroomsnelheden, zowel in het diepe, ondiepe als in het intergetijdengebied. De afwijkingen tussen het 2-dimensionale hydrodynamische numerieke model en de metingen blijven beperkt tot 15 cm/s, wat aanvaardbaar is. Indien dit model toegepast moet worden op andere slik- en schorgebieden, is het noodzakelijk ook voor deze gebieden een validatie uit te voeren alsvorens gebruik te maken van de gemodelleerde stroomsnelheden. De beschikbaarheid van goede terreingegevens is hiervoor noodzakelijk, doch deze studie heeft aangetoond dat dit mits een beperkte inspanning mogelijk is. Daarnaast biedt een beter inzicht in de lokale geomorfologie (o.a. aanwezigheid van bodemvormen) mogelijks meer mogelijkheden in de onderbouwing van de keuze van modelparameters (stromingsweerstand). Met betrekking tot de doorvertaling naar de ecologie blijft het van belang bewust te zijn van de mogelijkheden en beperkingen van de modellen.

1 Introduction

The shallow waters, intertidal mudflats and marshes along the Sea Scheldt have an important ecological value. They form a habitat for the development of ecosystems. A good understanding of the impact of human interventions on the estuarine ecosystem is required to manage the river in a sustainable way.

From the historical analysis of the slikke and schorre areas (tidal flats and marshes) in the Sea Scheldt (*Van Braeckel et al*., 2006) it is clear that the schorre, slikke and undeep sublitoral areas along the Scheldt estuary and its tidal tributaries strongly decreased over the passed 150 years. This loss of habitats is a result of river straightening actions in the Upper Sea Scheldt, poldering along the river, construction of dikes and other infrastructural works. In the last decades the relative importance of the indirect loss of habitats (i.e. loss of habitats because of erosion) strongly increased as a result of the increased tidal energy in the estuary. Different natural processes and human interventions in the estuary can be a reason for this. However up to this moment it is not clear what is the impact of the individual changes (both natural as human) on the observed evolution. But it is clear that the change in tidal penetration is an important factor contributing to this.

The influence of different factors on the hydrodynamics of the estuary is studied by the use of a 2D hydrodynamic model (NEVLA model). The model grid was adapted and extended to include all intertidal areas.

1.1 Study Area

The slikke and schorre areas Notelaer and Ballooi were chosen as a pilot study in the framework of the project “Vervolgstudie inventarisatie en historische analyse van slikken en schorren in de Zeeschelde”. These areas are located between Rupelmonde and Temse. Both zones form one of the most ecologically valuable areas of the Upper Sea Scheldt. Furthermore, both high and low dynamic zones are located on the slikke areas of the Notelaer and Ballooi (*Plancke et al*., 2009).

1.2 Structure of the report

Whithin this study both a calibration and validation of flow velocities on the intertidal areas were performed. After the description of the model (chapter 2), the measurements are described in chapter 3. Before the calibration, a sensitivity analysis (chapter 4) is performed. The calibration and validation results are described in chapters 5 and 6.

2 The numerical model

At Flanders Hydraulics Research the NEVLA model was developed for the Western Scheldt, the Sea Scheldt and connected Flemish rivers. The model was developed in the SIMONA software and it includes a broad sea area and all Flemish tidal rivers, such as Schelde, Durme, Rupel, Nete (Beneden, Grote and Kleine), Dijle and Zenne. These rivers are represented until their tidal border (*Vanlede et al*., 2008). A calibration of the NEVLA model of the Scheldt estuary – including all tributaries which are under tidal influence – was executed in (*Maximova et al*., 2009).

Since the grid resolution of the calibrated NEVLA model is too rough to represent the water movement in the intertidal areas correctly, it is necessary to refine the model grid. However, refinement of the model grid results in an increase of the computation time. The Delft 3D modeling software is used for 2D computations in this study. It is based on the same modeling principles as the SIMONA-WAQUA hydrodynamic model. The Delft 3D modeling software allows to use the domain decomposition technique, which is necessary when different resolutions have to be used for different parts of the model grid. The domain decomposition technique helps to decrease computation time. The input files from the calibrated NEVLA model are adapted for the use in the Delft 3D software.

The map of the Scheldt estuary is shown on Figure 1. The downstream boundary of the model used in this study is located at Antwerp. The model includes all Flemish tidal rivers. These rivers are represented until their tidal border. Figure 2 presents the study area: Ballooi and Notelaer.

The model developed for this study is a 2D model.

2.1 Model grid

Domain decomposition is a technique in which a modeling domain is subdivided into several smaller model domains, which are called sub-domains. The subdivision is based on the horizontal and vertical model resolution required for adequately simulating physical processes. Then, the computations can be carried out separately on these sub-domains. The communication between the sub-domains takes place along internal open boundaries, or so called DD-boundaries. If these computations are carried out concurrently, we speak of parallel computing. Parallel computing can reduce the computational time for multiple domain simulations.

Domain decomposition also allows for local grid refinement, both in horizontal direction and in vertical direction. Grid refinement in horizontal direction means that in one sub-domain smaller mesh sizes (fine grid) are used than in other sub-domains (coarse grid). In case of vertical grid refinement one sub-domain e.g. uses ten vertical layers and other domains five layers, or a single layer (depth-averaged) (*WL/Delft Hydraulics*, 2007a).

Grid refinement in horizontal direction is used in this study. Since different grid resolutions can be used in different model sub-domains, it is possible to define a finer resolution for the study area without refinement of the entire model grid.

2.2 Topo-bathymetry

The bathymetric samples provided by INBO (laser altimetry measurements from 2004) are used to define the bathymetry for the intertidal areas. In the middle of the river the channel bathymetry is defined based on the samples delivered by the Maritime Acces Division (Single Beam measurements):

- The Upper Sea Scheldt, Rupel and Durme: Single Beam measurements from 2001
- The Lower Sea Scheldt: Single Beam measurements from 2004-2005

A higher bathymetry (+ 6 m NAP) is assigned to all areas lying outside the border between the schorre area and dry zone. This is done in order to prevent unrealistic flooding of these areas.

For the first and third model sub-domains the same bathymetry as in the calibrated NEVLA model is used in all model runs. In the second sub-domain (the study area) the bathymetry is redefined every

time when the grid resolution is changed. The same bathymetrical samples are used for all model runs. These samples are interpolated to the refined grids in order to calculate the bathymetry for each grid cell.

Depth, height and water levels are expressed in meter NAP (Normaal Amsterdams Peil). A bathymetric depth is positive below the reference plane, water levels are positive above the reference plane.

2.3 The boundary conditions

In order to refine the model grid for the study area without refinement of the entire grid, the domain decomposition technique is used. The model is divided in three sub-domains (Figure 3):

1. from Antwerp to Rupelmonde (including Rupel and its tributaries);
2. from Rupelmonde to Tielrode: the study areas Notelaer and Ballooi are located in the second sub-domain Figure 2);
3. from Tielrode to Merelbeke.

The measured 10 min time series of the water level in Antwerp are used as downstream boundary conditions for the first sub-domain.

The discharges for tributaries are available from the Hydrometry group of Flanders Hydraulics Research. Zero discharge is specified for Durme – Waasmunster, Schelde – Gentbrugge, Bovenschelde – Zwijnaarde because there is no or negligible discharge during the period of the analysis. The daily discharge series are available for Zenne – Zemst, Dijle – Haacht, Grote Nete – Itegem and Kleine Nete – Grobbendonk. They are specified as discharge sources for the first sub-domain.

For the second sub-domain no discharge sources, downstream and upstream boundaries are specified. Several monitoring stations are defined for the areas Notelaer and Ballooi (Figure 4 and Figure 5).

The discharges at Dendermonde and Merelbeke are specified for the third model sub-domain. 10 min discharge time series are available for Dendermonde (Appels), measured by the Hydrometry group of Flanders Hydraulics Research. The data series of the discharge at Merelbeke measured by IMDC are available as 5 min values.

All boundary conditions are specified for a period from 24/06/2002 to 17/07/2002. This period is chosen because for the period June – July 2002 5 min averaged discharge time series are available at Merelbeke. From the sensitivity analysis *(Ides et al.*, 2008) it is found that the use of daily averaged discharges at this location worsens the calculated discharges in the Upper Sea Scheldt up to Hemiksem compared to hourly averaged discharges. When 5 min averaged discharges are used, the correspondence between calculation and measurement is even better; however the difference between the two results is small.

2.4 Time step

The time step for the model simulations was chosen based on analysis of the Courant number. The Courant number is a ratio of a time step to a cell residence time. It specifies a maximum internal time step the solver may take during the time integration and is not the same as the time step of the simulation. The Courant number specifies a maximum value of a time step. This number should be smaller than 10. Otherwise, the time step of the simulation should be decreased.

During the sensitivity analysis to the grid resolution the time step had to be adapted for different model runs because a change of the grid resolution results in a change of the Courant number. The time step of the reference model run is 7.5 seconds. The time step of the model runs with 2x2, 3x3 and 4x4 grid refinement is 3.75; 3.0 and 1.5 seconds respectively. Therefore, grid refining results in a significant increase of the computational time.

3 Velocity measurements

The availability of the flow data for the slikke and schorre areas along the Scheldt estuary is limited. To enable the model calibration and validation for these zones and to improve the understanding of the flow in the slikke and schorre areas an extensive measurement campaign took place on 10 and 11 June 2009 in the intertidal areas Notelaer and Ballooi in the Upper Sea Scheldt.

The following measurement techniques were used:

- ADCP (Acoustic Doppler Current Profiler) measurements in the Scheldt;
- ADCP measurements on the slikke area;
- GPS-float measurements on the slikke area.

More detailed information about the measurement campaign can be found in (*Plancke et al*., 2009).

During the first day (10 June 2009) velocities were measured with floats at the Notelaer together with the ADCP measurements along the longitudinal profile. In the same day a transverse ADCP profile was measured by MS Parel II near the Ballooi (Figure 6). During the second day (11 June 2009) the float measurements and the ADCP measurements along the longitudinal profile were performed at the Ballooi; a transverse ADCP profile was measured by MS Parel II near the Notelaer. Results of the ADCP measurements can be found in (*Aqua Vision,* 2010).

Based on the float measurements from 10 and 11 June 2009 it can be concluded that the flow change during the tidal cycle is similar in the intertidal areas Ballooi and Notelaer. During the period around low water the flow is concentrated in the river channel. The flow velocity in the river channel in the beginning of the flood (about 80 cm/s) is lower than in the end of the ebb (about 100 cm/s). When the water level increases the slikke areas are gradually inundated. About one hour before the high water the velocity on the slik reaches maximum. Along the river bank the maximal velocities (about 65 cm/s) are lower than on the slikke area near the river channel (about 80 cm/s). The maximal velocities measured in the Ballooi area are about 5 cm/s higher than in the Notelaer. Velocities of maximum 65 cm/s are observed on the slikke area during the initial phase of the ebb (*Plancke et al*., 2009).

The measurements from 10 June 2009 are used for the model calibration and the measurements from 11 June 2009 are used for the model validation in this study.

4 Sensitivity analysis

4.1 Introduction

The sensitivity analysis of the Delft 3D model is performed in order to understand the impact of different model parameters (grid resolution, bed roughness, bathymetry, …) on the model results. The sensitivity analysis is performed only for the study area (second model sub-domain). The results of the reference run are compared with a simulation where only one of the parameters is changed. The results of the sensitivity analysis give necessary information for the model calibration.

The effect of the changes of model parameters on the model results is analyzed based on the maps and histories of velocity. The maps of the differences in velocity magnitude for different model simulations are found for several moments during one tide (Figure 7). The average absolute differences in velocity in observation points are calculated based on the history files.

4.2 The simulation period

The simulation period from 24/06/2002 9:00 to 26/06/2002 1:00 is chosen for the model simulations for the sensitivity analysis. This period includes three spring tides. The maps and histories of the velocity are analyzed for the one tide from 25/06/2002 12:00 to 26/06/2002 00:30 (Figure 7).

4.3 Sensitivity to grid resolution

4.3.1 Introduction

To study the effect of the grid resolution on the model results the grid cells - which are about 100 m long and 35 m wide in the original model in the second sub-domain - were refined in the directions perpendicular and parallel to the flow. Several refinements were used (Table 4-1).

Table 4-1. Model runs for the analysis of sensitivity to the grid resolution

Model run	Grid resolution
DDref	original
DD2x2	2x2 refinement
DD3x3	3x3 refinement
DD4x4	4x4 refinement

A finer grid resolution results in a better representation of topo-bathymetry. It is expected that a model with a refined grid produces more accurate results. Thus, modeling of the velocities in the intertidal areas and river channel improves. However, grid refining results in a significant increase of the calculation time. Therefore, the choice of an optimal grid resolution involves a trade-off between increased accuracy of the model and increased computation time.

Very often, a coarse grid resolution can introduce approximations and uncertainties into model results. Sometimes, a finer grid resolution does not necessarily result in more accurate predictions (*Sastry S. Isukapalli*, 1999). We expect that differences between two model runs with different grid resolutions

become very small when a well refined grid is used in both simulations, so that there is no need to further refine a grid. Therefore, it is necessary to find an optimal grid resolution which provides a balance between the model accuracy and the calculation time.

4.3.2 Results

We expect that 4x4 grid refinement produces the most accurate results. Therefore, the results of the model runs DDref, DD2x2 and DD3x3 are compared with the results of run DD4x4. The average values of the absolute differences in velocities are calculated based on the velocity histories (Table A-1). This table shows that in general the differences between the model runs with different grid resolution decrease when the resolution becomes finer. The smallest average differences in velocity (less than 5cm/s for most observation points) are observed between runs DD4x4 and DD3x3. However, there are some exceptions in the Ballooi area. In points B4 and B12 the results of run DD2x2 with a rougher grid resolution are closer to the results of run DD4x4 than the model results DD3x3. The analysis of the velocity histories shows that the ebb and flood velocities calculated in run DD3x3 are higher in these points than the ones calculated in run DD4x4 (Figure 8).

The average differences in velocity in the slikke area are larger than in the schorre area (Table A-1). This is because the model calculates that there is no water flow in some observation points located in the schorre area. Therefore, the velocity differences in these points are zero.

The maps of the differences in velocity magnitude between model run DD4x4 and the runs with other grid resolutions are calculated for several time moments of one tide (Figure 7). These maps are shown on Figure 9 - Figure 23. They are obtained by triangular interpolation of the velocity samples exported from the model runs with different grid resolutions. All samples are triangulated to the 4x4 grid. Therefore, it is necessary to bear in mind possible interpolation errors.

Figure 9 - Figure 23 show that the largest differences in the calculated velocities are observed between model runs DD4x4 and DDref. The velocity differences between runs DD4x4 and DD3x3 are very small on most maps. Only on maps 3 (the end of the flood period) and 4 (before the high water slack) the differences are large in some grid cells.

On map 3 the velocities calculated in run DD3x3 are larger than the velocities in run DD4x4 in several grid cells located in the eastern part of the Ballooi (Figure 14). This can be explained by the differences in bathymetry for the different grid resolutions. Figure 24 shows that bathymetry of several grid cells in the eastern part of the Ballooi area is deeper in run DD3x3 than in run DD4x4. The water flow in these points is not blocked in run DD3x3 and velocities are larger than in run DD4x4. The differences in bathymetry in these cells affect the velocities in the upstream area because the water flow moves upstream during flood.

On map 4 the differences in velocities between runs DD4x4 and DD3x3 are large in several grid cells in the schorre area of the Notelaer (Figure 17). The velocity maps 4 for simulations DD4x4 and DD3x3 show that velocities calculated in run DD4x4 in this area are larger than velocities in run DD3x3 (Figure 25). The differences in velocity in the schorre area of the Notelaer can be explained by the differences in bathymetry in runs DD3x3 and DD4x4. Figure 26 shows that bathymetry for 4x4 grid is deeper in some grid cells than bathymetry for 3x3 grid. The water flow in the schorre area of the Notelaer is hindered by the shallower bathymetry in run DD3x3 on map 4 while in run DD4x4 water can flow in this area faster.

Grid refining results in a significant increase of the computational time because a time step of model simulations decreases and a number of grid cells increases. Simulation of a period of 40 hours takes about 13 hours in run DDref, 35 hours in run DD2x2, 41 hours in run DD3x3 and about 119 hours in run DD4x4.

4.3.3 Conclusions

The analysis of the maps and histories of the water level and velocity showed that model runs with the grid refinement 3x3 and 4x4 produce similar results for most periods of the tide. There are velocity differences in some areas in the end of the flood period and around high slack. They are related to the small differences in bathymetry and uncertainties due to the interpolation of velocity samples for the calculation of the velocity differences. However, in general similar velocities are calculated in runs DD3x3 and DD4x4 in the study area. Since the computation time for run DD3x3 is much smaller than for run DD4x4, it was chosen to use the grid with refinement 3x3 for further sensitivity analysis. The cells of this grid are about 33 m long and 11 m wide.

4.4 Sensitivity to bed roughness

4.4.1 Introduction

The effect of the bed roughness on the water movement is studied. It is analyzed how a variation of the roughness in a certain area affects the modeled velocities. This gives a better insight for a more efficient approach for the model calibration. The grid with 3x3 refinement (compared with NEVLA) is used for the sensitivity analysis to the bed roughness.

First, the same bed roughness as in the calibrated NEVLA model with the extended grid (*Maximova et al.*, 2009) is used for all model sub-domains. A uniform bed roughness of 0.018 $m^{-1/3}s$ is assigned for the area between Rupelmonde and Temse (second sub-domain). No distinction is made in the NEVLA model between the bed roughness values of the river channel, slikke and schorre areas due to the limited effect on the water movement in general. The model run with this bed roughness field is used as a reference. Afterwards, different bed roughness fields for the slikke and schorre areas in the second model sub-domain are defined. The bed roughness in the first and third sub-domains does not differ from the values of the reference simulation. The following definitions are used:

- the border between the slikke area and river channel is defined as a mean spring low water;
- the border between the slikke and schorre area is defined as a mean neap high water.

Mean spring low water (-2.34 m NAP) and mean neap high water (+2.65 m NAP) are calculated based on the measured water levels at Temse in 2008[1].

A uniform bed roughness is used for the slikke area and a depth dependent roughness is defined for the schorre area. The roughness for the schorre area varies as a function of bathymetry: a higher roughness is defined for a higher bathymetry. In the river channel the same roughness as in the reference run is used (0.018 $m^{-1/3}s$). Table 4-2 shows the model runs for the analysis of the model sensitivity to the bed roughness.

Table 4-2. Model runs for the analysis of sensitivity to the bed roughness

Model run	Bed roughness ($m^{-1/3}s$)	
	slikke areas	schorre areas
DD3x3 (reference)	0.018	
DD3x3rgh1	0.017	from 0.017 to 0.050
DD3x3rgh2	0.013	from 0.013 to 0.035
DD3x3rgh3	0.021	from 0.021 to 0.065
DD3x3rgh4	0.013	from 0.013 to 0.050

[1] personal communication Marc Wouters

4.4.2 Results

The absolute values of the average differences in velocity calculated in runs with different roughness fields are presented in Table A-2. These differences are calculated for the slikke and schorre areas of the Ballooi and Notelaer. Table A-2 shows that velocities in the Ballooi are more sensitive to the changes of the bed roughness than velocities in the Notelaer. The slikke area is affected more by the roughness change than the schorre area. This is because the model calculates that there is no water flow in some observation points in the schorre area. The velocity differences in these points are zero.

Figure 27 - Figure 40 show the maps of differences in velocity for the runs with different roughness and the reference run. The time for each map is shown on Figure 7. The largest differences in velocity are observed on map 3 (second half of the flood period, the moment of the maximal flood velocity) for all model runs with different roughness fields. The slikke and schorre areas are inundated during the flood period. The change of the roughness field of these zones affects the flow velocities calculated by the model.

In the beginning of the flood and during the ebb the differences in velocities decrease. The smallest differences (less than 0.05 m/s) are calculated in the end of the ebb period (map 7) when there is no water flow in the intertidal areas and a changed roughness of these areas does not affect the model results.

The change of the roughness in run DD3x3rgh1 affects mainly velocities in the Ballooi. The velocities in the Notelaer area do not change significantly. In the end of the flood (map 3) the velocity calculated in run DD3x3rgh1 is 0.05 to 0.20 m/s smaller than in the reference run DD3x3 in some parts of the Ballooi area (Figure 28). This decrease of the velocity is related to the change of the roughness field. In run DD3x3rgh1 the roughness of the slikke areas decreases only a little (from 0.018 to 0.017 $m^{-1/3}s$) while the roughness of a large part of the schorre areas increases in comparison to the reference run. Therefore, resistance to the flow movement in the schorre area increases. This results in a decrease of the velocities on a border between the slikke and schorre areas. A lower velocity of the water flow in several grid cells in the eastern part of the Ballooi (Figure 28) results in a slower movement of the water flow more upstream during the period of the maximal flood velocity (map 3).

There are still some differences in velocities (from 0.05 to 0.10 m/s) on map 4 but they are smaller than the differences on map 3 (Figure 29). Map 4 shows the time moment before the slack period when velocities decrease. The differences in velocities calculated in runs DD3x3 and DD3x3rgh1 in the beginning of the flood and during the ebb are small (Figure 27, Figure 30).

Figure 31 - Figure 34 show maps 1, 3, 5 and 6 with the differences in velocity between the reference run and run DD3x3rgh2. The velocities calculated in run DD3x3rgh2 are larger than the velocity in the reference run for a large part of the slikke area. Maximal differences of 0.05 to 0.15 m/s are observed on map 3 (Figure 32). The roughness of the slikke area in run DD3x3rgh2 decreases from 0.017 to 0.013 $m^{-1/3}s$. This results in a faster water flow in the intertidal zone of the Ballooi and Notelaer.

The roughness of the schorre area in run DD3x3rgh2 changes from 0.013 to 0.035 $m^{-1/3}s$ as a function of bathymetry. Therefore, the roughness of some part of the schorre area is larger than the original roughness of 0.018 $m^{-1/3}s$. This explains a velocity decrease on map 3 in some parts of the schorre area of the Ballooi (Figure 32).

On maps 5 and 6 (the ebb period) velocity in some parts of the slikke area of the Ballooi and Notelaer increases by 0.05 to 0.20 m/s in run DD3x3rgh2 in comparison to the reference run (Figure 33 and Figure 34). Due to a decreased roughness of the slikke areas, the water flows faster over these areas during the ebb. There is no significant velocity change in the schorre area during the ebb period in run DD3x3rgh2.

In run DD3x3rgh3 the bed roughness of both slikke and schorre areas is increased. This affects mainly the velocities in the Ballooi. The roughness change in run DD3x3 rgh3 does not have a strong effect on the velocities in the Notelaer.

The water flow velocity decreases by 0.05 to 0.25 m/s in the slikke and schorre areas of the Ballooi on map 3 (Figure 36). This decrease of the velocity is larger than in run DD3x3rgh1. This is because in run DD3x3rgh1 only the roughness of the schorre area increased while in run DD3x3rgh3 the roughness of both slikke and schorre increased in comparison to the reference run. The roughness of the intertidal zones in run DD3x3rgh3 is higher than in run DD3x3rgh1.

There is still some effect of the roughness change on maps 4 and 5 (Figure 37 and Figure 38). The velocities decrease in the Ballooi area by 0.05 to 0.15 m/s. On other maps the differences in velocity are very small (Figure 35).

In run DD3x3rgh4 the same roughness field as in run DD3x3rgh2 is used for the slikke area (0.013 $m^{-1/3}s$). The roughness value for the schorre area varies from 0.013 to 0.05 $m^{-1/3}s$. The average velocity differences (Table A-2) and the maps of the differences in velocity (Figure 32, Figure 34, Figure 39 and Figure 40) between the reference run and runs DD3x3rgh2 and DD3x3rgh4 show that these two runs produce very similar results. This shows that a change of a roughness of the schorre area does not have a significant effect on the model results. The change of the roughness of the slikke area is more important.

4.4.3 Conclusions

The sensitivity analysis showed that change of the bed roughness of the intertidal area can have an important effect on the velocities in this area. However, this effect is not equally important during the entire tidal period. The largest changes are observed during the period with a maximal flood velocity and in the first phase of ebb. An increase of the roughness of the littoral zone results in a decrease of the velocities in this zone and a decrease of the roughness results in an increase of the flow velocities. The roughness of the slikke areas plays a more important role for the velocities than the roughness of the schorre areas.

The analysis of the histories and maps shows that a change of the bed roughness results in a larger velocity changes in the Ballooi area than in the Notelaer. An increase of the roughness in runs DD3x3rgh1 and DD3x3rgh3 does not have a strong effect on the velocities in the Notelaer area (velocities change by less than 0.05 m/s). A decrease of the roughness in runs DD3x3rgh2 and DD3x3rgh4 results in an increase of the velocities on the Notelaer by 0.05 to 0.10 m/s.

4.5 Sensitivity to horizontal eddy viscosity

4.5.1 Introduction

Viscosity is a measure of the resistance of a fluid which is being deformed by either shear stress or extensional stress. Viscosity describes a fluid's internal resistance to flow and may be thought of as a measure of fluid friction. In the study of turbulence in fluids, a common practical strategy for calculation is to ignore the small-scale vortices (or eddies) in the motion and to calculate a large-scale motion with an eddy viscosity that characterizes the transport and dissipation of energy in the smaller-scale flow (*Wikimedia Foundation, Inc*., 2009).

It is analyzed what effect the horizontal eddy viscosity has on the flow velocity in the intertidal areas and river channel. In the original model a horizontal eddy viscosity of 1 m^2/s is used. To study the model sensitivity to this parameter, the eddy viscosity is changed in all three model sub-domains in model runs DD3x3V1 and DD3x3V2 (Table 4-3).

Table 4-3. Model runs for the analysis of sensitivity to the horizontal eddy viscosity

Model run	Horizontal eddy viscosity (m^2/s)
DD3x3 (reference)	1
DD3x3V1	5
DD3x3V2	0.2

4.5.2 Results

The average absolute differences in velocity between the reference run and the runs with the changed viscosity are presented in Table A-3. The change of the horizontal eddy viscosity affects the velocities in the areas Ballooi and Notelaer. An increase of the viscosity has a little stronger effect on the velocities in

the slikke areas than a decrease of the viscosity. The velocity difference in some observation points in the schorre area is zero. This is because the model calculates that there is no water flow in these points.

Increased viscosity

The maps of the differences in velocities calculated for the reference run and run DD3x3V1 with an increased viscosity are presented on Figure 41 – Figure 47. Map 1 shows the beginning of the flood (Figure 41). The velocities in the river channel decrease in run DD3x3V1 in comparison to the reference run by 0.05 to 0.20 m/s. The water flow has a lower fluidity due to an increased viscosity and moves slower in the river channel. However, the velocities on the border of the slikke area and undeep zone increase by 0.05 to 0.15 m/s on map 1. In the second half of the flood period (map 2) velocities in a large part of the slikke areas of the Ballooi and Notelaer increase (Figure 42). This is because the velocity profile along the cross section changes when the viscosity changes. When the viscosity increases, the velocity profile becomes less convex (Figure 57). This means that velocities in the middle of the river decrease and they increase in the intertidal areas.

Besides the velocity profile, the horizontal eddy viscosity affects a discharge through a cross section. Figure 55 and Figure 56 show the comparison of the instantaneous and cumulative discharges in the reference model run and runs with a changed viscosity. An increase of viscosity results in a decrease of the discharge. This is due to the fact that velocities in the river channel decrease. This decrease is not compensated by an increase of the velocities in the intertidal zones which have a smaller area than the river channel. The cumulative discharge decreases by about 4 Mm^3 in run DD3x3V1 (Figure 56).

A maximal decrease of the velocity in the river channel (more than 0.25 m/s in some areas) in run DD3x3V1 is observed on map 3 (the moment of the maximal flood velocity) (Figure 43). The velocities in the part of the intertidal area closest to the river channel decrease on map 3 too. The velocities in a more shallow part of the intertidal zone increase. A maximal increase of the velocity (from 0.05 to 0.25 m/s) on the slikke areas of the Ballooi and Notelaer is observed on map 4 in the end of the flood period (Figure 44).

There is a strong decrease of the velocity in the river channel and in a small part of the slikke area in the first half of the ebb (Figure 45). However, the velocities in a large part of the slikke and schorre areas do no change on map 5.

On map 6 (the middle of the ebb) velocity differences in the slikke area become larger again (Figure 46). In the end of the ebb (map 7), velocity decreases in the middle of the river channel in comparison to the reference run and it increases on the sides of the river channel near the slikke areas (Figure 47).

Decreased viscosity

Figure 48 - Figure 54 show the differences in velocities calculated in the reference run and run DD3x3V2 with a decreased viscosity. In the beginning of the flood (map1) the velocities in the river channel increase by 0.05 to 0.15 m/s in run DD3x3V2 (Figure 48). Less viscous water can move easier than water with a higher viscosity. However, the velocities on the border of the slikke area and undeep zone decrease by 0.05 to 0.20 m/s. This is explained by a more convex shape of the velocity profile along the cross section as a result of a decreased viscosity (Figure 57). A decreased viscosity results in an increase of the velocities in the middle of the river while the velocities in the intertidal areas decrease. A flow discharge through a cross section increases a little as a result of a decreased viscosity (Figure 55, Figure 56).

On map 2 velocities decrease in the middle of the slikke areas (Figure 49). At the moment of the maximal flood velocity (map 3) velocities decrease on the border of the slikke and schorre areas (Figure 50). However, the velocities in a part of the slikke area of the Ballooi increase. In the end of the flood period (map 4) velocities in the river channel increase. An opposite effect is observed on the slikke area of the Ballooi where velocities decrease by 0.05 to 0.15 m/s. On the slikke and schorre areas of the Notelaer velocities increase by more than 0.25 m/s in some grid cells in run DD3x3V2 (Figure 51). This is because the flow velocity in these cells is close to zero in the reference run on map 4. In run DD3x3V2 velocities in this area increase.

In the middle of the flood period (maps 5 and 6) velocities in the river channel increase. In some parts of the slikke area velocities decrease. Only in the western part of the Ballooi slikke area velocity increases on map 5 (Figure 52). On map 6 velocities decrease mainly not in the middle of the slikke area but on the border with the undeep zone (Figure 53).

In the end of the ebb (map 7) velocity increases in the middle of the river channel and it decreases on the sides of the river channel near the slikke areas. There are no differences in velocity on the intertidal areas (Figure 54).

4.5.3 Conclusions

An increase of the horizontal eddy viscosity results in a decrease of the flow velocities in the river channel, while a decrease of the viscosity results in an increase of the velocities in the river. An opposite effect is observed in some parts of the slikke and schorre areas. The flow velocities there increase when viscosity increases and they decrease when viscosity decreases. This is because the velocity profile along the cross section changes when viscosity changes. When viscosity increases, the velocity profile becomes less convex. When viscosity decreases, the velocity profile becomes more convex (Figure 57). However, at some moments during the tide velocities in some parts of the intertidal area change similar to the velocities in the river channel.

A change of the viscosity has different effects on the velocities in the intertidal areas Ballooi and Notelaer during some periods of the tide. Different results are obtained at both sites due to the different shape of the slikke area at the Notelaer and Ballooi. Where the bathymetry of the Notelaer has a quasi constant shape, the Ballooi is located at the inner side of a bend and is characterized by an extensive sandbar in the undeep and the lower part of the littoral zone.

4.6 Sensitivity to wind

4.6.1 Introduction

Wind can be an important factor in shallow water. It can have a strong effect on the water levels and velocities in the intertidal areas. To analyze the model sensitivity to wind, the model run DD3x3 is performed with and without wind (Table 4-4). Wind data are available from the Hydro Meteo Centrum Zeeland (HMCZ) database. The wind data measured at station Hansweert are imposed as a uniform wind field influencing the whole model area. This station is chosen as being representative for the entire estuary. The wind data consist of wind magnitude (10 min average value) and direction (10 min average value in degrees towards North).

Table 4-4. Model runs for the analysis of sensitivity to wind

Model run	Wind condition
DD3x3 (reference)	with wind
DD3x3 no wind	without wind

4.6.2 Results

Figure 58 and Figure 59 show the time series of the wind magnitude and direction at Hansweert. The wind direction changes from approximately 240 to 320 degrees during the analyzed tidal period. The wind magnitude changes from about 1 to 7 m/s (1 to 4 Beaufort: light air to moderate breeze).

The average differences in velocity between the runs with and without wind are presented in Table A-4. These differences are very small (6 mm/s on average). This means that velocities in the slikke and schorre areas of the Ballooi and Notelaer are less sensitive to the changes in wind than to other model parameters analyzed in the previous chapters.

Wind has a similar effect on the slikke areas of the Ballooi and Notelaer. The average velocity changes in the schorre areas due to the wind are negligible (Table A-4). This is because the model calculates that there is no water flow in some observation points located in the schorre area.

The maps of the velocity differences are presented on Figure 60 - Figure 63. These maps show that wind has only a very small effect on the velocities in the slikke and schorre areas. The changes of the velocities do not exceed 0.05 to 0.10 m/s for most locations. The velocities in a large part of the slikke and schorre areas are not affected by the wind.

The velocity in some parts of the slikke areas of the Notelaer and Ballooi increases a little in the model simulation without wind (by less than 0.10 m/s). This is probably because the wind direction (240 to 320 degrees) in the reference run is opposite to the water flow in these areas at these moments in time. Therefore, in the model run without wind water can flow a little faster in these areas. There is almost no effect of the wind on maps 1 and 2 (Figure 60 and Figure 61). During the period of maximal flood velocity and in the beginning of ebb velocities in a very small part of the slikke areas increase a little in the simulation without wind. However, the changes are very small (Figure 62, Figure 63).

4.6.3 Conclusions

The analysis of the model sensitivity to wind showed that wind implementation in the model has a smaller effect on the velocities than other model parameters (grid resolution, bed roughness and viscosity). It affects a smaller area and differences in velocity are less than 0.10 m/s. The velocities on most locations are not affected by the wind. The wind magnitude does not exceed 7m/s during the analyzed tidal period. If a period with a stronger wind is analyzed, the wind can have a stronger effect on the velocities in the intertidal areas.

4.7 Sensitivity to bathymetry

4.7.1 Introduction

A topo-bathymetric survey of the river produces a field of points where the depth of each point is known. However, location of the topo-bathymetric measurement points can differ from the grid points of the numerical model. Therefore, it is necessary to use interpolation in order to calculate the depth for each grid point. Different interpolation techniques exist that can be used to change measured bathymetric data to the model bathymetry with a certain depth value per calculation point. The use of different interpolation methods can affect water mass movement landwards and seawards. In this chapter it is analyzed how the use of different interpolation methods affects the model velocities.

The bathymetric samples provided by INBO (laser altimetry measurements) are used to define the bathymetry for the intertidal areas. In the middle of the river channel bathymetry is defined based on the samples delivered by the Maritime Acces Division (Single Beam measurements). A higher bathymetry (+ 6 m NAP) is assigned to all areas lying outside the border between the schorre area and the dry zone. This is done in order to prevent unrealistic flooding of these areas.

The interpolation methods used for the analysis are presented in Table 4-5. The *Closest value* interpolation method is compared with the *Shepard* method. These two algorithms take into account the distance between the depth measurement point and the calculation grid point. The *Closest value* method uses the value of the closest sample point within the vicinity to define the bathymetry for a grid cell. The *Shepard* method is a weighted averaging method, with weights depending on the reciproke of the squared distance between the grid point and the surrounding sample points (*WL/Delft Hydraulics*, 2007b).

The *Shepard* interpolation technique is used in run DD3x3shepard only for the second model sub-domain. For the first and third sub-domains the same bathymetry as in the reference run is used (the bathymetry of the model calibrated in (*Maximova et al*., 2009)).

Table 4-5. Model runs for the analysis of sensitivity to bathymetry

Model run	Interpolation method
DD3x3 (reference)	*Closest value*
DD3x3shepard	*Shepard*

4.7.2 Results

The sensitivity analysis shows that the change of the interpolation method does not have a strong effect on the flow velocities. The average differences in velocity calculated in runs with different bathymetries

are presented in Table A-5. They are less than 0.01 m/s.

Figure 64 - Figure 67 show the maps of the velocity differences. There is almost no difference between the results of runs DD3x3 and DD3x3shepard on most maps. Some differences are observed on maps 3 and 4. On map 3 velocities decrease in several grid cells of the Ballooi in run DD3x3shepard (Figure 65). On map 4 velocities in several grid cells of the Notelaer schorre area increase by 0.05 to 0.15 m/s when the *Shepard* interpolation technique is used (Figure 66). In the reference run DD3x3 the water flow is hindered in this area on map 4 (Figure 25). The use of the Shepard technique results in a deeper bathymetry of several grid cells of the schorre area of the Notelaer and an increase of the velocities there (Figure 68 and Figure 69). However, the changes are very small.

4.7.3 Conclusions

Comparison of the *Closest value* and *Shepard* methods shows that these methods give very similar results. The preference is given to the *Shepard* method because the use of this interpolation technique in the model with 3x3 grid refinement results in a water flow in the Notelaer schorre area in the end of the flood period. The water flow in this area is also observed in 4x4 model. Nevertheless, the *Closest value* method can be used too because it produces very similar results for most model maps.

4.8 Conclusions

A sensitivity analysis was performed in order to analyze what effect different numerical parameters have on velocities in the intertidal areas Ballooi and Notelaer and in the river channel. The sensitivity analysis provides important information for the model calibration.

The sensitivity analysis to the grid resolution showed that at least a 3x3 grid refinement should be used in the model. The model with a rougher resolution can not accurately represent the water movement in the intertidal areas Ballooi and Notelaer correctly. The model with 3x3 grid refinement was used for the further sensitivity analysis. The cells of this grid are about 33 m long and 11 m wide in the study area.

The model sensitivity to the bed roughness was studied. First, a uniform roughness was analyzed and then different roughness values were defined for the slikke and schorre areas. A uniform roughness value was used for the slikke areas and varying depth dependent roughness was defined for the schorre areas. The sensitivity analysis showed that the change of the bed roughness of the slikke and schorre areas has an important effect on the velocities in these areas. An increase of the roughness results in a decrease of the velocities and a decrease of the roughness results in an increase of the flow velocities. The largest changes are observed during the period with the maximal flood velocity and in the first phase of ebb.

Another important model parameter that has a strong effect on the velocities is a horizontal eddy viscosity. The change of the viscosity results in a change of the velocity profile along the cross section. When viscosity increases, the velocity profile becomes less convex. Therefore, flow velocities decrease in the river channel and increase in the intertidal areas. A decrease of the viscosity has an opposite effect: the velocity profile becomes more convex. Velocities in the river channel increase and velocities in the slikke and schorre areas decrease. However, at some moments during tide the velocities in some parts of the intertidal area change similar to the velocities in the river channel.

The analysis of the model sensitivity to wind showed that the wind implementation in the model did not affect the results very much. The velocities changed by less than 0.05 to 0.10 m/s in a very small part of the areas Ballooi and Notelaer. The velocities in a large part of the intertidal zones were not affected by the wind.

Two different methods for interpolation of the bathymetric measured data to the model grid were studied. The analysis showed that the *Closest value* and *Shepard* methods produce very similar results. However, the preference is given to the *Shepard* method because the model with 3x3 grid refinement and *Shepard* interpolation calculates a little faster water flow in a small part of the Notelaer schorre area in the end of the flood period. This result is similar to the result of 4x4 model.

5 Model calibration

5.1 Introduction

The calibration is performed in order to improve the model accuracy. In this study the primary objective of the model calibration is to improve the representation of the flow velocities on the intertidal areas Ballooi and Notelaer. Besides the intertidal areas the model calibration was performed in the river channel. During the calibration several model runs were performed in which some model parameters were changed based on the results of the sensitivity analysis.

The calibration was executed on the available flow measurement data. From the available ADCP measurements (chapter 3) two transects were used for this calibration, while another transect was used for the validation (chapter 6).The GPS-float measurements were also used for the validation.

It was opted not to simulate the period of June 2009 due to the extra efforts to gather all the necessary data (boundary conditions, validation of water levels). Therefore, the (available) validated period of June – July 2002 was used in the model.

Based on the results of the sensitivity analysis, the numerical model with 3x3 grid refinement and *Shepard* interpolarion method was used for the calibration. Wind was included in the model runs.

5.2 Methodology

Bed roughness and horizontal eddy viscosity are used as the calibration parameters because the sensitivity analysis showed that they have the strongest effect on the flow velocities. The results of model simulations are compared with the results of the ADCP measurements on 10/06/2009 for the Ballooi – transverse profile and Notelaer – longitudinal profile. The location of the ADCP profiles is shown on Figure 6.

Velocity maps are calculated in the Delft3D model for every 15 min. The time of the ADCP measurements in 2009 is converted to the corresponding time in 2002 by fitting the corresponding high waters in the beginning of the ebb period (Figure 72). The number of longitudinal measurements is smaller than the number of the model maps, while the number of transverse measurements is larger than the number of the model maps. The transverse ADCP profile was measured every 3 min. For the comparison of the model results with the ADCP measurements for the Ballooi - transverse profile, the closest in time transect of the ADCP measurements was found for each model map. Each measurement along the longitudinal profile takes more time than along the transverse profile. The longitudinal ADCP profile was measured every 20 min. For the comparison of the model results with the ADCP measurements for the Notelaer - longitudinal profile, the closest in time model map was found for each ADCP measurement.

The calculated and measured depth-average velocities with the corresponding coordinates and time are found and plotted versus each other on scatter plots for 3 depth zones (deep, undeep and littoral). The plots are made for velocity magnitude and direction. The boundaries between the deep, undeep and littoral zones are defined as follows:

- the limit between deep water and undeep water is - 7.5 m NAP;
- the limit between undeep water and littoral zone (which includes slikke and schorre areas) is - 2.5 m NAP (it is about mean spring low water in the study area).

It was chosen to use a fixed height as a limit between depth zones. In reality this will be different (based on local water levels). However, the differences are supposed to be small enough to opt for this approximation.

The tide is divided in 6 time periods for the analysis (Figure 73):

- the first phase of ebb (from about 30 min after the high water slack to the middle of ebb);
- the second phase of ebb (from the middle of ebb to about 30 min before the low water slack);

- the period around low water slack (about 30 min before and after the slack);
- the middle of flood (from about 30 min after the low water slack to 30 min before the moment of the peak flood velocity);
- the period of the maximal flood velocity (30 min before and after the moment of the peak flood velocity);
- the period around high water slack (about 30 min before and after the slack),

The periods around high and low water slack include, besides the slack moment itself, some period in the end and beginning of ebb and flood. During the model calibration the most attention is paid to the analysis of the model results for the ebb, middle of flood and for the period of maximal flood velocity. The periods around high and low water slacks are less important because velocities around the slack periods are low and have limited importance for ecology.

The total bias and root mean squared error are calculated for each analyzed model map. Furthermore, mean bias, root mean squared error and standard deviation are found for each analyzed period of the tide for deep, undeep and littoral zones (Table A-6 and Table A-7). The definition of the different statistical parameters is given in appendix 1.

The most important plots used during the model calibration are presented in Figure 70 - Figure 138. The figures for all simulations used for the model calibration and validation can be found on the CD.

5.3 Simulation period

The simulation period for the model calibration is chosen based on the comparison of the tidal amplitudes at Schelle during the measurement campaign on 10/06/2009 (Figure 71) and during the period represented in the numerical model (June – July 2002) (Figure 70). This is done in order to obtain a better representation of the velocities in the model. The water level station Schelle is chosen for the comparison because it is located near the Notelaer and Ballooi. Temse could not be used for the analysis because the measured low waters at Temse are not accurate (the measurement instrument is located in the muddy environment during low water periods)[2].

The simulation period for the model calibration is chosen from 15/07/2002 5:00 to 15/07/2002 22.30 (model runs start from the restart files). The model maps for one full tidal cycle from 15/07/2002 8:45 to 15/07/2002 21:30 are used for the analysis. The tidal amplitude during the measurement campaign on 10/06/2009 (5.6 m) is similar to the tidal amplitude on 15/07/2002 (5.8 m) (Figure 72).

The wind magnitude was about 5 to 9 m/s on 15/07/2002, NW - NNW wind direction (wind station Hansweert is taken in the model as representative for the entire estuary) (Figure 74, Figure 75). The wind magnitude during the measurement campaign on 10/06/2009 was changing from about 1 to 4 m/s (wind station Haasdonk), with a peak velocity of about 6 m/s (*Plancke et al.*, 2009). Wind had SW – SSW direction on 10/06/2009. The sensitivity analysis showed that the model is not sensitive to the differences in wind (the maximal wind magnitude was about 7 m/s during the period used for the sensitivity analysis, the wind direction was changing from SW to NNW). The differences in wind during the simulation period and measurement period are very small. Therefore, we expect that they do not affect the calibration results.

5.4 Overview of the calibration model runs

Table 5-1 presents an overview of the model simulations used for the model calibration. The bed roughness and horizontal eddy viscosity are used as calibration parameters. The sensitivity analysis showed that they have the strongest effect on the modeled velocities.

[2] personal communication Hydrometry department

Table 5-1. Model runs for the model calibration

Model run	Bed roughness ($m^{-1/3}s$)			Horizontal eddy viscosity (m^2/s)
	river channel	slikke area	schorre area	
DD3x3calibr	0.018	0.017	0.017...0.05	1
Runs with adapted roughness				
$n_{intertidal}$ decreased				
DD3x3calibr1	0.018	0.013	0.013...0.035	1
DD3x3calibr3	0.018	0.011	0.011...0.028	1
$n_{intertidal\ and\ channel}$ decreased				
DD3x3calibr4	0.015	0.011	0.011...0.028	1
DD3x3calibr7	deep: 0.018 undeep: 0.011	0.011	0.011...0.028	1
n increased				
DD3x3calibr8	0.021	0.017	0.017...0.05	1
DD3x3calibr13	0.018	0.021	0.021…0.065	1
Runs with adapted viscosity				
DD3x3calibr2	0.018	0.013	0.013...0.035	5
DD3x3calibr9	0.018	0.017	0.017...0.05	3
DD3x3calibr11	0.015	0.011	0.011...0.028	2
DD3x3calibr10	0.021	0.017	0.017...0.05	2
DD3x3calibr5	0.018	0.013	0.013...0.035	0.2
DD3x3calibr12	0.023	0.017	0.017...0.05	0.6
Run with depth dependent roughness for slikke area				
DD3x3calibr14	0.018	0.018 … 0.05		3

5.5 Results

5.5.1 First calibration run

A certain bed roughness and viscosity are chosen for the first calibration run DD3x3calibr. A horizontal eddy viscosity of 1 m²/s (default value) is defined in the first simulation. The same roughness field as in the calibrated NEVLA model (*Maximova et al*., 2009) is used everywhere except the second sub-domain. In the second model domain a bed roughness of 0.017 $m^{-1/3}s$ is defined for the slikke area. The roughness of the schorre area changes from 0.017 to 0.05 $m^{-1/3}s$ as a function of bathymetry. Higher roughness values are defined for a higher bathymetry. For the river channel the same roughness (0.018 $m^{-1/3}s$) as in the calibrated NEVLA model is used in the second sub-domain.

The results of the first calibration run are presented in Table A-6 and Table A-7. The scatter plots of the calculated and measured velocities can be found on the CD.

Velocity magnitude

Comparison of the results of the first model run with the ADCP measurements for the Ballooi (transverse profile) shows that the maximal flood velocities in the deep and undeep zones are overestimated in the model. The RMSE of maximal flood velocities is 0.21 m/s in the deep zone and 0.15 m/s in the undeep zone. The modeled maximal flood velocities in the littoral zone show a slightly better correspondence with the measurements (RMSE is 0.14 m/s) (Table A-6). However, they require improvement too. In the middle of flood the modeled velocities in the littoral zone are lower than the measurements (RMSE is 0.18 m/s), while the velocities in the deep and undeep zones are represented better. The modeled ebb velocity in the littoral zone has smaller differences with the measurements than in the deep and undeep zones where some values of the ebb velocities are too high and some values are too low (Table A-6).

The model results are also compared with the ADCP measurements for the Notelaer (longitudinal profile) (Table A-7). Since only a few velocity points are available in the deep zone, no analysis was done for this zone. In the undeep zone the maximal flood velocity is calculated too high in the model (RMSE is 0.19 m/s). This is similar to the results of the comparison with the transverse ADCP measurements. In the littoral zone some of the maximal flood velocities are reproduced accurately. However, some values are too low. The RMSE of the maximal flood velocities in the littoral zone (0.12 m/s) is lower than in the undeep zone (0.19 m/s). In the middle of flood most of the calculated velocities in the undeep and littoral zones are lower than the measurements. However, the differences are not large for most points (RMSE is 0.08 m/s) (Table A-7).

During the ebb period some velocities are calculated too low and some too high in the undeep zone in comparison to the ADCP measurements along the longitudinal profile. Most of the calculated velocities are too low. In the littoral zone the calculated velocities for the ebb period have to be increased too.The velocities for the first ebb phase are modeled better in the undeep zone (RMSE is 0.12 m/s) than in the littoral zone (RMSE is 0.15 m/s). This is opposite for the second ebb phase: the velocities in the littoral zone have smaller differences with measurements (RMSE is 0.11 m/s) than the velocities in the undeep zone (RMSE is 0.15 m/s).

Velocity direction

At the Ballooi - transverse profile the velocity direction is close to 90 degrees during the ebb. The direction during the flood is about 270 degrees. At the Notelaer – longitudinal profile the velocity direction changes from about 45 to 85 degrees during the ebb period and from about 220 to 260 degrees during the flood. The analysis of the time series of the bias and RMSE of the calculated velocity direction shows that the differences between the model results and ADCP measurements are smaller than 10 degrees for most moments. The largest differences are observed during the slack.

Conclusion

Comparison of the model results with the ADCP measurements shows that maximal flood velocities in the deep and undeep zones should be decreased in the model. Some of the calculated maximal flood velocities in the littoral zone have to be increased. The calculated velocities for the middle of the flood have to be increased too in the littoral zone.

The conclusions about the ebb velocities obtained from the analysis of the ADCP measurements are a little different for the transverse and longitudinal profiles. Comparison of the model results with the measurements along the Ballooi - transverse profile shows that some of the calculated ebb velocities are too high and some are too low in all depth zones. Comparison with the longitudinal ADCP measurements at the Notelaer shows that most of the calculated ebb velocities are too low.

The differences in the results of the analysis of the transverse and longitudinal profiles can be related to the methodology of the analysis. The model map closest in time to the average time of the measured ADCP profile is used for the comparison. The transverse measurements are performed during a shorter period of time than the longitudinal measurements. The average time of the measured transverse profile does not differ much from the start and end time of the measurement. Therefore, the closest in time model map represents the velocities for a period of a transverse measurement better than for a longer period of a longitudinal measurement.

Another possible reason for the differences is the fact that the longitudinal ADCP measurements represent the velocities along a longer distance than the transverse ADCP measurements. Therefore, comparison of the model results with the transverse and longitudinal measurements can produce different results.

5.5.2 Model runs with adapted bed roughness

An attempt is made to improve the model results by the adaptation of the bed roughness. A change of the roughness value affects hydrodynamics, both the vertical (tidal penetration) and the horizontal (flow velocities) tide. A decreased roughness allows a further penetration of the tide and increases the flow velocities, while an increased roughness results in a less tidal penetration and a decrease of the velocities. The sensitivity analysis showed that change of the bed roughness of the intertidal area has an important effect on the velocities in this area. However, this effect is not equally important during the entire tidal period. The largest changes are observed during the period with the maximal flood velocity and in the first phase of ebb. Higher water levels on the littoral zones are observed during these periods. A change of the bed roughness of the littoral zones affects the velocities only in a part of the littoral zone.

Several model runs with different roughness fields were performed. The analysis showed that a change of the bed roughness on the intertidal areas has a rather limited effect on the model velocities. If the roughness of the littoral zone is changed together with the roughness of the river channel, the effect on the model velocities is larger.

Model runs with decreased roughness of the intertidal area

In model runs DD3x3calibr1 and DD3x3calibr3 a lower bed roughness is defined for the intertidal areas than in run DD3x3calibr. The same roughness as in the calibrated NEVLA model (Maximova et al., 2009) is used for the river channel (Table 5-1).

A decrease of the bed roughness of the intertidal zone has almost no effect on the velocities in the **deep** zone. The effect on the calculated velocities for the Notelaer – longitudinal profile is a little larger in the **undeep** zone. The calculated flood and ebb velocities increase (Table A-6, Table A-7). This results in a better representation of the calculated velocities for the middle of flood and ebb in the model in comparison to run DD3x3calibr. The representation of the maximal flood velocities in the model worsens. The changes in the velocities for the Ballooi – transverse profile in runs DD3x3calibr1 and DD3x3calibr3 in the undeep zone are only small.

The calculated flood and ebb velocities in the **littoral** zone increase as a result of a decreased roughness (Table A-6, Table A-7). Since the longitudinal ADCP measurements show that the middle of flood and ebb velocities are calculated too low in the littoral zone in run DD3x3calibr, a decreased roughness of the littoral zone helps to improve the model results (Table A-7).

However, the calculated maximal flood velocities and ebb velocities for the Ballooi – transverse profile

increase too much in the littoral zone and become higher than the measurements. The calculated velocities increase only a little in the middle of flood and they are still lower than the transverse ADCP measurements (Table A-6).

Model runs with decreased roughness of the intertidal area and river channel

In model runs DD3x3calibr7 and DD3x3calibr4 the bed roughness of the intertidal areas is decreased together with the roughness of the river channel. Very low bed roughness values are used in these simulations. This is done in order to check if a strong decrease of the bed roughness can help to improve some of the calculated velocities. In run DD3x3calibr7 a very low value of the bed roughness (0.011 $m^{-1/3}s$) is defined for the undeep zone. The roughness of the deep zone is not changed. In run DD3x3calibr4 the bed roughness of the river channel is decreased to 0.015 $m^{-1/3}s$. The same low roughness as in DD3x3calibr3 is defined for the intertidal areas (Table 5-1).

The change of the roughness in DD3x3calibr7 has a little stronger effect on the calculated velocities than in run DD3x3calibr4. The change of the velocities in the **deep** zone in these two runs is very small. The results are similar to run DD3x3calibr. Some velocities increase and some decrease, however, the effect is not significant. Maximal flood velocities decrease a little and improve in comparison to run DD3x3calibr in the deep zone of the Ballooi – transverse profile in run DD3x3calibr7 (Table A-6).

A decrease of the bed roughness results in an increase of the velocities in the **undeep** zone (Table A-6, Table A-7). This effect is smaller in run DD3x3calibr4 than in run DD3x3calibr7. The calculated flood and ebb (the first ebb phase) velocities for the Ballooi – transverse profile are represented worse in the undeep zone in run DD3x3calibr7 in comparison to run DD3x3calibr. The calculated velocities have a better agreement with the transverse ADCP measurements in the second ebb phase.

The calculated ebb velocities for the Notelaer – longitudinal profile increase and improve in the undeep zone (Table A-7). Most of the calculated velocities for the middle of flood improve too, however, some velocities become too high. The correspondence between the model results and measurements for the maximal flood velocities worsens.

The calculated velocities in the **littoral** zone increase too. The ebb and maximal flood velocities for the Ballooi – transverse profile become too high, while most of the velocities in the middle of flood are still too low in the model (Table A-6).

The calculated ebb velocities for the Notelaer – longitudinal profile increase and improve in the littoral zone (Table A-7). The calculated velocities improve in the middle of flood in run DD3x3calibr4. In run DD3x3calibr7 some of them become too high. The maximal flood velocities in the littoral zone increase and worsen in run DD3x3calibr7 and improve just a little in run DD3x3calibr4.

Model runs with increased roughness

The bed roughness is increased in simulations DD3x3calibr8 and DD3x3calibr13. In model run DD3x3calibr8 the bed roughness of the river channel is increased to 0.021 $m^{-1/3}s$. The same values of the bed roughness as in run DD3x3calibr are used for the intertidal area. In the model simulation DD3x3calibr13 the roughness of the intertidal area is increased while the roughness of the river channel is not changed (Table 5-1).

An increase of the roughness of the river channel results in a very small decrease of the velocities in the **deep zone** in run DD3x3calibr8. This decrease is very small and it does not result in a significant improvement of the maximal flood velocities, which remain too high (Table A-6). The calculated velocities in the **undeep** zone decrease. The change is very small and there is no improvement of the calculated velocities. The velocities in the **littoral** zone change only a little in run DD3x3calibr8. Some of the maximal flood velocities increase and some of them decrease in the littoral zone. But the changes are minor.

An increase of the roughness of the intertidal areas in run DD3x3calibr13 has almost no effect on the velocities in the **deep zone**. The calculated velocities in the **undeep** zone decrease a little but the changes are not significant (Table A-6). The maximal flood velocities in the undeep zone become a little closer to the longitudinal ADCP measurements at the Notelaer (Table A-7).

As a result of an increased roughness of the intertidal areas the velocities in the **littoral** zone decrease. Analysis of the ADCP measurements shows that the calculated velocities worsen in the middle of flood and during the ebb in run DD3x3calibr13 in comparison to run DD3x3calibr.

5.5.3 Model runs with adapted viscosity

The sensitivity analysis showed that an increase of the horizontal eddy viscosity results in a decrease of the flow velocities in the river channel, while a decrease of the viscosity results in an increase of the velocities in the river channel. An opposite effect is observed in a part of the slikke and schorre areas. The flow velocities there increase when the viscosity increases and they decrease when the viscosity decreases. However, at some moments during the tide the velocities in some parts of the intertidal area change similar to the velocities in the river channel.

Model run with increased viscosity

In run DD3x3calibr9 the horizontal eddy viscosity is increased to 3 m²/s. The same bed roughness as in run DD3x3calibr is used (Table 5-1). An increase of the viscosity results in a decrease of the calculated velocities in the **deep** zone. Comparison of the model results with the transverse ADCP measurements at the Ballooi shows that the correspondence between the calculated and measured maximal flood velocities improves a little, while the velocity becomes too low in the middle of flood. The representation of the ebb velocities in the model improves (Table A-6).

In the **undeep** zone some of the calculated flood velocities increase and some of them decrease. The deviation with the transverse ADCP measurements is reduced. Furthermore, the calculated maximal flood velocities have a better agreement with the longitudinal ADCP measurements at the Notelaer. A large part of the calculated ebb velocities for the Ballooi – transverse profile in the undeep zone decreases in run DD3x3calibr9 in comparison to DD3x3calibr. This results in an improvement of the ebb velocities for the first phase of the ebb. Most velocities in the second phase of the ebb become too low (Table A-6). The calculated velocities for the Notelaer – longitudinal profile increase and improve in the second phase of the ebb. The velocities for the first phase of the ebb decrease and become less accurate (Table A-7).

The calculated flood and ebb velocities for the Ballooi – transverse profile decrease a little in the **littoral zone** as a result of an increased viscosity. The flood velocities that are calculated too high in run DD3x3calibr improve when the viscosity is increased. However, a part of the calculated flood velocities and most of the ebb velocities worsen (Table A-6). Some of the calculated flood and ebb velocities for the Notelaer – longitudinal profile increase and some decrease in the littoral zone. The velocities improve in the middle of the flood and in the second phase of the ebb in run DD3x3calibr9 (Table A-7).

Model runs with increased viscosity and decreased bed roughness

In model runs DD3x3calibr2 and DD3x3calibr11 a decreased bed roughness and an increased viscosity are used (Table 5-1). In run DD3x3calibr2 the viscosity is increased to 5 m²/s (more than in run DD3x3calibr9). The changes in the velocities are similar to run DD3x3calibr9 but more pronounced.

Analysis of the model bias shows that on average the calculated velocities in run DD3x3calibr2 become lower than the transverse ADCP measurements at the Ballooi as a result of an increased viscosity. The root mean squared error increases. However, analysis of the model bias for the Notelaer - longitudinal profile shows that some of the modeled velocities increase and some decrease. This is because an increase of viscosity has different effects on the velocities in the littoral zones of the Ballooi – transverse and Notelaer – longitudinal profiles during some periods of the tide. The sensitivity analysis showed that velocities in a part of the littoral zone of the Ballooi – transverse profile decrease (similar to the velocities in the river channel) during some periods of the tide. Velocities in the littoral zone of the Notelaer – longitudinal profile increase as a result of an increased viscosity (Figure 43 and Figure 6).

The maximal flood velocities in the **deep zone** decrease and become closer to the transverse ADCP measurements in run DD3x3calibr2. However, the ebb and middle of flood velocities are calculated too low (Table A-6).

In the **undeep zone** the differences between the calculated and measured maximal flood velocities become smaller for the transverse Ballooi profile. Some of the calculated maximal flood velocities become closer to the longitudinal ADCP measurements at the Notelaer but some worsen (Table A-7). The calculated ebb velocities become lower than the transverse ADCP measurements. However, in the second phase of the ebb the differences between the calculated velocities and longitudinal ADCP measurements become smaller.

In run DD3x3calibr9 most of the calculated maximal flood velocities for the Ballooi – transverse profile decrease in the **littoral zone** as a result of an increased viscosity. A higher increase of the viscosity in

run DD3x3calibr2 results not only in a decrease but also in an increase of the part of the maximal flood velocities. As a result, too low maximal flood velocities increase, too high velocities decrease and the model result has a better agreement with the transverse ADCP measurements. However, the calculated ebb velocities decrease and become less accurate (Table A-6). The maximal flood and middle of flood velocities for the Notelaer – longitudinal profile increase too much in the littoral zone in run DD3x3calibr2. Some of the calculated ebb velocities increase, some do not change. The differences between the calculated velocities and longitudinal ADCP measurements become smaller in the second phase of the ebb in the littoral zone (Table A-7).

In run DD3x3calibr11 the viscosity is increased to 2 m²/s (less than in run DD3x3calibr9). Low roughness values are defined for the intertidal area and for the river channel (Table 5-1). The changes in velocities in run DD3x3calibr11 are similar to run DD3x3calibr9 but they are less pronounced. There are some improvements in the results of run DD3x3calibr11 in comparison to run DD3x3calibr9 and DD3x3calibr.

The calculated velocities for the Notelaer – longitudinal profile increase and improve in the second phase of the ebb in the **undeep** zone in run DD3x3calibr11. This is similar to the result of run DD3x3calibr9. However, the velocities for the first phase of the ebb are higher than in run DD3x3calibr9 and they show a better agreement with measurements (Table A-7).

The maximal flood velocities in the **littoral zone** of the Ballooi – transverse profile do not decrease in run DD3x3calibr11 as in run DD3x3calibr9 as a result of an increased viscosity. In run DD3x3calibr11 they increase a little (Table A-6). The velocities in the middle of flood increase a little and improve. The ebb velocities in the littoral zone increase and become closer to the longitudinal ADCP measurements (Table A-7). They are modeled better in run DD3x3calibr11 than in run DD3x3calibr9.

Model run with increased viscosity and increased bed roughness

In run DD3x3calibr10 an increase of the viscosity is combined with an increase of the roughness of the river channel. The viscosity is increased to 2 m²/s (the same as in run DD3x3calibr11). A higher bed roughness is defined for the river channel and intertidal areas in run DD3x3calibr10 than in run DD3x3calibr11 (Table 5-1).

The velocities in **deep** zone are similar in these two runs. The velocities that decrease in run DD3x3calibr11 in the **undeep** zone decrease a little more in run DD3x3calibr10 because of a higher bed roughness. The velocities that increase in run DD3x3calibr11 increase less in run DD3x3calibr10.

The calculated velocities for the Ballooi – transverse profile decrease in the **littoral** zone in run DD3x3calibr10 in comparison to run DD3x3calibr as a result of an increased viscosity and a higher roughness. However, the calculated velocities for the Notelaer - longitudinal profile increase in the littoral zone. They increase less in run DD3x3calibr10 than in run DD3x3calibr11 because of a higher bed roughness in run DD3x3calibr10 (Table A-6, Table A-7).

Model run with decreased viscosity and decreased bed roughness

In model run DD3x3calibr5 an effect of a decreased viscosity is studied (Table 5-1). A viscosity of 0.2 m²/s is defined in this simulation and a lower roughness of the intertidal area is used than in run DD3x3calibr. The analysis of the model bias shows that on average the calculated velocities in run DD3x3calibr5 become higher than the transverse ADCP measurements at the Ballooi. The root mean squared error increases. However, the model bias for the Notelaer - longitudinal profile becomes closer to zero in the beginning of the ebb and becomes more negative in the end of ebb. The sensitivity analysis showed that a decrease of viscosity has different effects on the velocities in the littoral zones of the Ballooi – transverse and Notelaer – longitudinal profiles during some periods of the tide (Figure 50 and Figure 6).

A decreased viscosity results in a small increase of the velocities in the **deep** zone in run DD3x3calibr5. The calculated velocities do not improve in the deep zone (Table A-6).

In the **undeep** zone some of the calculated flood and ebb velocities increase and some decrease. Comparison to the transverse ADCP measurements shows that most of the calculated velocities do not improve in run DD3x3calibr5 in the undeep zone. The differences between the calculated ebb velocities and transverse ADCP measurements become smaller in the second ebb phase. The flood velocities for the transverse profile do not change significantly. However, the maximal flood velocities become much higher than the longitudinal ADCP measurements (Table A-7). The modeled ebb velocities become

closer to the longitudinal ADCP measurements in the first ebb phase in the undeep zone. However, the model accuracy for the second ebb phase for the longitudinal profile worsens.

The ebb and flood velocities increase in the **littoral** zone of the Ballooi – transverse profile in run DD3x3calibr5. The calculated ebb and maximal flood velocities become much higher than the transverse ADCP measurements. The differences between the calculated and measured velocities become a little smaller for the transverse profile in the middle of the flood. However, the velocities are still too low in the model (Table A-6). Some of the calculated velocities in the littoral zone of the Notelaer – longitudinal profile increase and some decrease. The correspondence between the calculated and measured maximal flood velocities worsens. The differences between the modeled and measured ebb velocities for the longitudinal ADCP profile become smaller in the first phase of the ebb (Table A-7).

Model run with decreased viscosity and increased bed roughness

In run DD3x3calibr12 the viscosity is decreased a little less (to 0.6 m³/s) than in run DD3x3calibr5 and a higher roughness of the river channel is used than in run DD3x3calibr (Table 5-1). The changes of the calculated velocities in the **deep** zone are not significant. Some of the calculated velocities increase and some decrease, they become a little closer to the transverse ADCP measurements at the Ballooi in the middle of flood but the changes are very small.

The modeled flood and ebb velocities for the Ballooi – transverse profile decrease a little in the **undeep** zone in comparison to run DD3x3calibr. Comparison with the longitudinal ADCP measurements shows that some of the calculated maximal flood velocities increase a little and some decrease. The changes are only minor and do not result in an improvement of the velocities.

The velocities in the **littoral** zone increase a little in run DD3x3calibr12 in comparison to run DD3x3calibr. However, there is not significant improvement of the model results.

Model run with increased viscosity and depth dependent bed roughness of the slikke area

In run DD3x3calibr14 the horizontal eddy viscosity of 3 m²/s is used. This value is the same as in run DD3x3calibr9. A depth dependent bed roughness is defined for the slikke and schorre area in run DD3x3calibr14. The roughness of the intertidal areas is higher than in run DD3x3calibr9 while the roughness of the river channel is the same (Table 5-1).

The change of the bed roughness of the littoral zone has only a minor effect on the velocities in the **deep** zone. The model accuracy for the maximal flood velocities worsens a little. In general the results of run DD3x3calibr14 in the deep zone are similar to the results of run DD3x3calibr9 (Table A-6).

The calculated maximal flood velocities for the Notelaer – longitudinal profile in the **undeep** zone decrease in run DD3x3calibr14 and become closer to the measurements (Table A-7). However, most of the ebb and middle of flood velocities are too low in the model. The agreement of the calculated flood velocities for the undeep zone of the Ballooi – transverse profile does not change in run DD3x3calibr14 in comparison to run DD3x3calibr9 (Table A-6). The calculated ebb velocities decrease and worsen.

The model accuracy for the velocities in the **littoral zone** worsens in run DD3x3calibr14 in comparison to run DD3x3calibr9. An increased roughness of the intertidal area results in a decrease of the calculated velocities in the littoral zone and they become too low (Table A-6, Table A-7).

5.5.4 Intermediate conclusion

The “best” simulation, which represents the velocities at the Notelaer and Ballooi most accurately, is chosen based on the analysis of the statistics. Table A-6 – Table A-7 show the root mean squared errors calculated for different model runs for different zones and different periods of the tide. Furthermore, total root mean squared errors are calculated for each model run for the Ballooi – transverse, Notelaer – longitudinal profiles and for both profiles together (

Table A-8 – Table A-10).

Comparison of the root mean squared errors for different simulations shows that model run DD3x3calibr11 produces the best agreement with the measurements. In this run horizontal eddy viscosity is increased to 2 m²/s. A very low bed roughness is defined for the intertidal areas (Table 5-1). The roughness of the slikke area is 0.011 $m^{-1/3}s$. The roughness of the schorre area is depth dependent; it changes from 0.011 to 0.028 $m^{-1/3}s$ as a function of bathymetry. Since the schorre areas have a high bathymetry, the roughness of the largest part of the schorre area is higher than 0.020 $m^{-1/3}s$. The

roughness of the slikke area is lower than the roughnees of the river channel in this simulation. This can be explained by the fact that slikke areas are composed of muddy sediment and are not vegetated. The slikke areas are relatively flat and smooth areas. Furthermore, the smoothness of these zones can be increased due to the existence of biological films, which smooth the surface.

The total root mean squared error for this simulation is about 0.12 m/s (Table A-10). The largest differences between the calculated and measured velocities for both Ballooi – transverse and Notelaer – longitudinal profiles are observed during the period of the maximal flood velocity (Table A-6, Table A-7). The model overestimates maximal flood velocities. The simulation results are more accurate in the middle of the flood and during the ebb. The possible reasons for the differences between the calculated and measured velocities are studied in the next chapter.

5.5.5 Time shift of the measured water levels

The calibration period was chosen based on the comparison of the tidal amplitude at Schelle during the measurement campaign on 10/06/2009 (Figure 71) and the tidal amplitude during the period represented in the numerical model (June – July 2002) (Figure 70). This was done in order to obtain the best representation of the vertical and horizontal tide in the model. The tidal amplitude during the measurement campaign on 10/06/2009 is similar to the tidal amplitude on 15/07/2002. For the calibration described in the previous chapters the time of the ADCP measurements in 2009 is converted to the corresponding time in 2002 by fitting the corresponding high waters in the beginning of the ebb (Figure 107).The calculated and measured tidal curves are similar during the ebb period. However, the flood period observed on 10/06/2009 is shorter than the modeled flood for 15/07/2002, which causes a shift of 10 minutes in the high water after the flood period.

During post processing the effect of 10 min shift of the measured velocities on the model results is analyzed. The time of the ADCP measurements in 2009 is converted to the corresponding time in 2002 by fitting the corresponding high waters in the end of the flood (Figure 108). The water levels on Figure 108 are shifted by 10 min in comparison to Figure 107. After 10 min shift the water levels for 2009 become closer to the water levels for 2002 during the flood period, while the correspondence between the water levels for the ebb period slightly worsens (Figure 108).

Figure 109 and Figure 110 present comparison of the rate of the water level change (dh/dt values) for 2002 and 2009. The calculated and measured dh/dt values correspond well in the middle of flood and ebb. During the period of the maximal flood velocity (around 19:00 to 20:00) the differences become larger. The peak value of dh/dt is observed later in the model (Figure 109). This explains higher differences in calculated and measured velocities during the period of the maximal flood velocity. When measured water levels for 2009 are shifted by 10 min the correspondence between the calculated and measured dh/dt values improves in the end of flood (Figure 110) and remains good during the ebb.

Figure 111 and Figure 112 show comparison of the calculated and measured velocities (ADCP measurements for the Ballooi – transverse profile) in two different observation points in the deep zone. There is a shift in the phase of the calculated velocities. The largest shift is observed in the end of flood. If the measured velocities are shifted by 10 min, the correspondence between the model result and measurements improves in the end of the flood and ebb periods and slightly worsens in the beginning of the flood and ebb.

Mean bias, root mean squared error and standard deviation are calculated for run DD3x3calibr11 when the ADCP measurements are shifted by 10 min for the analysis. The results are presented in Table A-6 – Table A-10 and Figure 135 - Figure 138. The scatter plots of the velocity for different depth zones and different tidal periods are shown on Figure 113 - Figure 134. Root mean squared errors of the flood velocities decrease because the correspondence between the calculated and measured water levels improved during the flood. The most significant improvement of the model accuracy is observed during the period of the maximal flood velocity.

Some of the ebb velocities in the undeep zone of the Notelaer – longitudinal profile decrease a little and improve during the first phase of the ebb. However, most of the calculated ebb velocities do not improve or worsen slightly when 10 min time shift is implemented. This is because the correspondence between the calculated and measured tidal curves for the ebb period worsened.

5.6 Conclusions

A detailed 2D model is set up in the Delft3D suite. It is calibrated in order to improve the representation of flow velocities in the intertidal areas Ballooi and Notelaer and in the river channel. The calibration is based on the comparison of the calculated and measured ADCP velocities for the Ballooi - transverse profile and Notelaer - longitudinal profile. The calculated and measured velocities were compared for the analysis, using special scripts in which corresponding in time and space points were selected. They were plotted versus each other on scatter plots for different depth zones and different periods of the tide. Mean bias, root mean squared error and standard deviation were calculated for each model run.

The simulation period for the model calibration was chosen based on the comparison of the tidal amplitudes during the measurement campaign on 10/06/2009 and during the period for which the numerical model was validated in the earlier studies (June – July 2002). The tide on 15/07/2002 is used for the model calibration. In order to find the velocities with the corresponding time, the time of the ADCP measurements in 2009 was converted to the model time in 2002 by fitting the corresponding high waters in the beginning of the ebb. Since the modeled flood period is longer than the measured flood, the 10 minutes time shift of the ADCP measurements resulted in a better correspondence between the modeled and measured velocities.

The model is calibrated using bed roughness and horizontal eddy viscosity as calibration parameters.

Model run DD3x3calibr11 with an increased horizontal eddy viscosity of 2 m²/s and a low bed roughness of the intertidal areas produced the most accurate results. A lower bed roughness was defined for the slikke area than for the river channel in this simulation. This can be explained by the fact that slikke areas are composed of muddy sediment and are not vegetated.

The largest differences between the calculated and measured velocities are observed in the deep zone during the period of the maximal flood velocity and in the undeep zone in the second phase of ebb (RMSE is 0.14 m/s). The model overestimates maximal flood velocities for both profiles (the mean bias is 0.08 m/s in the deep and undeep zones). The smallest differences between the modeled and measured velocities are found in the undeep zone of the longitudinal profile in the middle of flood and first phase of ebb and in the littoral zone in the middle of flood and second phase of ebb (RMSE is 0.07 m/s). The correspondence between the model results and measurements is the best in the littoral zone for most tidal periods and in the middle of flood for most depth zones. The total root mean squared error of the calibrated model is smaller than 0.11 m/s.

6 Validation

6.1 Introduction

After calibration of the model it is necessary to check how the calibrated model performs against a measured dataset which has not been used during the calibration (validation).

The ADCP measurements for the Notelaer – transverse profile from 11 June 2009 and the GPS float measurements from 10 and 11 June 2009 are used for the model validation in this study.

6.2 Simulation period

During the model calibration it was found that it is very important that the tide represented in the model is very similar to the tide during the measurement campaign. The tidal amplitudes, duration of the flood and ebb periods and the rate of rising and falling (which is crucial for the flow velocities) should be similar in the model and in reality.

The best agreement for the tidal amplitude on 11/06/2009 was found (within the period for which the numerical model (June – July 2002) was validated) on 16/07/2002. Therefore, the simulation period from 16/07/2002 5:00 to 16/07/2002 23.30 is chosen for the model validation (the model runs start from the restart files). The model maps from 16/07/2002 9:15 to 16/07/2002 22:15 with 15 min interval are used for the analysis.

In order to find the velocity vectors with the corresponding time, the time of the ADCP measurements in 2009 should be converted to the time in 2002 by fitting the corresponding high waters. The flood period on 16/07/2002 (model) is longer than the flood period on 11/06/2009 (measurements). Fitting of the corresponding high waters at the beginning of the ebb results in a better representation of the ebb period in the model (Figure 139). Fitting of the high waters at the end of the flood helps to improve the model accuracy for the flood period (Figure 140).

Figure 141 and Figure 142 show comparison of the rate of the water level change (dh/dt values) for 2002 and 2009. On Figure 141 the differences between the calculated and measured dh/dt values are large during the flood period. On Figure 142 the flood period is represented better. However, the differences are larger during the ebb period. Therefore, calculated and measured dh/dt values for the validation period correspond better when different time shifts are used for the flood and ebb periods (Figure 139 and Figure 140).

Two different time shifts are used for the model validation. The ebb period is analyzed with the time shift shown on Figure 139. Figure 140 presents the time shift used for the analysis of the flood period.

6.3 Results

6.3.1 Comparison to ADCP measurements

The same methodology for comparison of measurements and model results was applied as during the calibration. The calculated and measured velocities with the corresponding coordinates and time are plotted versus each other on the scatter plots for different depth zones and different periods of the tide (Figure 144 - Figure 155). The most attention is paid to the analysis of the model results for the ebb, middle of flood and for the period of maximal flood velocity. The mean values of the bias and root mean squared error for each timestep are presented on Figure 165 - Figure 168. Furthermore, mean bias, root mean squared error and standard deviation are found for each analyzed period of the tide for deep, undeep and littoral zones (Table A-11). Total root mean squared errors for the model validation are shown in Table A-12.

Mean bias of the velocity magnitude changes from -0.10 to 0.10 m/s during the ebb and flood periods. Mean bias of the velocity direction is smaller than 10 degrees for most moments during the flood and ebb Figure 165, Figure 166). Root mean squared error of the velocity magnitude varies between 0.07

and 0.15 m/s. Root mean squared error of the velocity direction is about 10 degrees during the ebb period and it changes from about 10 to 20 degrees during the flood (Figure 167, Figure 168).

Figure 169 and Figure 170 show the comparison of the calculated and measured velocities (ADCP measurements for the Notelaer – transverse profile) in the observation point in the deep zone. The ebb and flood periods are presented on two different plots because two different time shifts are used for the model validation for the ebb and flood (Figure 139, Figure 140). There is no shift in the phase of the modeled velocities during the ebb period (Figure 169). However, the simulated flood period is 15 min longer than the measured one, causing differences in the period just after low water slack, beginning of the flood (Figure 170). The middle and the end of the flood are represented in the model better.

Comparison of the model results to the ADCP measurements for the Notelaer – transverse profile shows that the maximal flood velocities are overestimated in the model in the **deep zone**. This is similar to the results of the calibration. In the middle of flood and during the ebb the differences between the calculated and measured velocities in the deep zone are smaller (Table A-11, Figure 144, Figure 145).

In the **undeep zone** the calculated maximal flood velocities are more accurate than the velocities in the middle of flood, which are calculated too low (Table A-11, Figure 148). The modeled ebb velocities are lower than the measurements too (Figure 149).

The largest differences in the **littoral zone** are calculated for the first ebb phase (Table A-11, Figure 153). This can be related to a limited number of available velocity measurements for the ebb period in the littoral zone. The velocities for the first ebb phase and middle of flood are underestimated in the model. The calculated maximal flood velocities are closer to the ADCP measurements in the littoral zone than the velocities in the middle of flood (Table A-11, Figure 152).

Table A-12 presents an overview of the total root mean squared errors calculated for different periods of the tide and for different depth zones. Comparison of the model results to the ADCP measurements shows that root mean squared errors for the ebb are smaller than for the flood. The model accuracy in the littoral zone is a little worse than in the deep and undeep zones. The total root mean squared error of the model result for the validation period is about 0.12 m/s. This is similar to the total root mean squared error of the final calibration run DD3x3calibr11 10min shift (Table A-10).

6.3.2 Comparison to GPS float measurements

Besides the ADCP measurements, the GPS float measurements (1 m below water surface) are used for the model validation. The first and last 30 seconds of each float measurement are excluded from the analysis in order to avoid a measurement error (disturbance of vessel). The float measurements are divided in 13 groups for each hour of the tide (6 hours before the high water, the period of high water and 6 hours after the high water). Each group of measurements includes 30 min before and after high water, high water plus 1 hour, high water plus 2 hours, etc. (*Plancke et al.*, 2010). For each float measurement, the corresponding velocity field is determined.

The velocity data from the model map is compared with the float measurements for the closest time period and the same location. The corresponding model output and float measurements are plotted versus each other on the scatter plots for deep, undeep and littoral zones. The plots are made for different tidal periods (Figure 156 - Figure 164). Mean bias, root mean squared error and standard deviation are found for each analyzed period of the tide for deep, undeep and littoral zones (Table A-11, Table A-12). Since the measurements are grouped in 1 hour periods, differences can occur because in the numerical model only one map was taken into account for each group of float measurements.

Comparison of the model results with the float measurements shows that the maximal flood velocities are overestimated in the model in the **deep zone**. The velocities in the middle of flood are more accurate (Figure 156). The differences between the model results and float measurements are smaller than the differences between the calculations and ADCP measurements in the deep zone for the flood period and larger for the ebb period (Table A-11). The ebb velocities are calculated too low in the model in the deep zone (Figure 157).

In the **undeep zone** the largest differences are calculated for the second ebb phase: the calculated velocities are systematically too low (Figure 160). Some of the calculated velocities are too low in the middle of the flood. Some of the calculated maximal flood velocities are too high (Figure 159).

In the **littoral zone** most of the calculated velocities for the flood and ebb periods are lower that the float measurements. The model accuracy for the flood is better than for the ebb period (Table A-11, Figure

162, Figure 163). The largest differences between the modeled and measured velocities are found for the second phase of the ebb: modeled velocities are too low.

It should be mentioned that these differences (underestimation by the model) can partly be explained by the set up of float measurements. During the measurement campaign floats were used at a depth of about 1 m (*Plancke et al*., 2010), while the model calculates depth averaged velocities. In general the top layer of the water column is characterized by higher velocities than the depth averaged velocities. This was checked for some of the ADCP transects. The velocity for the top cell is plotted versus the depth average measured velocity on Figure 171 - Figure 174 for one of the measured profiles. It can be seen that most of the velocities measured in the top layer of the water overestimate the depth averaged velocities. The velocity for the top layer is on average about 12% higher than the depth averaged velocity.

Table A-12 presents an overview of the total root mean squared errors calculated for different periods of the tide and for different depth zones. A smaller root mean squared error is calculated in the middle of the flood when floats are used for the analysis instead of ADCP measurements. Comparison of the model results to the float measurements shows that root mean squared error is maximal in the second ebb phase. The model results for the second ebb phase are closer to the ADCP transverse measurements at the Notelaer than to the float measurements in all depth zones (Table A-11). Therefore, the root mean squared error in different depth zones and the total root mean squared error of the model are larger when the float measurements are used for the analysis.

6.4 Conclusions

Model validation was based on comparison of the calculated and measured velocitites for the Notelaer and Ballooi. The ADCP measurements from 11/06/2009 and float measurements from 10/06/2009 and 11/06/2009 were used for the analysis. The model was validated for one tide on 16/07/2002 because the tidal amplitude during this period was similar to the measured tidal amplitude on 11/06/2009.

The calculated and measured velocities with the corresponding coordinates and time were found for the analysis. They were plotted versus each other on the scatter plots. Mean bias, root mean squared error and standard deviation were calculated for different depth zones and different periods of the tide.

The total root mean squared error of the model is 0.12 m/s for the ADCP measurements and 0.16 m/s for the GPS-float measurements. The model systematically underestimates the float measurements becase the flow velocities in the top layer of the water (measured with floats) are higher than the depth averaged velocities (modeled).

The model validation showed that the calibrated model performs slightly better in the deep zone than in the undeep and littoral zones. In general the ebb period is represented in the model better than the flood period.

In the deep zone the modeled ebb velocities have a good agreement with the measurements (RMSE is 0.09 m/s). The modeled maximal flood velocities in the deep zone are overestimated (bias is 0.13 m/s, RMSE is 0.16 m/s). Maximal flood velocities in the undeep zone correspond well with the measurements (RMSE is 0.09 m/s). The modeled velocities in the middle of flood are underestimated in the model (bias is -0.09 m/s, RMSE is 0.15 m/s). The ebb period is represented in the model a little better than the middle of flood in the undeep zone. In the littoral zone the modeled velocities in the first ebb phase are too low in comparison to the float and ADCP measurements. The modeled flood velocities in the littoral zone show a better agreement with the measurements (RMSE for the period of maximal flood velocity is 0.09 m/s, RMSE for the middle of flood is 0.15 m/s).

The validation results may further improve if the modeled tide is a better approximation of the tide observed during the measurement campaign. The tidal amplitudes and the rate of the water level change should be very similar in the model and in the reality.

7 Conclusions and recommendations

7.1 General conclusions

The shallow waters, intertidal mudflats and marshes along the Sea Scheldt have an important ecological value. They form a habitat for the development of ecosystems. A good reproduction in the numerical model of the velocity on the intertidal areas is necessary to answer ecological questions. The slikke and schorre areas Notelaer and Ballooi were chosen as a pilot study in the framework of the project "Vervolgstudie inventarisatie en historische analyse van slikken en schorren in de Zeeschelde". These areas are located between Rupelmonde and Temse. Both zones form one of the most ecologically valuable areas of the Upper Sea Scheldt.

Whithin this study a sensitivity analysis, calibration and validation of flow velocities on the intertidal areas and in the river channel were performed. The sensitivity analysis showed that at least 3x3 grid refinement should be used in the model. The cells of this grid are about 33 m long and 11 m wide. The change of the bed roughness of the slikke and schorre areas has an important effect on the velocities in these areas. An increase of the roughness results in a decrease of the velocities and a decrease of the roughness results in an increase of the flow velocities. Change of the horizontal eddy viscosity affects the flow velocity along the cross section. When viscosity increases, the velocity profile becomes less convex. Therefore, flow velocities decrease in the river channel and increase in the intertidal areas. A decrease of the viscosity has an opposite effect: the velocity profile becomes more convex. Wind and interpolation method for the calculation of bathymetry have only a very small effect on the modeled velocities.

A detailed model set up in the Delft3D suite was calibrated and validated in order to improve the representation of the flow velocities in the intertidal areas Ballooi and Notelaer and in the river channel. The calibration and validation were executed on the available flow measurement data (measurement campaign 10 and 11 June 2009). From the available ADCP measurements two transects were used for the calibration, while another transect was used for the validation. The GPS-float measurements were also used for the validation.

The model was calibrated using bed roughness and horizontal eddy viscosity. Model run DD3x3calibr11 with an increased horizontal eddy viscosity of 2 m²/s and a low bed roughness of the intertidal areas produced the most accurate results. A lower bed roughness was defined for the slikke area than for the river channel in this simulation. This can be explained by the fact that slikke areas are composed of muddy sediment and are not vegetated. The slikke areas are relatively flat and smooth areas. Furthermore, the hydraulic smoothness of these zones can be increased due to the existence of biological films.

The total root mean squared error of the calibrated model is smaller than 0.11 m/s. The largest differences between the calculated and measured velocities are observed in the deep zone during the period of the maximal flood velocity and in the undeep zone in the second phase of ebb (RMSE is 0.14 m/s). The model overestimates maximal flood velocities. The smallest differences between the modeled and measured velocities are calculated in the undeep zone in the middle of flood and first phase of ebb and in the littoral zone in the middle of flood and second phase of ebb (RMSE is 0.07 m/s). The best correspondence between the model results and measurements is observed in the littoral zone for most tidal periods and in the middle of flood for most depth zones.

The total root mean squared error for the validation period is 0.12 m/s if the model results are compared with the ADCP measurements and it is 0.16 m/s if the GPS-float measurements are used for the analysis. The model systematically underestimates the float measurements because the flow velocities in the top layer (measured with floats) are higher than the depth averaged velocities (modeled).

The model validation showed that the calibrated model performs better in the deep zone than in the undeep and littoral zones. In general the ebb period is represented in the model better than the flood period. The largest differences between the modeled and measured ADCP velocities are calculated in the deep zone for the period of maximal flood velocity and in the undeep and littoral zones in the middle of flood. The model overestimates measured maximal flood velocities in the deep zone (bias is 0.13 m/s, RMSE is 0.16 m/s) and it underestimates measured velocities in the middle of flood in the undeep and

littoral zones (bias is -0.10 m/s, RMSE is 0.15 m/s). The smallest differences between the model results and ADCP measurements are calculated for the ebb period in the deep zone and for the maximal flood velocities in the undeep and littoral zone (RMSE is 0.09 m/s).

7.2 Recommendations

7.2.1 Water levels

The calibration and validation were executed on the available flow measurement data. The correspondence between the model results and measurements may improve if the tide represented in the model is exactly the same as the tide observed during the measurement campaign. The tidal amplitudes and the rate of the water level change, which is crucial for the flow velocities, should be very similar in the model and in the reality.

7.2.2 Topo-bathymetry

A topo-bathymetry used in the model can have an important effect on the model results. The laser altimetry measurements from 2004 were used to define bathymetry for the intertidal areas. The use of the bathymetry from 2009 for the study area can result in a better correspondence between the modeled and measured (10 – 11 June 2009) velocities.

7.2.3 Study area

A period of June – July 2002 was simulated in the model because more detailed boundary conditions are available for this period. The model was calibrated for one tide for the study area Ballooi and Notelaer. If another location should be used in the model, a new model calibration and validation should be performed. A model calibration and validation are based on the available flow measurement data. Therefore, measured velocities should be available if the model has to be calibrated for another study area.

7.2.4 Bed roughness

A bed roughness was used in this study as a calibration parameter. The bed roughness-coefficient expresses the resistance the flow experiences from the riverbed. Flow resistance is often attributed to, on one hand, the roughness of surface grains and, on the other hand, the form drag due to irregularities of the bed (bedforms) (*Spekkers et al*., 2008). In the final calibration run a uniform bed roughness was assigned for all slikke areas in the study area and a depth dependend roughness was assigned for the schorre area. No distinction was made between different geomorphological zones (bedforms) of the intertidal areas. In reality different fluvial bedforms can be present on the intertidal areas and in the river channel, such as dunes, ripples, or no bedforms. These bedforms can interact with the flow and result in different turbulence conditions. Different bedforms form a different obstacle to the flow; therefore, they have different bed roughness values.

The model simulation with the bed roughness values related to the bedforms can be performed. A spatially distributed approach to a hydraulic modelling scheme must be based on a map of the roughness elements over the floodplain at different scales. Theoretically, the topographic representation must characterise the terrain surface over which the fluid flows at an adequately discretised scale in order to reflect the flow processes of interest. Similarly, roughness parameterisation must account for energy losses due to geometric variability of the surface produced at scales finer than those represented in the mesh (discretisation scale) (*Lane*, 2005). A higher resolution model will explicitly encompass smaller topographic variations, provided the associated topographic data are at the same resolution. With a coarser model resolution, smaller topographic variations will need to be parameterised, either explicitly through a porosity type treatment (e.g. *Yu and Lane*, 2006) or upscaling of a roughness parameter.

The main problem of assessing spatial subscale effects upon flow is that, in practice, roughness parameterization must account not only for discrepancies between the intrinsic scale of the surface variability and the scale represented in a mesh, but also for the discrepancies between the intrinsic scale of the flow process and the processes explicitly represented in the numerical solution (i.e. the processes not explicitly represented because of the averaging of the flow equations in time or space, such as diffusive effects in the flow due to turbulence in a 2-D approach). Therefore, the roughness

parameter turns out to be an effective parameter commonly obtained through a calibration procedure (e.g. *Lane and Ferguson*, 2005). This situation complicates the scale-dependent relationship between roughness and topography (*Casas et al*., 2010).

(*Van Prooijen en Dam*, 2005) tested the performance of the FINEL model with different bed roughness fields: the bed roughness obtained from the calibration of water levels and the bed roughness obtained based on the geomorphological map. The analysis showed that the morphology dependent roughness field is not necessarily better for a good representation of the flow velocities in the model. The differences in velocities calculated in the models with two different bed roughness fields were small. Therefore, it was concluded that it was not necessary to define the bed roughness based on the geomorphological data.

Besides the variation of the bed roughness in space, it also varies in time. The direction of water movement and water levels change during the tidal cycle. Therefore, the bedforms interact with the flow differently during the flood and ebb periods and they have a different effect on the water movement. Since it is not possible to define a time varying bed roughness in the Delft3D model a constant in time bed roughness field was used in this study.

8 References

Adema, J. (2006). Evaluatie van hydraulische modellen voor operationele voorspellingen. Deelopdracht 3: Afregelen van Vlaamse rivieren in het Kustzuid model en vergelijking Kalman sturing. Rapport Alkyon A1401R3r2, in opdracht van WL Borgerhout (M.729-09)

Aqua Vision, (2010). Varende ADCP metingen Schelde 2009. AV_DOC_100456. Vlaamse Overheid, Departement Mobiliteit en Openbare Werken, Waterbouwkundig Laboratorium.

Casas, A., Lane, S.N., Yu, D., Benito G., (2010). A method for parameterising roughness and topographic sub-grid scale effects in hydraulic modeling from LIDAR data. Hydrology and Earth System Sciences Discussions, 7, 2261 – 2299.

Ides, S.; Vanlede, J.; De Mulder, T.; Mostaert, F., (2008). Vervolgstudie inventarisatie en historische analyse van slikken en schorren langs de Zeeschelde – Gevoeligheidsonderzoek 2D modellen. Ref. WL2008R713_21_2rev2_0.

Lane, S.N., (2005). Roughness-time for a re-evaluation? Earth Surf. Proc. Land, 30, 251 – 253.

Lane, S.N. and Ferguson, R.I., (2005). Modelling reach-scale fluvial flows, in: Computational Fluid Dynamics Applications in Environmental Hydraulics, edited by: Bates, P.D., Lane, S.N., Ferguson, R.I., John Wiley and Sons Ltd, 217 – 269.

Maximova, T.; Ides, S.; De Mulder, T.; Mostaert, F., (2009). Verbetering randvoorwaardenmodel. Deelrapport 4: Extra aanpassingen Zeeschelde. WL Rapporten, 753_09. Flanders Hydraulics Research: Antwerp, Belgium.

Plancke, Y.; Ides, S.; Mostaert, F., (2010). Vervolgstudie inventarisatie en historische analyse van slikken en schorren langs de Zeeschelde: Vlottermetingen Ballooi en Notelaer Juni 2009. Versie 2_0. WL Rapporten, 713_21. Waterbouwkundig Laboratorium: Antwerpen, Belgie

Sastry, S. Isukapalli, (1999). Types and origins of uncertainty in transport-transformation models [online]. Available from: http://ccl.rutgers.edu/~ssi/thesis/thesis-node11.html [Accessed 18/12/2009].

Spekkers, M.H.; Tuijnder, A.P.; Ribberink, J.S.; Hulscher, S.J.M.H. (2008). Bed roughness experiments in supply limited conditions. Marine and river dune dynamics, 1-3 April 2008. Leeds, United Kingdom.

Vanlede, J., Decrop, B., De Clercq, B., Ides, S., Demulder, T. en Mostaert, F. (2008). Permanente verbetering modelinstrumentarium: verbetering randvoorwaardenmodel. Deel 2: afregelen van het Scheldemodel. Ref. WL2008R753_09rev1.

Van Prooijen, B., Dam, G. (2005). Kalibratie waterbeweging Westerschelde. Ref. bvp/05365/1339. Svasek. Rotterdam, Nederland.

WL/Delft Hydraulics, (2007a). Delft3D-FLOW. Simulation of multi-dimensional hydrodynamic flows and transport phenomena, including sediments. User manual.

WL/Delft Hydraulics, (2007b). Delft3D-QUICKIN. Generation and manipulation of grid-related parameters such as bathymetry, initial conditions and roughness. User manual.

Wikimedia Foundation, Inc., (2009). Viscosity [online]. Available from: http://en.wikipedia.org/wiki/Viscosity [Accessed 11/12/2009].

Yu, D. and Lane, S.N., (2006). Urban fluvial flood modeling using a two-dimensional diffusion-wave treatment, part2: development of a sub-grid-scale treatment, Hydrol. Process., 20(7), 1567 – 1583.

Tables

Table A-1. Average absolute differences in velocity for runs with different grid resolution

Study area		Point number	Average absolute difference in velocity (m/s)		
			DD4x4 minus DD3x3	DD4x4 minus DD2x2	DD4x4 minus DDref
Ballooi	Slikke area	B1	0.032	0.041	0.098
		B3	0.016	0.034	0.049
		B4	0.037	0.021	0.031
		B5	0.011	0.032	0.032
		B6	0.053	0.061	0.077
		B7	0.017	0.027	0.025
		B8	0.012	0.012	0.050
		B9	0.016	0.024	0.079
		B10	0.016	0.027	0.034
		B12	0.073	0.030	0.083
		all points	0.028	0.031	0.056
	Schorre area	B2	0.000	0.028	0.032
		B11	0.000	0.000	0.000
		all points	0.000	0.014	0.016
Notelaer	Slikke area	N1	0.018	0.018	0.049
		N2	0.017	0.022	0.025
		N4	0.015	0.044	0.132
		N7	0.021	0.024	0.032
		all points	0.018	0.027	0.060
	Schorre area	N3	0.009	0.008	0.013
		N5	0.000	0.010	0.024
		N6	0.000	0.000	0.003
		N8	0.000	0.000	0.000
		N9	0.000	0.000	0.000
		N10	0.001	0.000	0.000
		all points	0.002	0.003	0.007

Table A-2. Average absolute differences in velocity for runs with different bed roughness

Study area		Point number	Average absolute difference in velocity (reference run DD3x3 minus run) (m/s)			
			DD3x3rgh1	DD3x3rgh2	DD3x3rgh3	DD3x3rgh4
Ballooi	Slikke area	B1	0.021	0.014	0.044	0.022
		B3	0.009	0.015	0.022	0.015
		B4	0.009	0.050	0.034	0.047
		B5	0.009	0.053	0.033	0.051
		B6	0.008	0.043	0.027	0.043
		B7	0.013	0.006	0.021	0.009
		B8	0.008	0.029	0.026	0.027
		B9	0.010	0.050	0.033	0.048
		B10	0.012	0.025	0.029	0.025
		B12	0.018	0.031	0.038	0.034
		all points	0.012	0.032	0.031	0.032
	Schorre area	B2	0.000	0.000	0.000	0.000
		B11	0.000	0.000	0.000	0.000
		all points	0.000	0.000	0.000	0.000
Notelaer	Slikke area	N1	0.006	0.026	0.013	0.026
		N2	0.002	0.006	0.003	0.006
		N4	0.005	0.028	0.014	0.028
		N7	0.002	0.012	0.005	0.012
		all points	0.004	0.018	0.009	0.018
	Schorre area	N3	0.002	0.001	0.003	0.002
		N5	0.000	0.000	0.000	0.000
		N6	0.000	0.000	0.000	0.000
		N8	0.000	0.000	0.000	0.000
		N9	0.000	0.000	0.000	0.000
		N10	0.001	0.000	0.001	0.000
		all points	0.000	0.000	0.001	0.000

Table A-3. Average absolute differences in velocity for runs with different viscosity

Study area		Point number	Average absolute difference in velocity (reference run DD3x3 minus run) (m/s)	
			DD3x3V1	DD3x3V2
Ballooi	Slikke area	B1	0.034	0.030
		B3	0.025	0.017
		B4	0.042	0.031
		B5	0.057	0.036
		B6	0.077	0.042
		B7	0.025	0.014
		B8	0.040	0.022
		B9	0.057	0.037
		B10	0.050	0.028
		B12	0.060	0.042
		all points	0.047	0.030
	Schorre area	B2	0.000	0.000
		B11	0.000	0.000
		all points	0.000	0.000
Notelaer	Slikke area	N1	0.063	0.044
		N2	0.021	0.015
		N4	0.063	0.042
		N7	0.031	0.021
		all points	0.044	0.031
	Schorre area	N3	0.006	0.004
		N5	0.000	0.000
		N6	0.000	0.000
		N8	0.000	0.000
		N9	0.000	0.000
		N10	0.001	0.001
		all points	0.001	0.001

Table A-4. Average absolute differences in velocity for runs with different wind conditions

Study area		Point number	Average absolute difference in velocity (m/s)
			DD3x3 minus DD3x3 without wind
Ballooi	Slikke area	B1	0.010
		B3	0.003
		B4	0.005
		B5	0.004
		B6	0.005
		B7	0.005
		B8	0.005
		B9	0.006
		B10	0.007
		B12	0.011
		all points	0.006
	Schorre area	B2	0.000
		B11	0.000
		all points	0.000
Notelaer	Slikke area	N1	0.009
		N2	0.002
		N4	0.005
		N7	0.004
		all points	0.005
	Schorre area	N3	0.001
		N5	0.000
		N6	0.000
		N8	0.000
		N9	0.000
		N10	0.000
		all points	0.000

Table A-5. Average absolute differences in velocity for runs with different bathymetry

Study area		Point number	Average absolute difference in velocity (m/s)
			DD3x3 (closest value) minus DD3x3 (shepard)
Ballooi	Slikke area	B1	0.009
		B3	0.008
		B4	0.005
		B5	0.004
		B6	0.009
		B7	0.010
		B8	0.005
		B9	0.006
		B10	0.006
		B12	0.016
		all points	0.008
	Schorre area	B2	0.003
		B11	0.004
		all points	0.004
Notelaer	Slikke area	N1	0.009
		N2	0.005
		N4	0.006
		N7	0.011
		all points	0.008
	Schorre area	N3	0.004
		N5	0.000
		N6	0.002
		N8	0.000
		N9	0.000
		N10	0.001
		all points	0.001

Table A-6. Mean bias, RMSE and standard deviation for Ballooi - transverse profile of ADCP measurements

Model run	Time period	Mean difference (model - measurement) (m/s)			RMSE (m/s)			Standard deviation (m/s)		
		Deep	Undeep	Littoral	Deep	Undeep	Littoral	Deep	Undeep	Littoral
DD3x3calibr	max flood velocity	0.15	0.08	0.02	0.21	0.15	0.14	0.15	0.12	0.14
	middle flood	-0.01	0.02	-0.16	0.09	0.11	0.18	0.09	0.11	0.09
	1st phase ebb	0.06	0.03	0.00	0.16	0.13	0.11	0.15	0.13	0.11
	2nd phase ebb	0.04	-0.07	no data	0.12	0.10	no data	0.12	0.08	no data
DD3x3calibr1	max flood velocity	0.14	0.09	0.07	0.20	0.15	0.16	0.15	0.12	0.14
	middle flood	-0.02	0.02	-0.12	0.09	0.11	0.16	0.09	0.11	0.09
	1st phase ebb	0.05	0.04	0.06	0.15	0.13	0.13	0.14	0.13	0.11
	2nd phase ebb	0.03	-0.06	no data	0.12	0.09	no data	0.12	0.08	no data
DD3x3calibr2	max flood velocity	0.02	0.03	-0.01	0.13	0.13	0.12	0.13	0.13	0.12
	middle flood	-0.13	-0.05	-0.15	0.16	0.10	0.18	0.08	0.09	0.09
	1st phase ebb	-0.11	-0.12	-0.12	0.15	0.15	0.17	0.09	0.08	0.12
	2nd phase ebb	-0.10	-0.19	no data	0.14	0.20	no data	0.09	0.07	no data
DD3x3calibr3	max flood velocity	0.13	0.09	0.10	0.20	0.15	0.17	0.15	0.12	0.14
	middle flood	-0.02	0.03	-0.11	0.09	0.11	0.14	0.09	0.11	0.10
	1st phase ebb	0.04	0.04	0.08	0.15	0.13	0.14	0.14	0.12	0.12
	2nd phase ebb	0.03	-0.05	no data	0.12	0.09	no data	0.12	0.08	no data
DD3x3calibr4	max flood velocity	0.14	0.10	0.09	0.21	0.16	0.16	0.15	0.12	0.14
	middle flood	-0.01	0.04	-0.11	0.10	0.13	0.15	0.10	0.12	0.09
	1st phase ebb	0.05	0.06	0.09	0.16	0.15	0.15	0.15	0.13	0.11
	2nd phase ebb	0.03	-0.03	no data	0.13	0.08	no data	0.12	0.08	no data
DD3x3calibr5	max flood velocity	0.18	0.07	0.13	0.23	0.14	0.20	0.15	0.13	0.15
	middle flood	0.02	0.05	-0.11	0.10	0.13	0.14	0.09	0.12	0.09
	1st phase ebb	0.10	0.10	0.16	0.19	0.17	0.19	0.16	0.14	0.11
	2nd phase ebb	0.09	0.01	no data	0.16	0.08	no data	0.14	0.08	no data

Model run	Time period	Mean difference (model - measurement) (m/s)			RMSE (m/s)			Standard deviation (m/s)		
		Deep	Undeep	Littoral	Deep	Undeep	Littoral	Deep	Undeep	Littoral
DD3x3calibr7	max flood velocity	0.13	0.13	0.12	0.19	0.18	0.19	0.14	0.12	0.14
	middle flood	-0.03	0.09	-0.08	0.10	0.16	0.12	0.10	0.13	0.09
	1st phase ebb	0.04	0.09	0.13	0.14	0.17	0.18	0.14	0.14	0.11
	2nd phase ebb	0.02	0.02	no data	0.11	0.08	no data	0.11	0.08	no data
DD3x3calibr8	max flood velocity	0.14	0.07	0.03	0.20	0.14	0.15	0.14	0.12	0.14
	middle flood	-0.03	0.00	-0.16	0.08	0.10	0.18	0.08	0.10	0.09
	1st phase ebb	0.04	0.01	-0.01	0.14	0.12	0.11	0.14	0.12	0.11
	2nd phase ebb	0.03	-0.08	no data	0.12	0.11	no data	0.11	0.08	no data
DD3x3calibr9	max flood velocity	0.08	0.05	-0.03	0.16	0.13	0.14	0.14	0.12	0.13
	middle flood	-0.09	-0.03	-0.17	0.12	0.10	0.19	0.08	0.09	0.09
	1st phase ebb	-0.04	-0.07	-0.10	0.12	0.12	0.15	0.11	0.10	0.12
	2nd phase ebb	-0.04	-0.15	no data	0.10	0.17	no data	0.10	0.07	no data
DD3x3calibr10	max flood velocity	0.10	0.06	0.00	0.17	0.13	0.14	0.14	0.12	0.14
	middle flood	-0.07	-0.02	-0.16	0.10	0.09	0.18	0.08	0.09	0.09
	1st phase ebb	-0.01	-0.05	-0.07	0.12	0.11	0.13	0.12	0.10	0.11
	2nd phase ebb	-0.02	-0.13	no data	0.10	0.15	no data	0.10	0.07	no data
DD3x3calibr11	max flood velocity	0.10	0.09	0.06	0.18	0.15	0.14	0.14	0.12	0.13
	middle flood	-0.05	0.02	-0.12	0.10	0.11	0.15	0.09	0.11	0.09
	1st phase ebb	0.00	0.00	0.02	0.13	0.11	0.12	0.13	0.11	0.12
	2nd phase ebb	-0.01	-0.08	no data	0.10	0.11	no data	0.10	0.08	no data
DD3x3calibr12	max flood velocity	0.15	0.07	0.06	0.21	0.14	0.16	0.14	0.12	0.15
	middle flood	-0.01	0.00	-0.15	0.08	0.10	0.17	0.08	0.10	0.09
	1st phase ebb	0.06	0.02	0.02	0.15	0.12	0.11	0.14	0.12	0.11
	2nd phase ebb	0.05	-0.07	no data	0.12	0.11	no data	0.11	0.08	no data

Model run	Time period	Mean difference (model - measurement) (m/s)			RMSE (m/s)			Standard deviation (m/s)		
		Deep	Undeep	Littoral	Deep	Undeep	Littoral	Deep	Undeep	Littoral
DD3x3calibr13	max flood velocity	0.16	0.08	-0.03	0.22	0.15	0.15	0.15	0.12	0.15
	middle flood	-0.01	0.01	-0.20	0.09	0.11	0.21	0.09	0.11	0.08
	1st phase ebb	0.07	0.02	-0.06	0.17	0.13	0.12	0.15	0.13	0.11
	2nd phase ebb	0.05	-0.08	no data	0.13	0.11	no data	0.12	0.08	no data
DD3x3calibr14	max flood velocity	0.10	0.04	-0.13	0.17	0.13	0.19	0.14	0.12	0.15
	middle flood	-0.08	-0.05	-0.24	0.11	0.10	0.26	0.08	0.09	0.08
	1st phase ebb	-0.03	-0.10	-0.20	0.12	0.14	0.22	0.12	0.10	0.11
	2nd phase ebb	-0.03	-0.18	no data	0.10	0.19	no data	0.10	0.08	no data
DD3x3calibr11 10min shift	max flood velocity	0.08	0.08	0.03	0.14	0.10	0.10	0.12	0.07	0.09
	middle flood	-0.04	0.05	-0.06	0.09	0.11	0.12	0.08	0.09	0.11
	1st phase ebb	0.02	0.01	0.06	0.13	0.13	0.11	0.13	0.13	0.09
	2nd phase ebb	-0.02	-0.07	no data	0.11	0.13	no data	0.11	0.11	no data

Table A-7. Mean bias, RMSE and standard deviation for Notelaer - longitudinal profile of ADCP measurements

Model run	Time period	Mean difference (model - measurement) (m/s)			RMSE (m/s)			Standard deviation (m/s)		
		Deep*	Undeep	Littoral	Deep*	Undeep	Littoral	Deep*	Undeep	Littoral
DD3x3calibr	max flood velocity	no data	0.14	-0.03	no data	0.19	0.12	no data	0.13	0.12
	middle flood	-0.03	-0.05	-0.05	0.03	0.08	0.08	0.02	0.07	0.06
	1st phase ebb	no data	-0.01	-0.12	no data	0.12	0.15	no data	0.12	0.09
	2nd phase ebb	0.23	-0.04	-0.09*	0.24	0.15	0.11*	0.08	0.15	0.06*
DD3x3calibr1	max flood velocity	no data	0.16	0.02	no data	0.21	0.12	no data	0.12	0.11
	middle flood	-0.03	-0.03	-0.02	0.03	0.08	0.07	0.02	0.07	0.06
	1st phase ebb	no data	0.01	-0.06	no data	0.11	0.10	no data	0.11	0.09
	2nd phase ebb	0.22	-0.02	-0.04*	0.24	0.15	0.07*	0.08	0.14	0.06*
DD3x3calibr2	max flood velocity	no data	0.13	0.08	no data	0.19	0.16	no data	0.13	0.13
	middle flood	-0.04	-0.02	0.05	0.05	0.09	0.09	0.02	0.09	0.08
	1st phase ebb	no data	-0.06	-0.08	no data	0.14	0.13	no data	0.12	0.11
	2nd phase ebb	0.17	0.04	0.03*	0.20	0.14	0.08*	0.10	0.14	0.07*
DD3x3calibr3	max flood velocity	no data	0.18	0.05	no data	0.22	0.12	no data	0.12	0.11
	middle flood	-0.03	-0.02	0.00	0.03	0.07	0.07	0.02	0.07	0.07
	1st phase ebb	no data	0.02	-0.03	no data	0.11	0.09	no data	0.11	0.08
	2nd phase ebb	0.22	-0.01	-0.01*	0.23	0.14	0.06*	0.08	0.14	0.06*
DD3x3calibr4	max flood velocity	no data	0.18	0.03	no data	0.22	0.11	no data	0.13	0.11
	middle flood	-0.02	-0.02	-0.01	0.03	0.08	0.07	0.02	0.07	0.07
	1st phase ebb	no data	0.02	-0.04	no data	0.11	0.09	no data	0.11	0.08
	2nd phase ebb	0.21	-0.01	-0.03*	0.23	0.14	0.07*	0.08	0.14	0.07*
DD3x3calibr5	max flood velocity	no data	0.23	0.03	no data	0.27	0.15	no data	0.15	0.15
	middle flood	0.00	-0.03	-0.07	0.02	0.08	0.09	0.02	0.07	0.06
	1st phase ebb	no data	0.03	-0.03	no data	0.09	0.08	no data	0.08	0.07
	2nd phase ebb	0.24	-0.09	0.08*	0.25	0.18	0.10*	0.06	0.16	0.06*

Model run	Time period	Mean difference (model - measurement) (m/s)			RMSE (m/s)			Standard deviation (m/s)		
		Deep*	Undeep	Littoral	Deep*	Undeep	Littoral	Deep*	Undeep	Littoral
DD3x3calibr7	max flood velocity	no data	0.25	0.06	no data	0.28	0.14	no data	0.13	0.12
	middle flood	0.00	0.03	0.03	0.02	0.09	0.07	0.02	0.08	0.07
	1st phase ebb	no data	0.04	-0.04	no data	0.11	0.09	no data	0.10	0.08
	2nd phase ebb	0.20	0.03	-0.01*	0.22	0.13	0.07*	0.09	0.13	0.07*
DD3x3calibr8	max flood velocity	no data	0.14	0.00	no data	0.19	0.12	no data	0.13	0.12
	middle flood	-0.03	-0.05	-0.04	0.03	0.09	0.08	0.02	0.07	0.06
	1st phase ebb	no data	-0.01	-0.11	no data	0.12	0.14	no data	0.12	0.10
	2nd phase ebb	0.23	-0.04	-0.08*	0.25	0.15	0.10*	0.08	0.15	0.06*
DD3x3calibr9	max flood velocity	no data	0.12	0.03	no data	0.18	0.13	no data	0.12	0.13
	middle flood	-0.04	-0.04	0.00	0.04	0.09	0.07	0.02	0.08	0.07
	1st phase ebb	no data	-0.05	-0.12	no data	0.14	0.15	no data	0.13	0.10
	2nd phase ebb	0.21	0.01	-0.03*	0.23	0.14	0.07*	0.10	0.14	0.06*
DD3x3calibr10	max flood velocity	no data	0.13	0.02	no data	0.18	0.13	no data	0.12	0.12
	middle flood	-0.03	-0.04	-0.02	0.04	0.09	0.07	0.02	0.08	0.07
	1st phase ebb	no data	-0.04	-0.11	no data	0.13	0.15	no data	0.13	0.10
	2nd phase ebb	0.21	-0.01	-0.05*	0.23	0.14	0.08*	0.10	0.14	0.06*
DD3x3calibr11	max flood velocity	no data	0.17	0.06	no data	0.20	0.13	no data	0.12	0.11
	middle flood	-0.03	0.00	0.03	0.03	0.08	0.08	0.02	0.08	0.07
	1st phase ebb	no data	0.00	-0.05	no data	0.12	0.10	no data	0.12	0.09
	2nd phase ebb	0.21	0.03	0.01*	0.23	0.14	0.07*	0.09	0.14	0.07*
DD3x3calibr12	max flood velocity	no data	0.15	0.01	no data	0.20	0.13	no data	0.13	0.13
	middle flood	-0.02	-0.05	-0.05	0.03	0.09	0.08	0.02	0.07	0.06
	1st phase ebb	no data	0.00	-0.09	no data	0.11	0.13	no data	0.11	0.09
	2nd phase ebb	0.25	-0.06	-0.08*	0.26	0.16	0.10*	0.08	0.15	0.06*

Model run	Time period	Mean difference (model - measurement) (m/s)			RMSE (m/s)			Standard deviation (m/s)		
		Deep*	Undeep	Littoral	Deep*	Undeep	Littoral	Deep*	Undeep	Littoral
DD3x3calibr13	max flood velocity	no data	0.11	-0.07	no data	0.17	0.13	no data	0.13	0.12
	middle flood	-0.03	-0.06	-0.08	0.03	0.09	0.10	0.02	0.07	0.06
	1st phase ebb	no data	-0.03	-0.16	no data	0.13	0.19	no data	0.12	0.10
	2nd phase ebb	0.23	-0.06	-0.13*	0.25	0.16	0.14*	0.08	0.15	0.06*
DD3x3calibr14	max flood velocity	no data	0.06	-0.07	no data	0.14	0.15	no data	0.12	0.13
	middle flood	-0.04	-0.07	-0.06	0.04	0.11	0.10	0.02	0.08	0.07
	1st phase ebb	no data	-0.09	-0.21	no data	0.17	0.24	no data	0.14	0.11
	2nd phase ebb	0.22	-0.04	-0.12*	0.24	0.16	0.13*	0.10	0.15	0.05*
DD3x3calibr11 10min shift	max flood velocity	no data	0.08	0.03	no data	0.12	0.10	no data	0.08	0.09
	middle flood	0.07	0.01	0.04	0.09	0.07	0.07	0.05	0.07	0.05
	1st phase ebb	no data	-0.03	-0.06	no data	0.07	0.10	no data	0.07	0.08
	2nd phase ebb	0.21	0.03	-0.03	0.23	0.14	0.07	0.10	0.14	0.07

* limited number of points is available for the analysis

Table A-8. Total root mean squared errors for Ballooi – transverse profile

Model run	RMSE for Ballooi - transverse profile							
	max flood velocity	middle flood	1st phase ebb	2nd phase ebb	deep zone	undeep zone	littoral zone	total RMSE
DD3x3calibr	0.18	0.10	0.15	0.12	0.14	0.12	0.15	0.14
DD3x3calibr1	0.18	0.10	0.14	0.12	0.13	0.12	0.15	0.13
DD3x3calibr2	0.13	0.15	0.15	0.15	0.14	0.14	0.15	0.14
DD3x3calibr3	0.18	0.10	0.14	0.11	0.13	0.12	0.16	0.13
DD3x3calibr4	0.18	0.11	0.15	0.12	0.14	0.13	0.16	0.14
DD3x3calibr5	0.20	0.11	0.19	0.15	0.16	0.14	0.19	0.16
DD3x3calibr7	0.19	0.12	0.15	0.11	0.13	0.15	0.17	0.14
DD3x3calibr8	0.17	0.10	0.14	0.12	0.13	0.12	0.15	0.13
DD3x3calibr9	0.14	0.12	0.12	0.12	0.12	0.12	0.15	0.13
DD3x3calibr10	0.15	0.11	0.12	0.11	0.12	0.12	0.15	0.12
DD3x3calibr11	0.16	0.11	0.12	0.10	0.12	0.12	0.14	0.12
DD3x3calibr12	0.18	0.09	0.14	0.12	0.13	0.11	0.15	0.13
DD3x3calibr13	0.18	0.11	0.15	0.13	0.14	0.13	0.16	0.14
DD3x3calibr14	0.17	0.13	0.14	0.12	0.12	0.14	0.22	0.14
DD3x3calibr11 10min shift	0.12	0.10	0.13	0.12	0.11	0.12	0.10	0.11

Table A-9. Total root mean squared errors for Notelaer – longitudinal profile

Model run	RMSE for Notelaer - longitudinal profile							
	max flood velocity	middle flood	1st phase ebb	2nd phase ebb	deep zone	undeep zone	littoral zone	total RMSE
DD3x3calibr	0.15	0.08	0.14	0.15	0.14	0.13	0.12	0.13
DD3x3calibr1	0.16	0.07	0.11	0.14	0.13	0.12	0.10	0.12
DD3x3calibr2	0.17	0.09	0.13	0.14	0.12	0.13	0.13	0.13
DD3x3calibr3	0.17	0.07	0.10	0.14	0.13	0.12	0.09	0.11
DD3x3calibr4	0.17	0.07	0.10	0.13	0.13	0.12	0.09	0.11
DD3x3calibr5	0.21	0.08	0.08	0.17	0.14	0.15	0.11	0.14
DD3x3calibr7	0.21	0.08	0.10	0.13	0.12	0.14	0.10	0.13
DD3x3calibr8	0.15	0.08	0.14	0.15	0.14	0.13	0.12	0.12
DD3x3calibr9	0.15	0.08	0.15	0.14	0.13	0.12	0.13	0.12
DD3x3calibr10	0.15	0.08	0.14	0.14	0.13	0.12	0.12	0.12
DD3x3calibr11	0.17	0.08	0.11	0.14	0.13	0.12	0.10	0.12
DD3x3calibr12	0.17	0.08	0.13	0.16	0.15	0.13	0.12	0.13
DD3x3calibr13	0.15	0.09	0.17	0.16	0.14	0.13	0.15	0.14
DD3x3calibr14	0.14	0.10	0.22	0.16	0.14	0.13	0.18	0.15
DD3x3calibr11 10min shift	0.11	0.07	0.10	0.14	0.15	0.10	0.09	0.10

Table A-10. Total root mean squared errors for transverse and longitudinal profiles together

Model run	**total RMSE (m/s)**
DD3x3calibr11 10min shift	0.105
DD3x3calibr11	0.119
DD3x3calibr3	0.123
DD3x3calibr1	0.123
DD3x3calibr10	0.123
DD3x3calibr9	0.125
DD3x3calibr4	0.126
DD3x3calibr8	0.126
DD3x3calibr12	0.129
DD3x3calibr	0.130
DD3x3calibr7	0.134
DD3x3calibr2	0.134
DD3x3calibr13	0.140
DD3x3calibr14	0.147
DD3x3calibr5	0.147

Table A-11. Mean bias, RMSE and standard deviation for model validation

Measurements	Time period	Model run for validation								
		Mean difference (model - measurement) (m/s)			RMSE (m/s)			Standard deviation (m/s)		
		Deep	Undeep	Littoral	Deep	Undeep	Littoral	Deep	Undeep	Littoral
ADCP Notelaer - transverse profile (fit high waters for flood)	max flood	0.13	-0.02	-0.05	0.16	0.09	0.09	0.09	0.09	0.07
	middle flood	0.00	-0.09	-0.10	0.11	0.15	0.15	0.11	0.12	0.12
ADCP Notelaer - transverse profile (fit high waters for ebb)	1st phase ebb	0.03	-0.03	-0.17*	0.09	0.12	0.20*	0.08	0.12	0.10*
	2nd phase ebb	-0.02	-0.09	no data	0.09	0.13	no data	0.09	0.10	no data
GPS float measurements	max flood	0.11	0.07	-0.06	0.13	0.13	0.13	0.07	0.12	0.12
	middle flood	-0.02	-0.04	-0.07	0.09	0.09	0.12	0.09	0.08	0.09
	1st phase ebb	-0.13	-0.02	-0.08	0.13	0.11	0.14	0.02	0.11	0.12
	2nd phase ebb	-0.20	-0.22	-0.12	0.21	0.27	0.20	0.07	0.15	0.16

* limited number of points is available for the analysis

Table A-12. Total root mean squared errors for model validation

Measurements	Time period	RMSE for model validation (m/s)				Total RMSE (m/s)
		different periods	different depth zones			
			Deep	Undeep	Littoral	
ADCP Notelaer - transverse profile (fit high waters for flood)	max flood	0.13	0.11	0.13	0.15	0.12
	middle flood	0.13				
ADCP Notelaer - transverse profile (fit high waters for ebb)	1st phase ebb	0.11				
	2nd phase ebb	0.11				
GPS float measurements	max flood	0.13	0.16	0.18	0.15	0.16
	middle flood	0.10				
	1st phase ebb	0.13				
	2nd phase ebb	0.23				

Figures

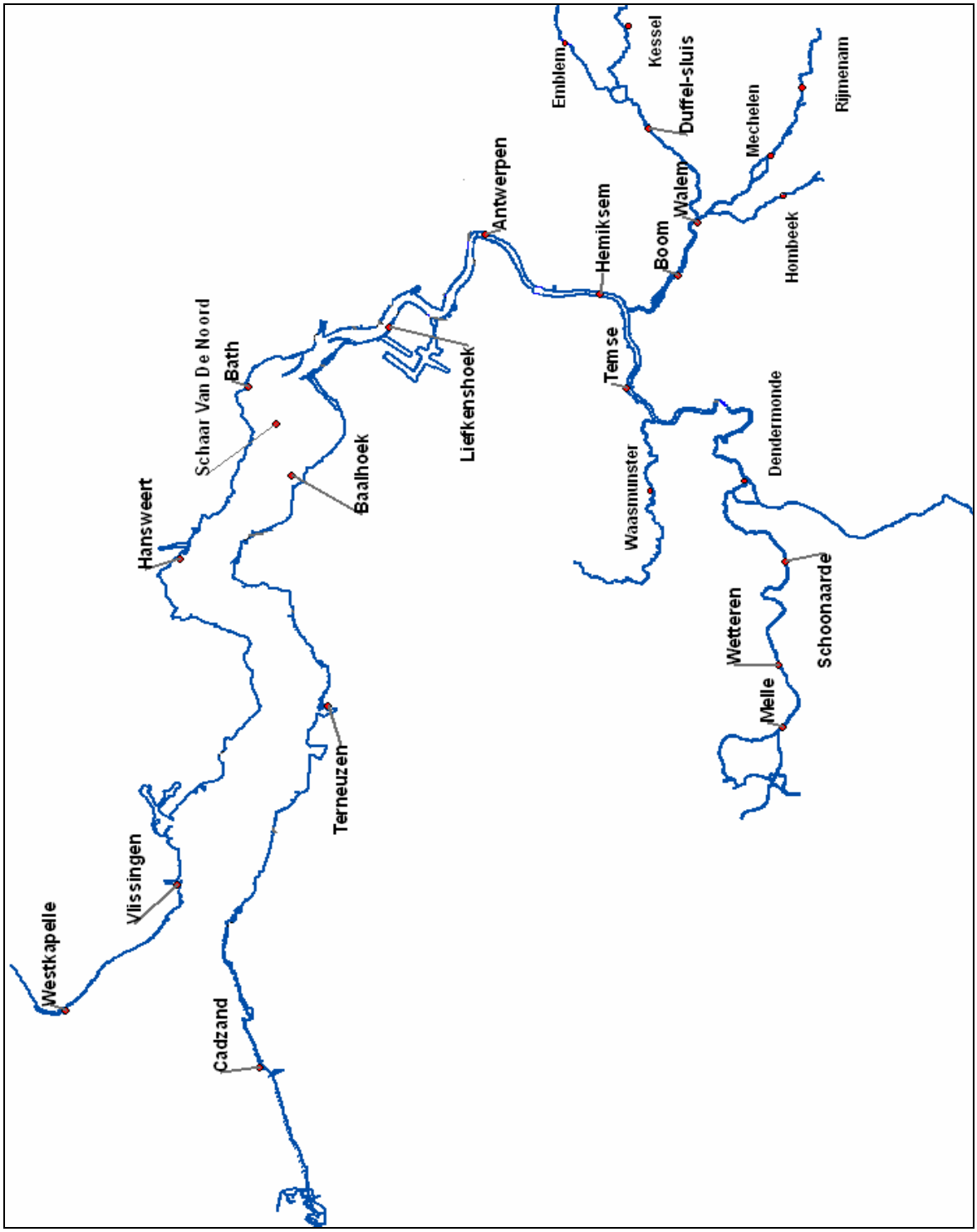

Figure 1 - The Scheldt estuary with different water level stations

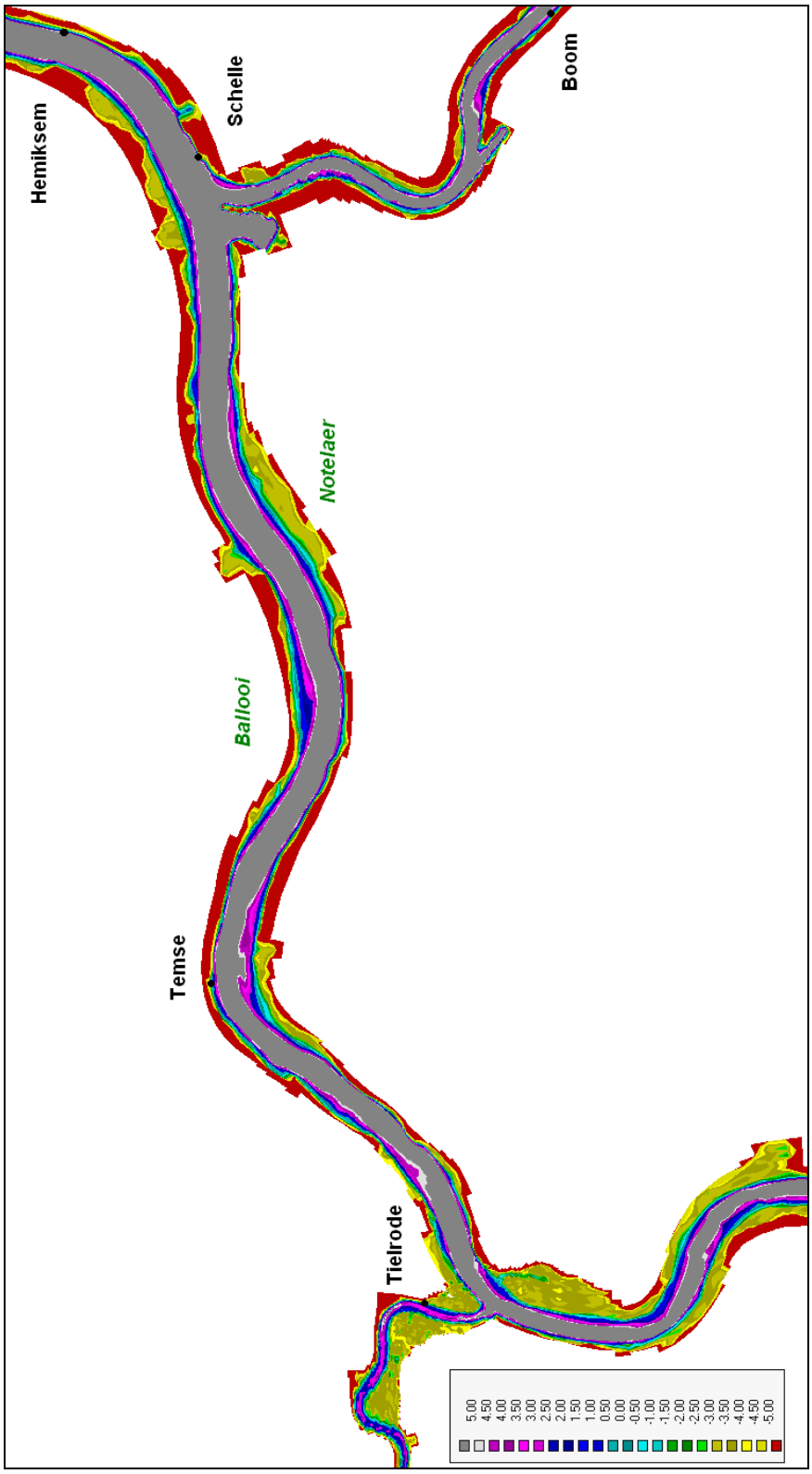

Figure 2 - Location of the areas Ballooi and Notelaer (bathymetry m NAP)

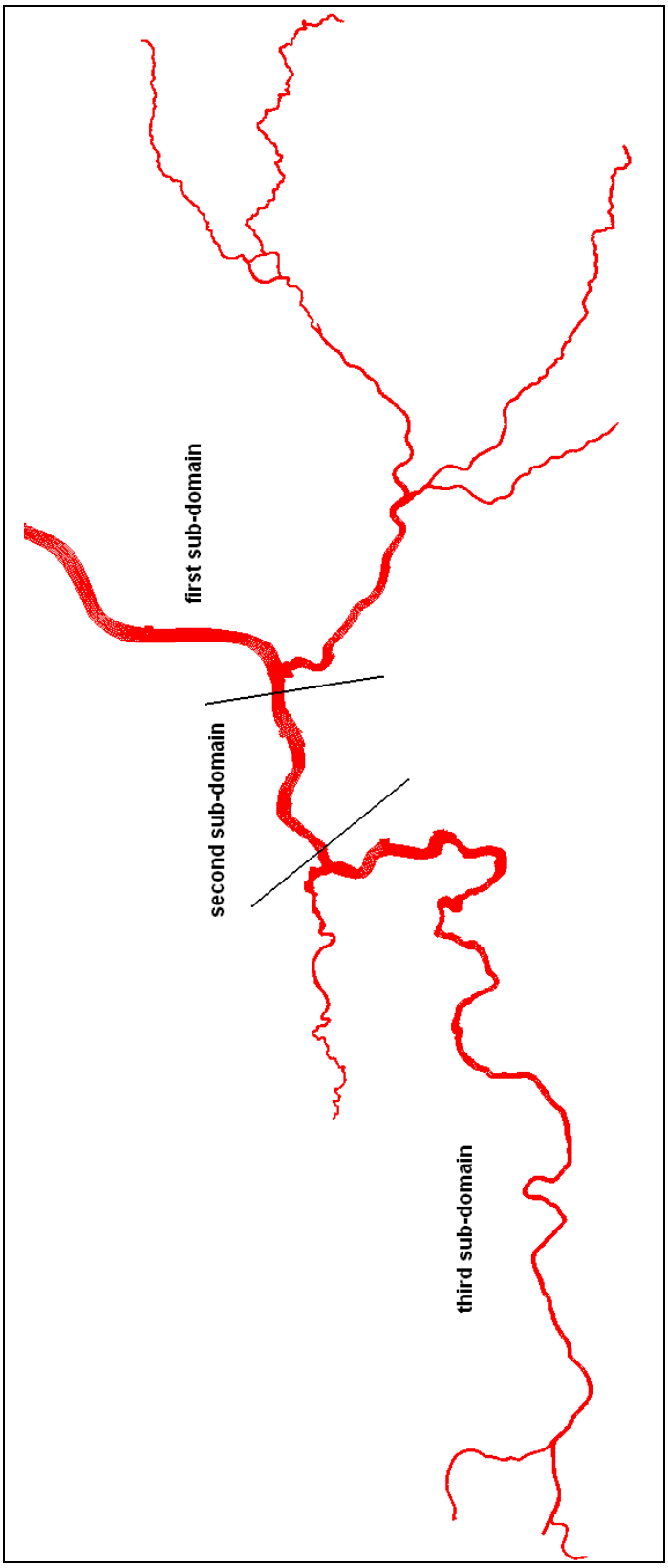

Figure 3 – Model grid with domain decomposition

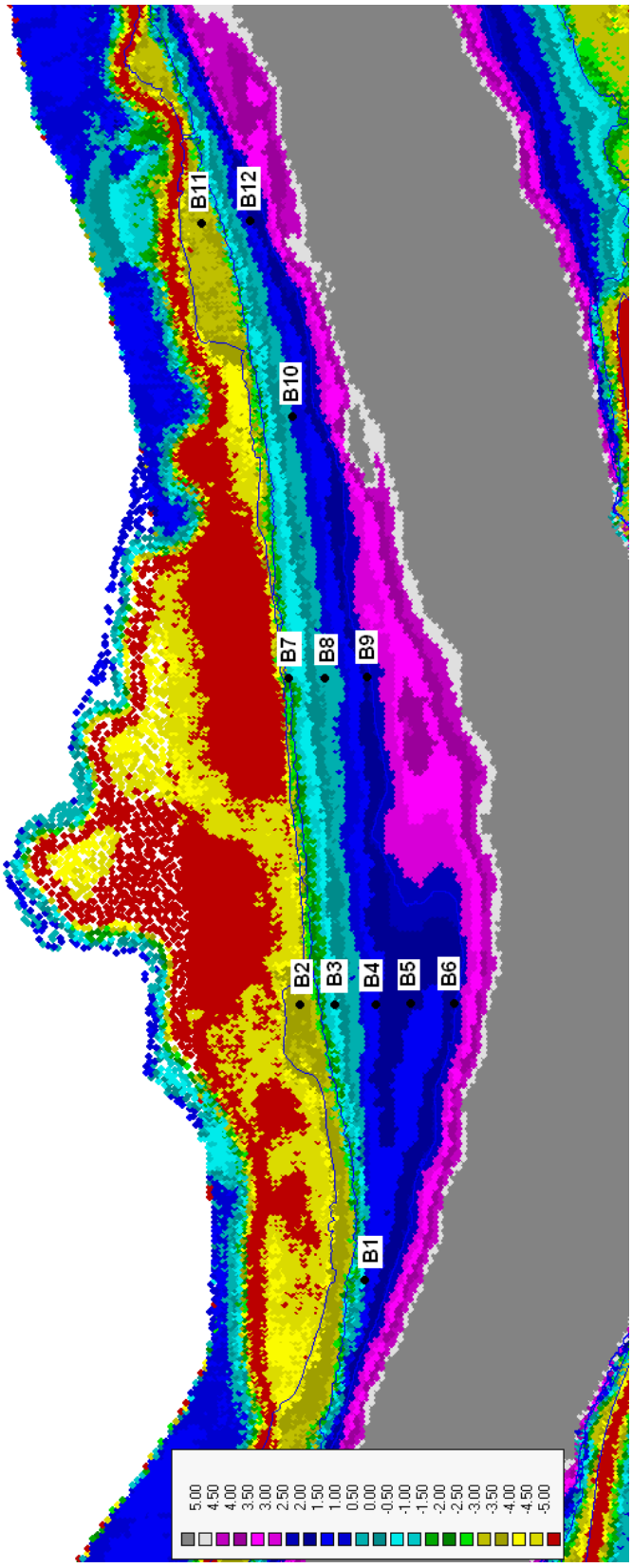

Figure 4 - The Ballooi area with the monitoring stations (m NAP)

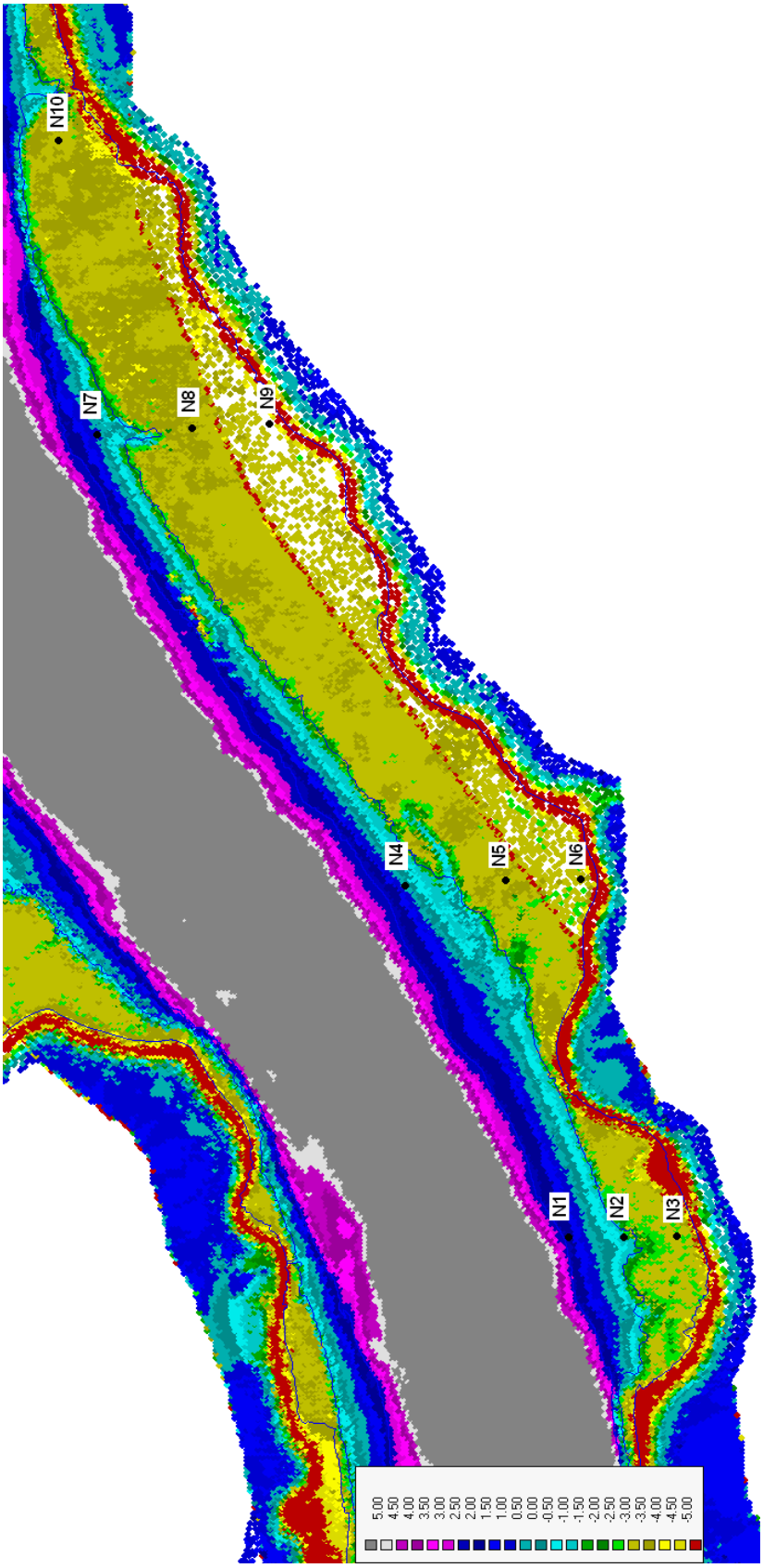

Figure 5 - The Notelaer area with the monitoring stations (m NAP)

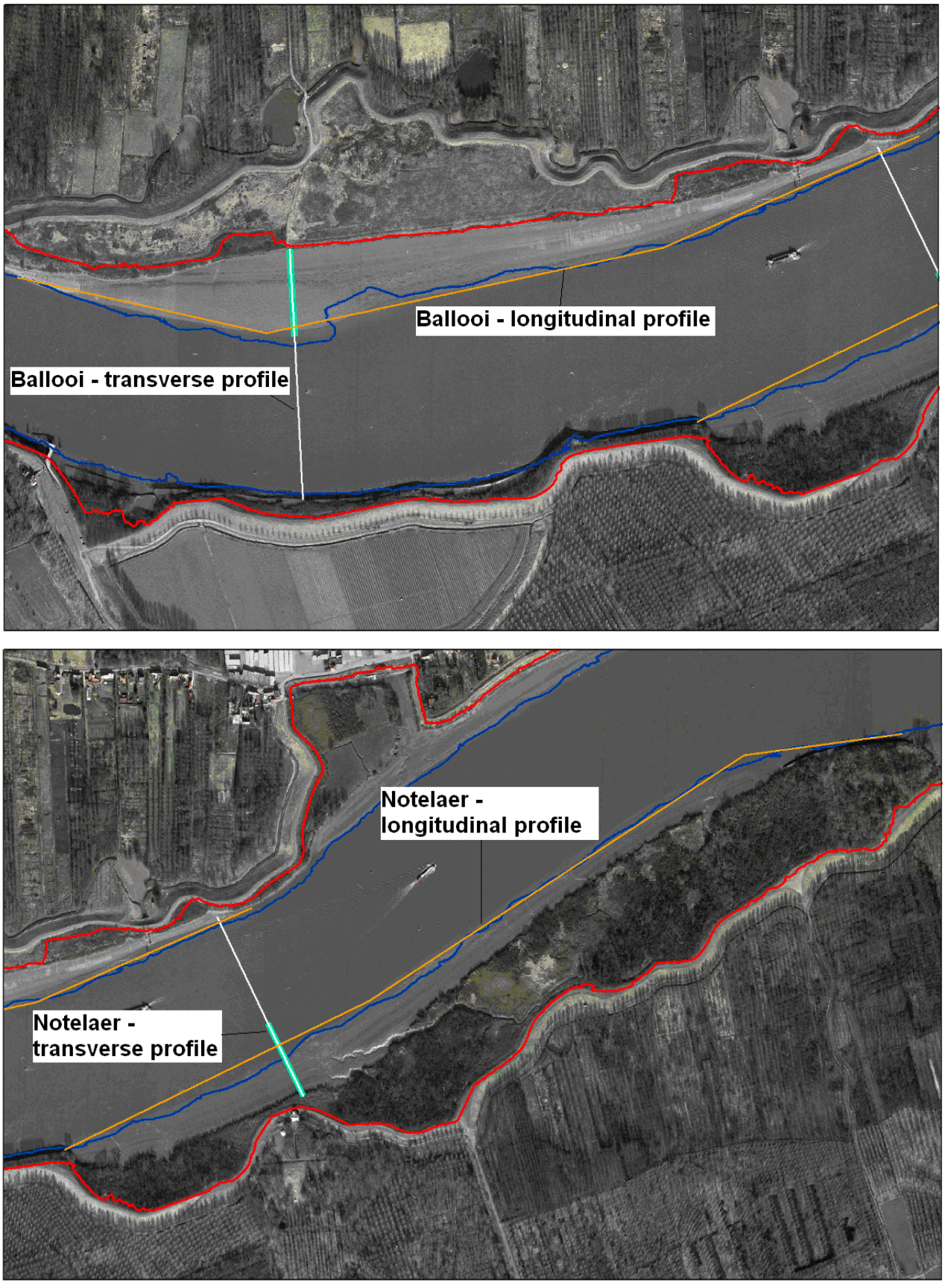

Figure 6 - Location of the ADCP measurements profiles (transverse profile: white, longitudinal profile: yellow,

slik – undeep water border: blue, schor – dry area border – red, sample points INBO - green)

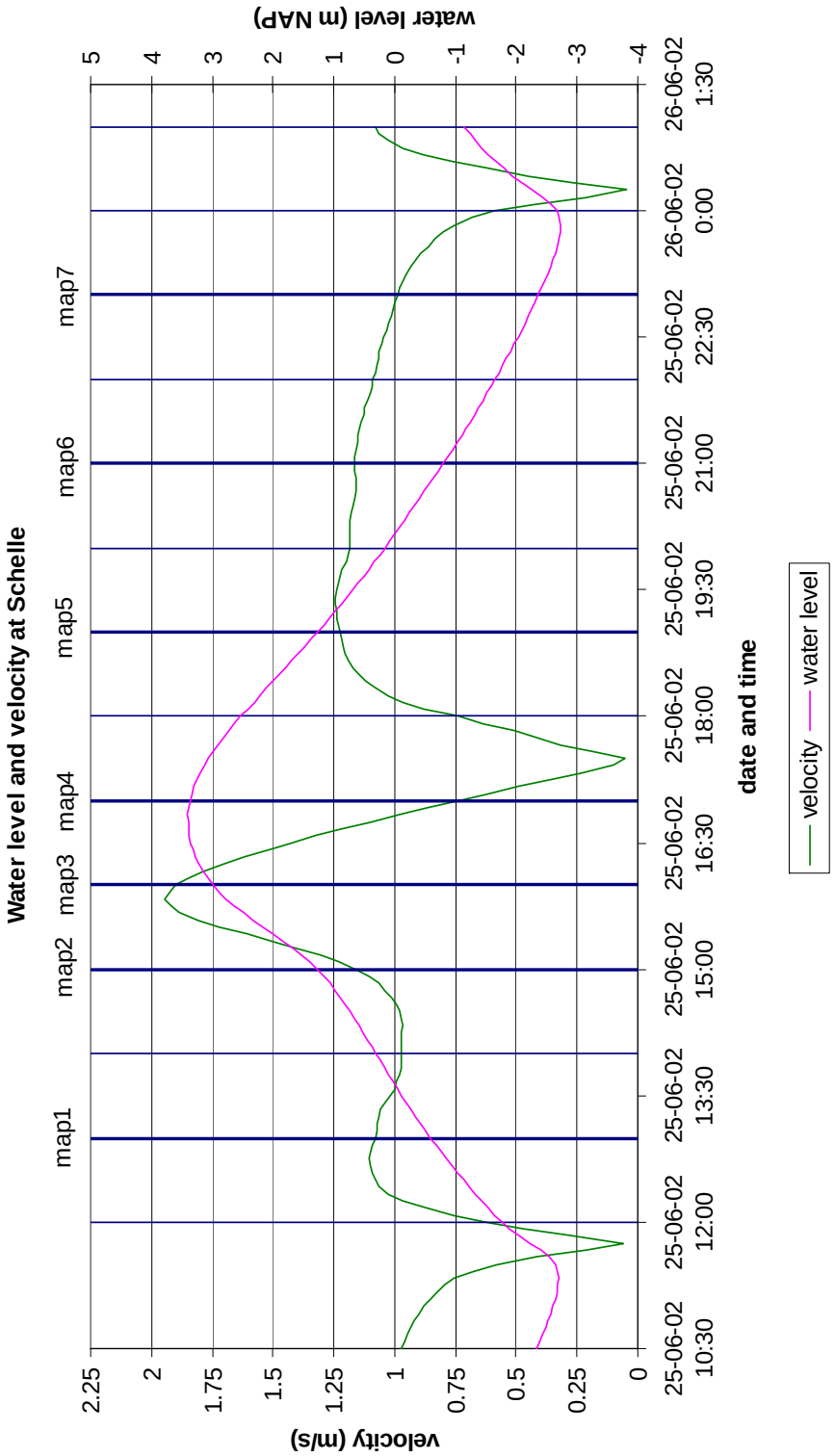

Figure 7 - Water level and velocity magnitude at Schelle during the period of the sensitivity analysis

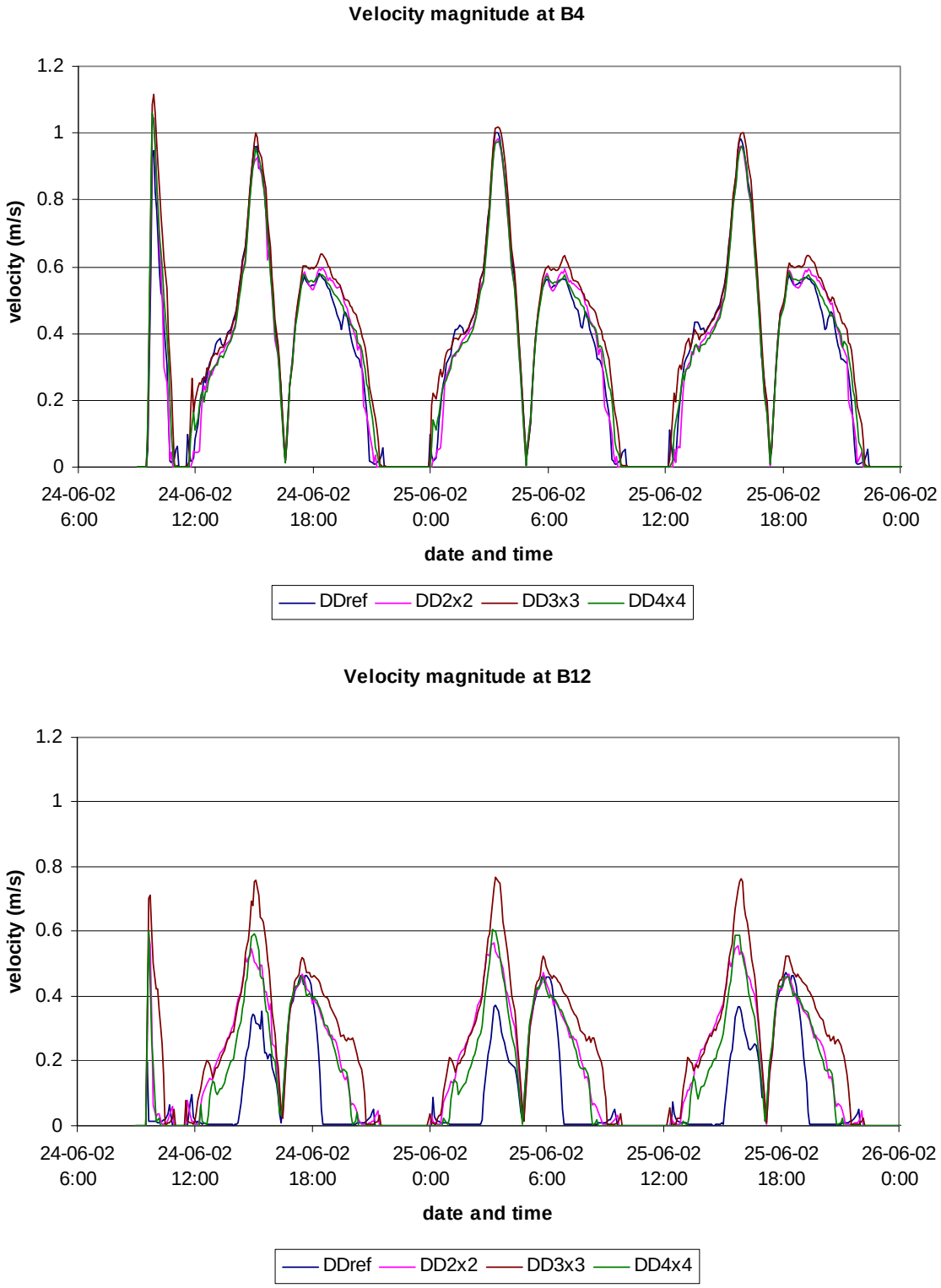

Figure 8 - Velocity in the observation points B4 and B12 for the model runs with different grid resolution

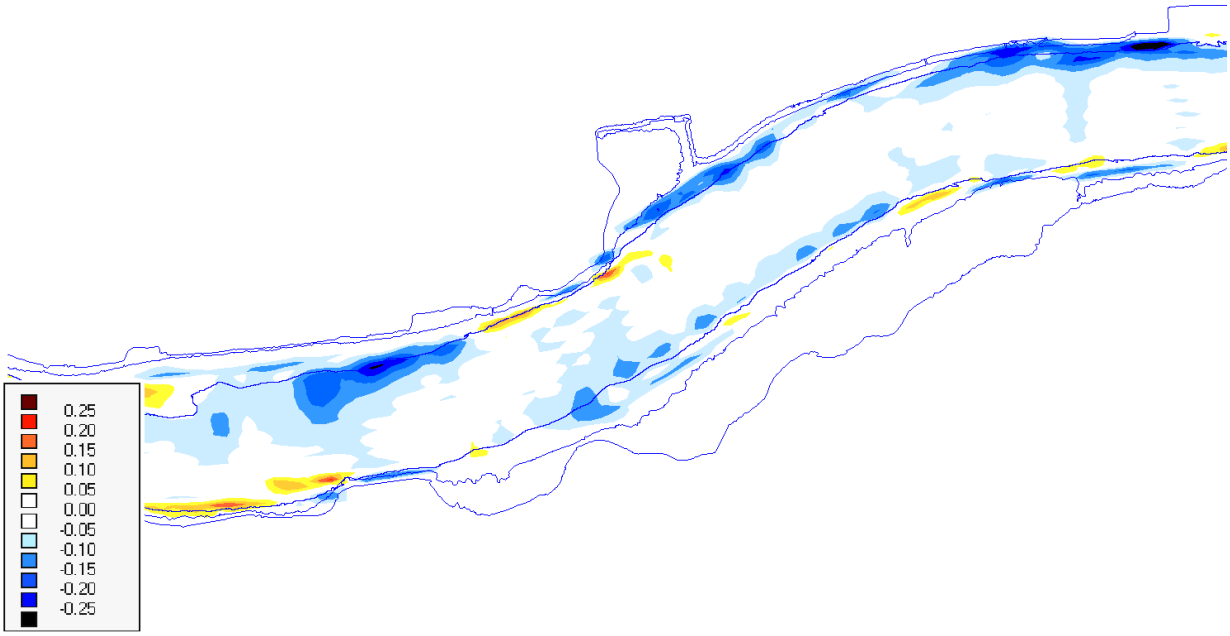

Figure 9 - Map 1 of differences in velocity (run DD4x4 minus run DDref)

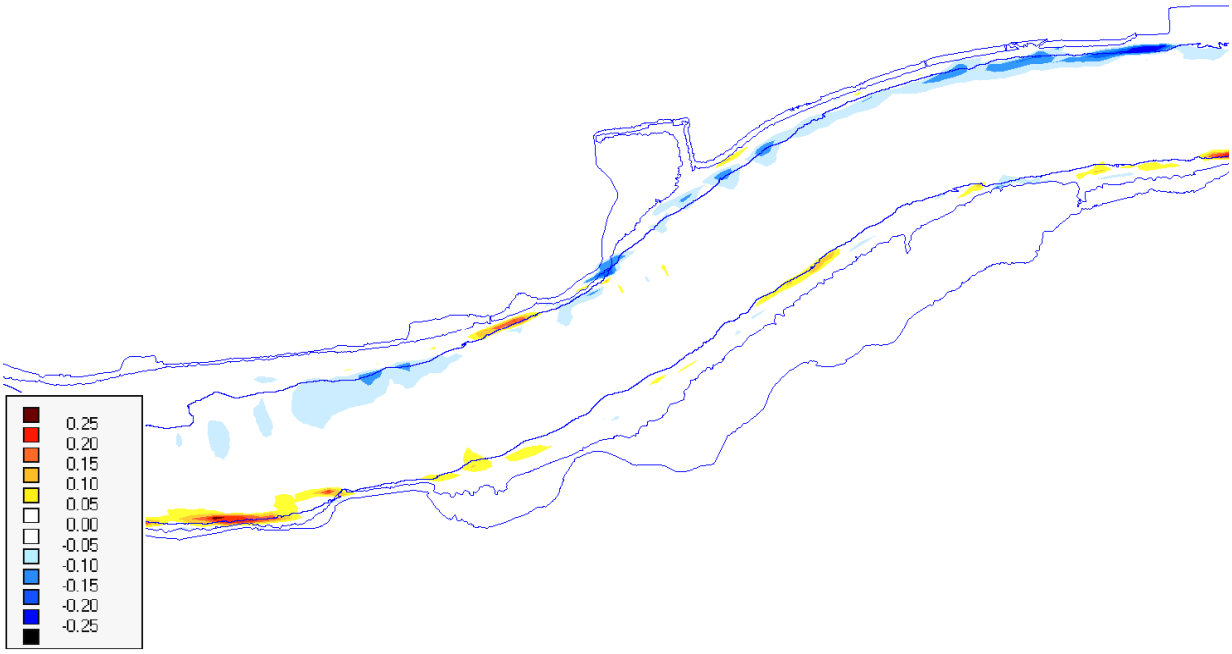

Figure 10 - Map 1 of differences in velocity (run DD4x4 minus run DD2x2)

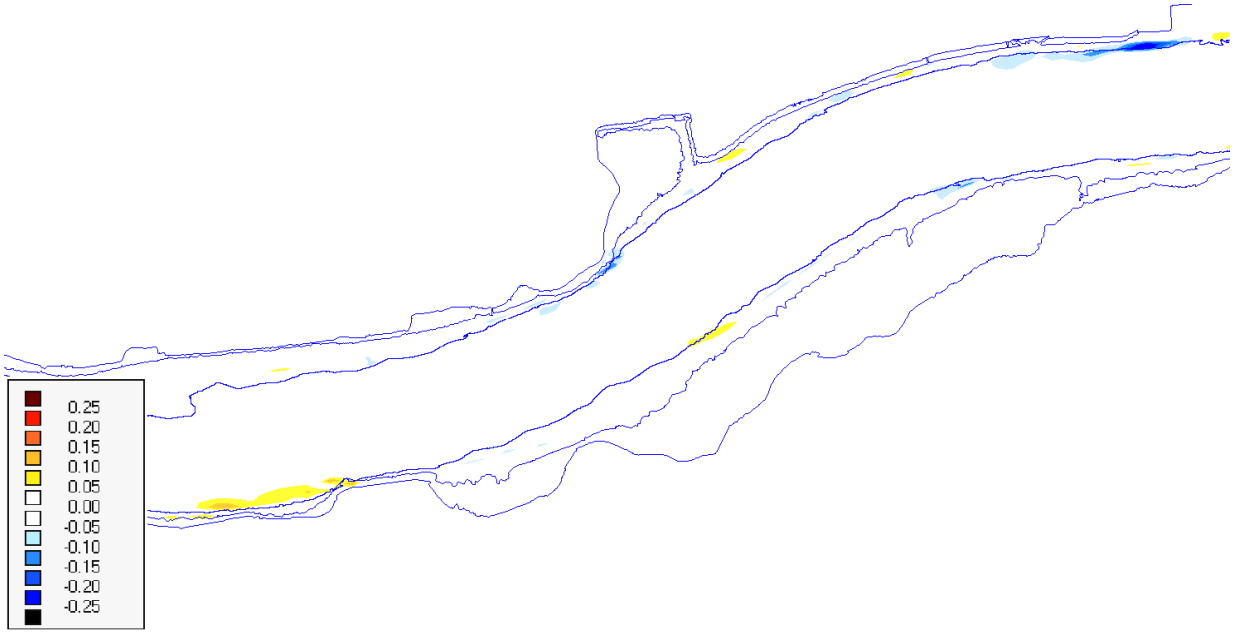

Figure 11 - Map 1 of differences in velocity (run DD4x4 minus run DD3x3)

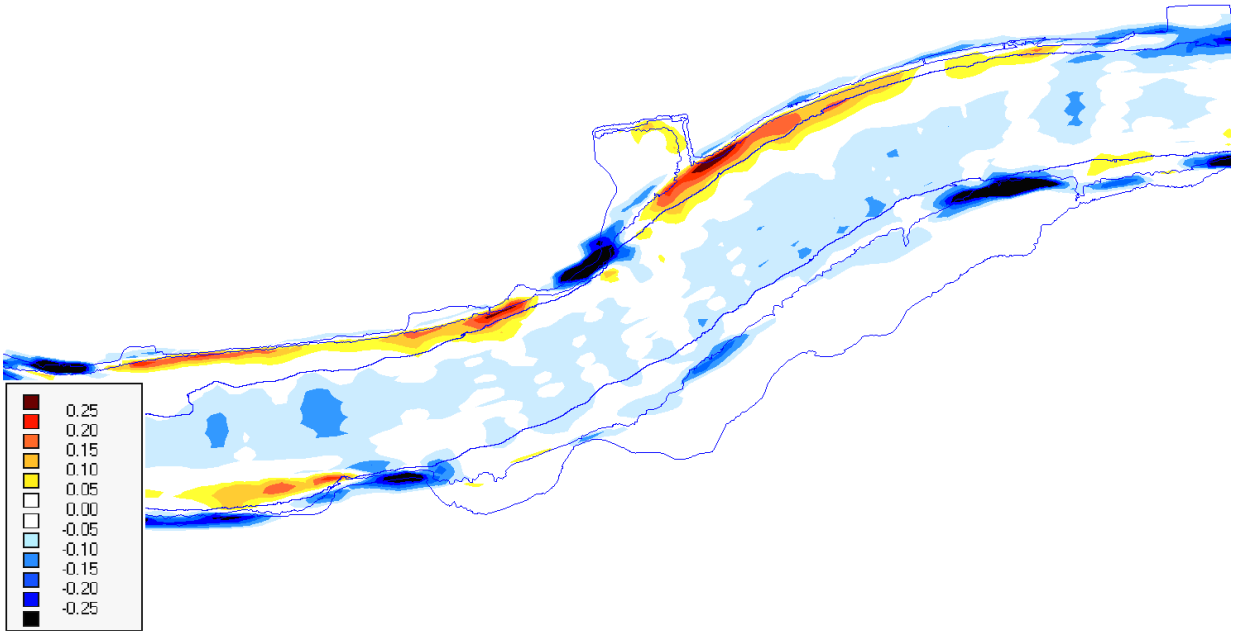

Figure 12 - Map 3 of differences in velocity (run DD4x4 minus run DDref)

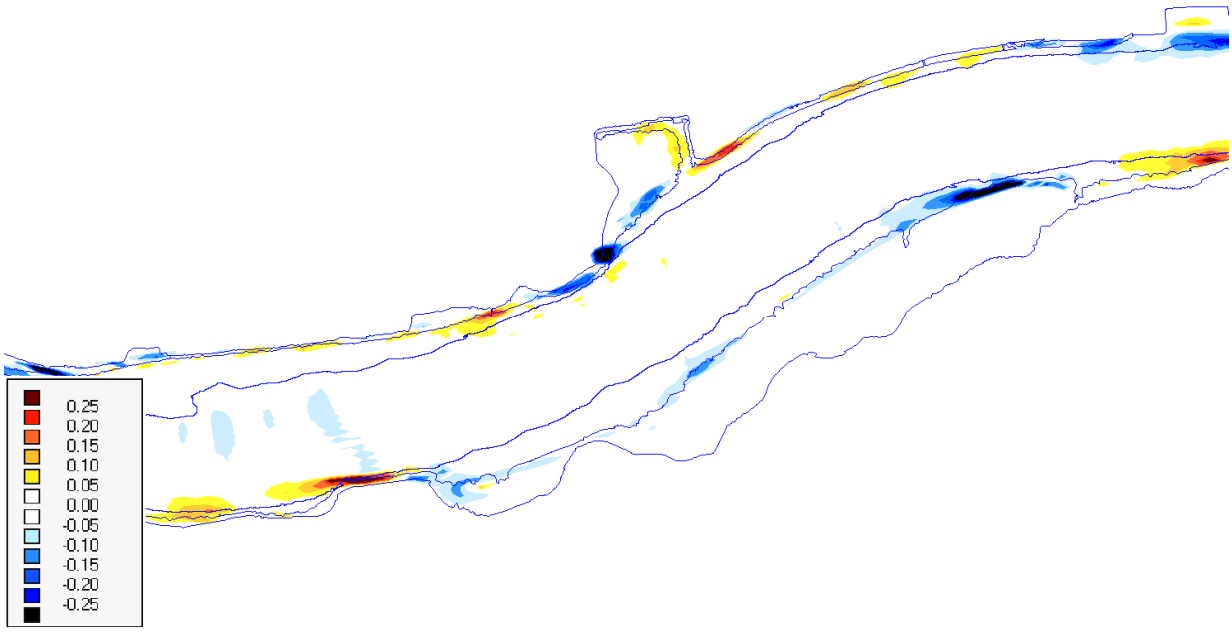

Figure 13 - Map 3 of differences in velocity (run DD4x4 minus run DD2x2)

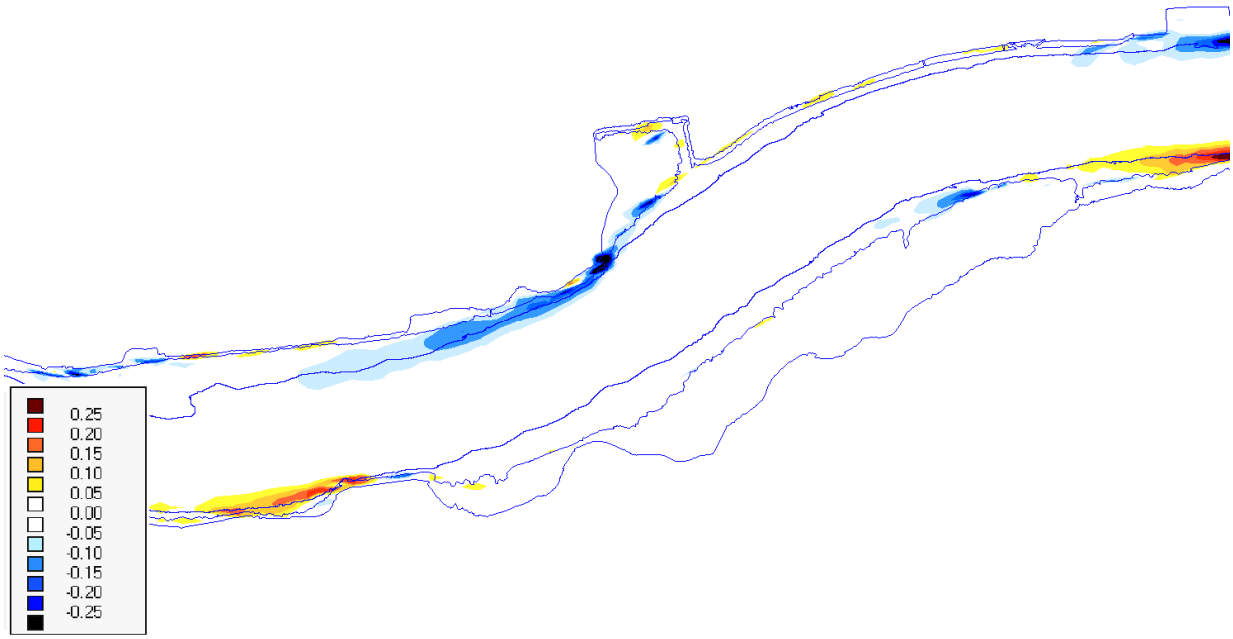

Figure 14 - Map 3 of differences in velocity (run DD4x4 minus run DD3x3)

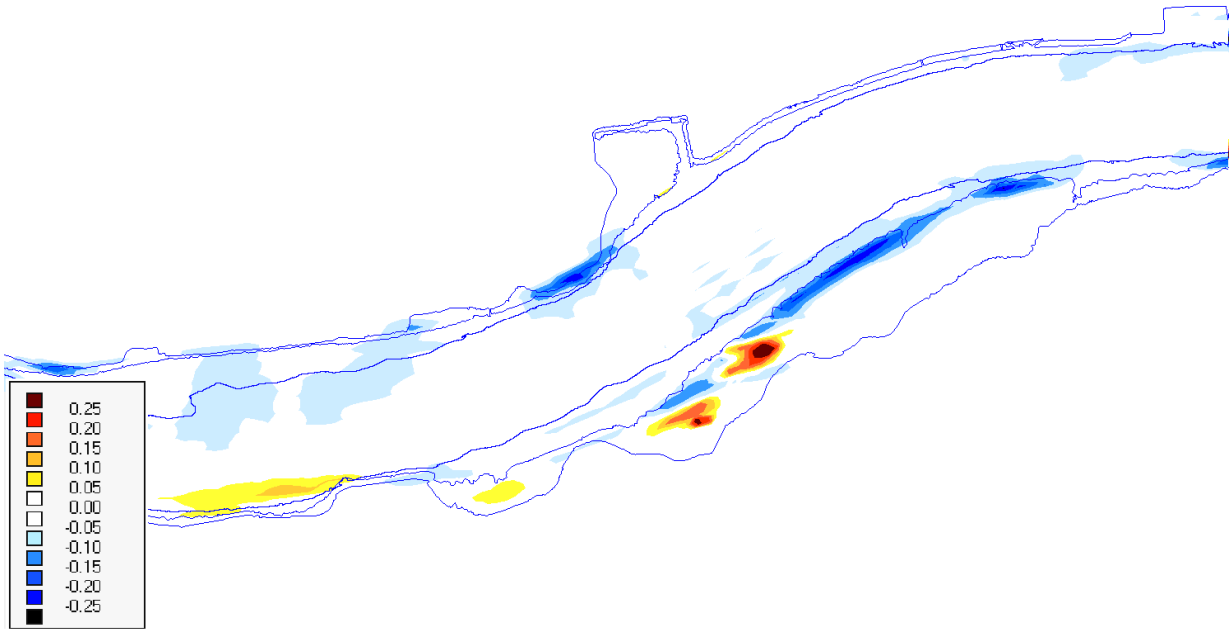

Figure 15 - Map 4 of differences in velocity (run DD4x4 minus run DDref)

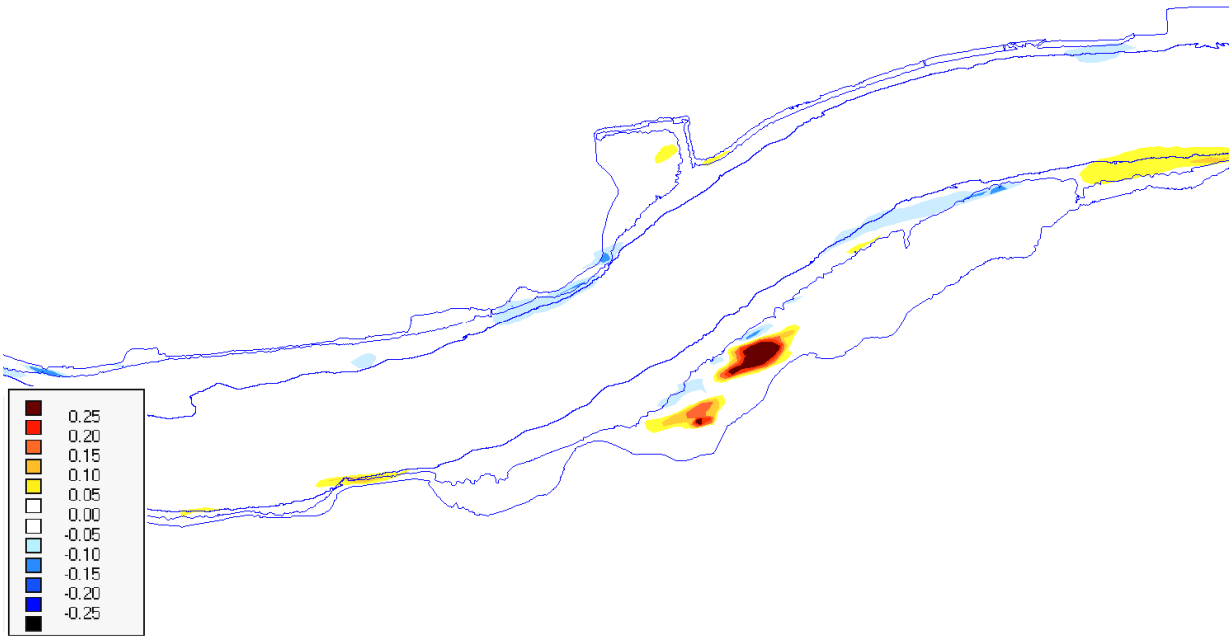

Figure 16 - Map 4 of differences in velocity (run DD4x4 minus run DD2x2)

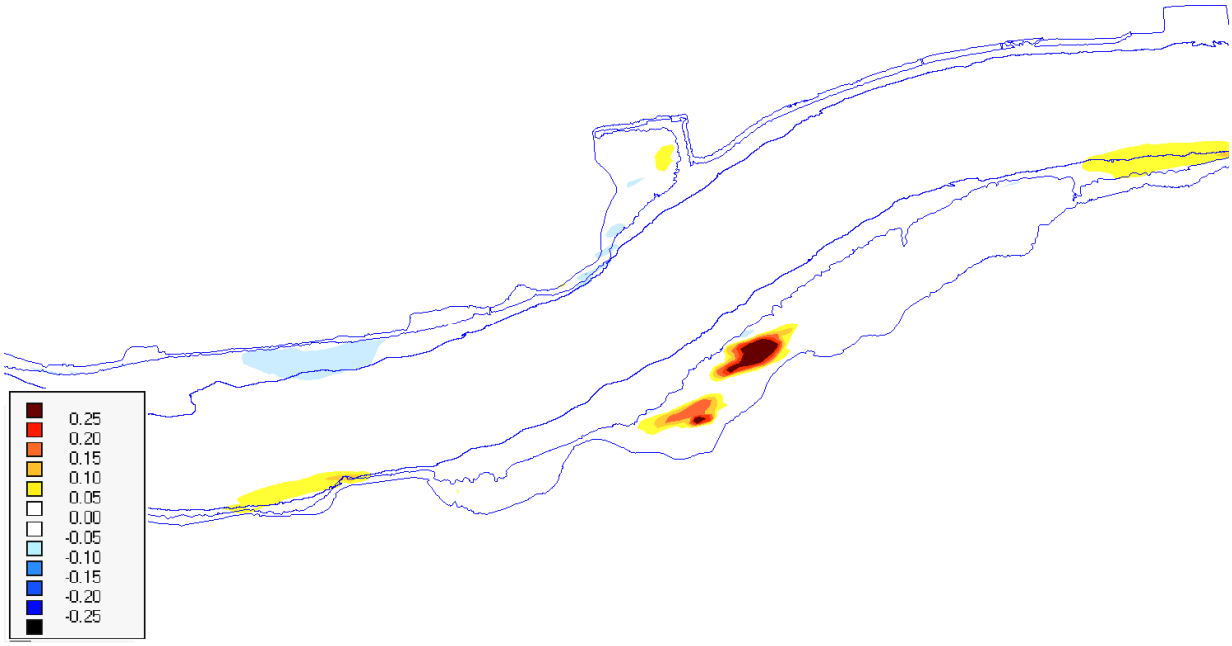

Figure 17 - Map 4 of differences in velocity (run DD4x4 minus run DD3x3)

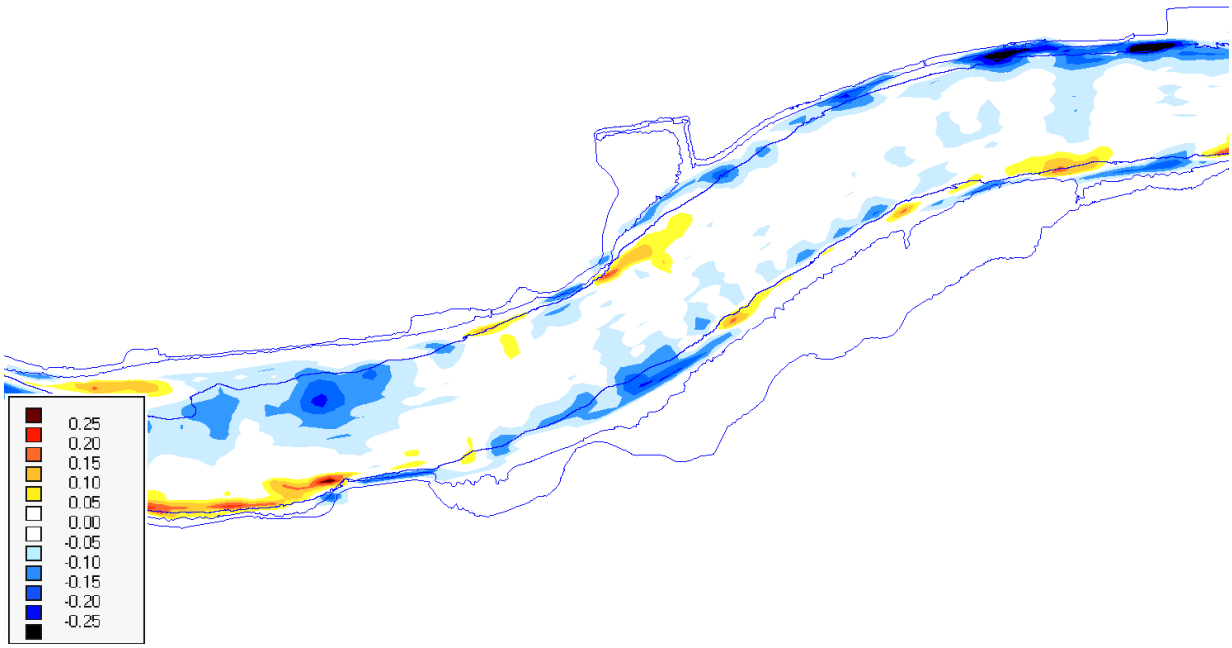

Figure 18 - Map 6 of differences in velocity (run DD4x4 minus run DDref)

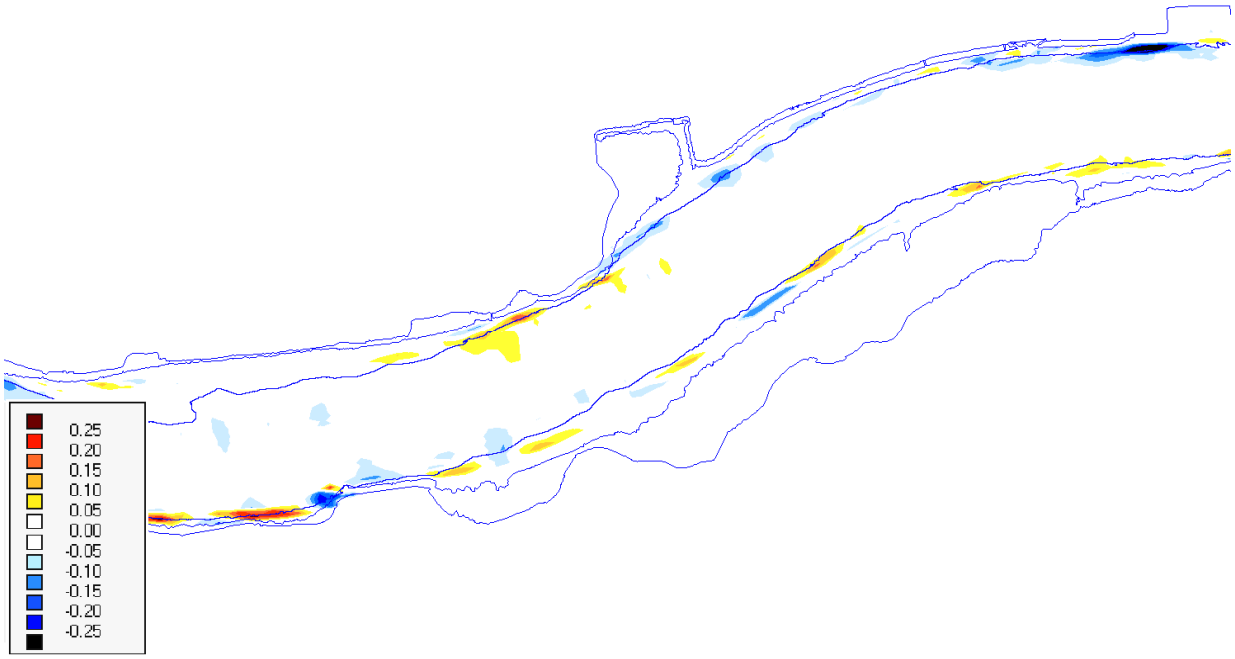

Figure 19 - Map 6 of differences in velocity (run DD4x4 minus run DD2x2)

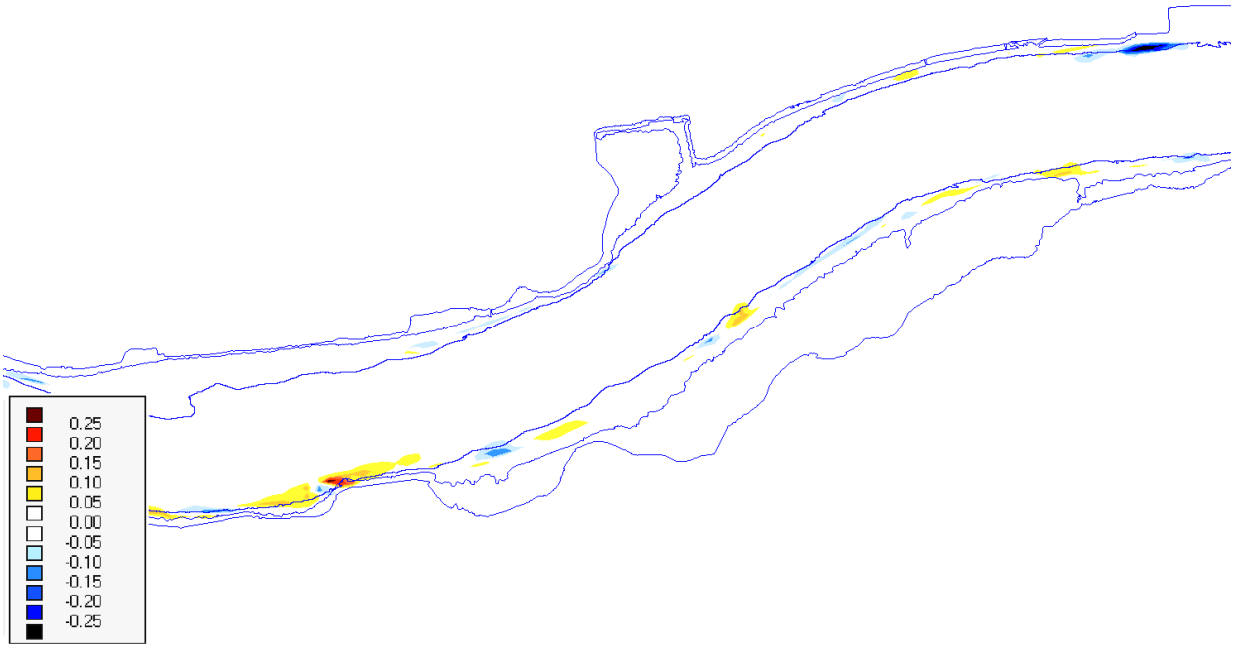

Figure 20 - Map 6 of differences in velocity (run DD4x4 minus run DD3x3)

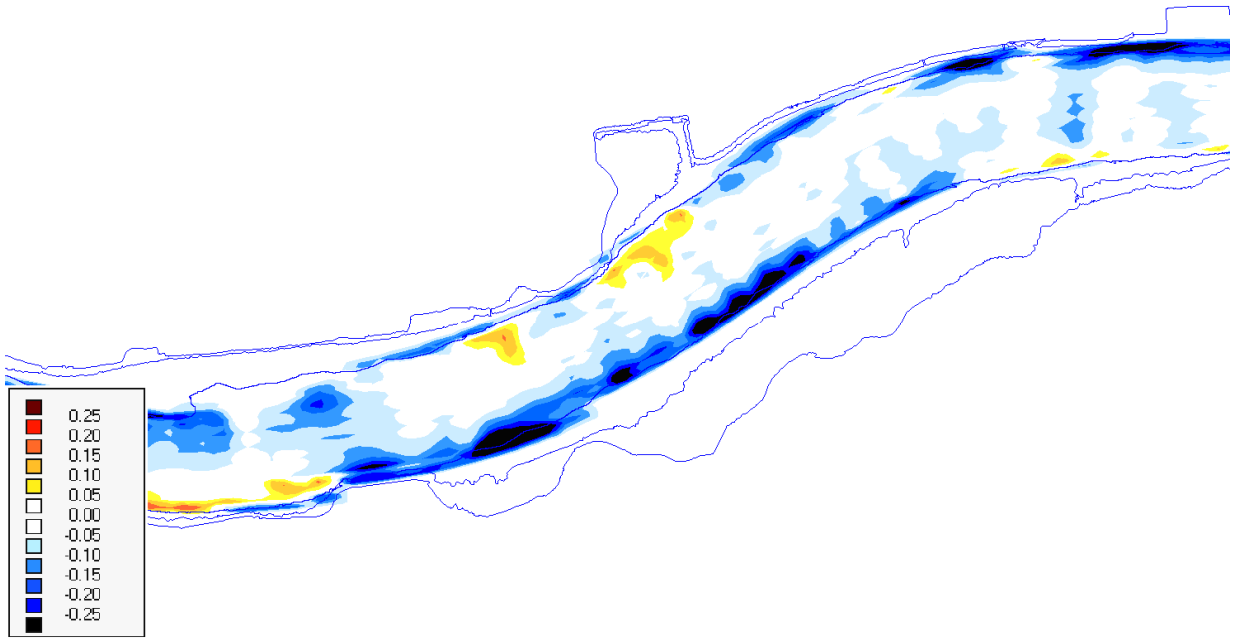

Figure 21 - Map 7 of differences in velocity (run DD4x4 minus run DDref)

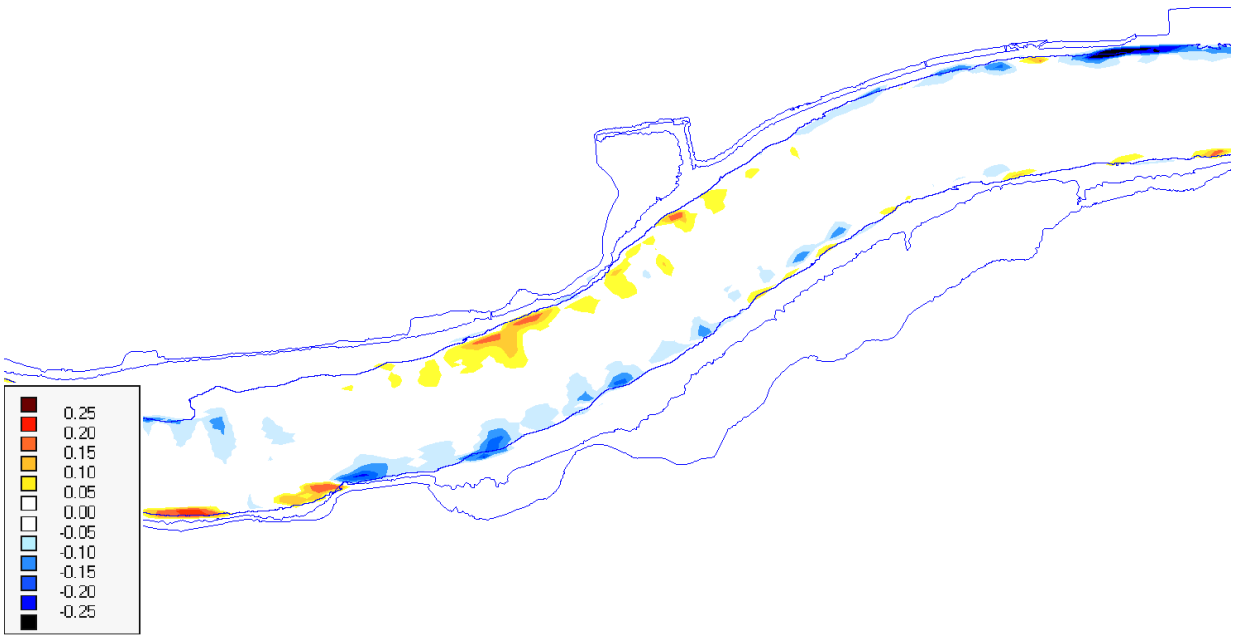

Figure 22 - Map 7 of differences in velocity (run DD4x4 minus run DD2x2)

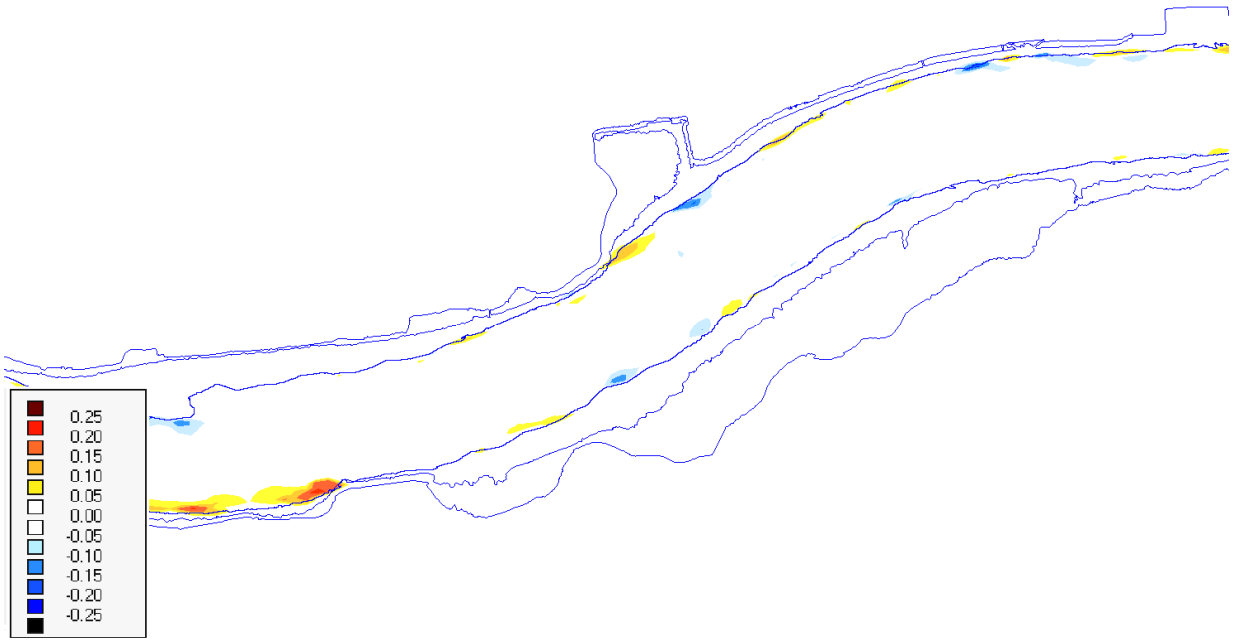

Figure 23 - Map 7 of differences in velocity (run DD4x4 minus run DD3x3)

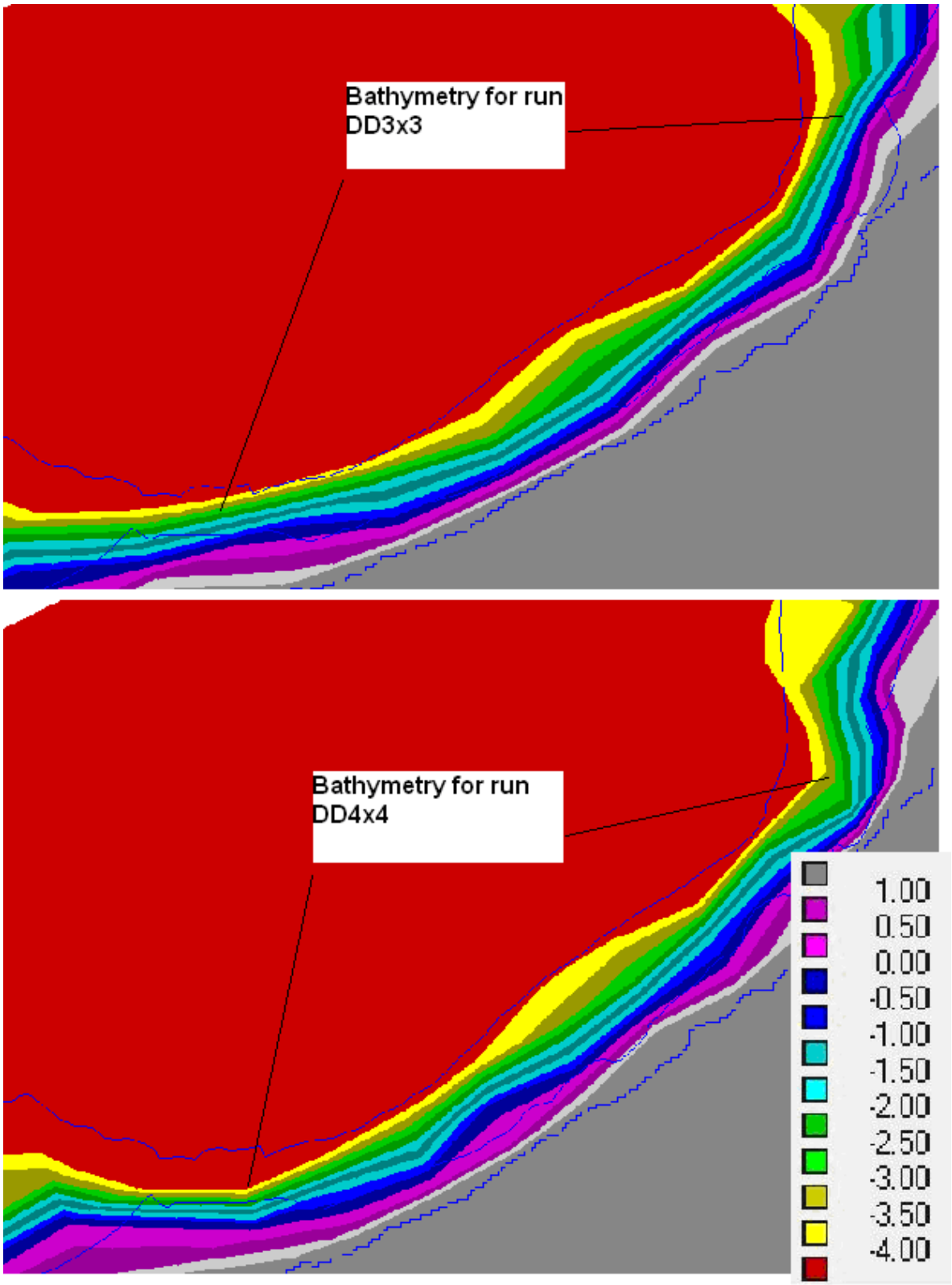

Figure 24 - Bathymetry of the eastern part of the Ballooi area for runs DD3x3 and DD4x4 (m NAP)

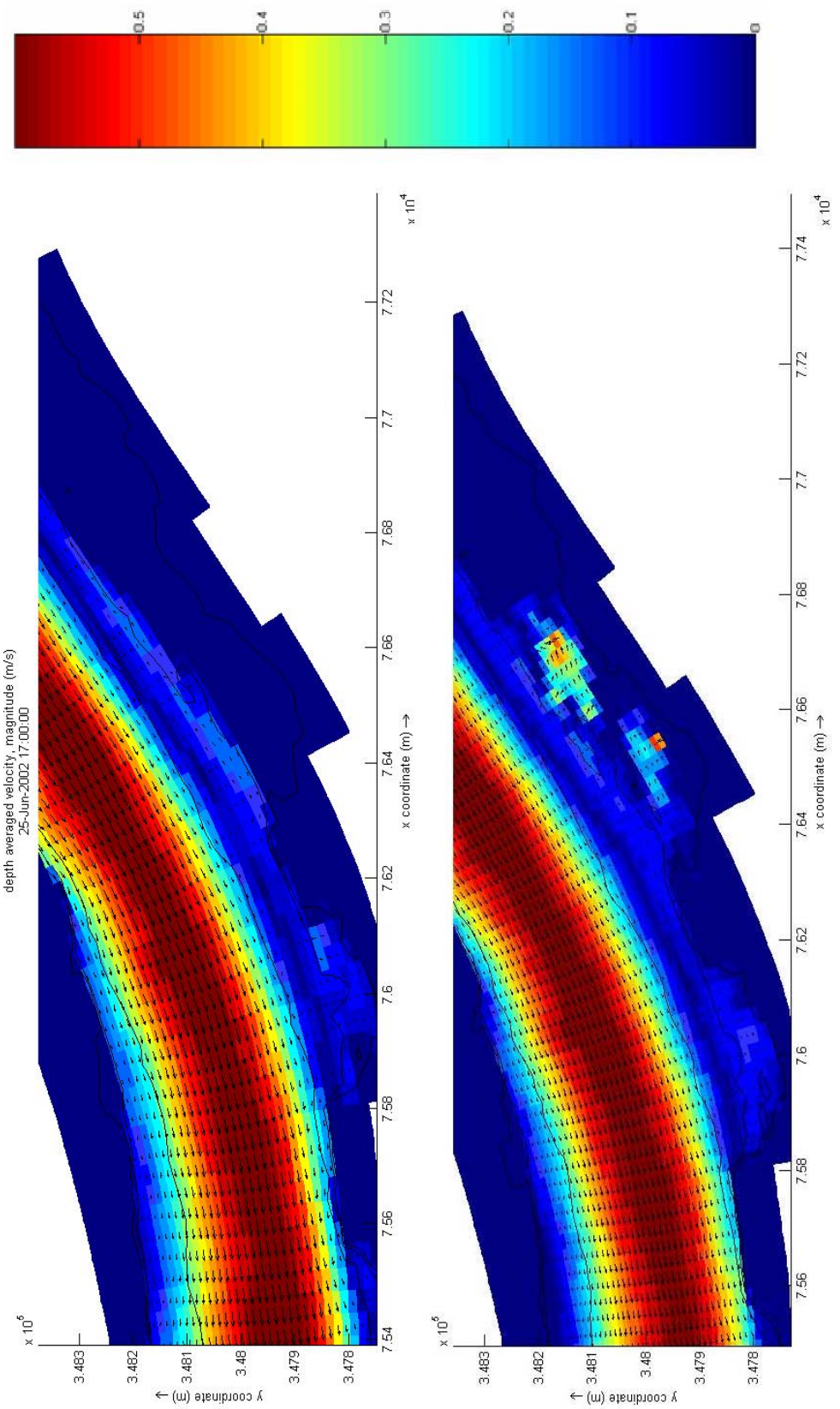

Figure 25 - Velocity map 4 for model runs DD3x3 (above) and DD4x4 (below) (m/s)

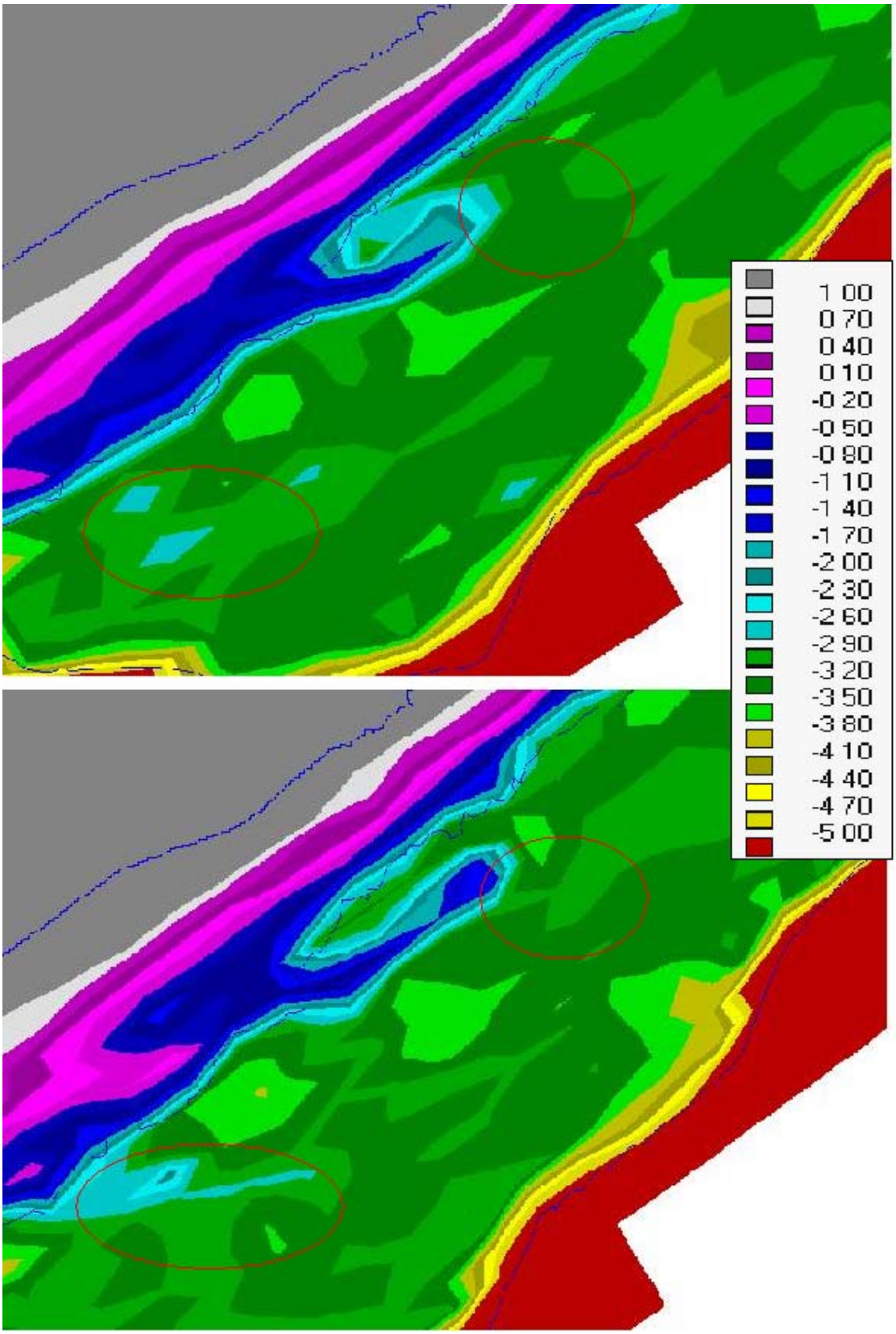

Figure 26 - Bathymetry of the Notelaer area for the grid resolution 3x3 (above) and 4x4 (below) (m NAP) (red circles: the differences in bathymetry resulting in velocity differences on map4)

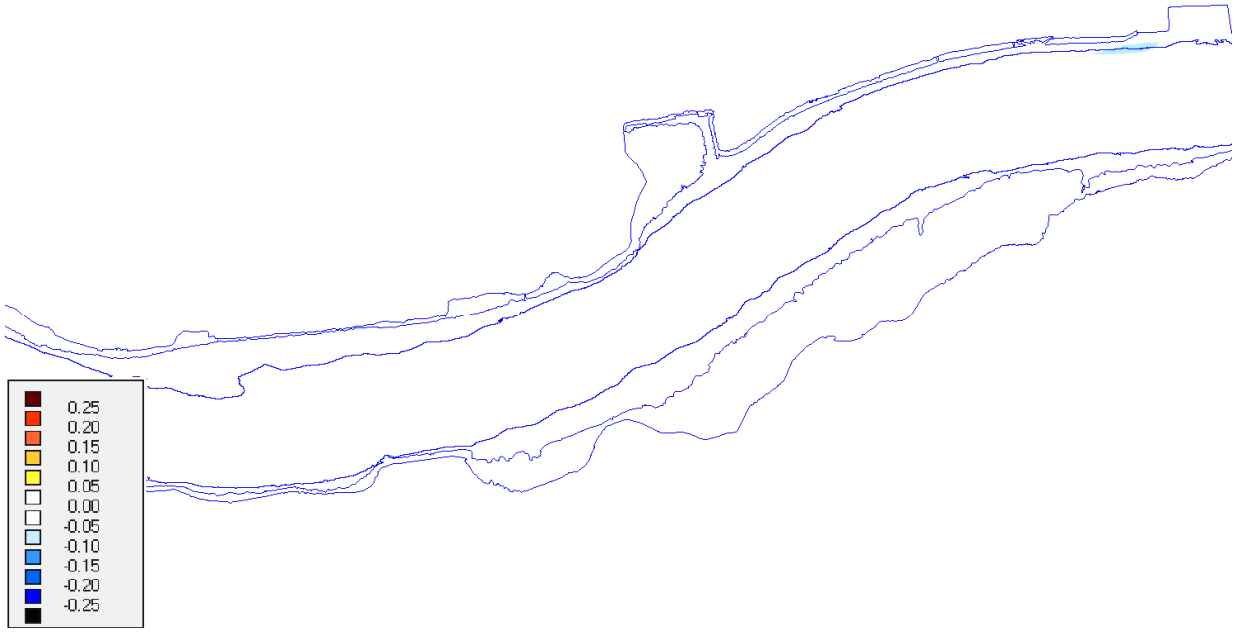

Figure 27 - Map 1 of differences in velocity (run DD3x3 rgh1 minus run DD3x3)

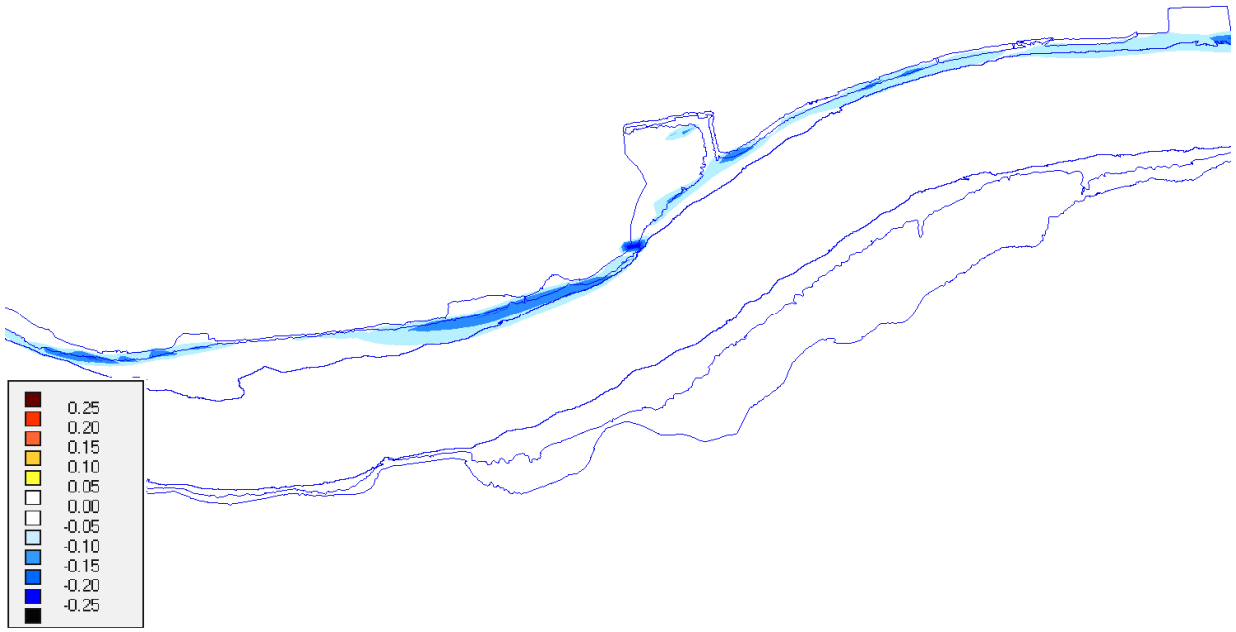

Figure 28 - Map 3 of differences in velocity (run DD3x3 rgh1 minus run DD3x3)

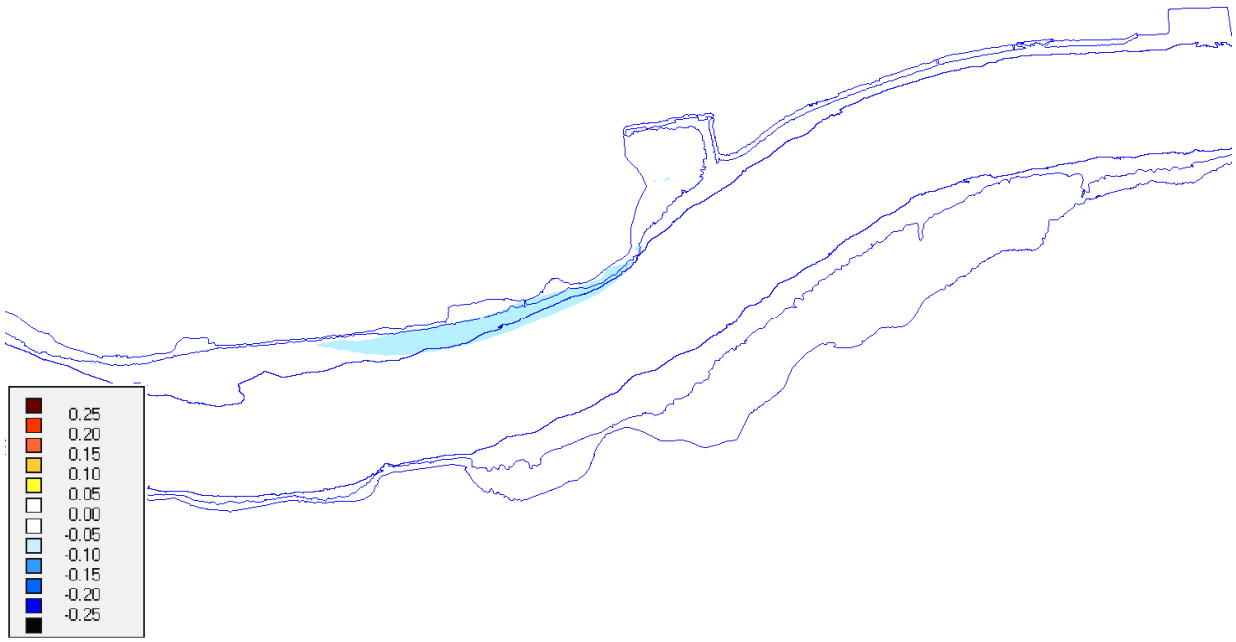

Figure 29 - Map 4 of differences in velocity (run DD3x3 rgh1 minus run DD3x3)

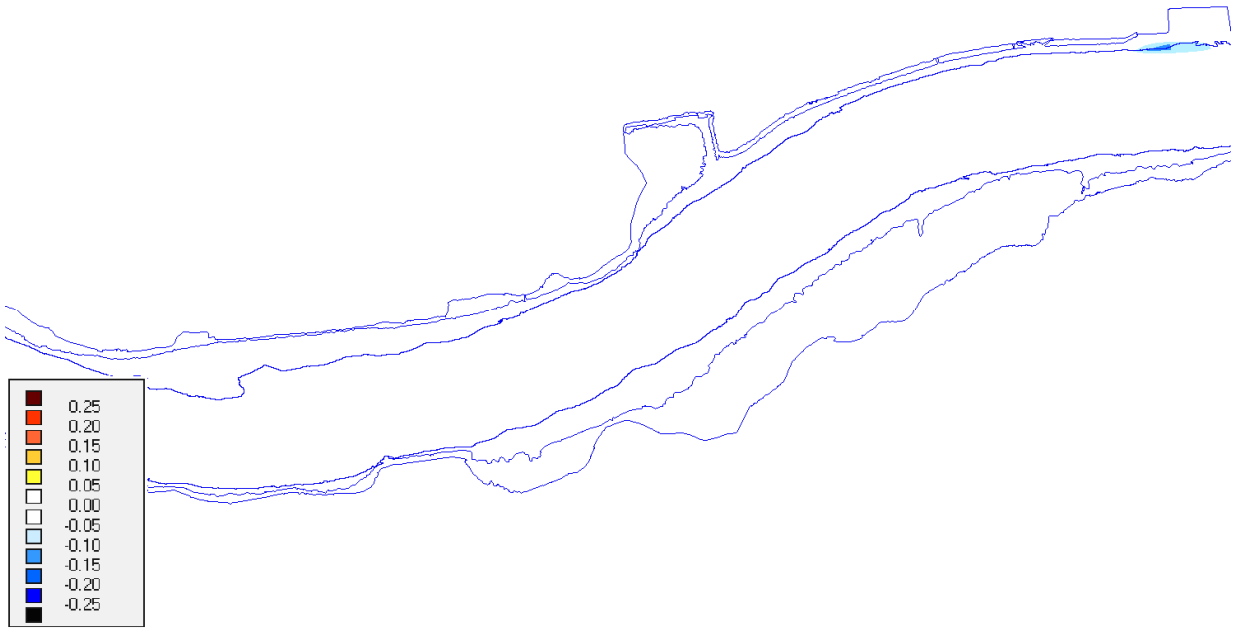

Figure 30 - Map 6 of differences in velocity (run DD3x3 rgh1 minus run DD3x3)

Figure 31 - Map 1 of differences in velocity (run DD3x3 rgh2 minus run DD3x3)

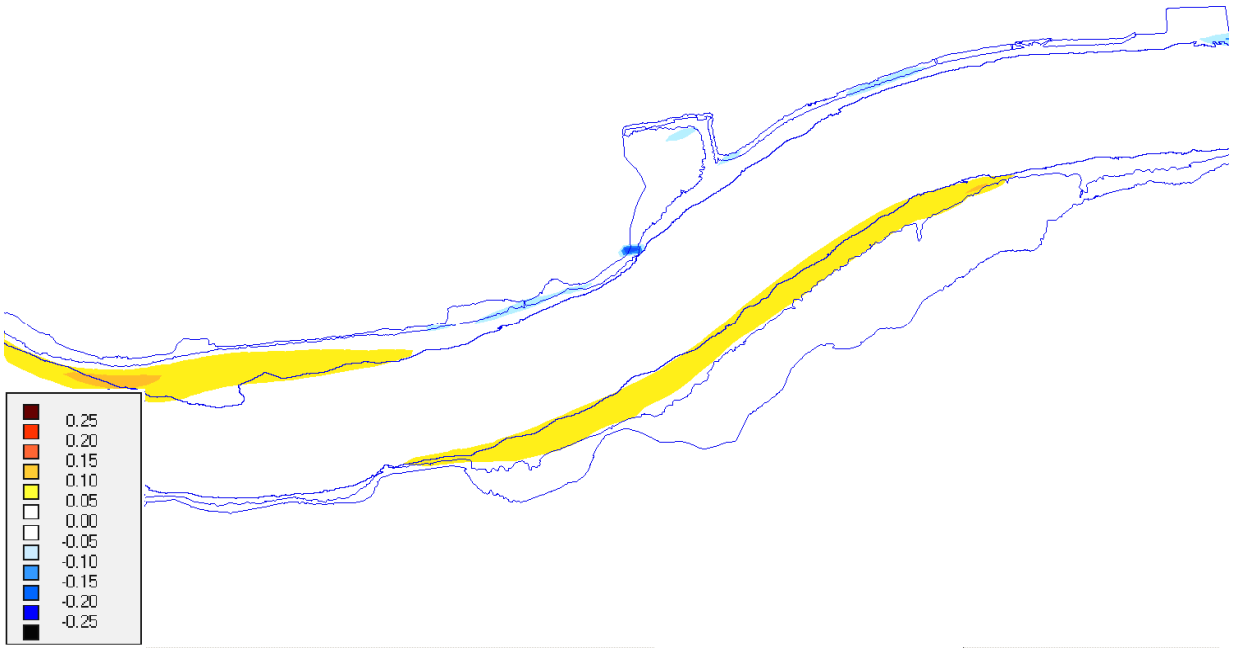

Figure 32 - Map 3 of differences in velocity (run DD3x3 rgh2 minus run DD3x3)

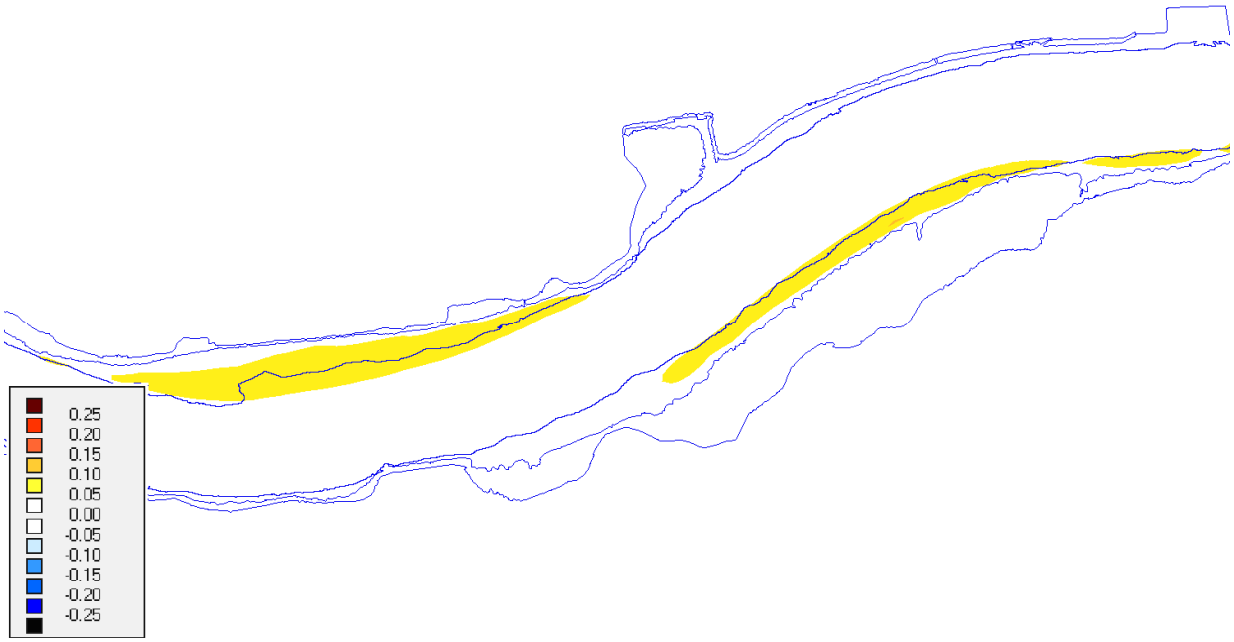

Figure 33 - Map 5 of differences in velocity (run DD3x3 rgh2 minus run DD3x3)

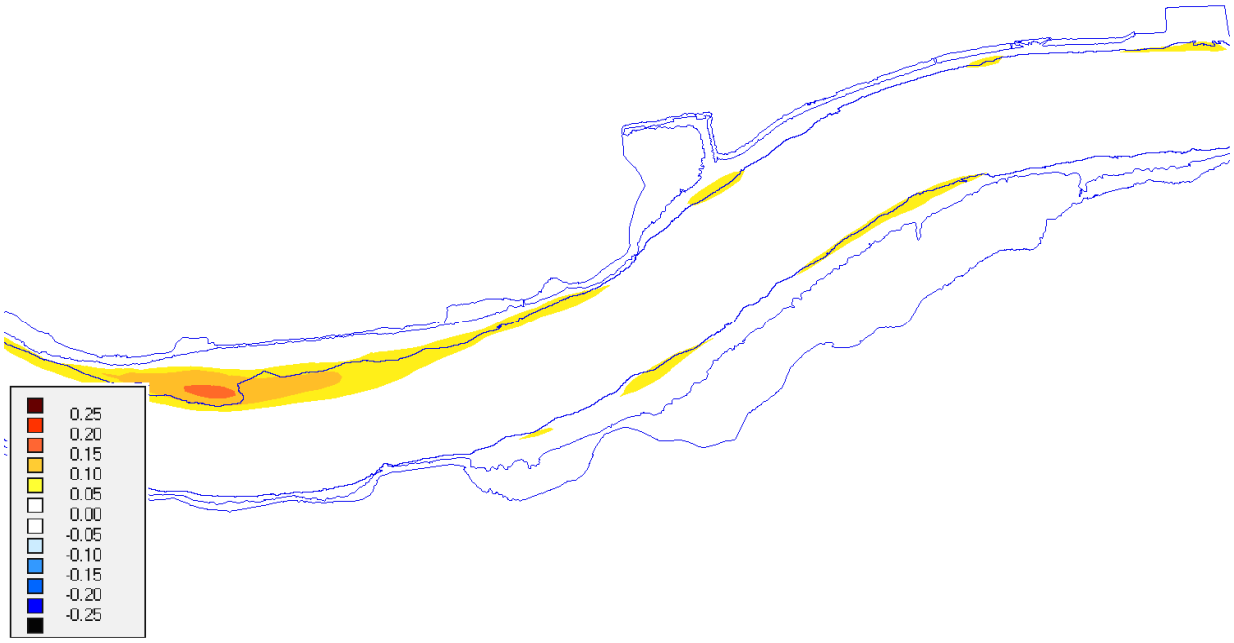

Figure 34 - Map 6 of differences in velocity (run DD3x3 rgh2 minus run DD3x3)

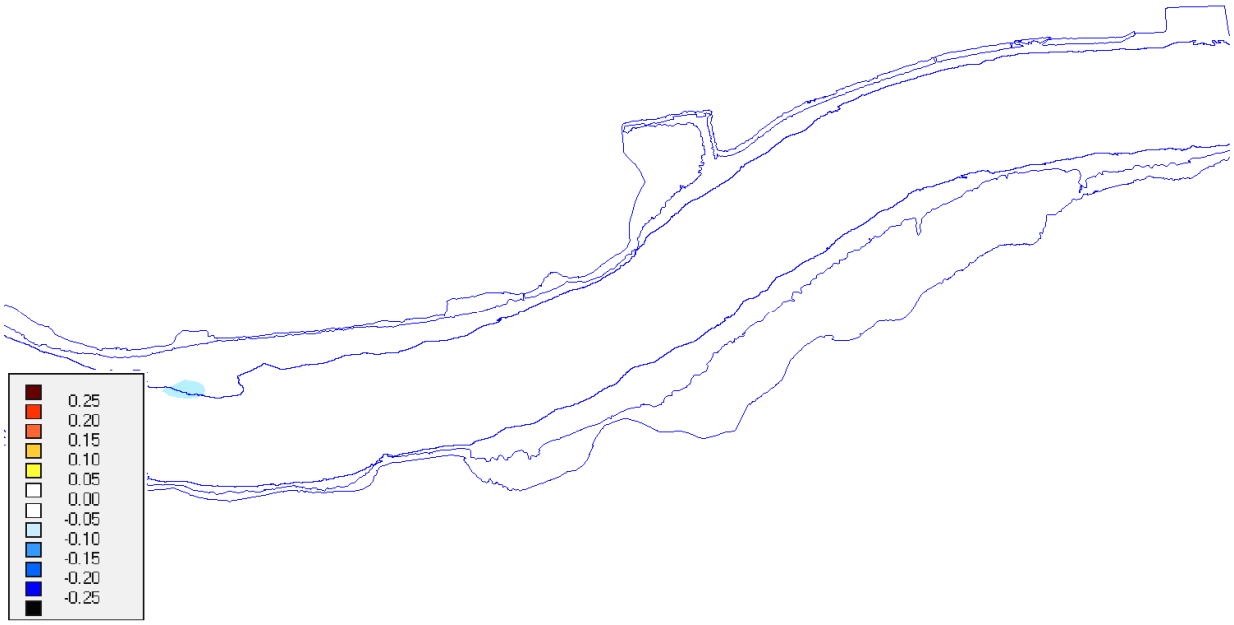

Figure 35 - Map 1 of differences in velocity (run DD3x3 rgh3 minus run DD3x3)

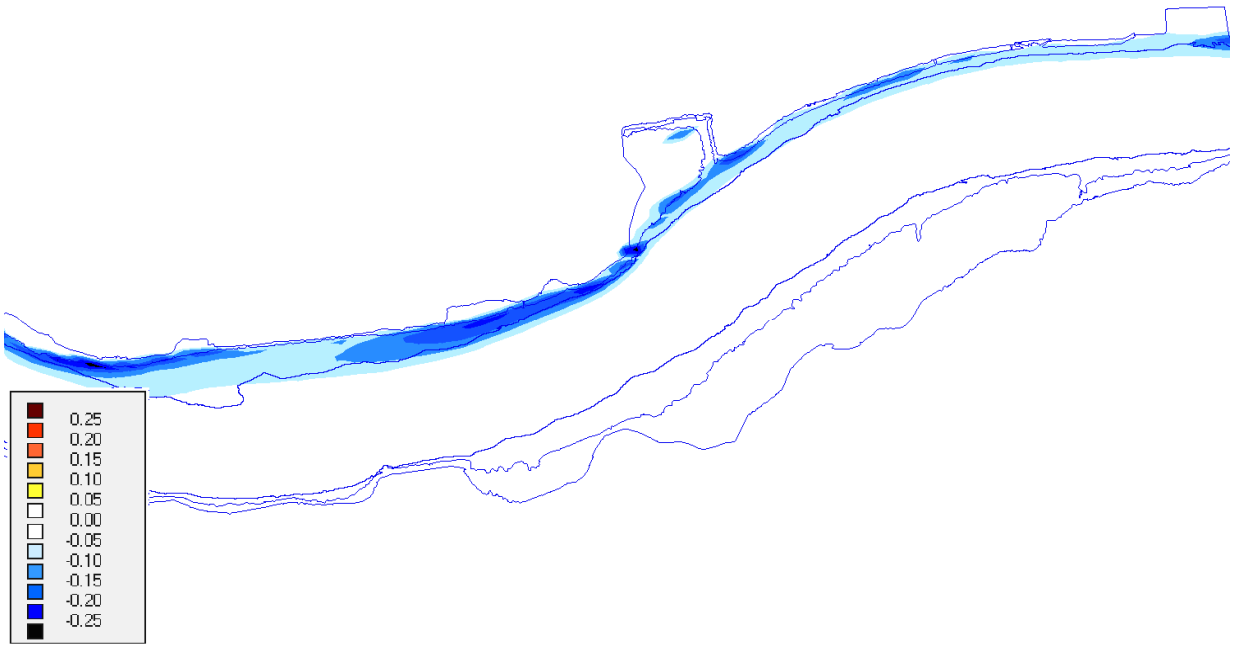

Figure 36 - Map 3 of differences in velocity (run DD3x3 rgh3 minus run DD3x3)

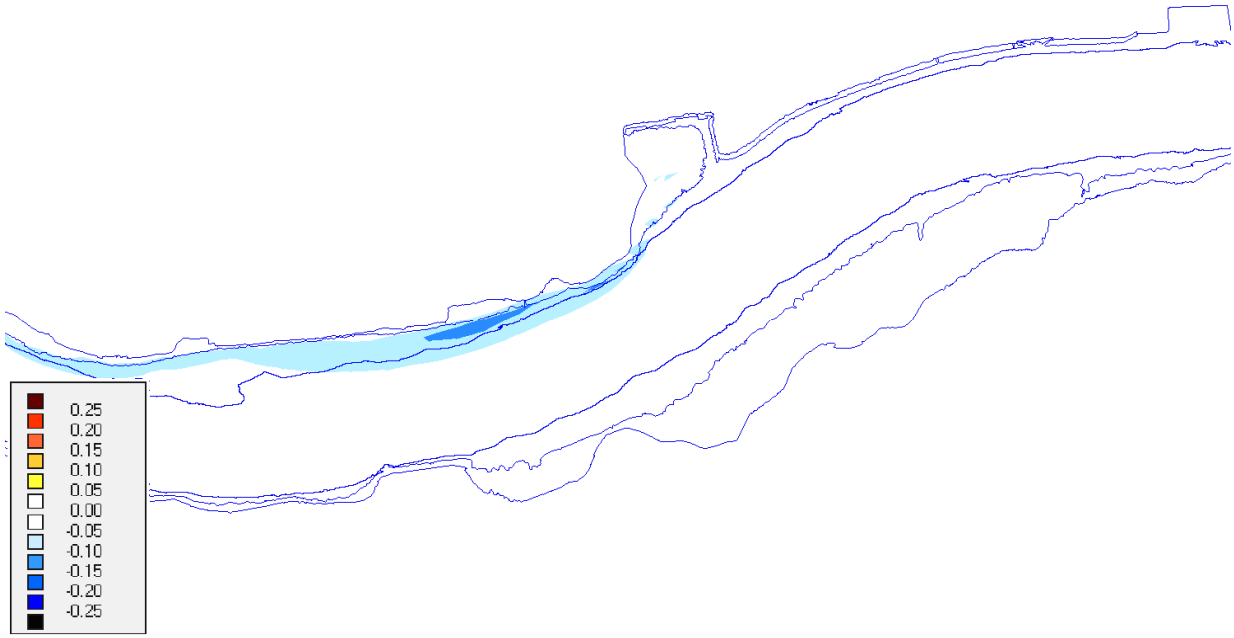

Figure 37 - Map 4 of differences in velocity (run DD3x3 rgh3 minus run DD3x3)

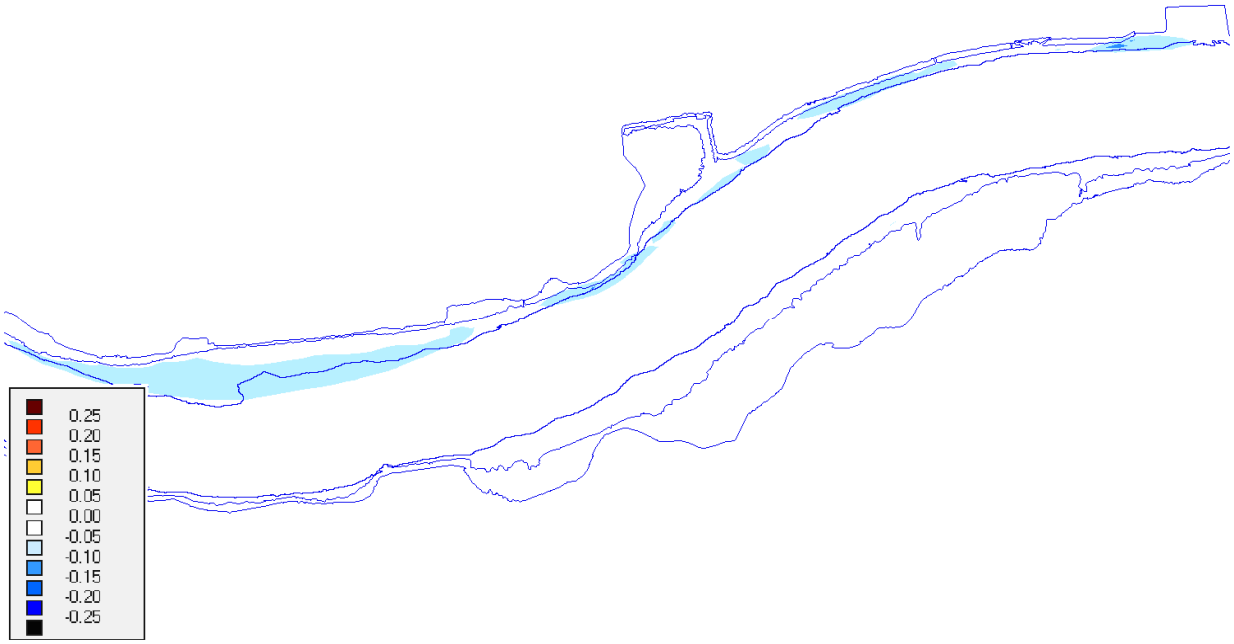

Figure 38 - Map 5 of differences in velocity (run DD3x3 rgh3 minus run DD3x3)

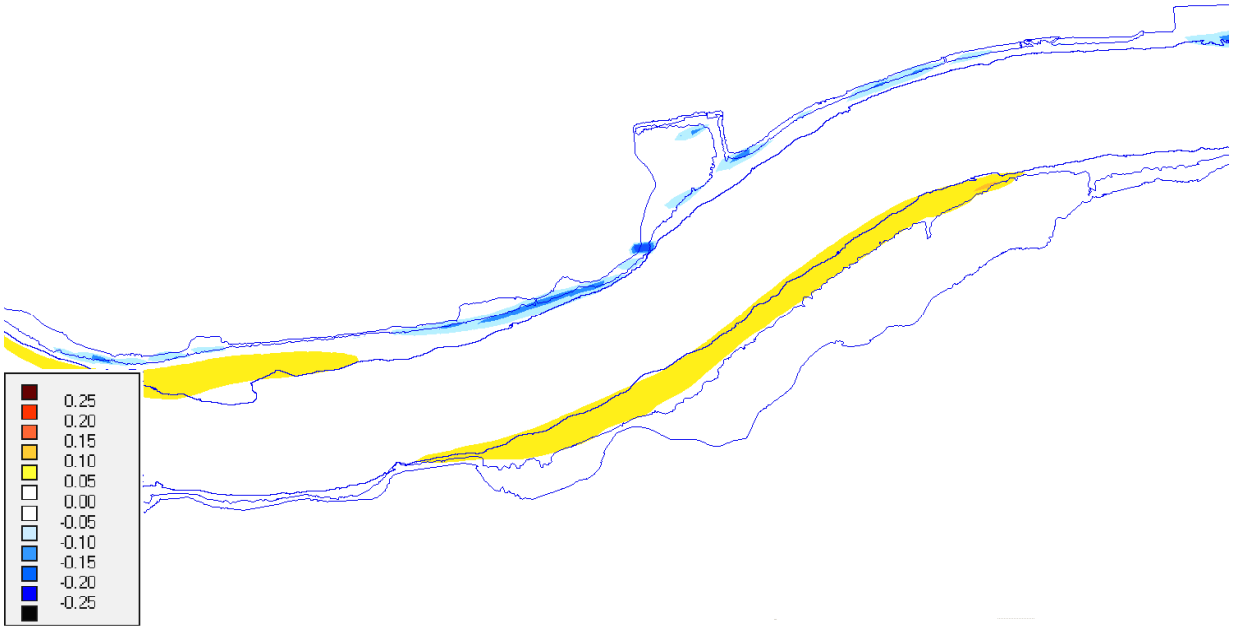

Figure 39 - Map 3 of differences in velocity (run DD3x3 rgh4 minus run DD3x3)

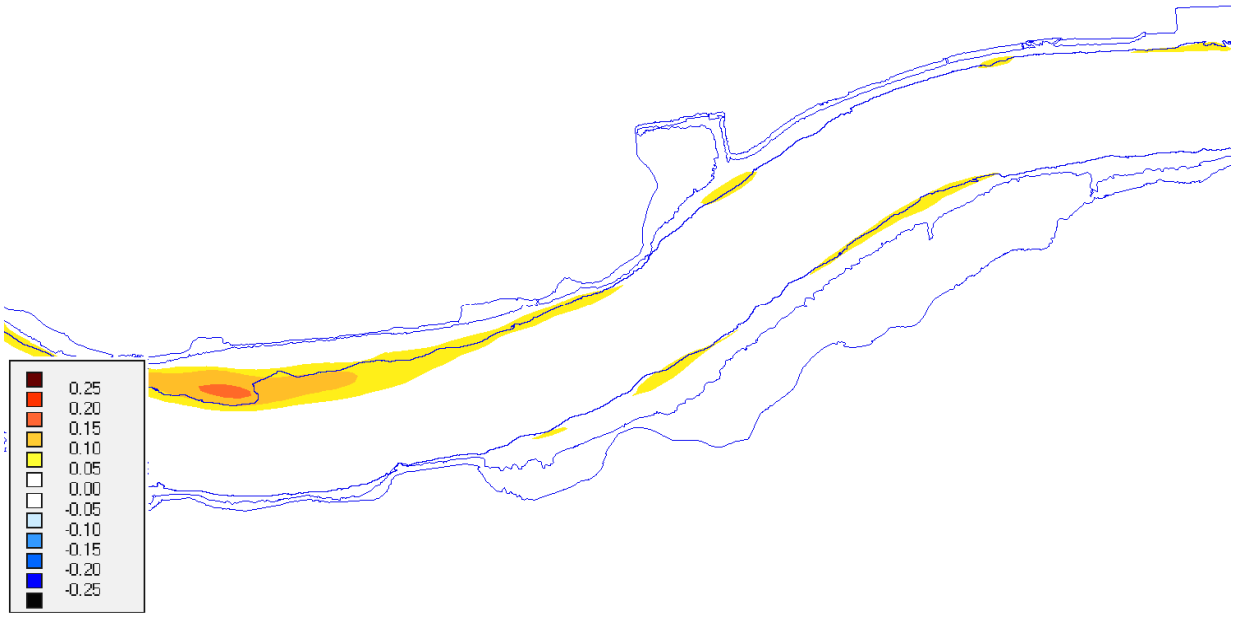

Figure 40 - Map 6 of differences in velocity (run DD3x3 rgh4 minus run DD3x3)

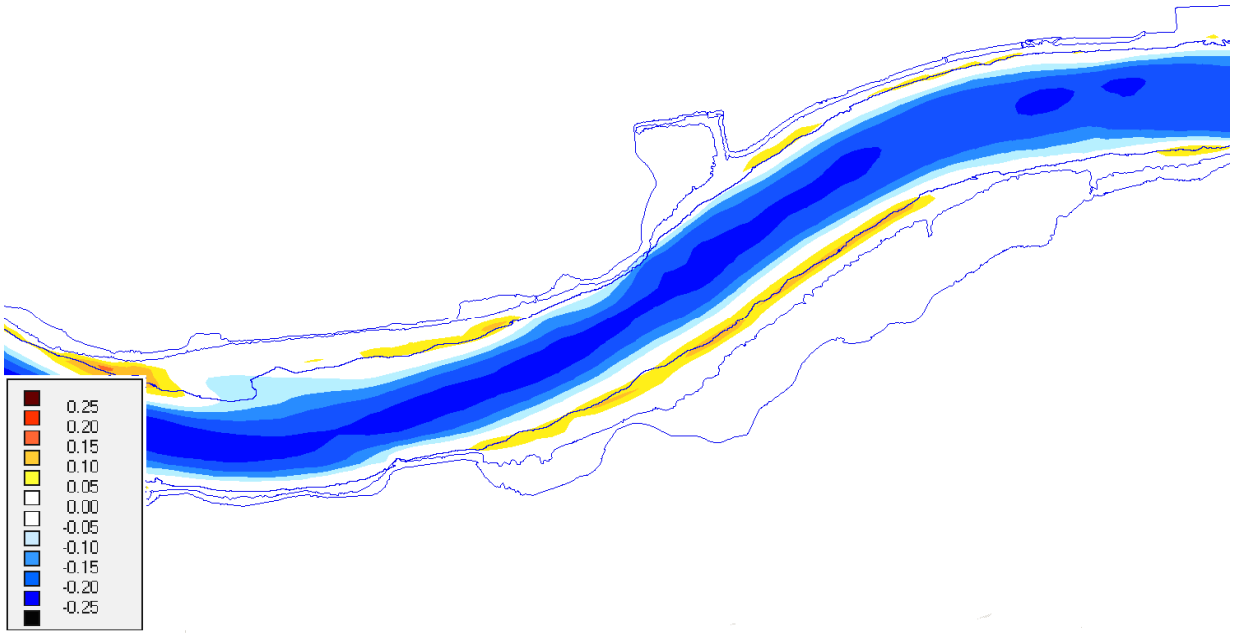

Figure 41 - Map 1 of differences in velocity (run DD3x3V1 minus run DD3x3)

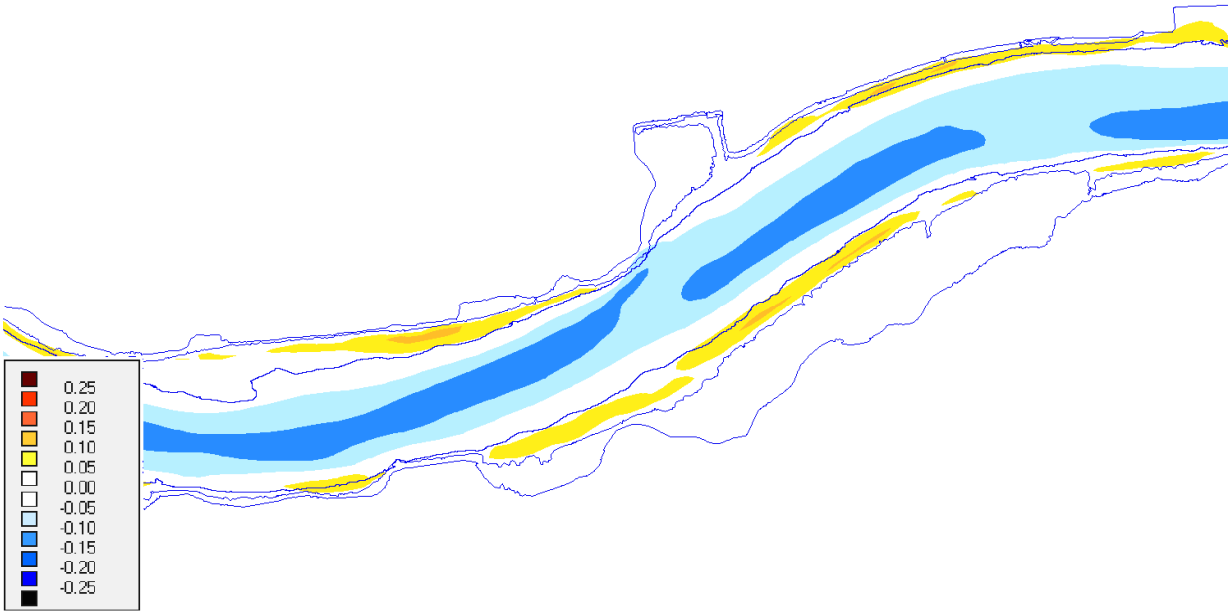

Figure 42 - Map 2 of differences in velocity (run DD3x3V1 minus run DD3x3)

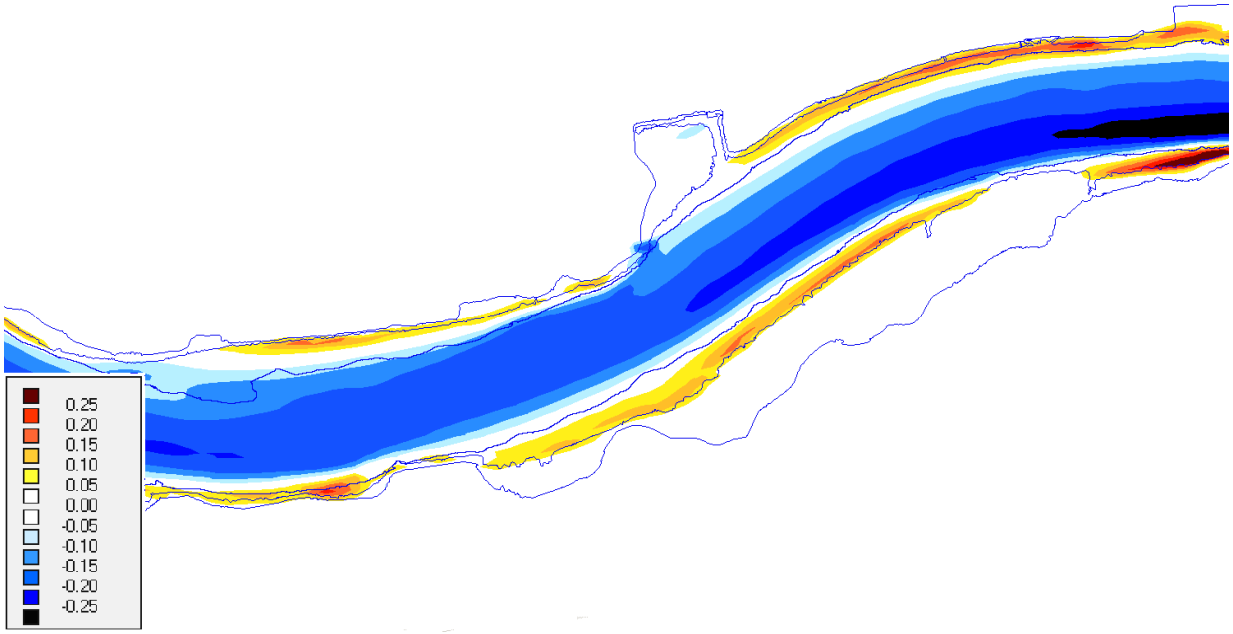

Figure 43 - Map 3 of differences in velocity (run DD3x3V1 minus run DD3x3)

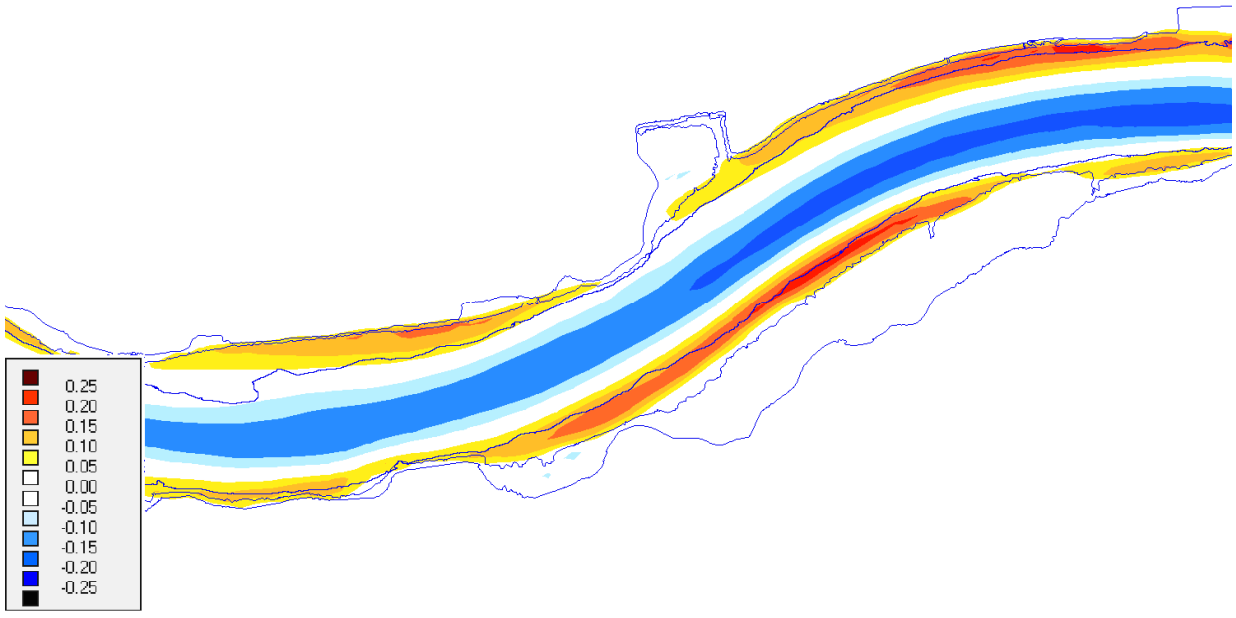

Figure 44 - Map 4 of differences in velocity (run DD3x3V1 minus run DD3x3)

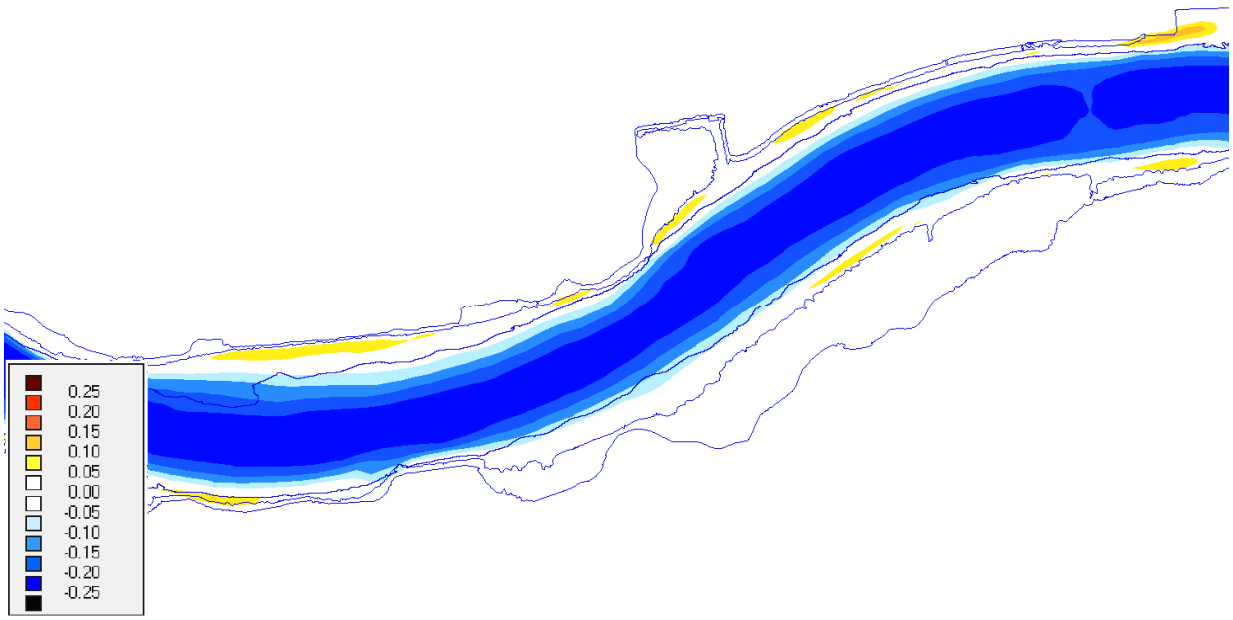

Figure 45 - Map 5 of differences in velocity (run DD3x3V1 minus run DD3x3)

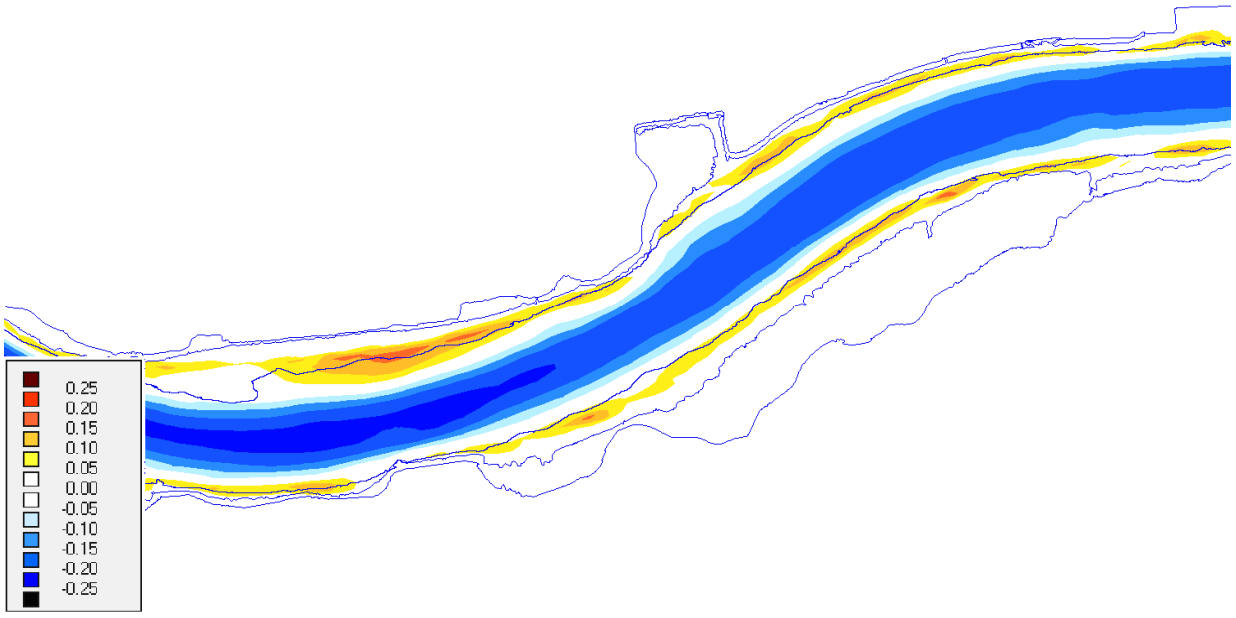

Figure 46 - Map 6 of differences in velocity (run DD3x3V1 minus run DD3x3)

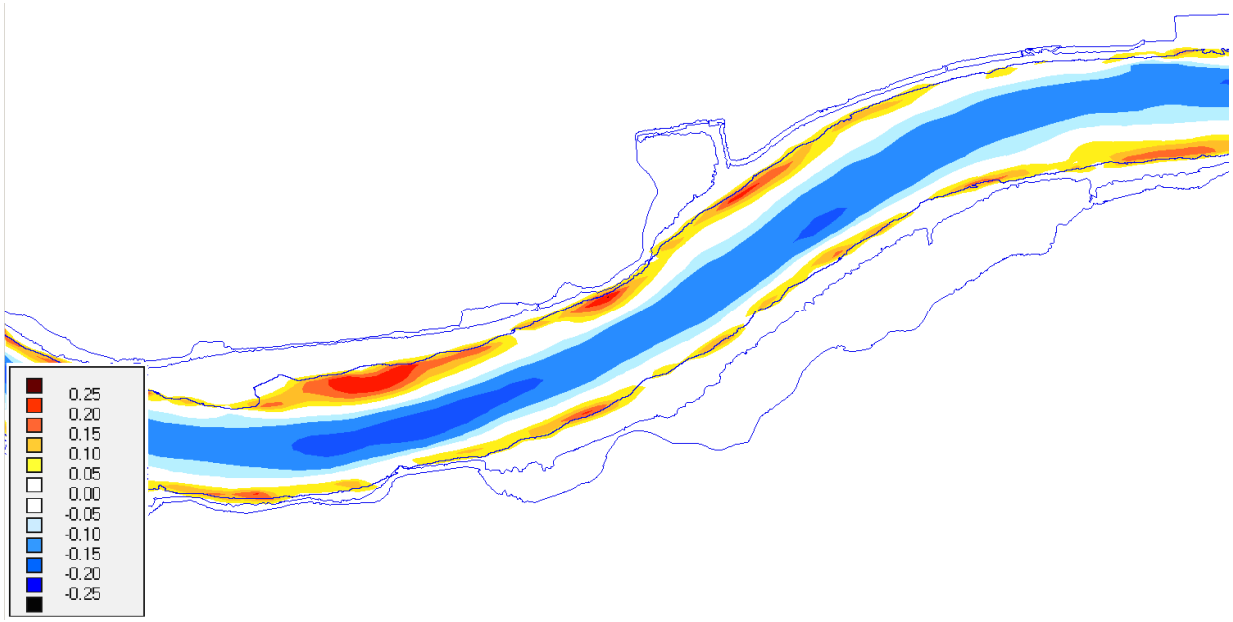

Figure 47 - Map 7 of differences in velocity (run DD3x3V1 minus run DD3x3)

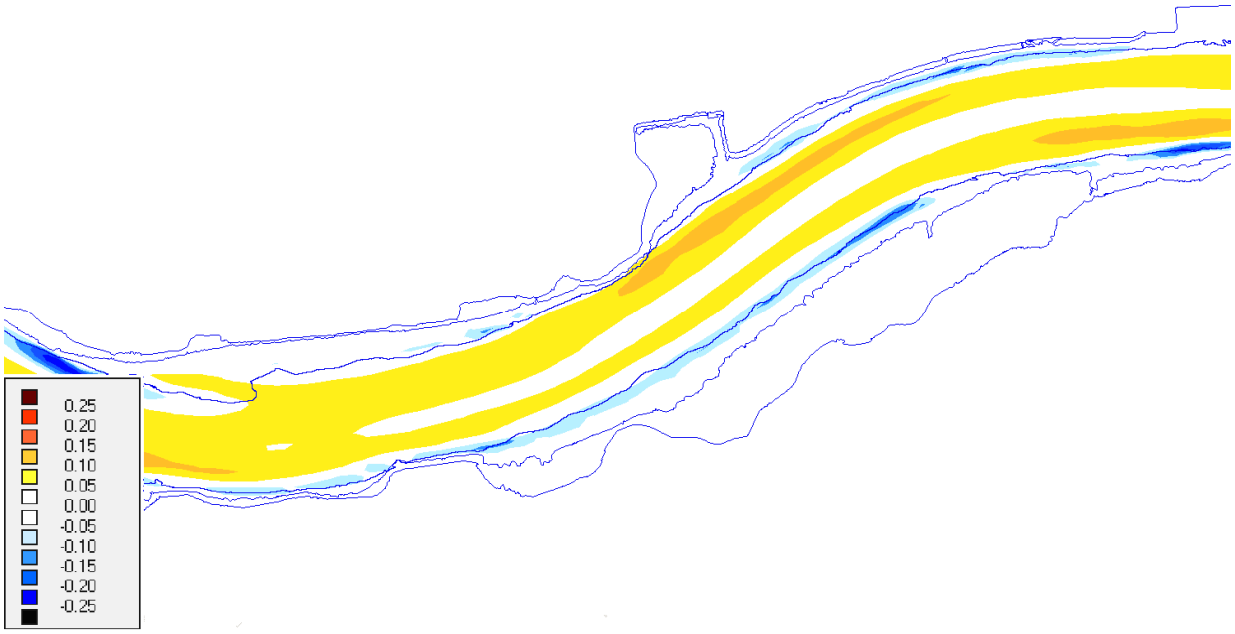

Figure 48 - Map 1 of differences in velocity (run DD3x3V2 minus run DD3x3)

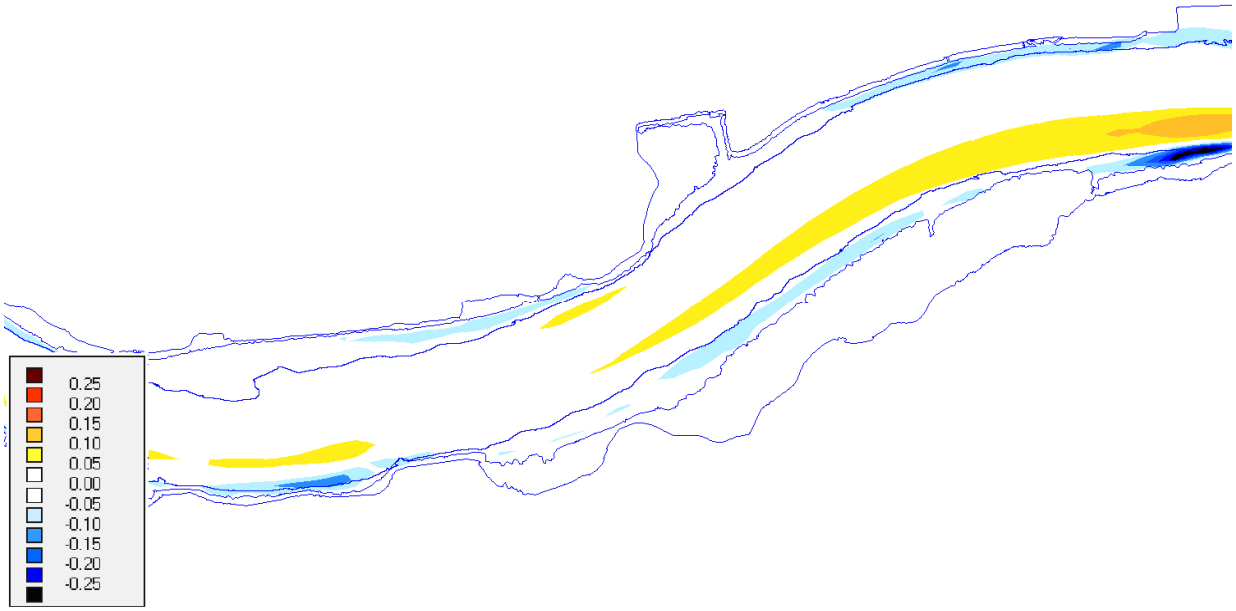

Figure 49 - Map 2 of differences in velocity (run DD3x3V2 minus run DD3x3)

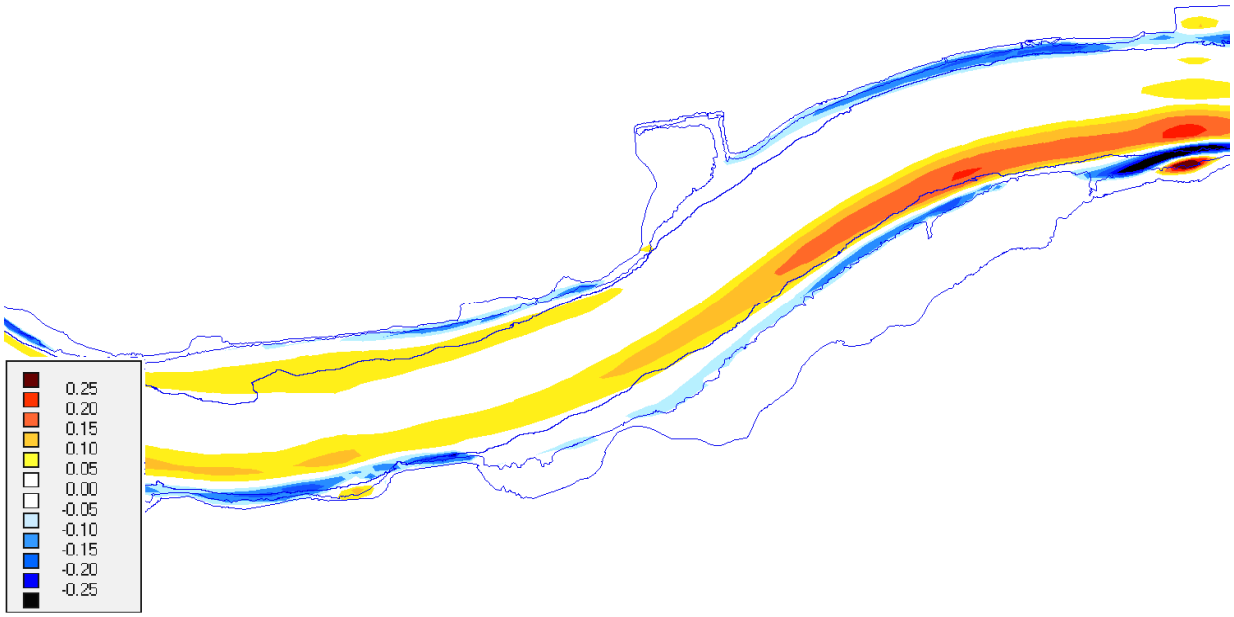

Figure 50 - Map 3 of differences in velocity (run DD3x3V2 minus run DD3x3)

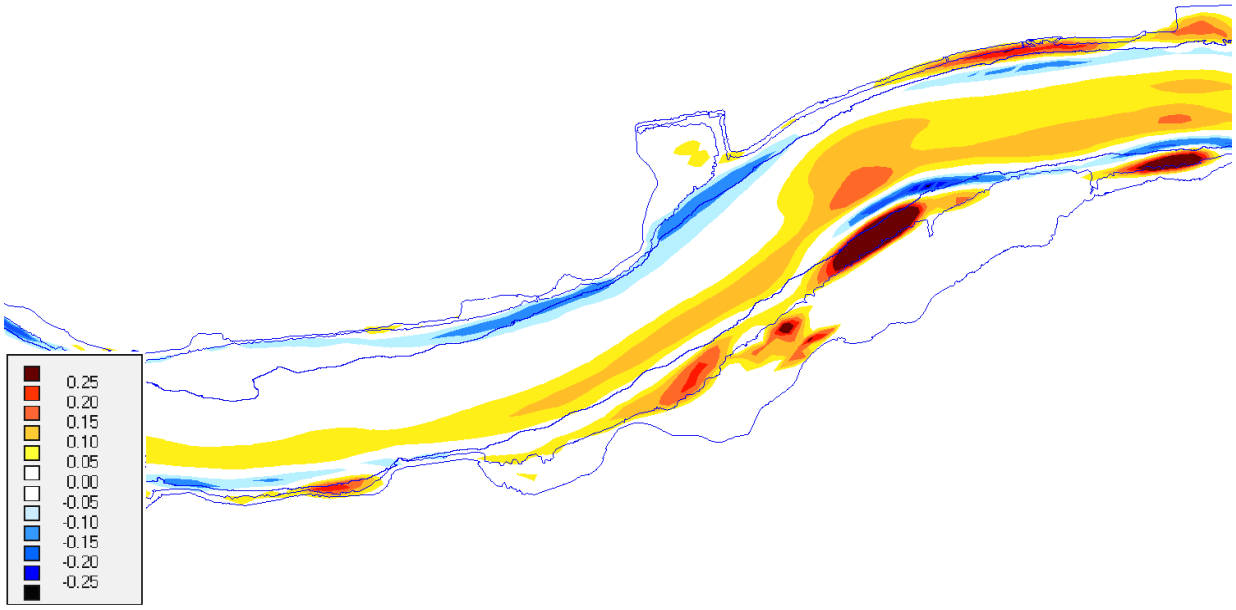

Figure 51 - Map 4 of differences in velocity (run DD3x3V2 minus run DD3x3)

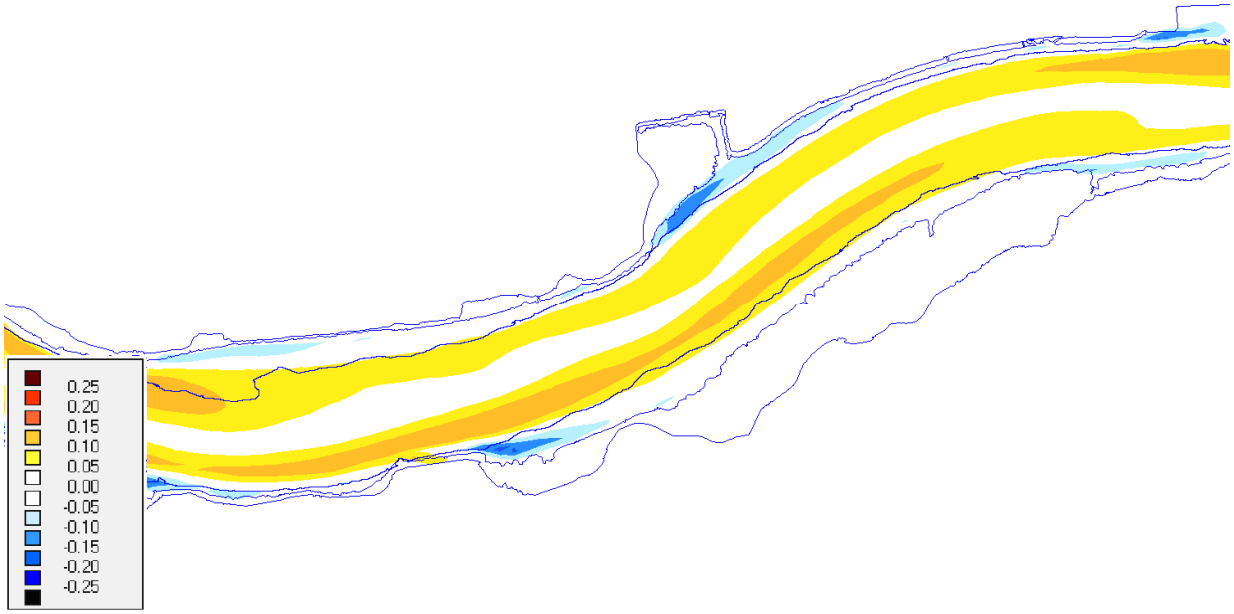

Figure 52 - Map 5 of differences in velocity (run DD3x3V2 minus run DD3x3)

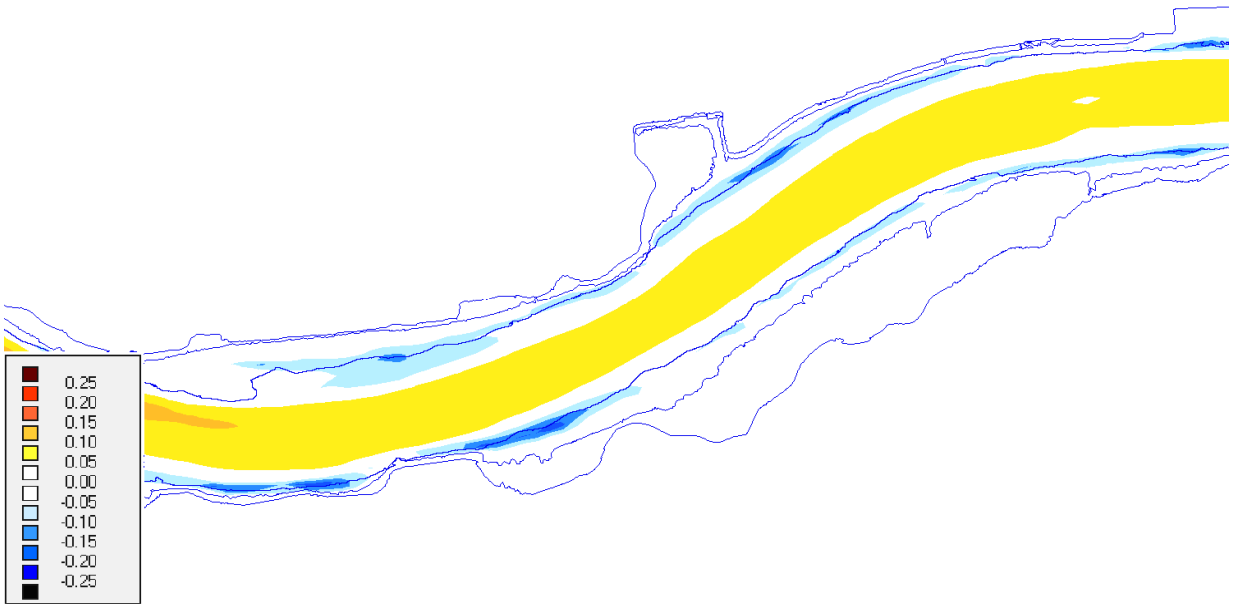

Figure 53 - Map 6 of differences in velocity (run DD3x3V2 minus run DD3x3)

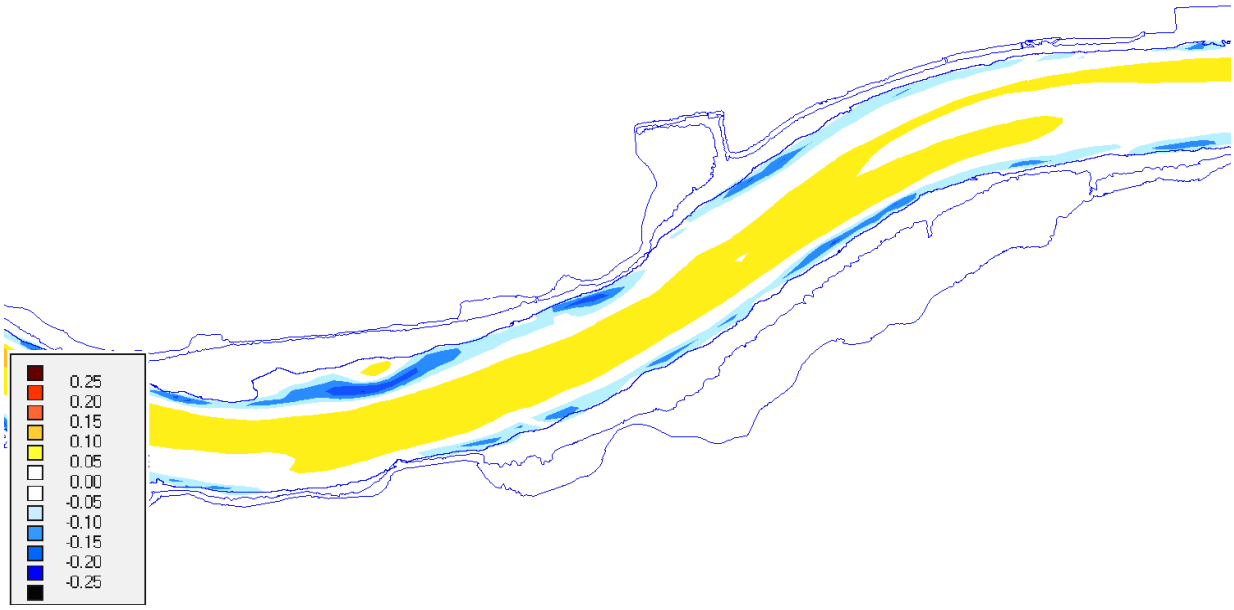

Figure 54 - Map 7 of differences in velocity (run DD3x3V2 minus run DD3x3)

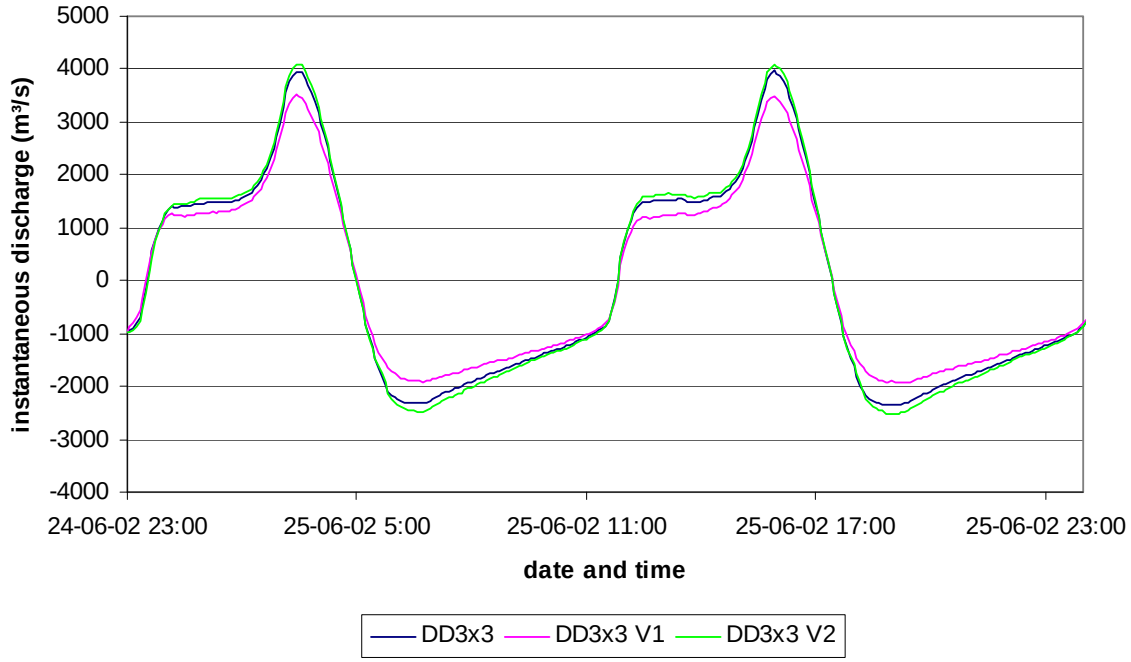

Figure 55 - Instantaneous discharge through cross section Steendorp

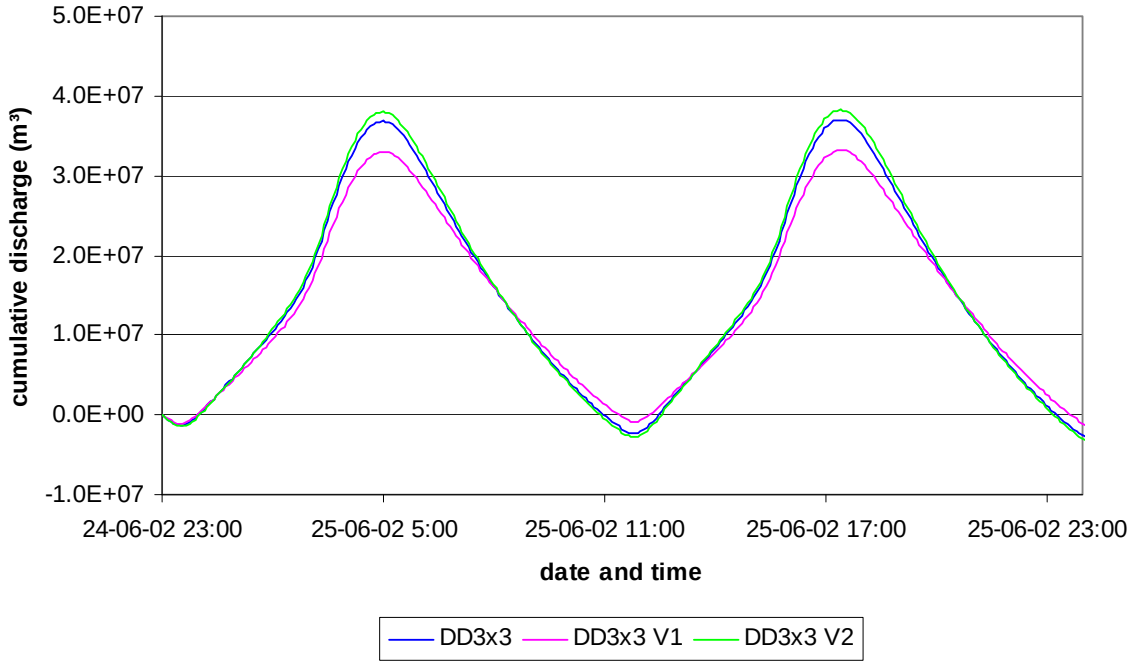

Figure 56 - Cumulative discharge through cross section Steendorp

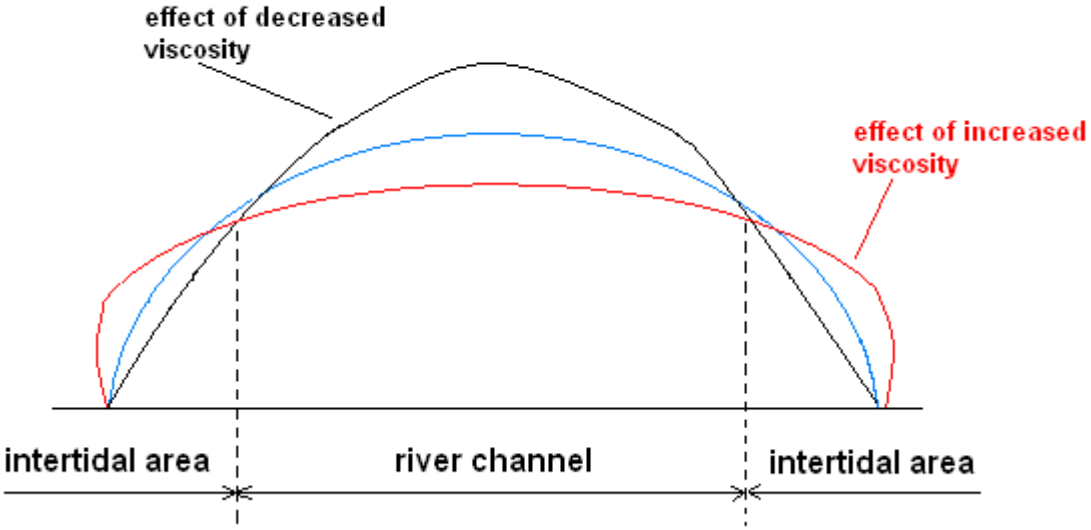

Figure 57 - Effect of horizontal eddy viscosity on the velocity profile

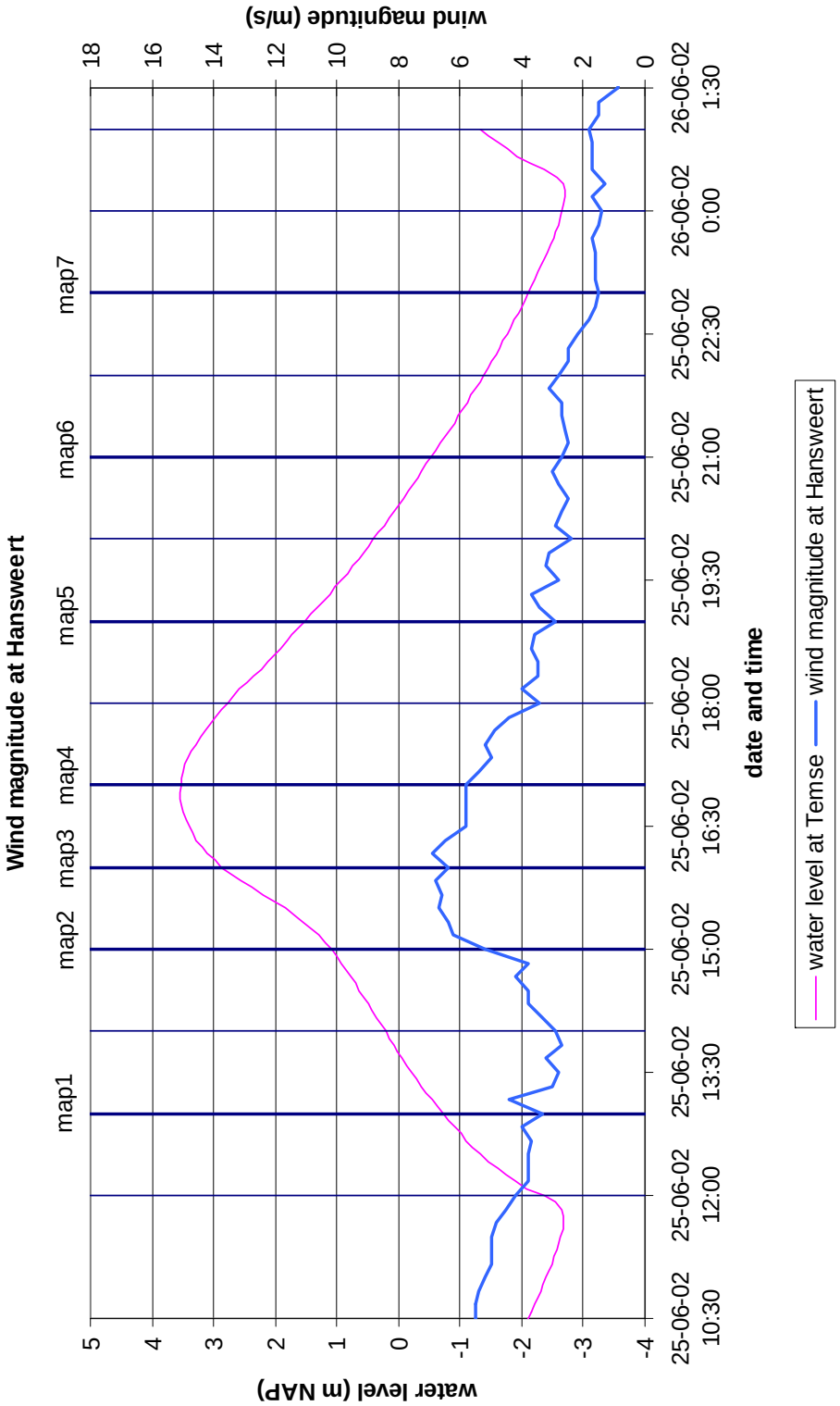

Figure 58 - Wind magnitude at Hansweert during the period of the sensitivity analysis

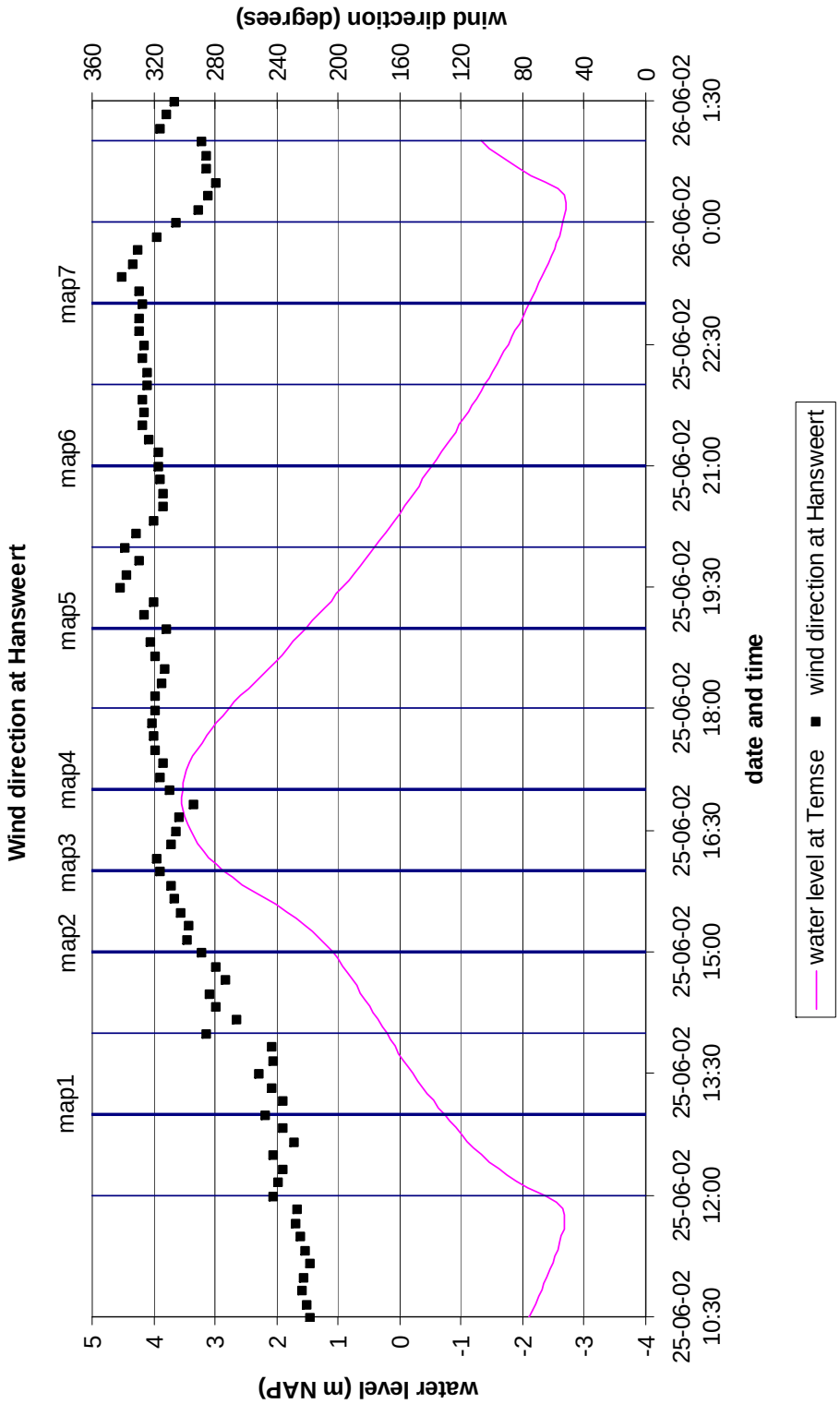

Figure 59 - Wind direction at Hansweert during the period of the sensitivity analysis

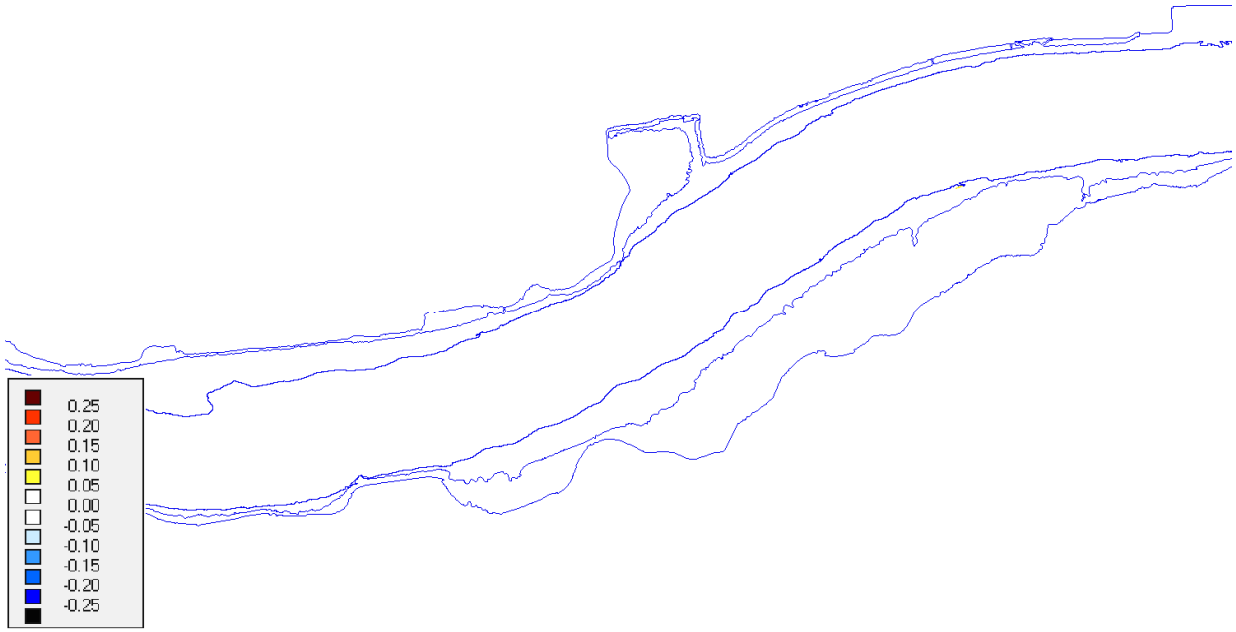

Figure 60 - Map 1 of differences in velocity (run DD3x3 no wind minus run DD3x3)

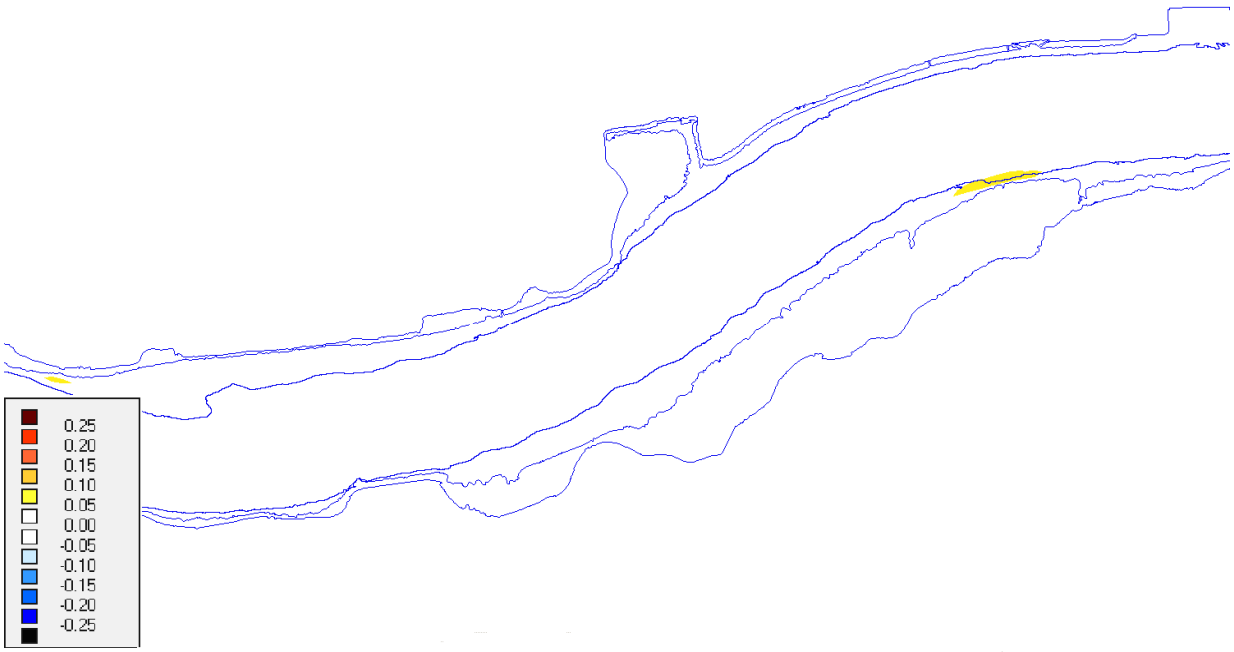

Figure 61 - Map 2 of differences in velocity (run DD3x3 no wind minus run DD3x3)

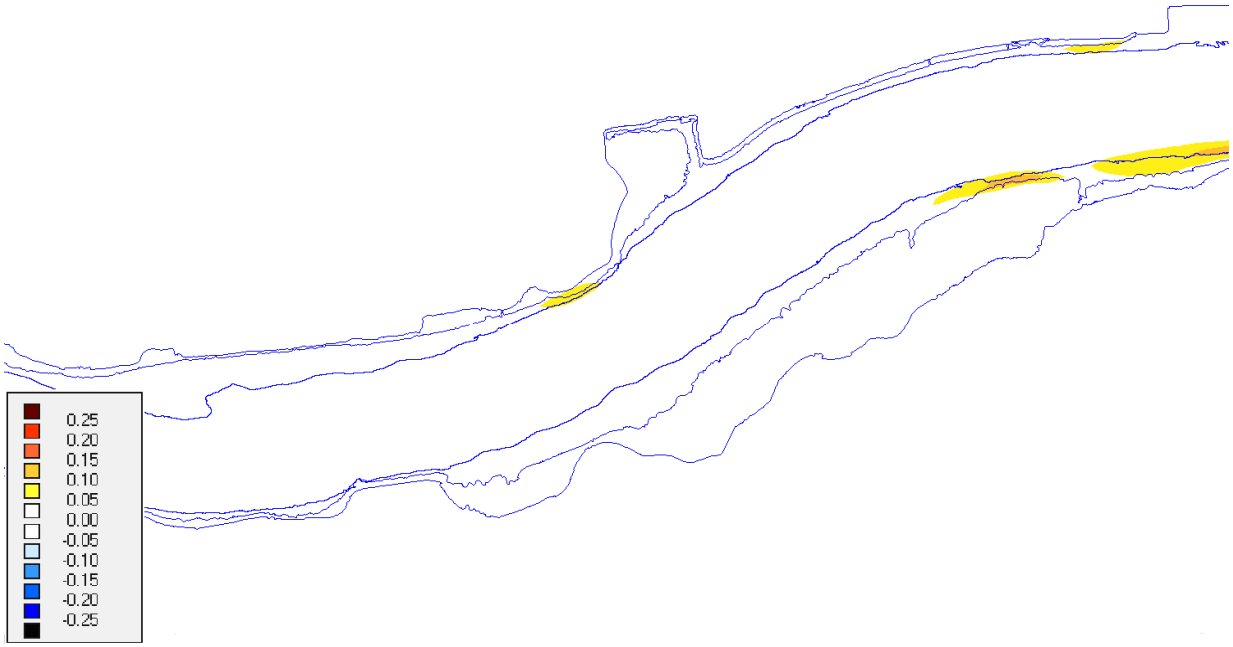

Figure 62 - Map 3 of differences in velocity (run DD3x3 no wind minus run DD3x3)

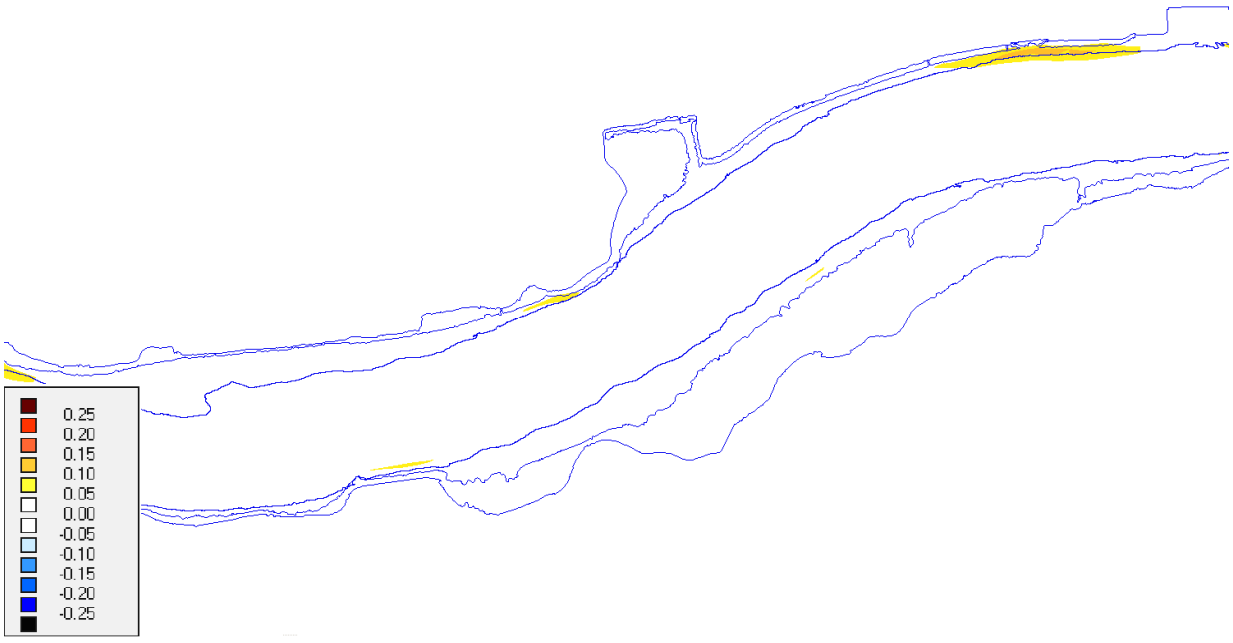

Figure 63 - Map 5 of differences in velocity (run DD3x3 no wind minus run DD3x3)

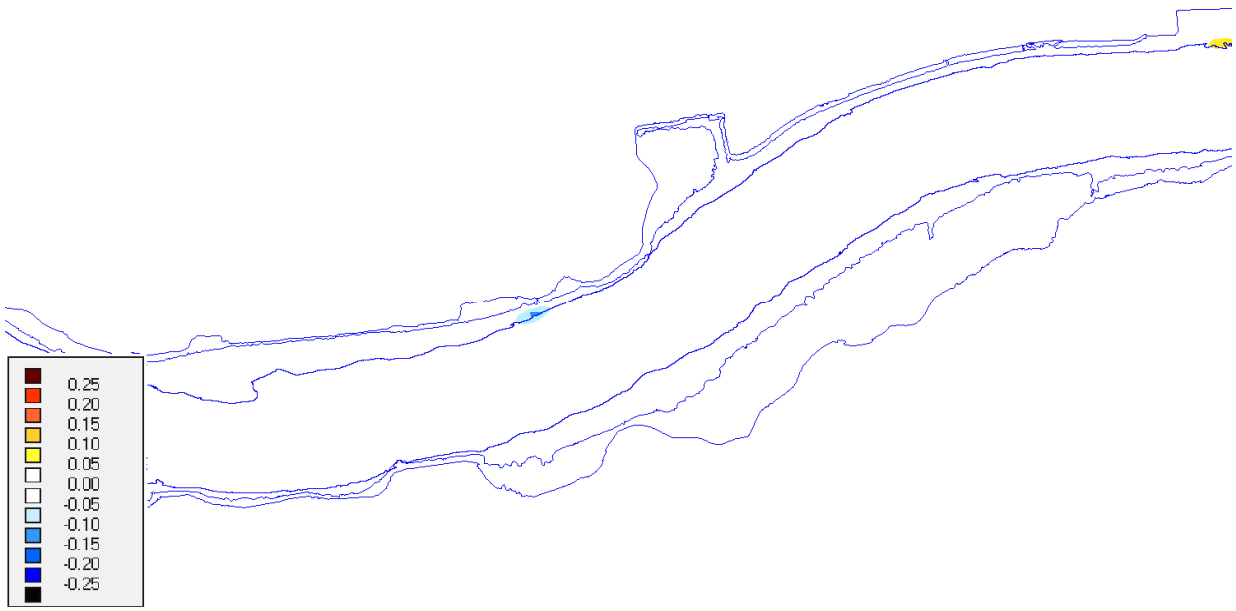

Figure 64 - Map 1 of differences in velocity (run DD3x3 shepard minus run DD3x3)

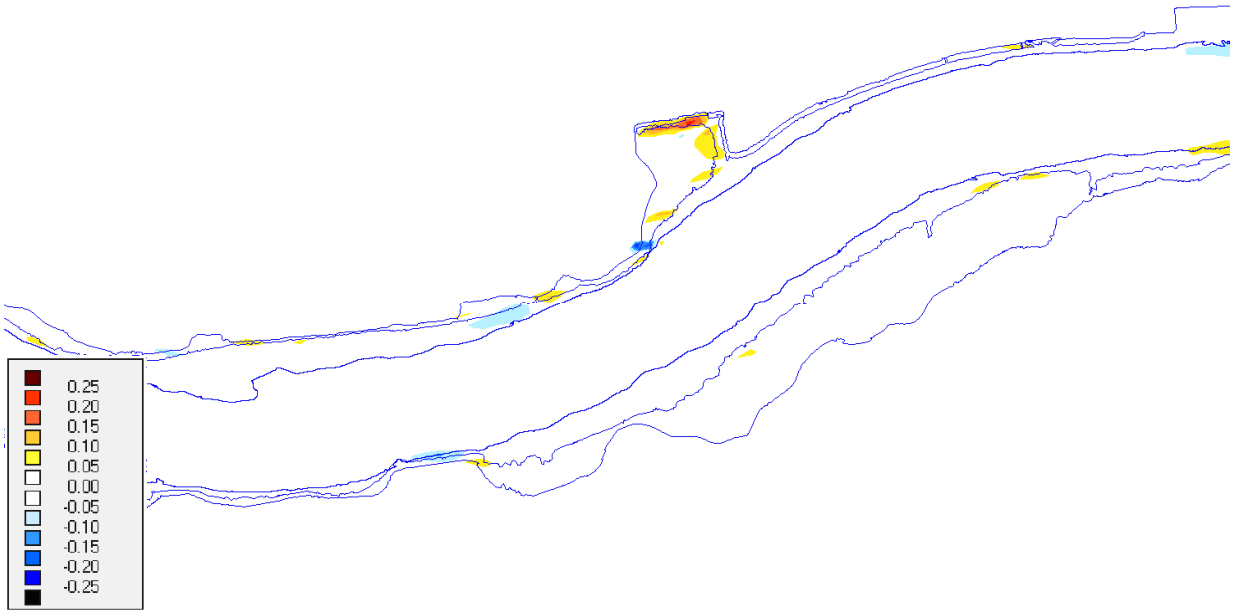

Figure 65 - Map 3 of differences in velocity (run DD3x3 shepard minus run DD3x3)

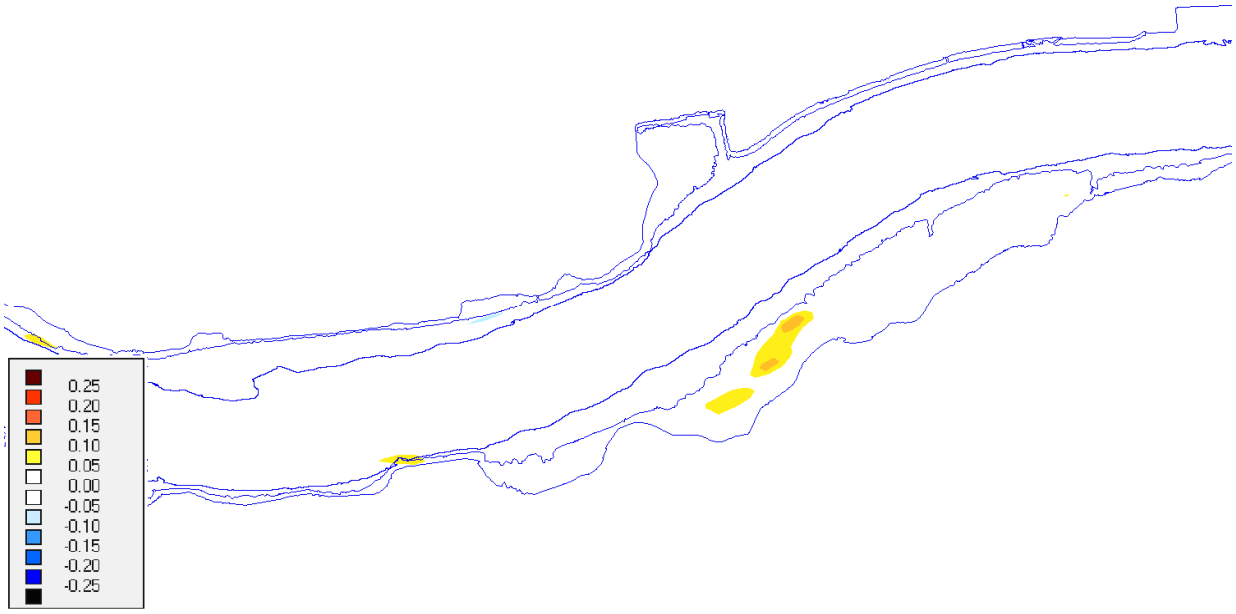

Figure 66 - Map 4 of differences in velocity (run DD3x3 shepard minus run DD3x3)

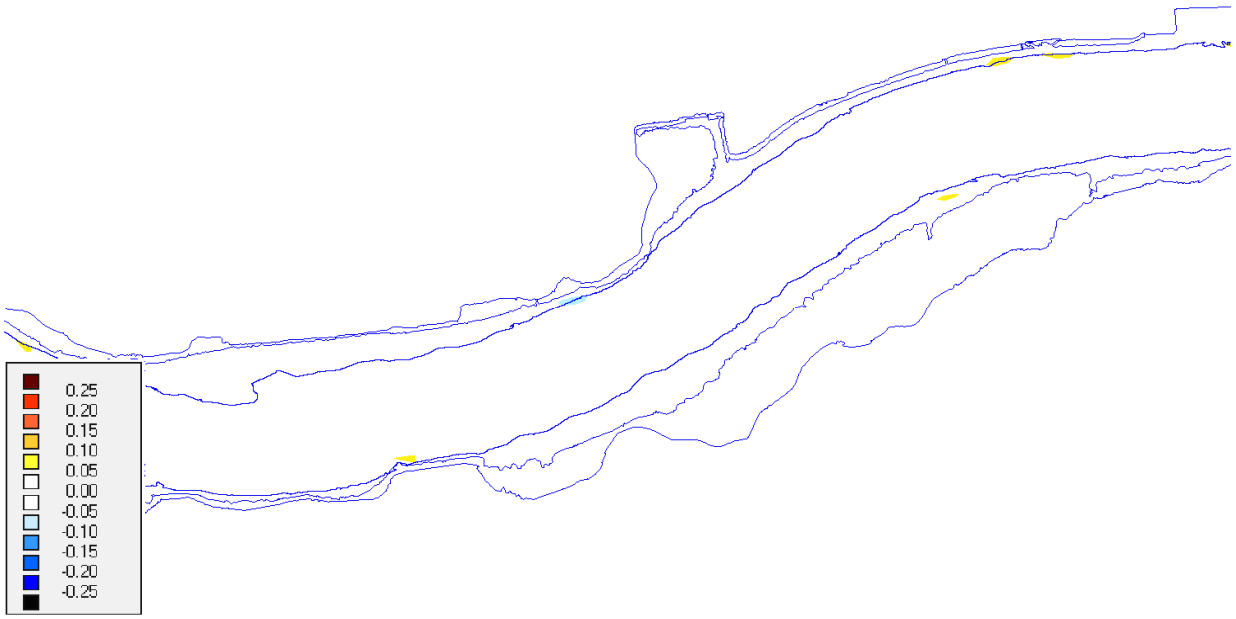

Figure 67 - Map 6 of differences in velocity (run DD3x3 shepard minus run DD3x3)

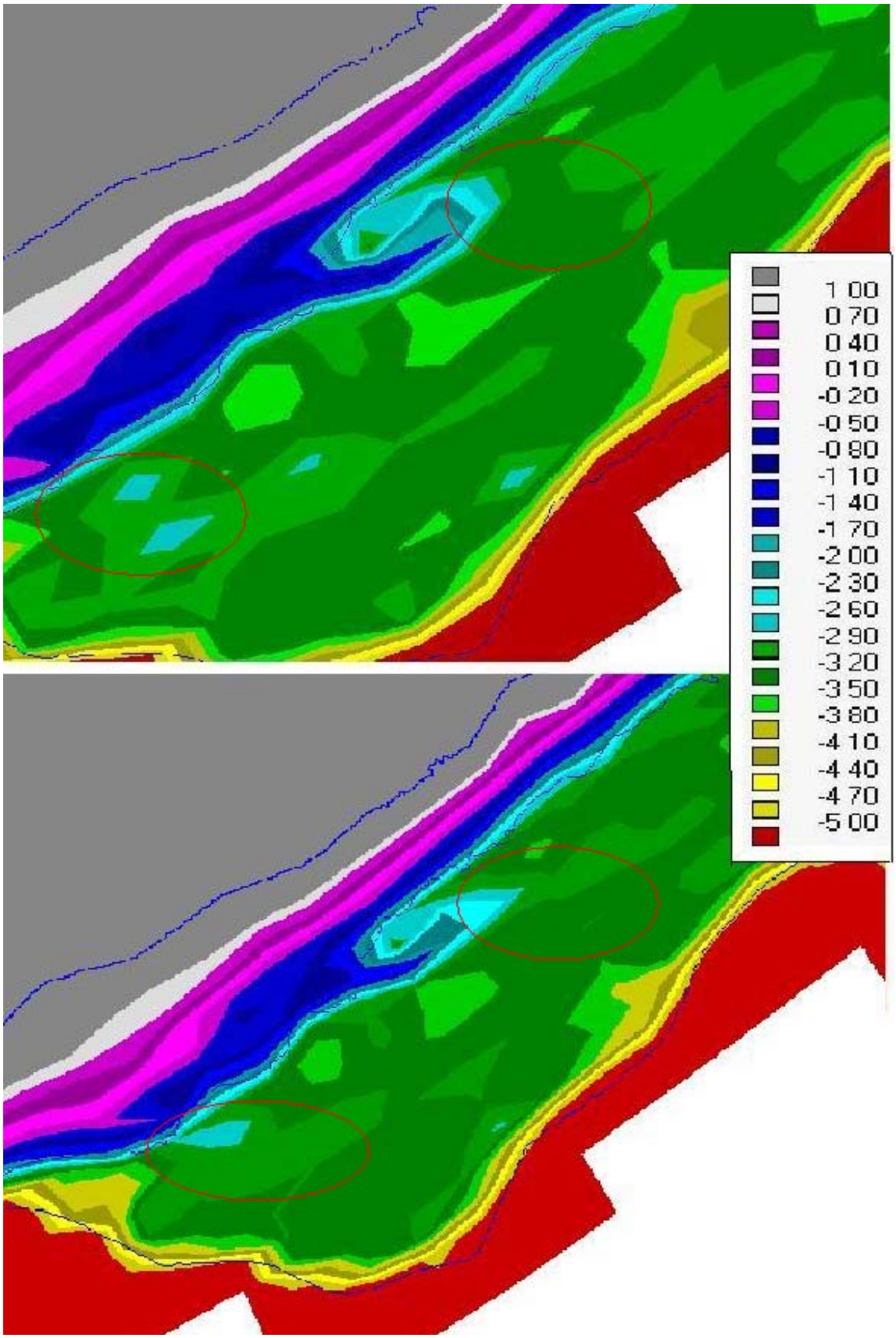

Figure 68 - Bathymetry of the Notelaer area: *Closest* method (above) and *Shepard* (below) (m NAP) for model DD3x3 (red circle: the differences in bathymetry resulting in velocity differences on map 4)

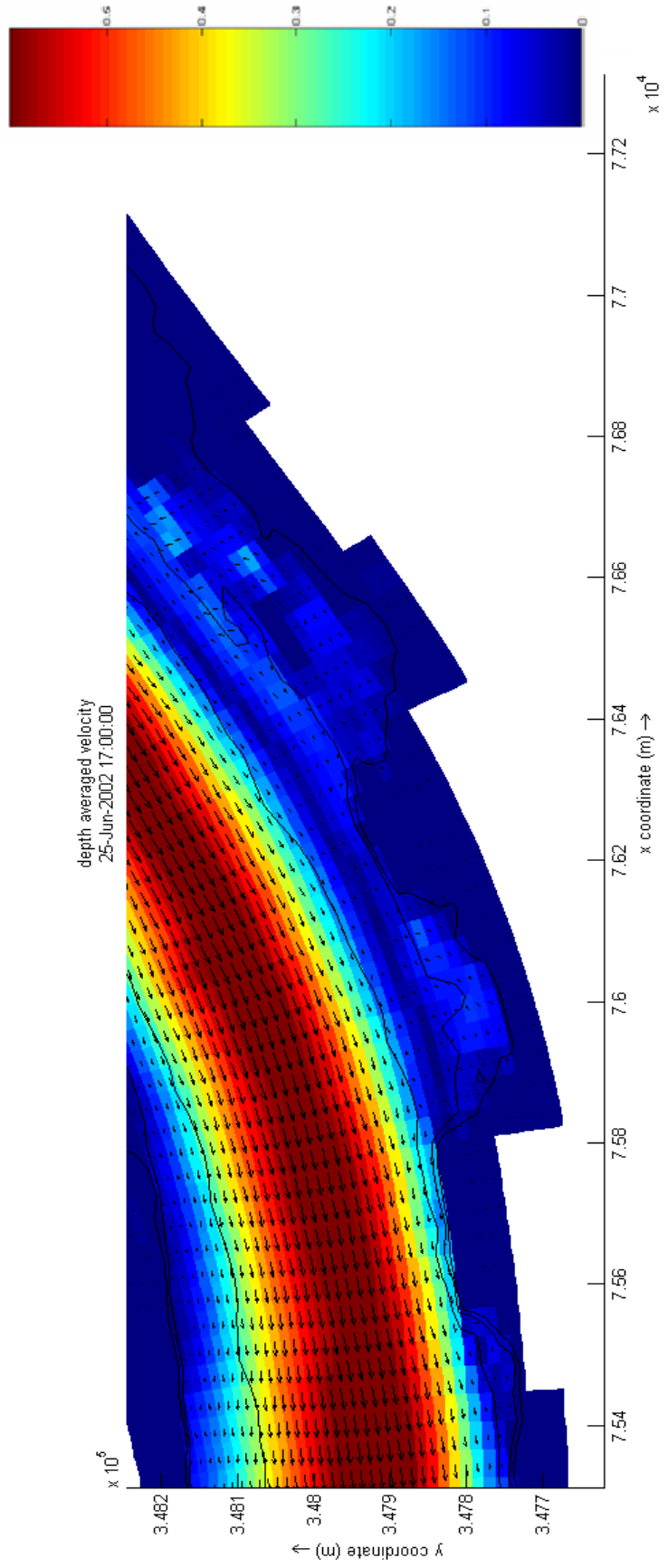

Figure 69 - Velocity map 4 in model run DD3x3shepard

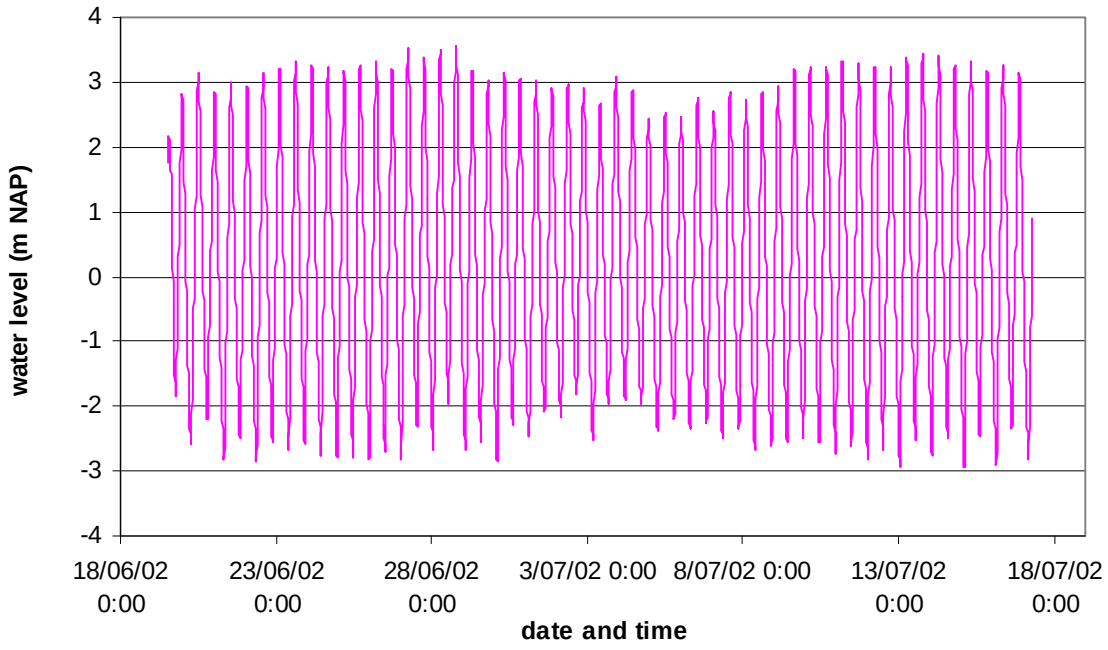

Figure 70 – Calculated water level at Schelle June – July 2002

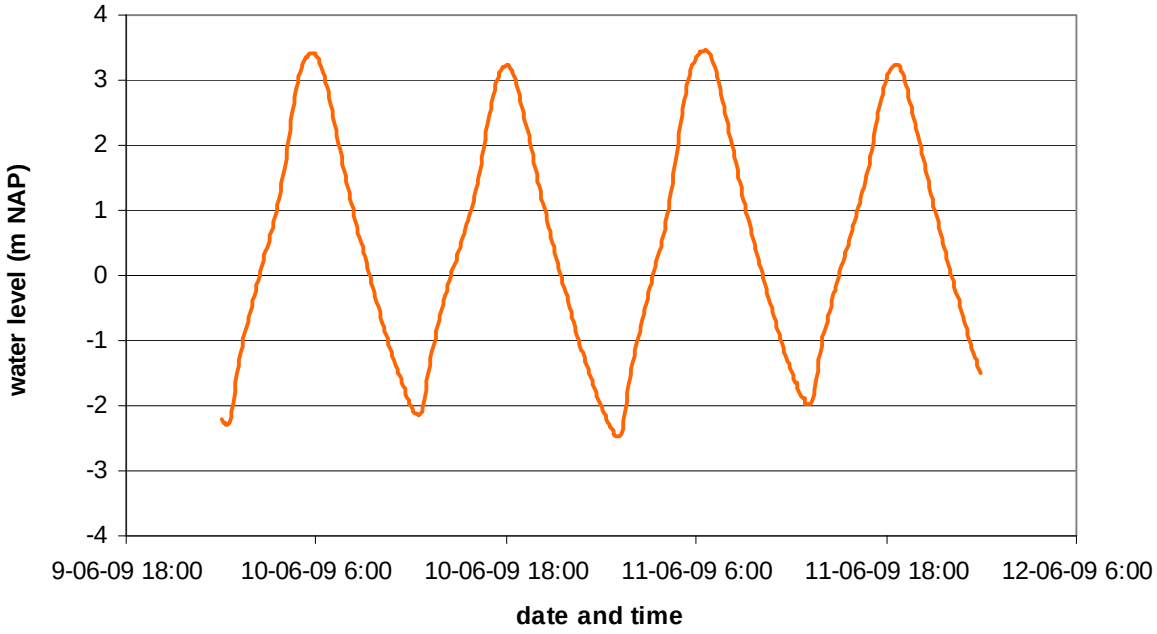

Figure 71 – Measured water level at Schelle 10 – 11 June 2009

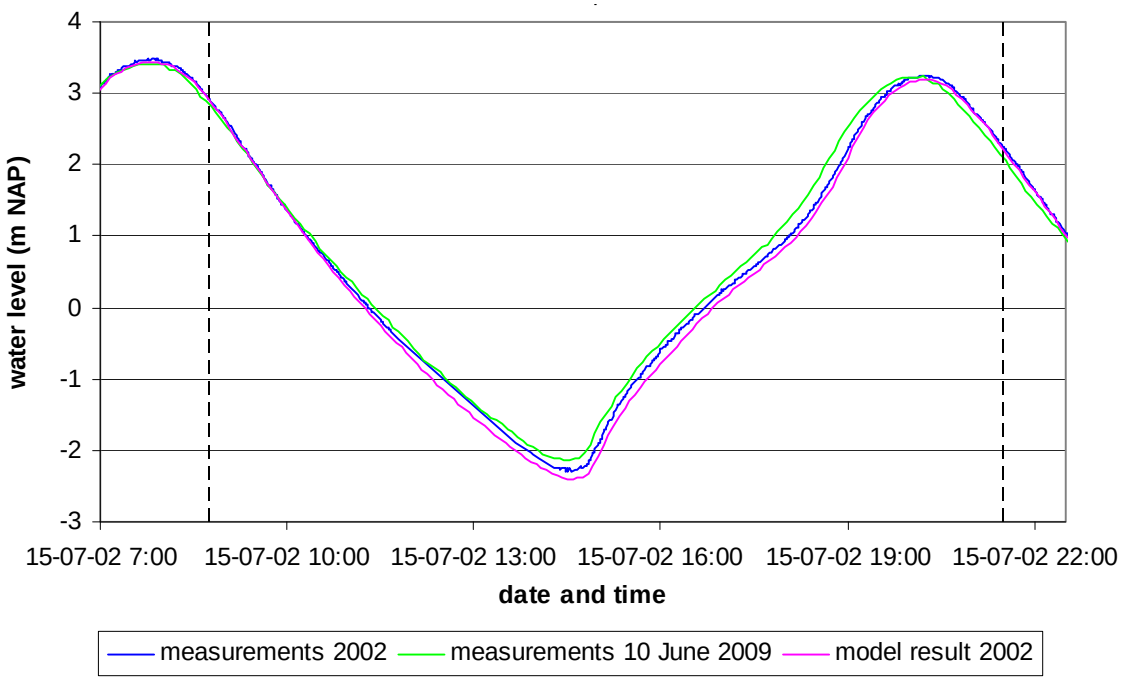

Figure 72 - Comparison of the water levels at Schelle in 2002 and 2009 for the calibration period

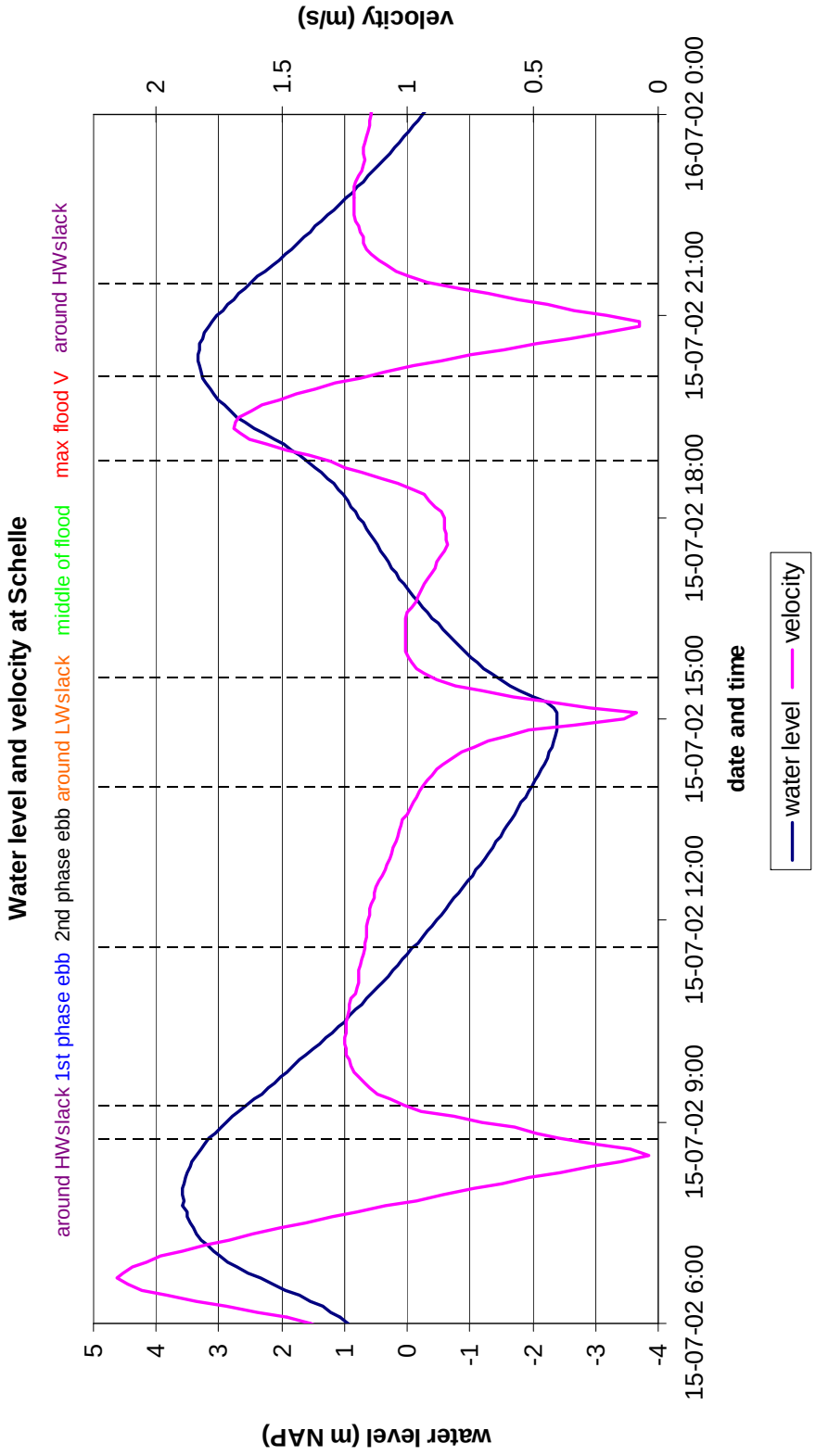

Figure 73 - Time periods for the comparison of the model results and measurements for the model calibration

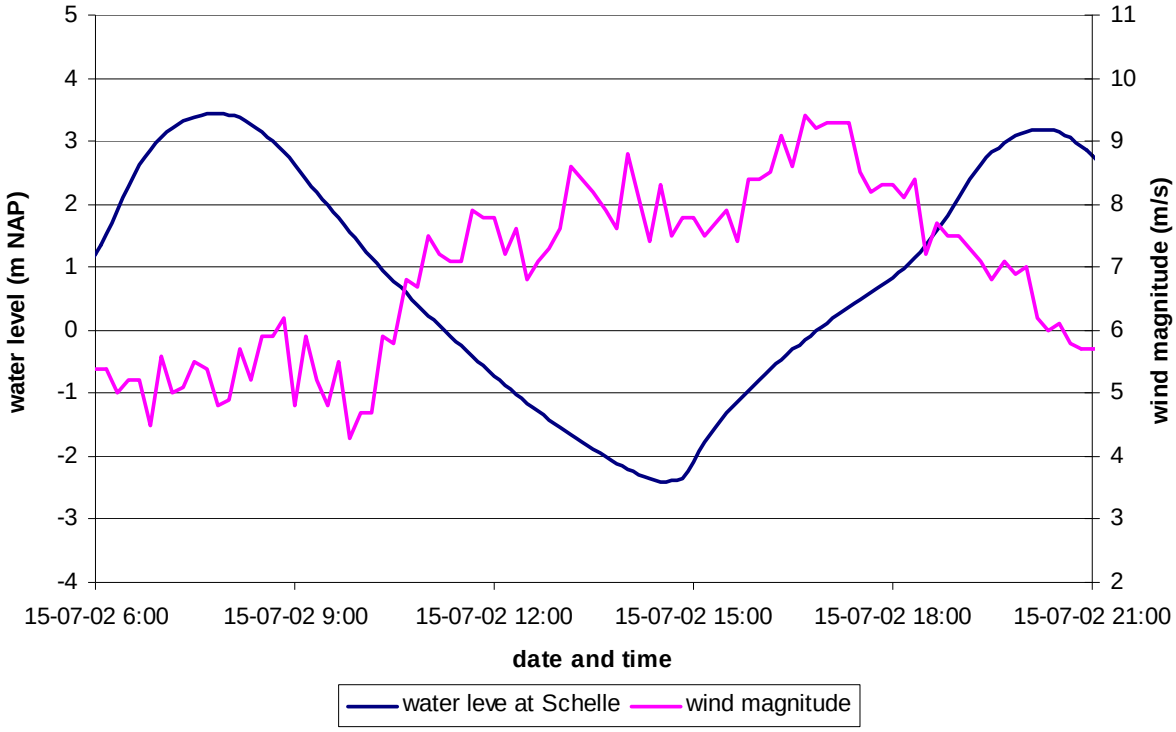

Figure 74 - Wind magnitude at Hansweert during the calibration period

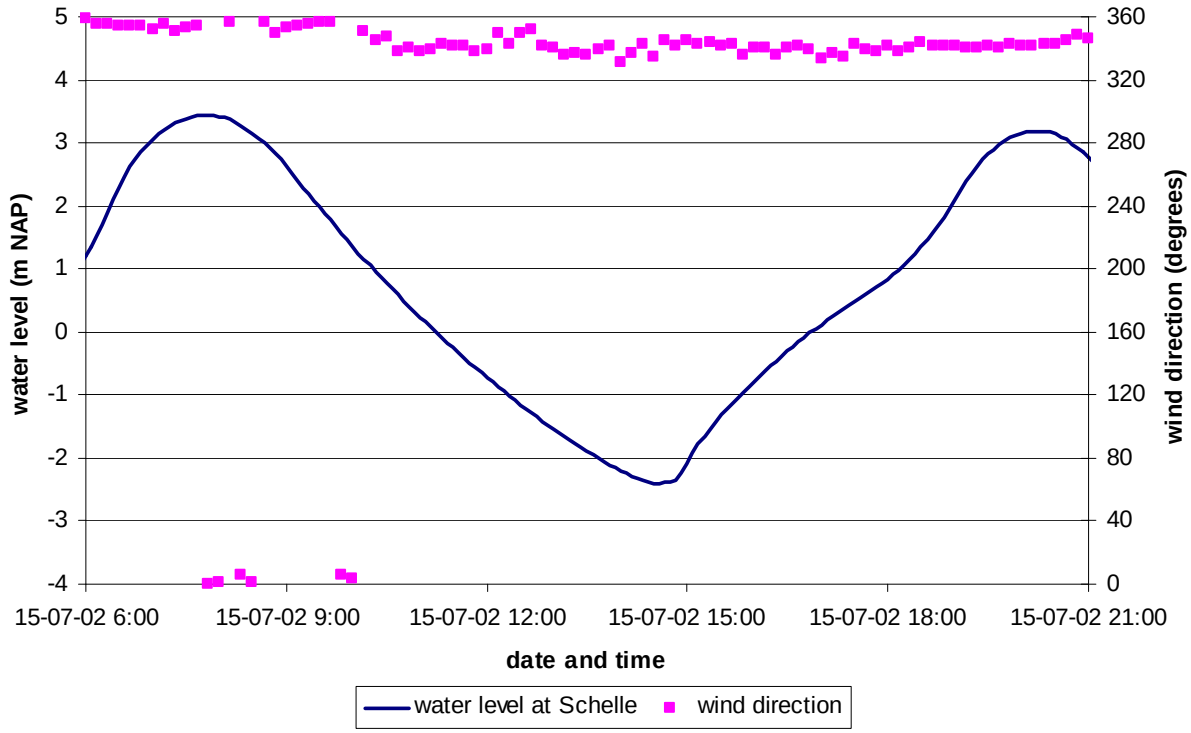

Figure 75 - Wind direction at Hansweert during the calibration period

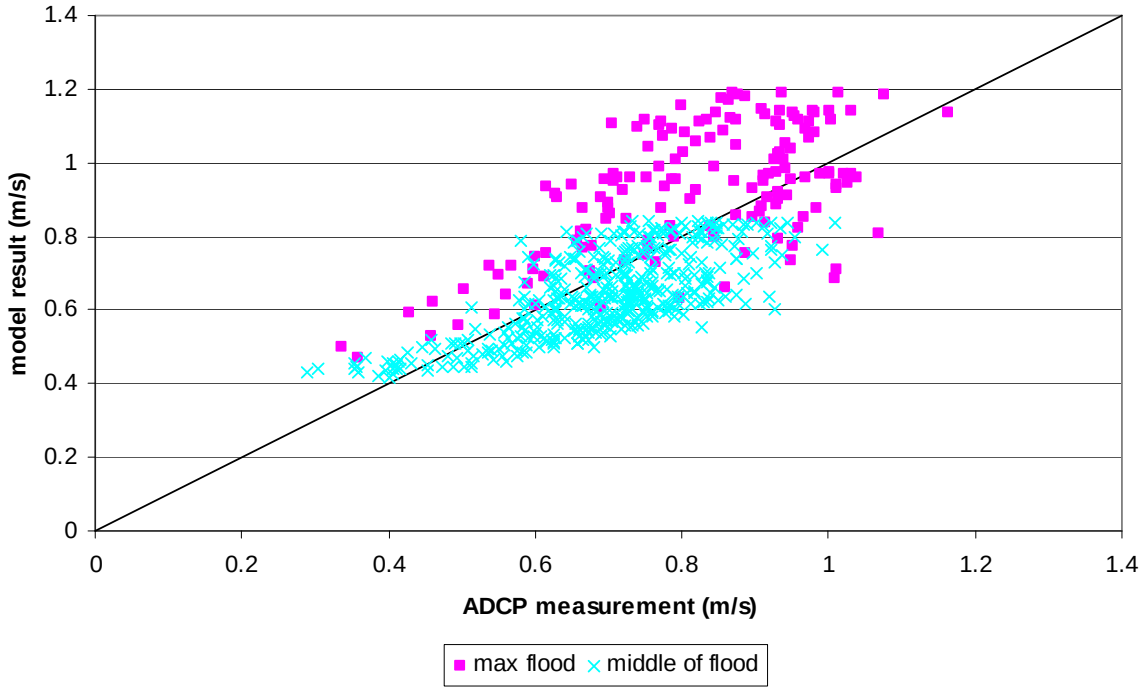

Figure 76 - Velocity magnitude for Ballooi – transverse profile in deep zone for flood
(model result DD3x3calibr11 vs ADCP measurement)

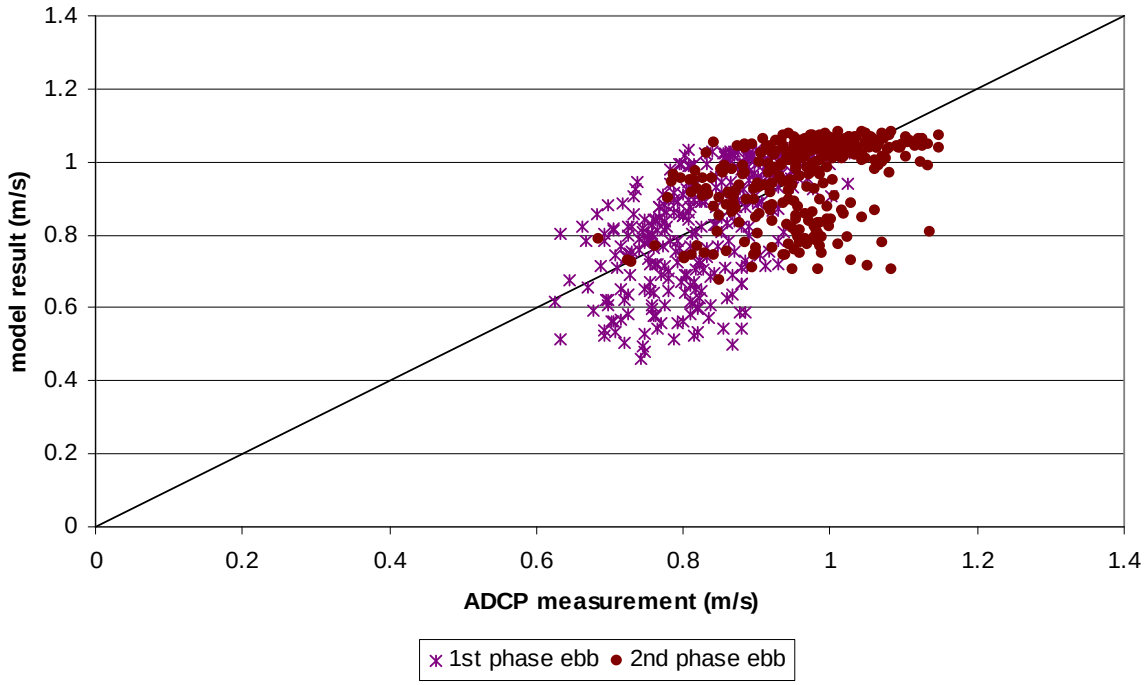

Figure 77 - Velocity magnitude for Ballooi – transverse profile in deep zone for ebb
(model result DD3x3calibr11 vs ADCP measurement)

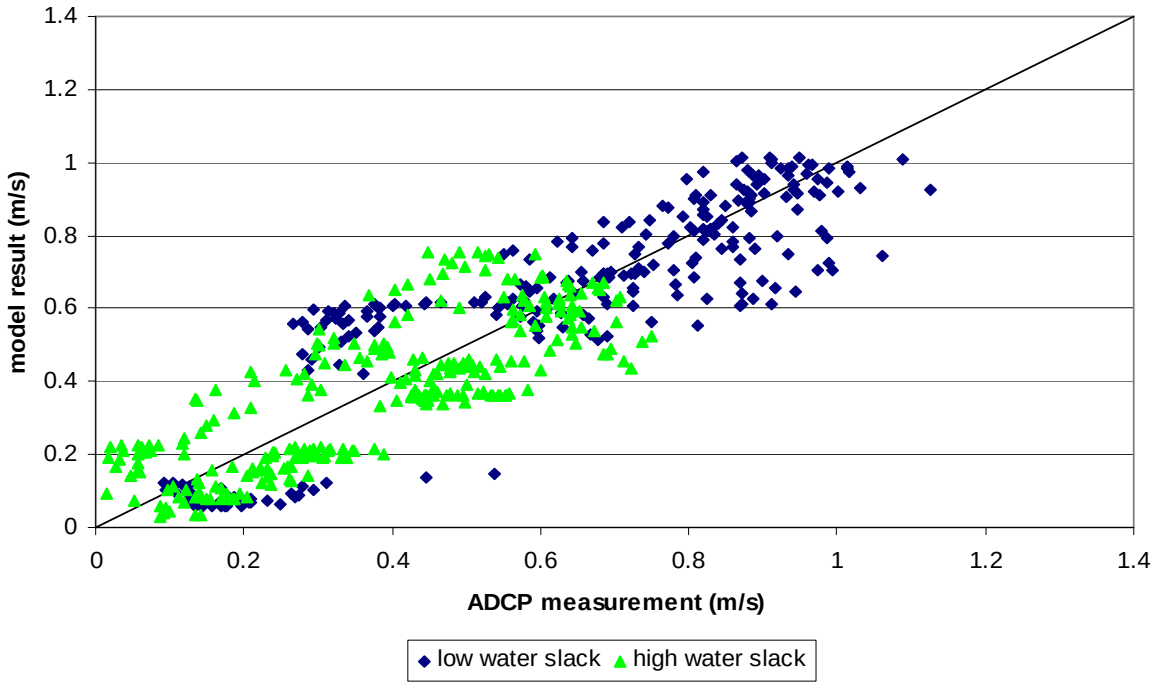

Figure 78 - Velocity magnitude for Ballooi – transverse profile in deep zone for slack
(model result DD3x3calibr11 vs ADCP measurement)

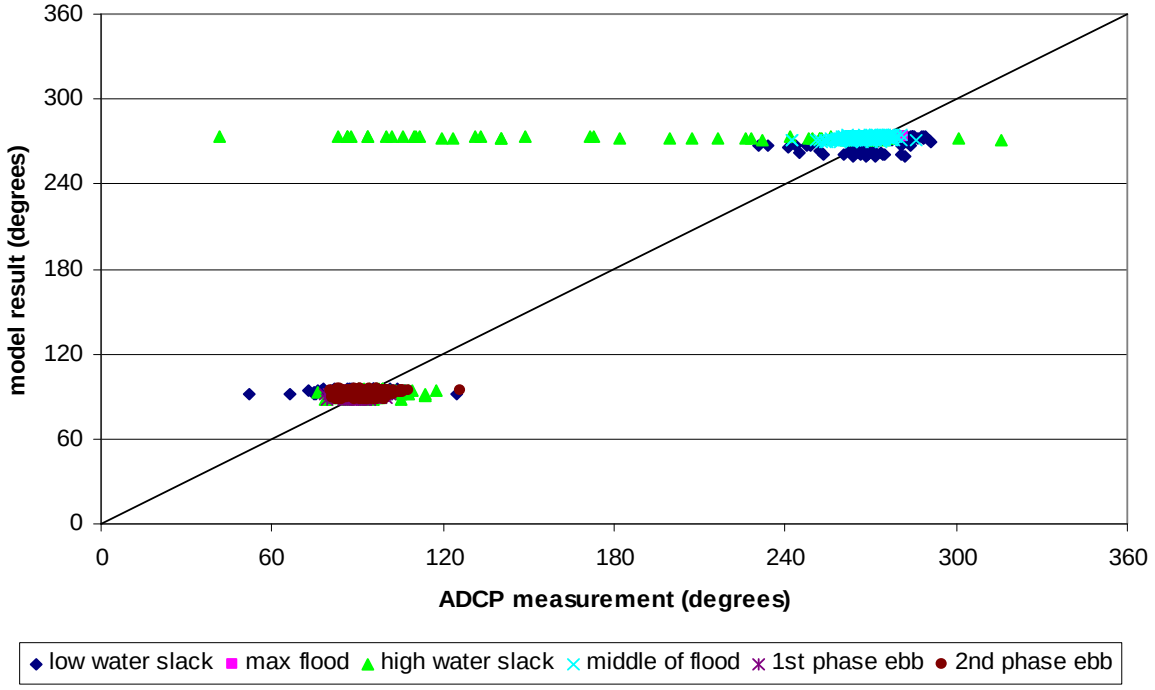

Figure 79 - Velocity direction for Ballooi – transverse profile in deep zone
(model result DD3x3calibr11 vs ADCP measurement)

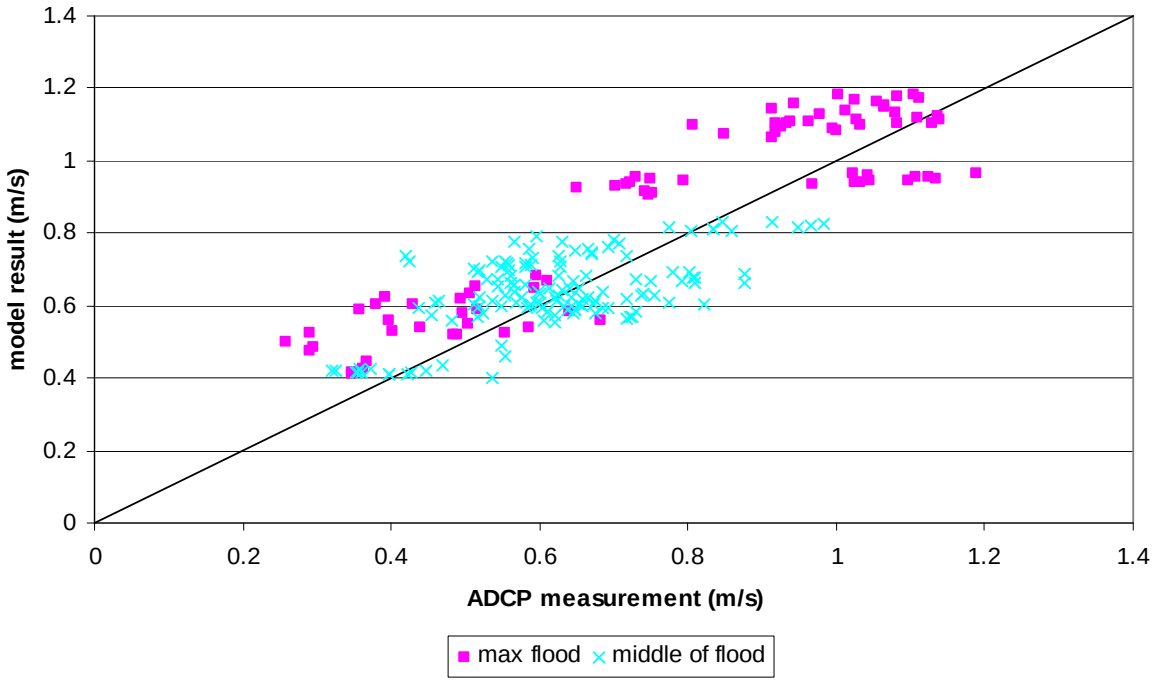

Figure 80 - Velocity magnitude for Ballooi – transverse profile in undeep zone for flood
(model result DD3x3calibr11 vs ADCP measurement)

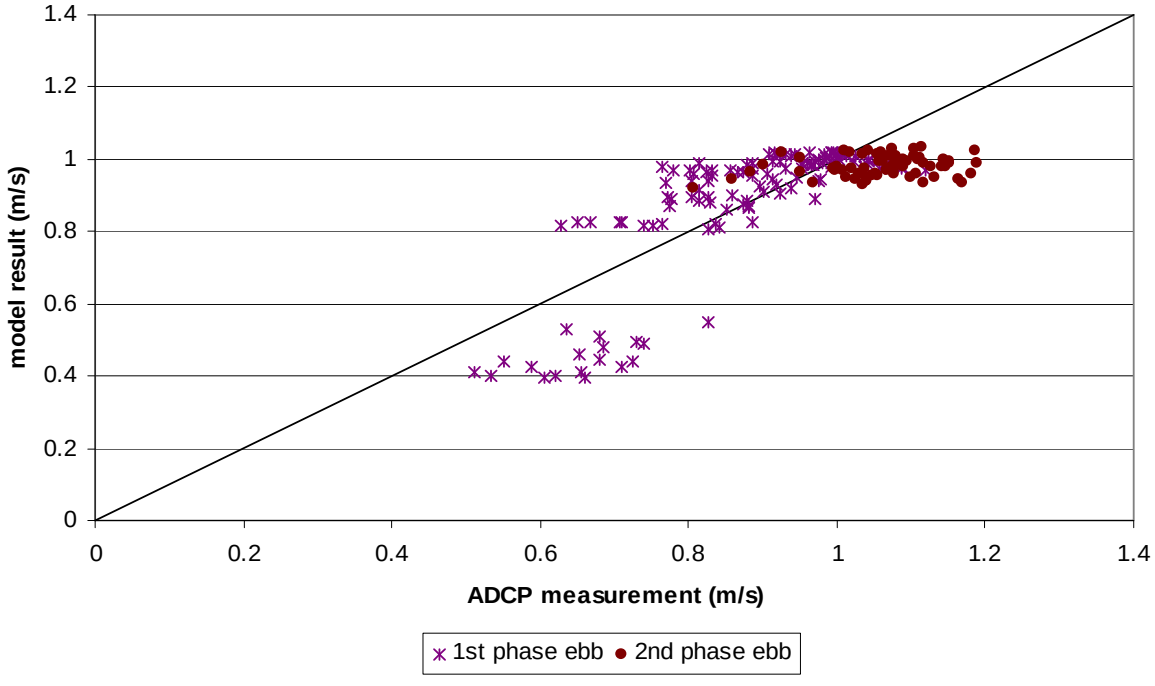

Figure 81 - Velocity magnitude for Ballooi – transverse profile in undeep zone for ebb
(model result DD3x3calibr11 vs ADCP measurement)

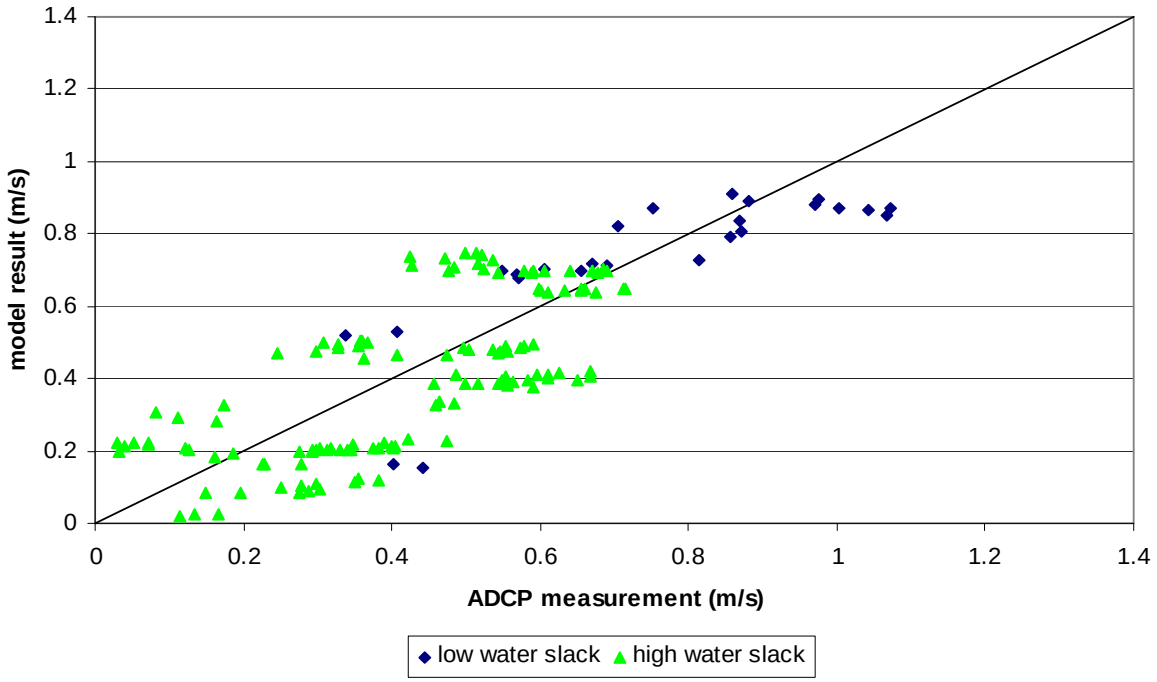

Figure 82 - Velocity magnitude for Ballooi – transverse profile in undeep zone for slack
(model result DD3x3calibr11 vs ADCP measurement)

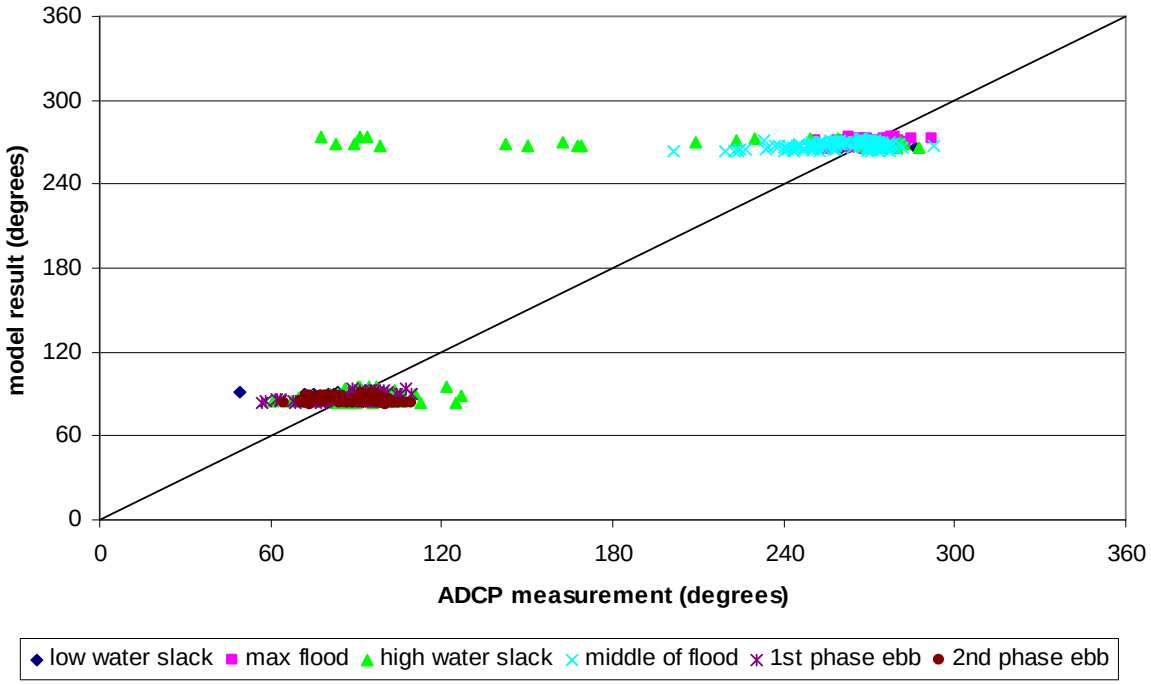

Figure 83 - Velocity direction for Ballooi – transverse profile in undeep zone
(model result DD3x3calibr11 vs ADCP measurement)

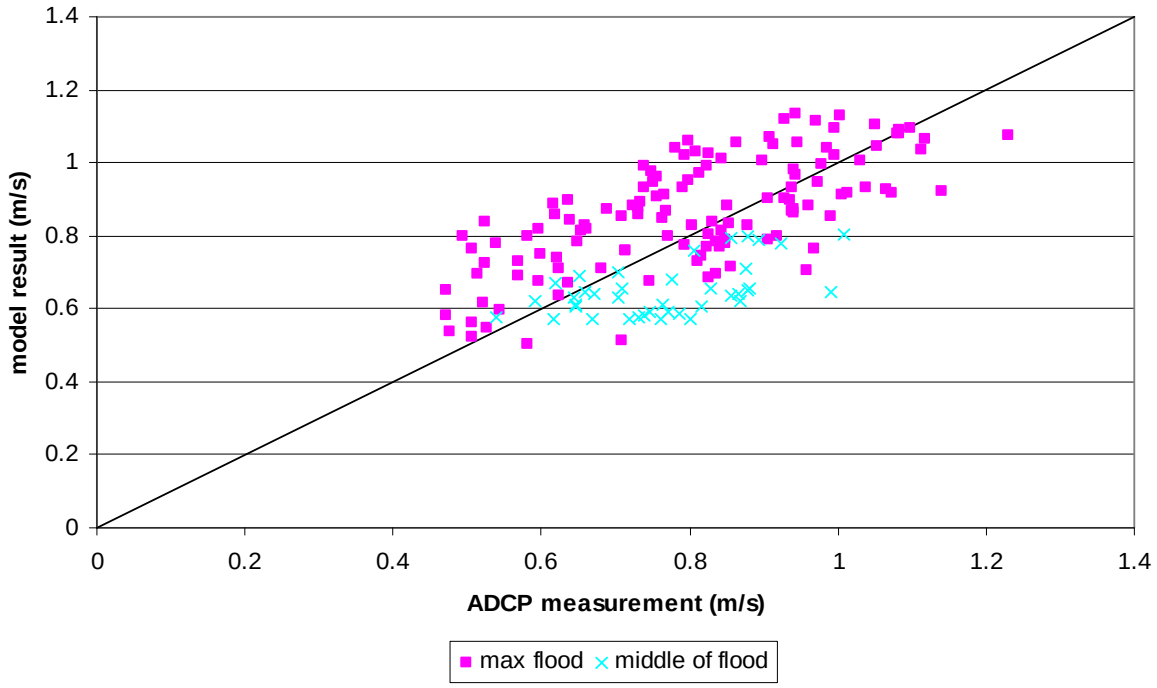

Figure 84 - Velocity magnitude for Ballooi – transverse profile in littoral zone for flood (model result DD3x3calibr11 vs ADCP measurement)

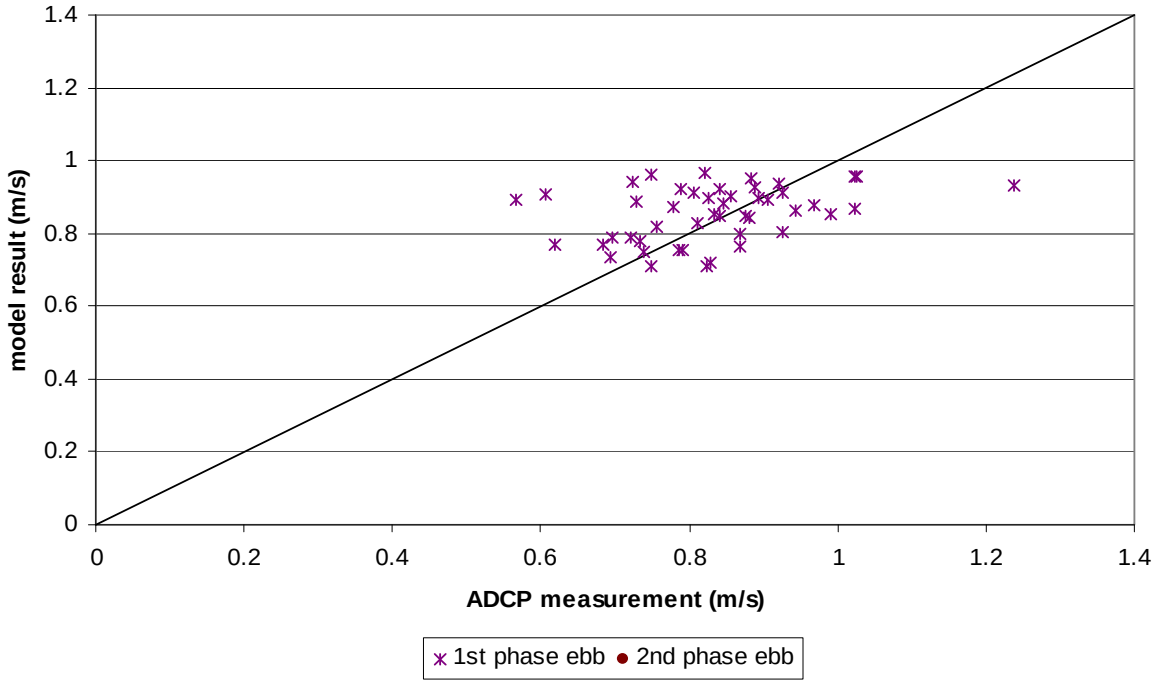

Figure 85 - Velocity magnitude for Ballooi – transverse profile in littoral zone for ebb (model result DD3x3calibr11 vs ADCP measurement)

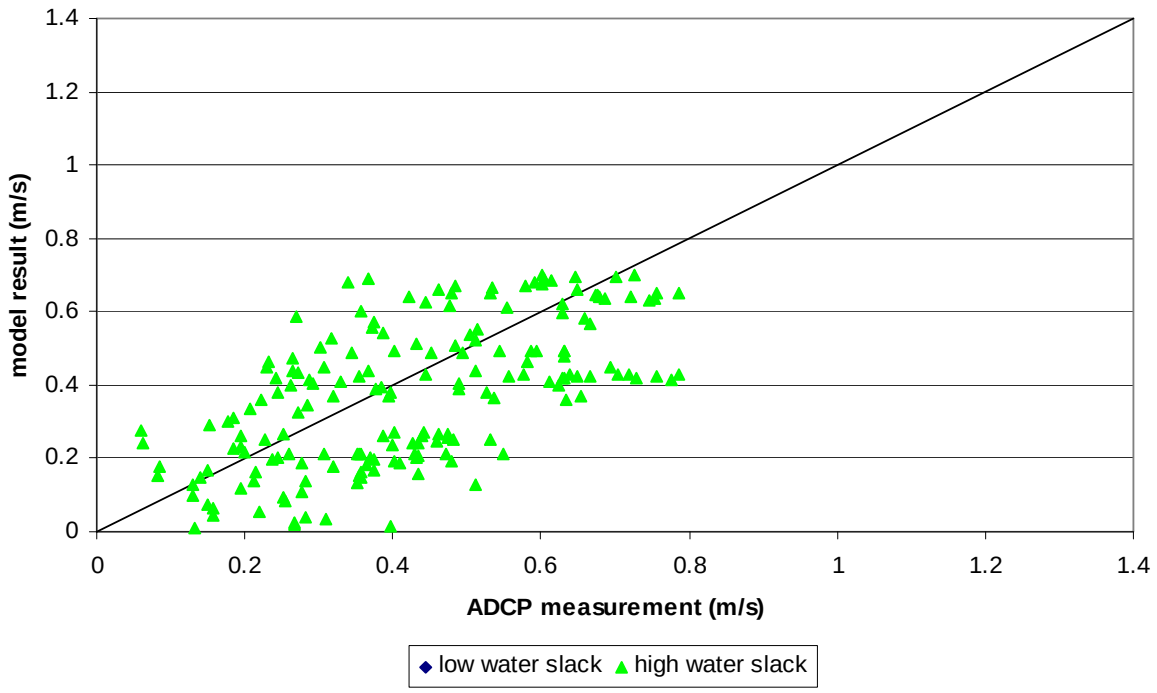

Figure 86 - Velocity magnitude for Ballooi – transverse profile in littoral zone for slack (model result DD3x3calibr11 vs ADCP measurement)

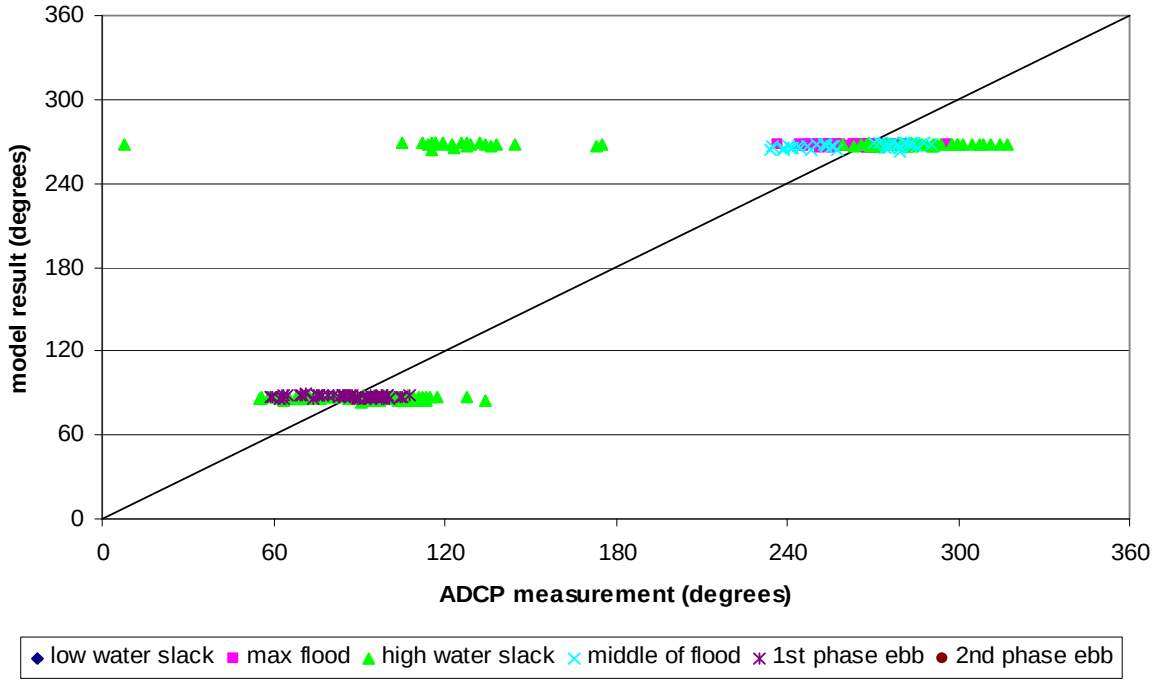

Figure 87 - Velocity direction for Ballooi – transverse profile in littoral zone (model result DD3x3calibr11 vs ADCP measurement)

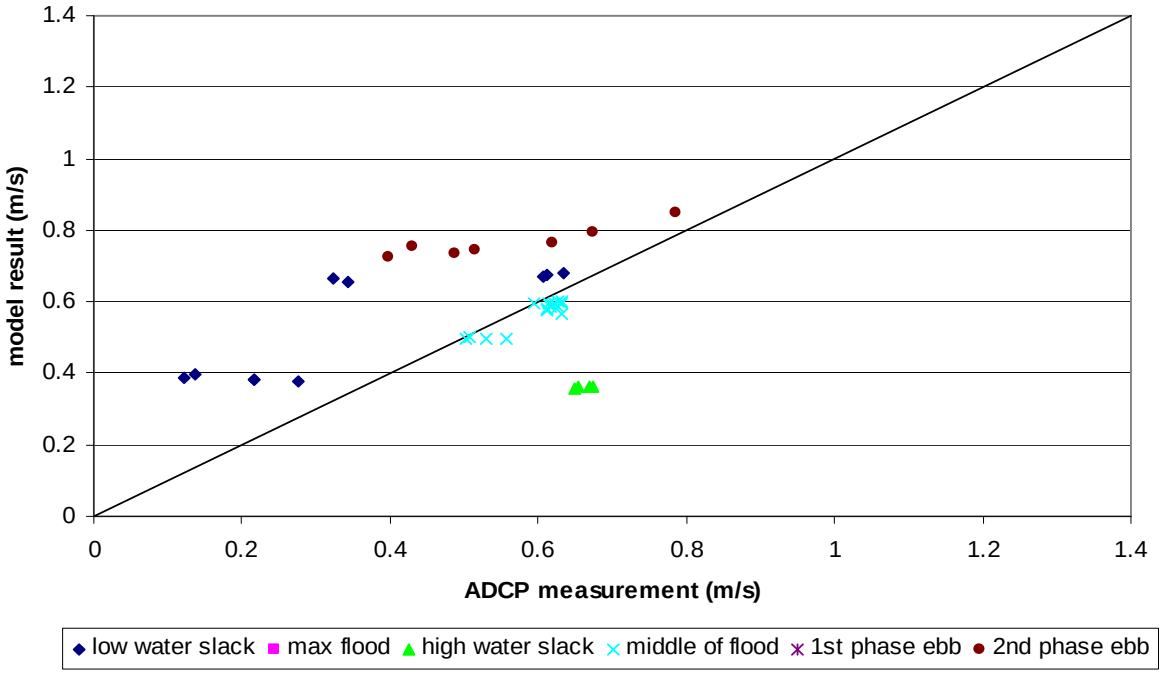

Figure 88 - Velocity magnitude for Notelaer – longitudinal profile in deep zone
(model result DD3x3calibr11 vs ADCP measurement)

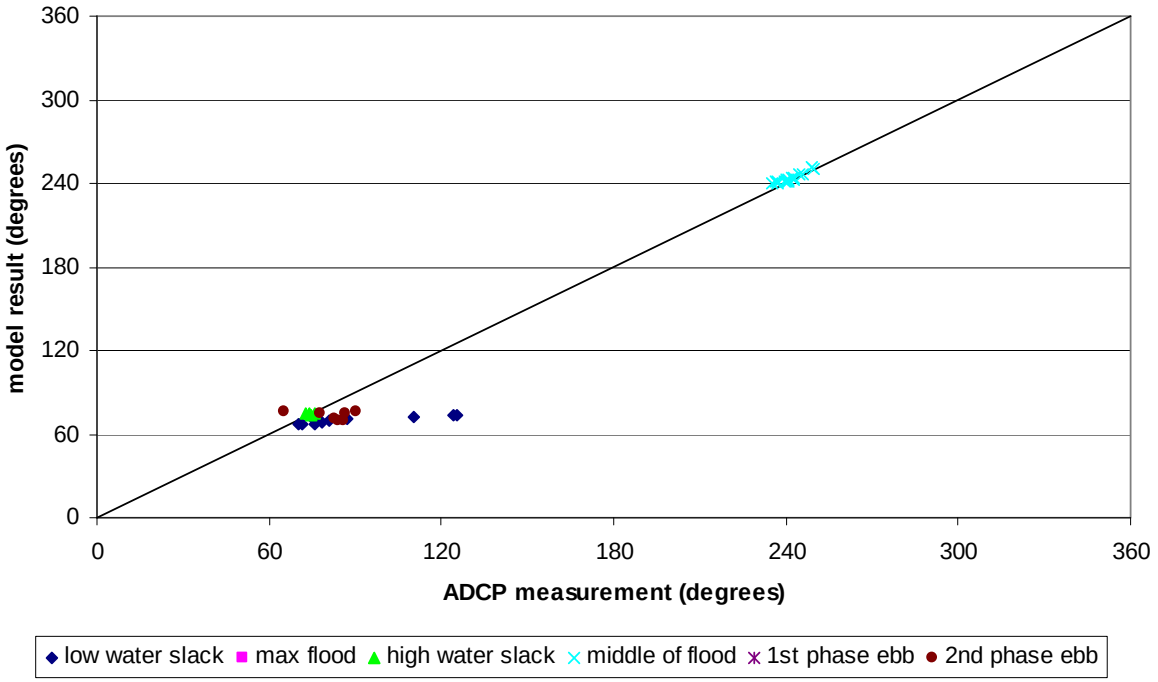

Figure 89 - Velocity direction for Notelaer – longitudinal profile in deep zone
(model result DD3x3calibr11 vs ADCP measurement)

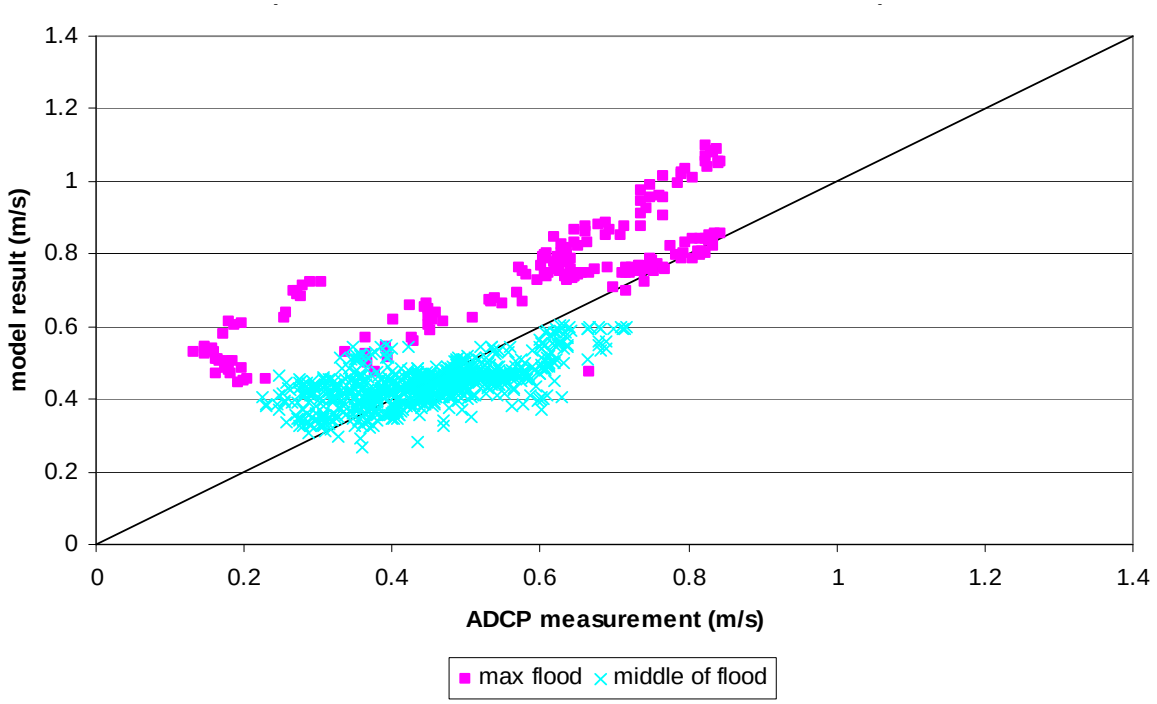

Figure 90 - Velocity magnitude for Notelaer – longitudinal profile in undeep zone for flood
(model result DD3x3calibr11 vs ADCP measurement)

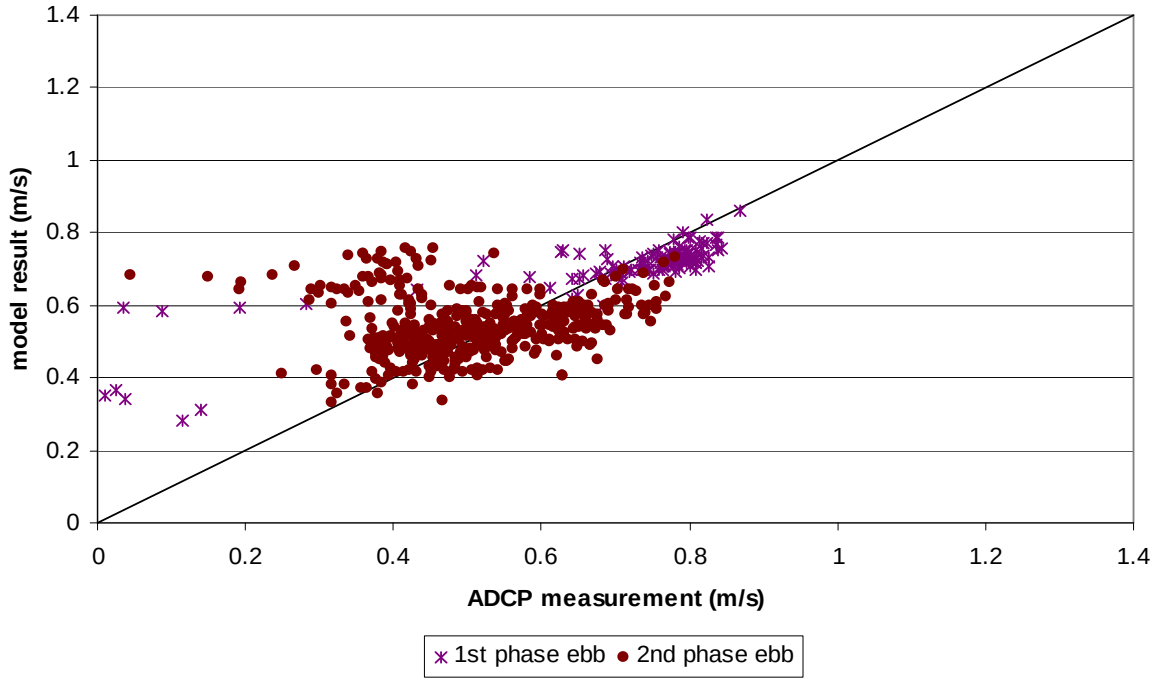

Figure 91 - Velocity magnitude for Notelaer – longitudinal profile in undeep zone for ebb
(model result DD3x3calibr11 vs ADCP measurement)

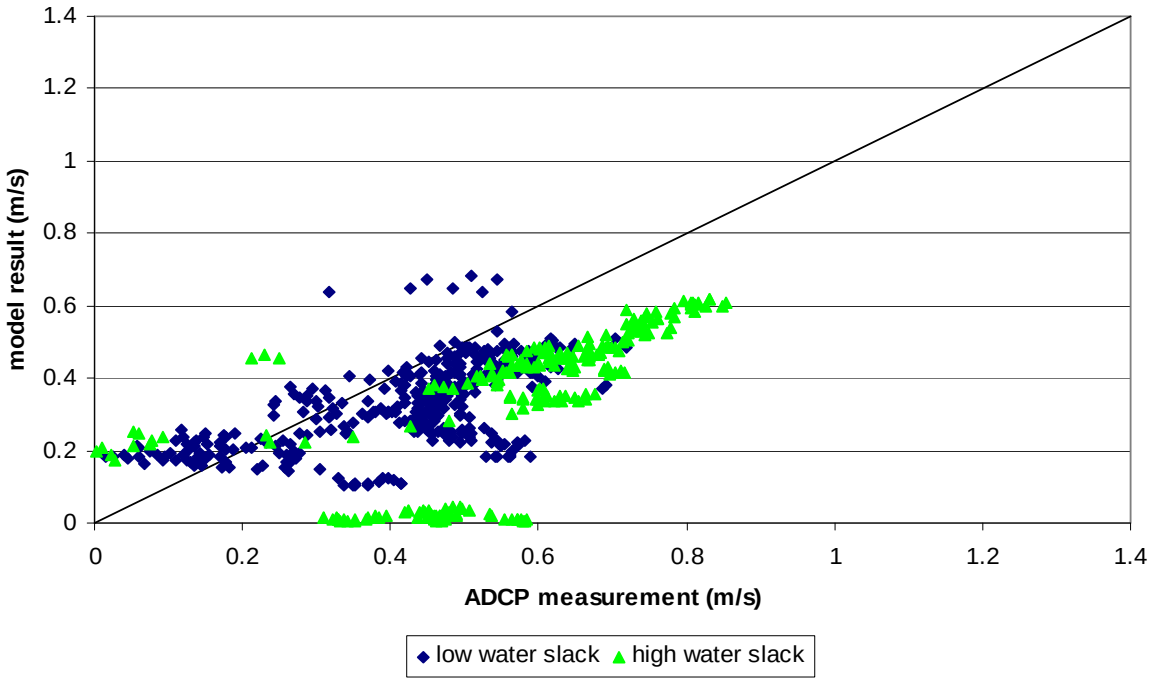

Figure 92 - Velocity magnitude for Notelaer – longitudinal profile in undeep zone for slack
(model result DD3x3calibr11 vs ADCP measurement)

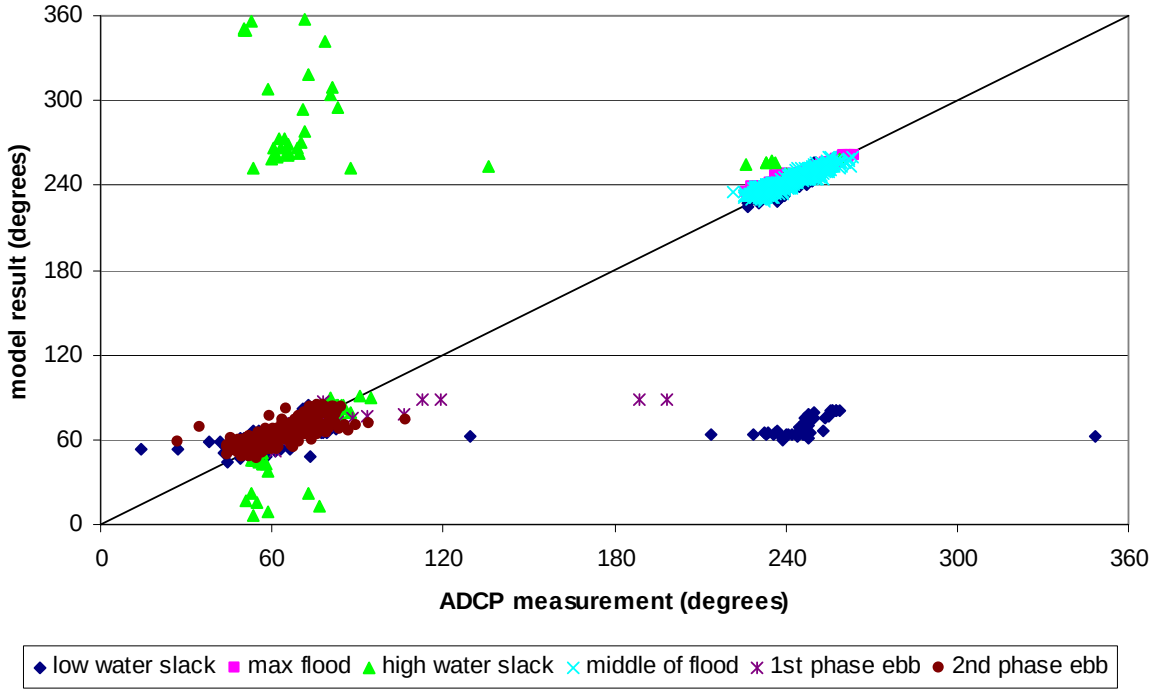

Figure 93 - Velocity direction for Notelaer – longitudinal profile in undeep zone
(model result DD3x3calibr11 vs ADCP measurement)

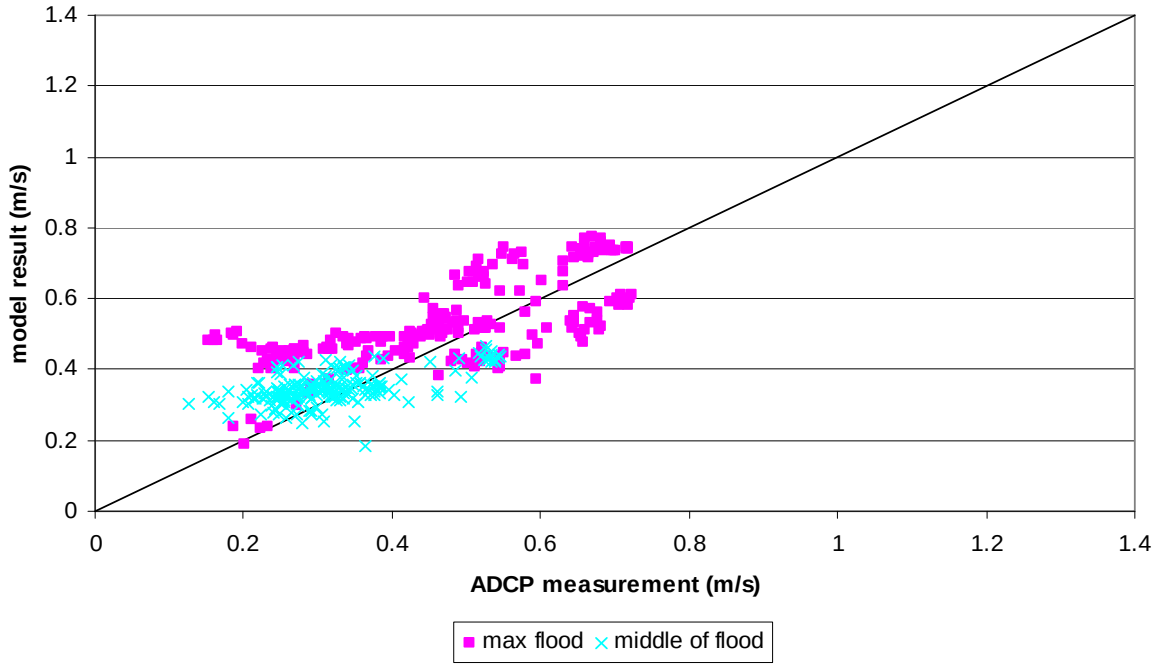

Figure 94 - Velocity magnitude for Notelaer – longitudinal profile in littoral zone for flood
(model result DD3x3calibr11 vs ADCP measurement)

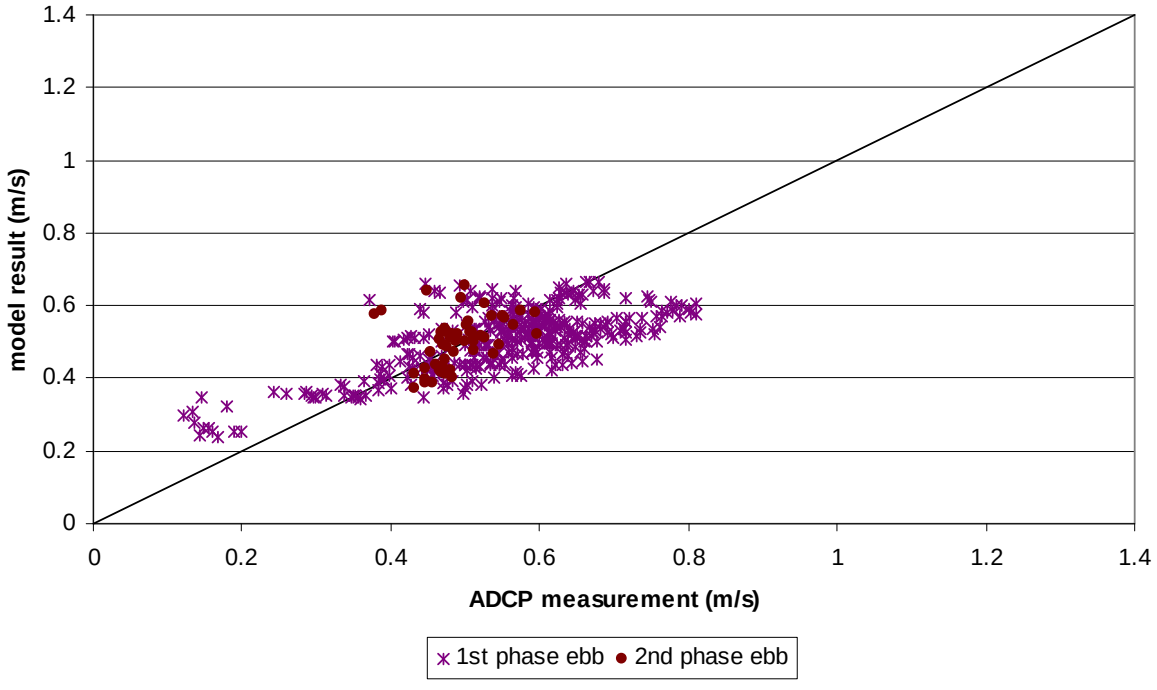

Figure 95 - Velocity magnitude for Notelaer – longitudinal profile in littoral zone for ebb
(model result DD3x3calibr11 vs ADCP measurement)

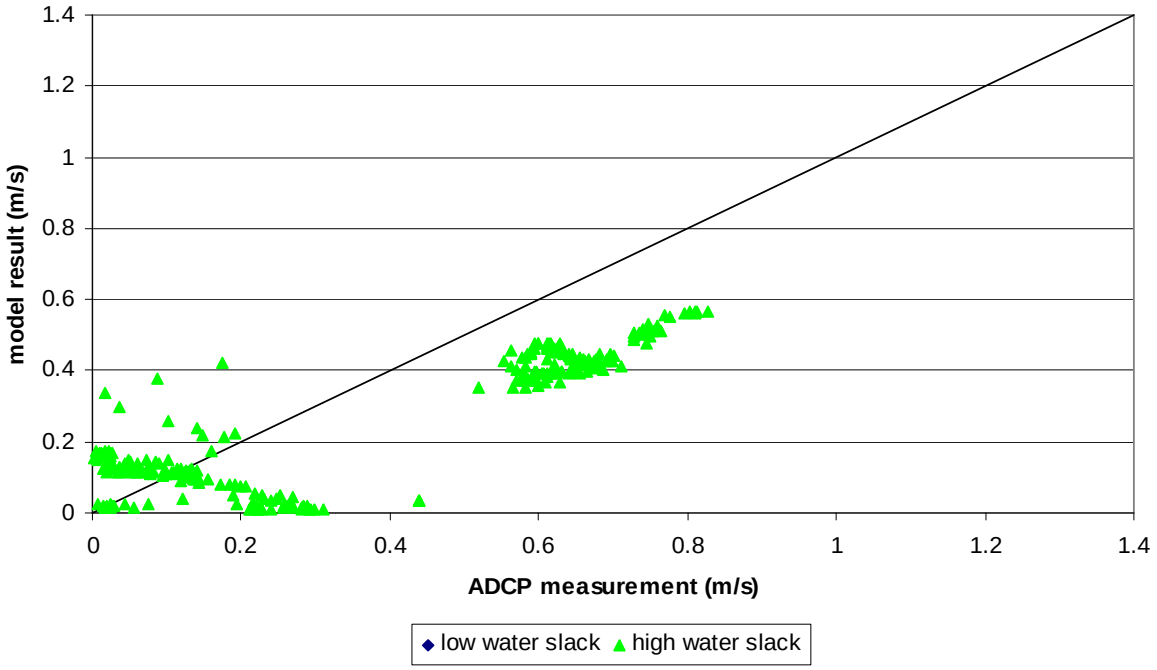

Figure 96 - Velocity magnitude for Notelaer – longitudinal profile in littoral zone for slack
(model result DD3x3calibr11 vs ADCP measurement)

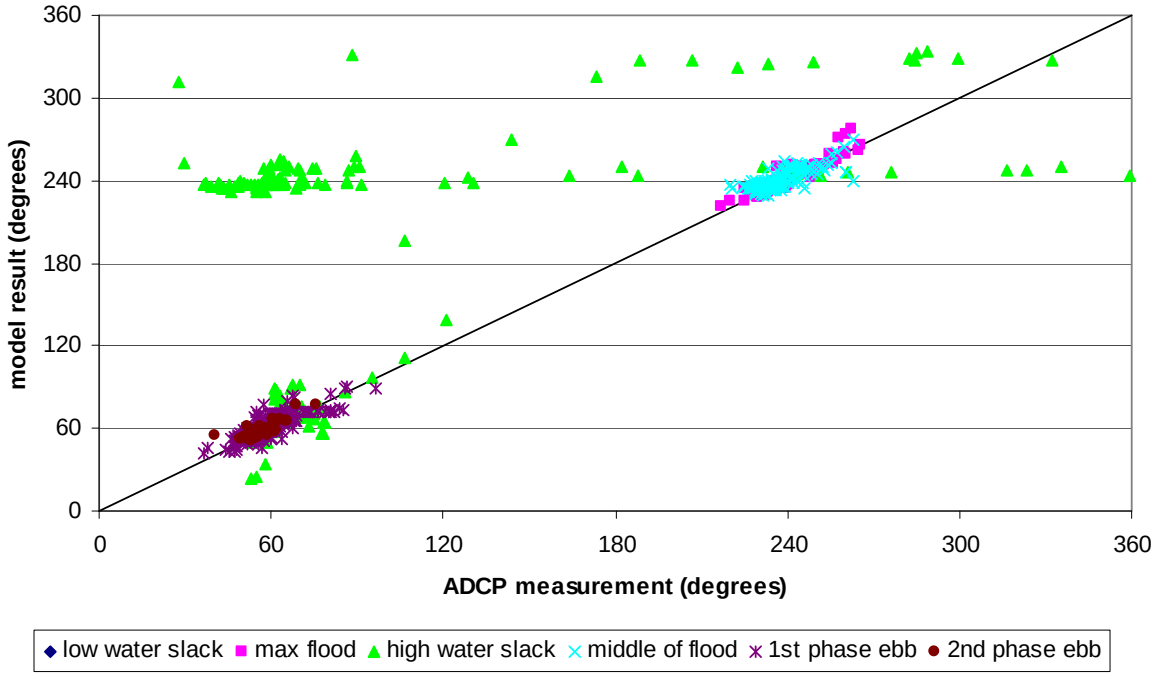

Figure 97 - Velocity direction for Notelaer – longitudinal profile in littoral zone
(model result DD3x3calibr11 vs ADCP measurement)

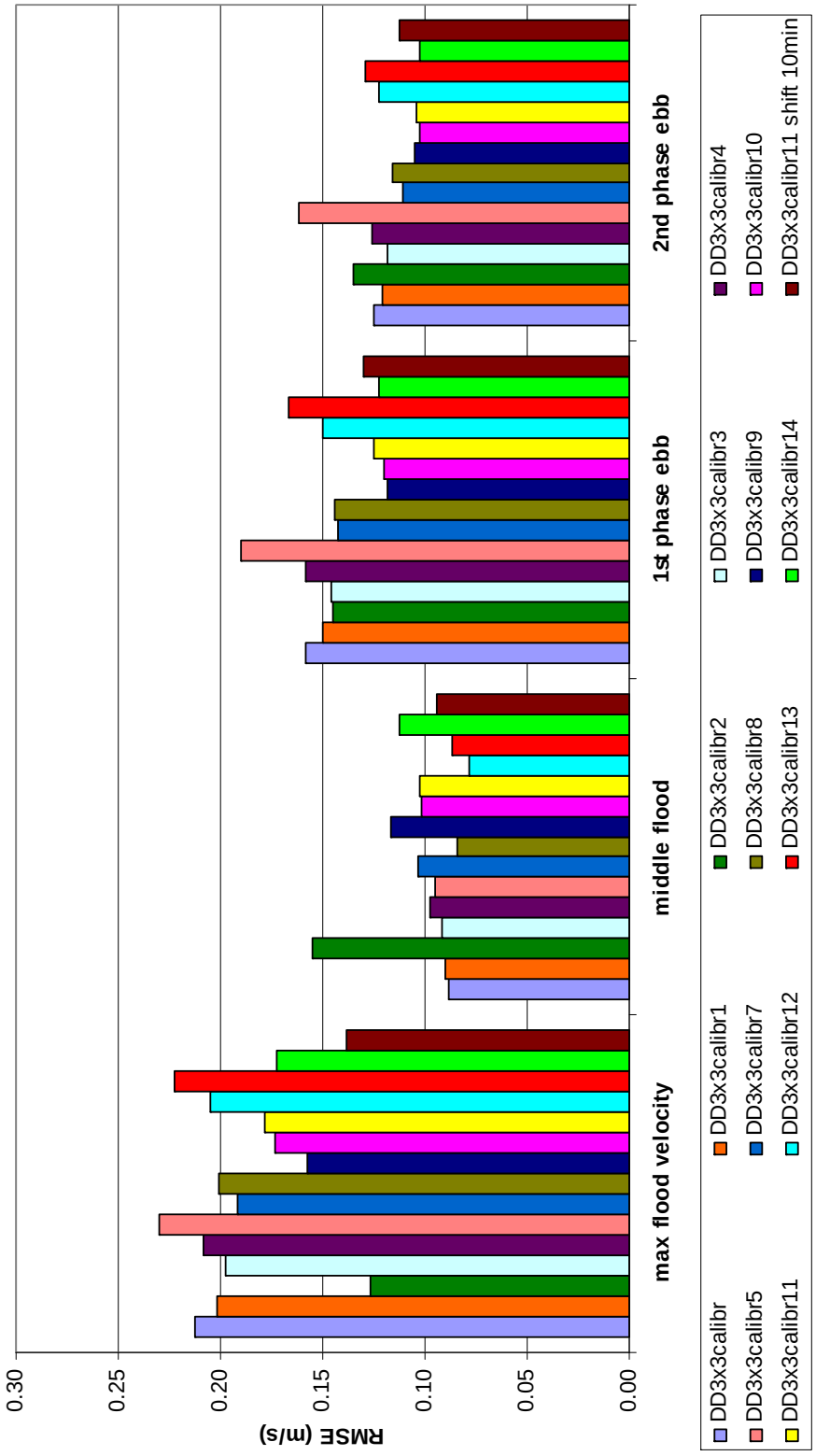

Figure 98 - Root mean squared error in the deep zone for the Ballooi – transverse profile

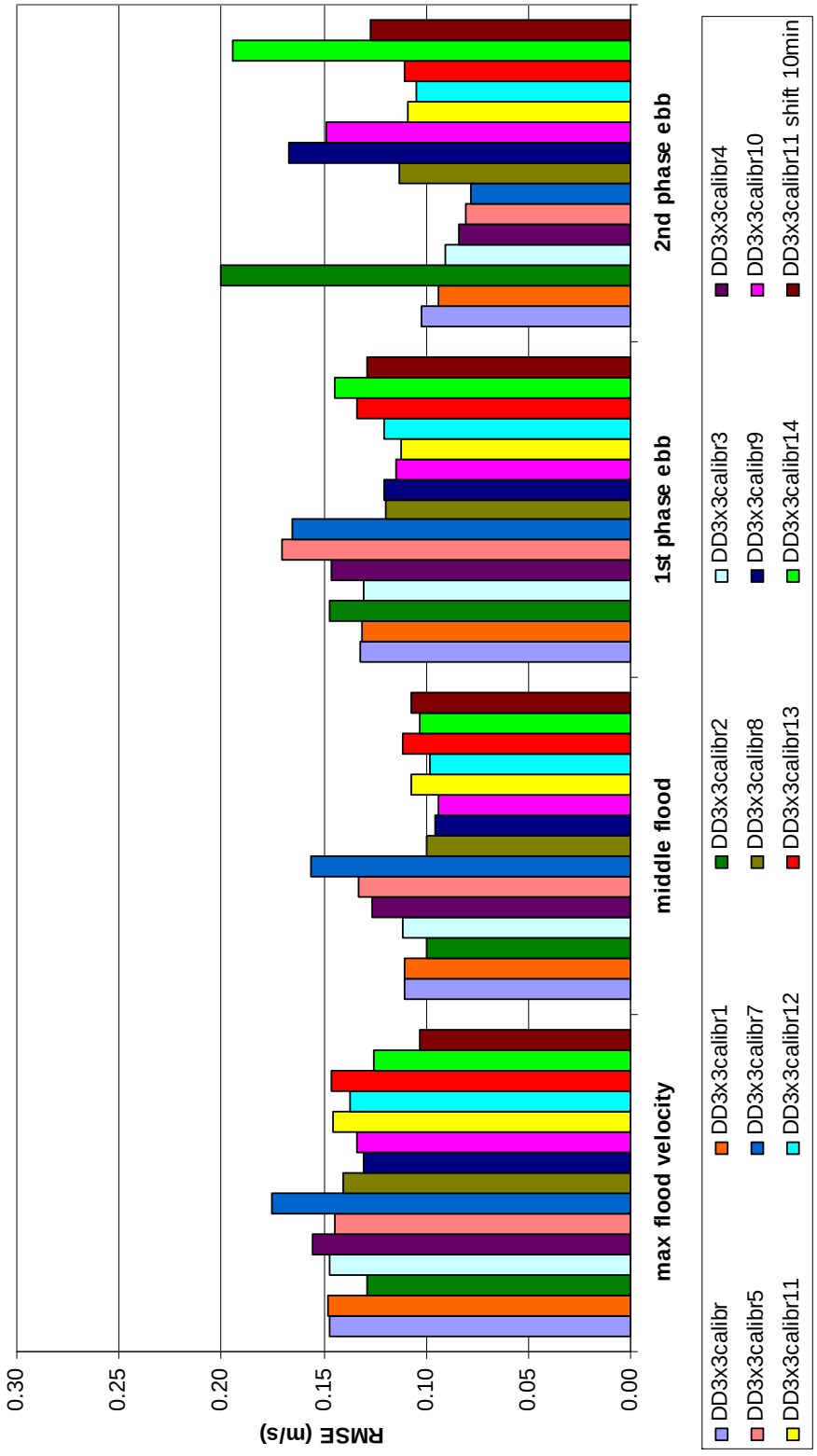

Figure 99 - Root mean squared error in the undeep zone for the Ballooi – transverse profile

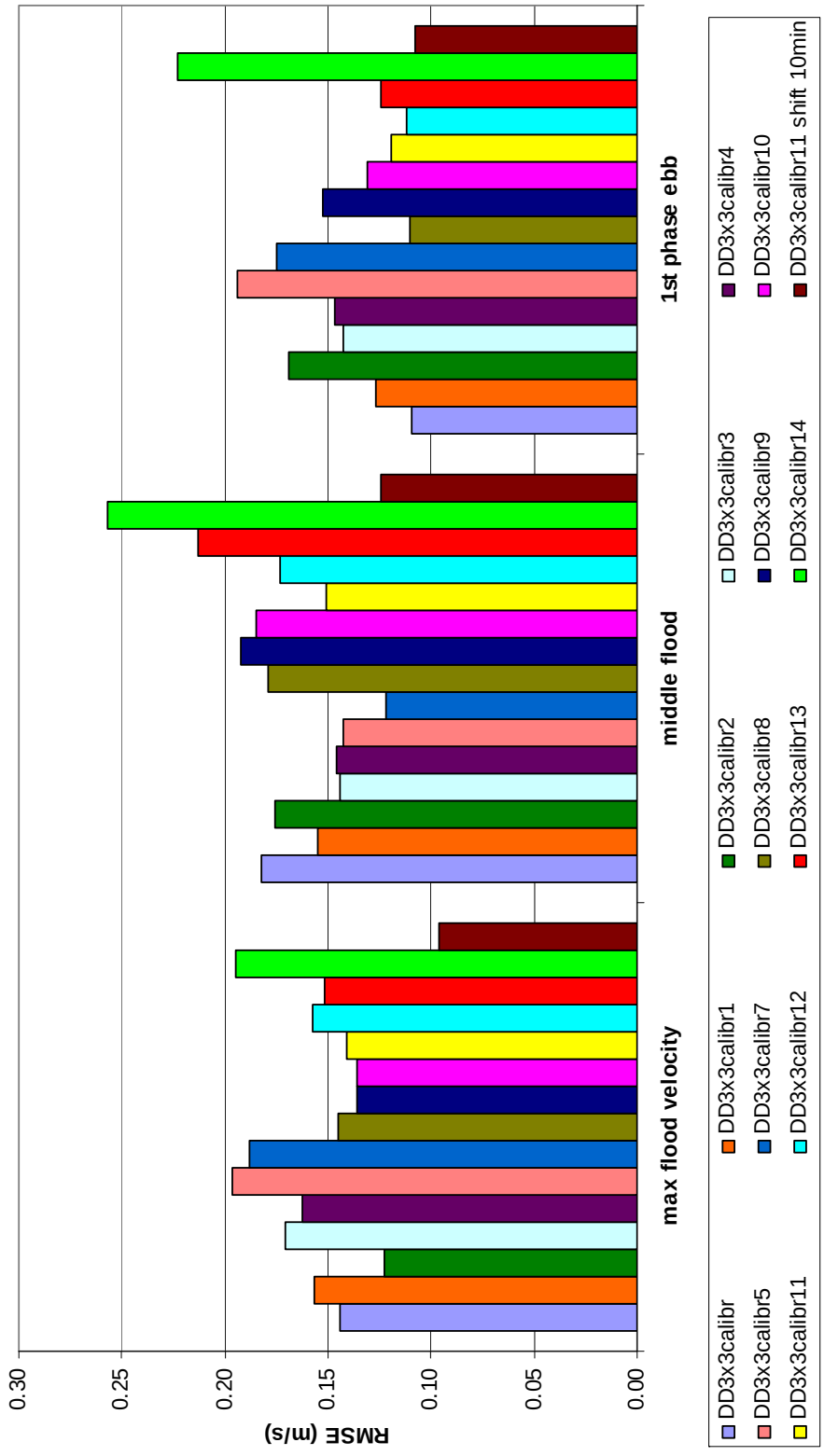

Figure 100 - Root mean squared error in the littoral zone for the Ballooi – transverse profile

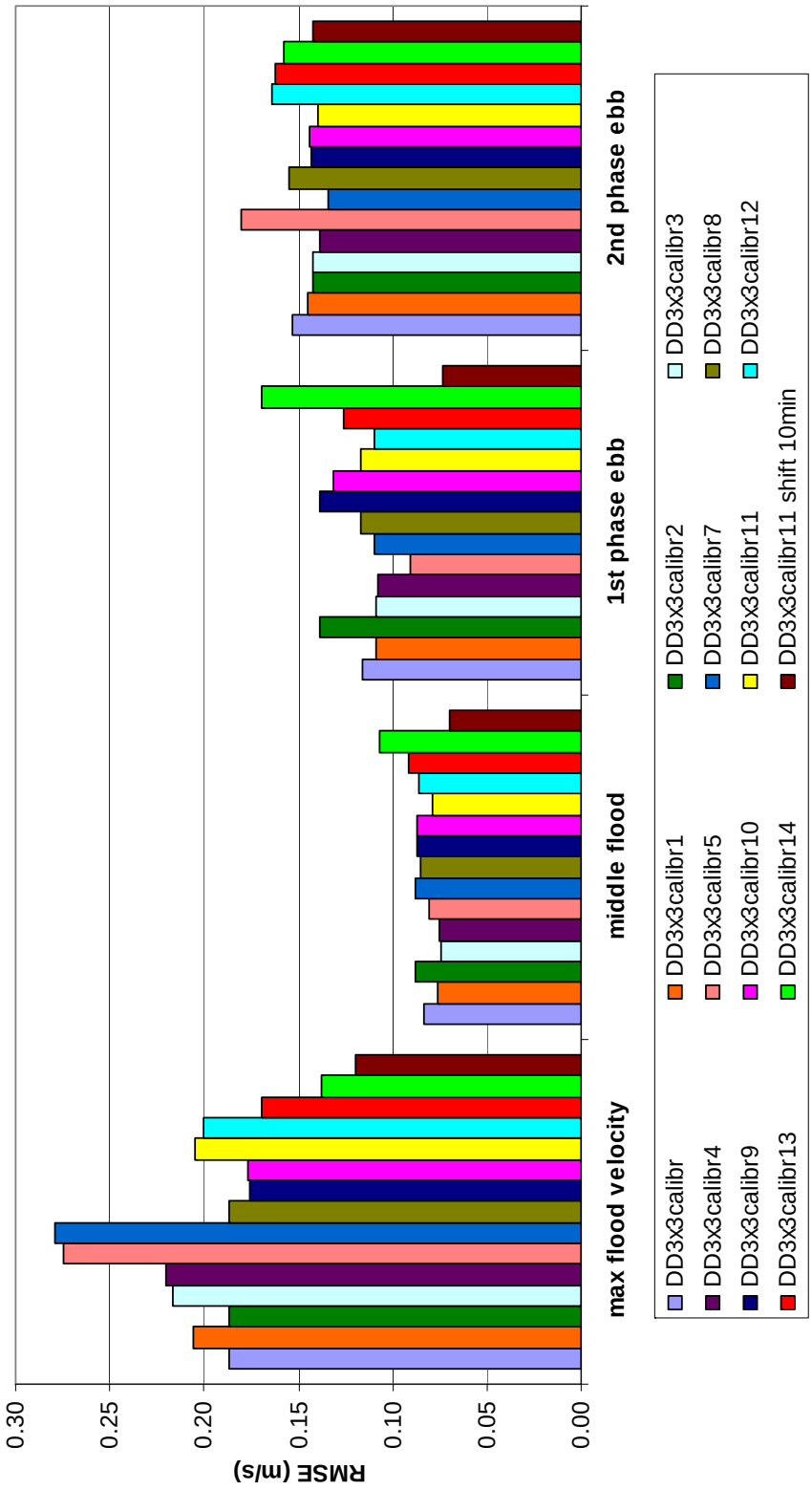

Figure 101 - Root mean squared error in the undeep zone for the Notelaer – longitudinal profile

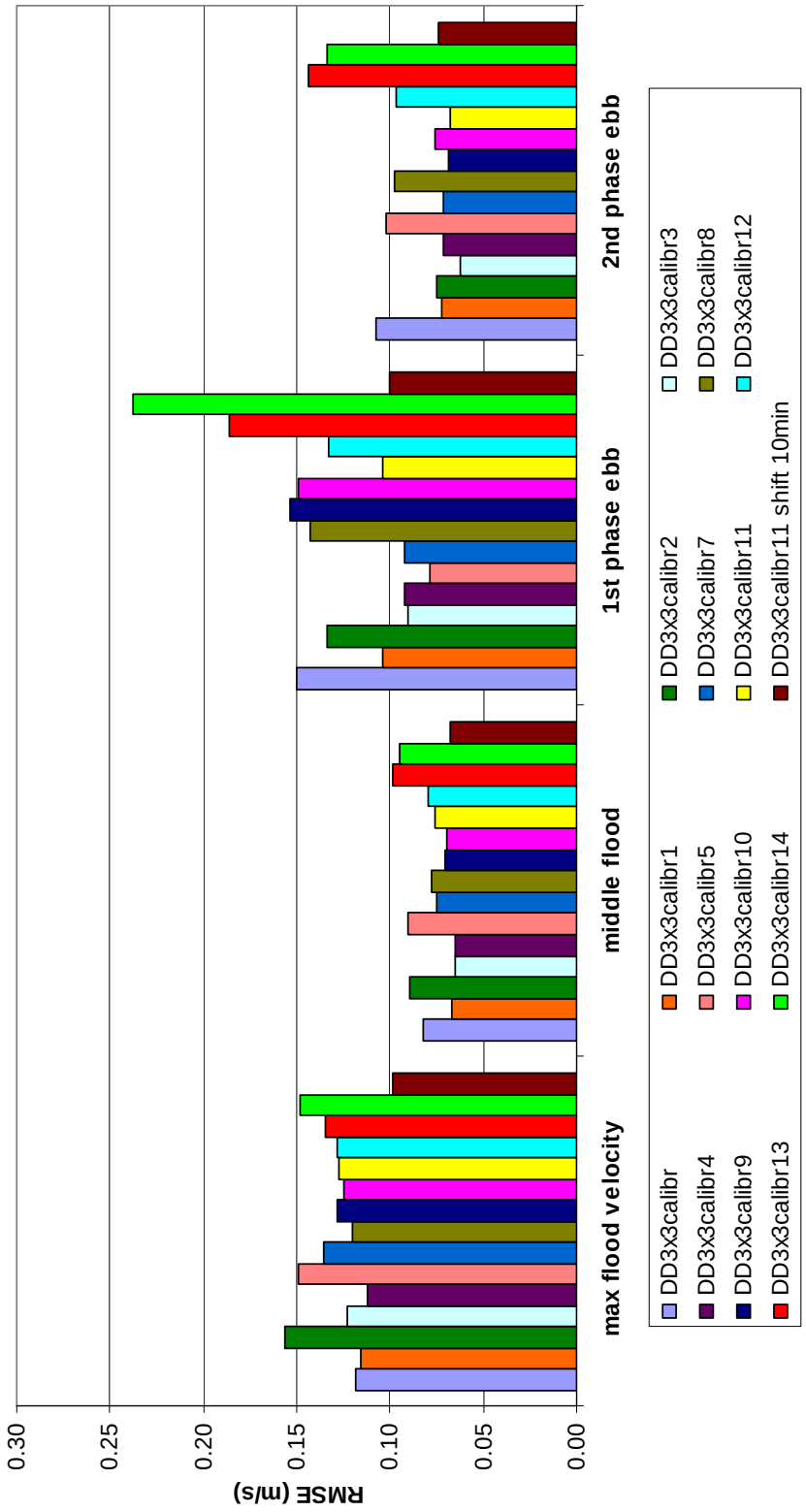

Figure 102 - Root mean squared error in the littoral zone for the Notelaer – longitudinal profile

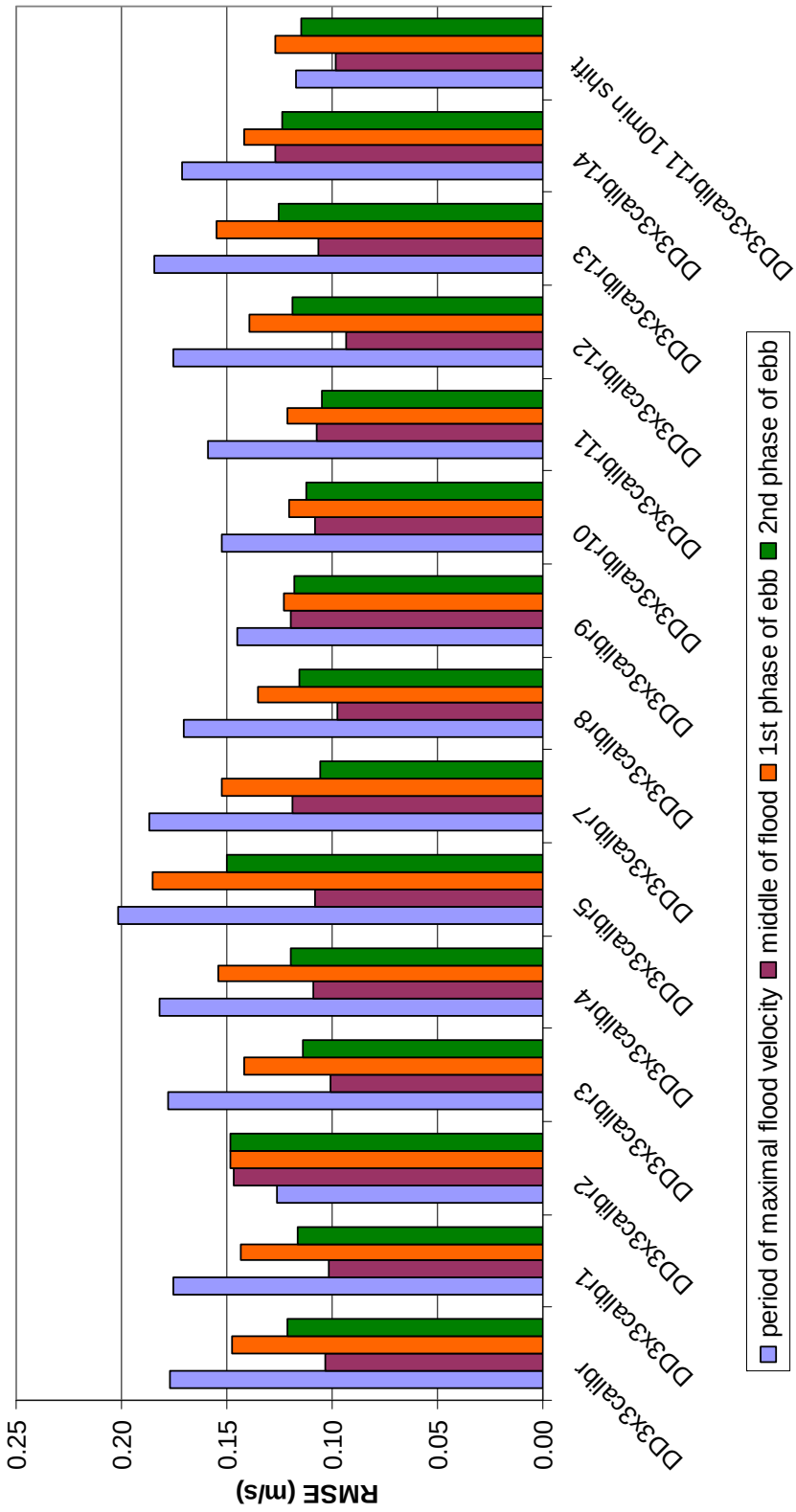

Figure 103 - Root mean squared errors for different tidal periods for the Ballooi – transverse profile

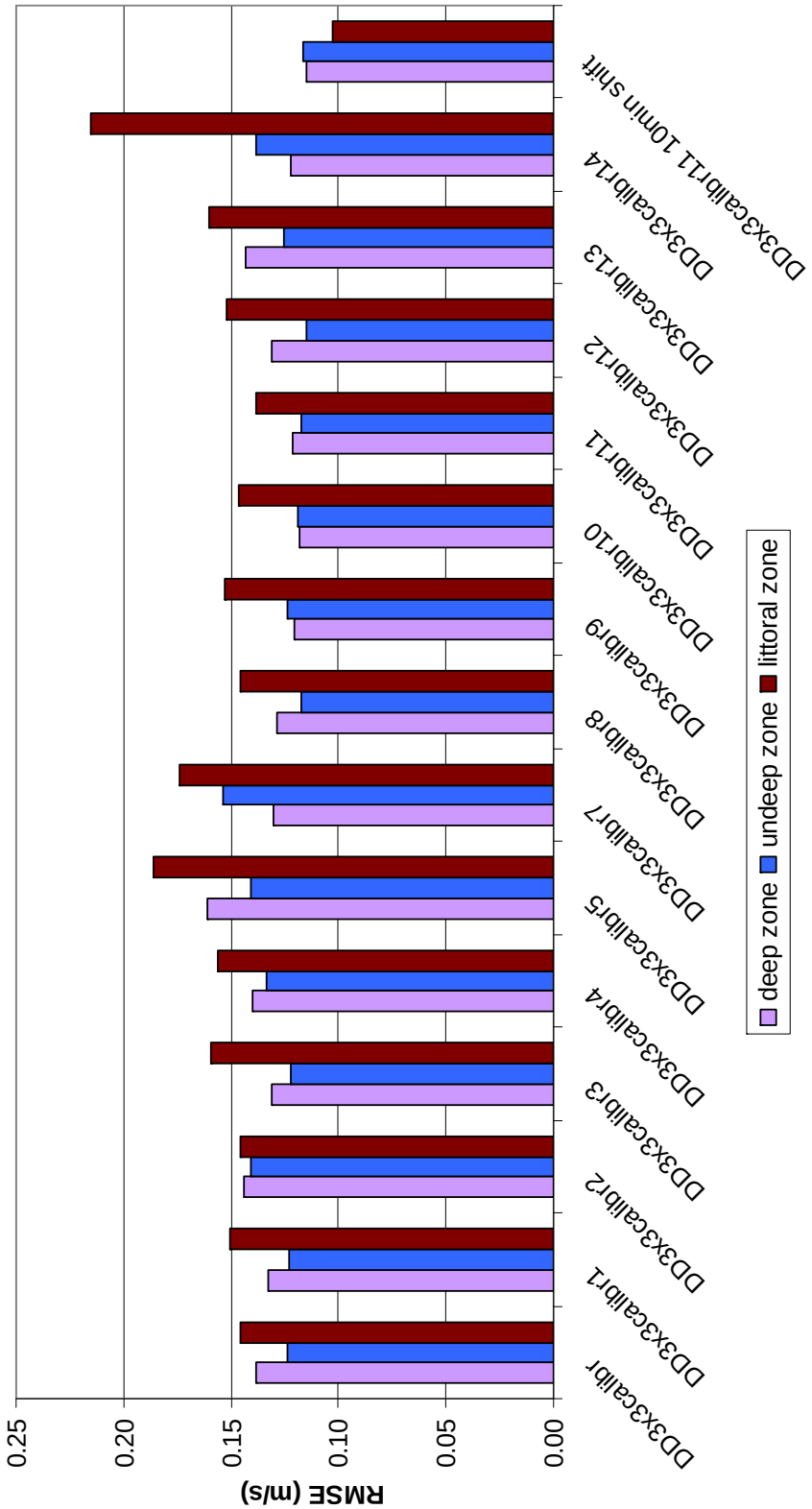

Figure 104 - Root mean squared errors for different depth zones for the Ballooi – transverse profile

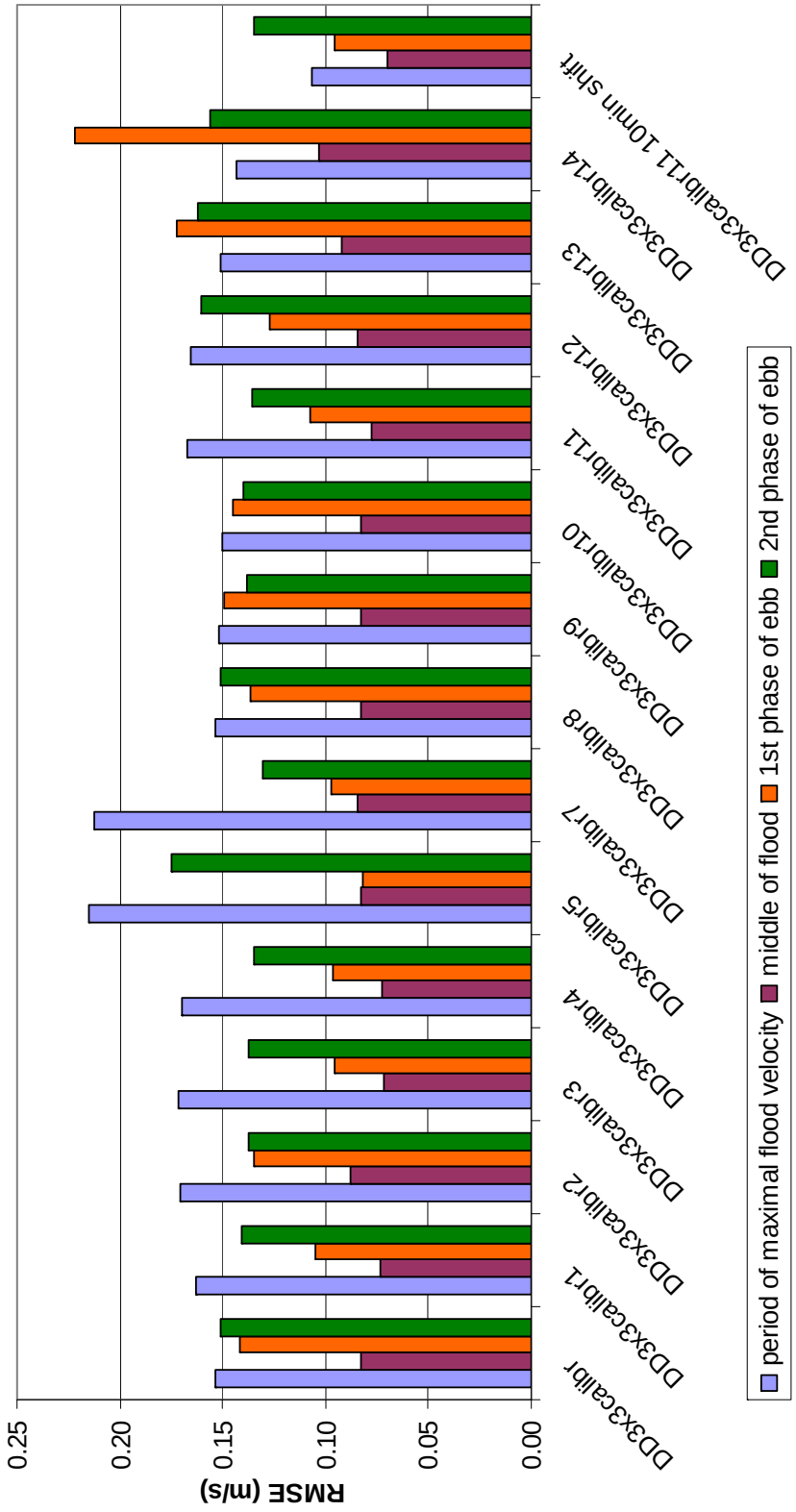

Figure 105 - Root mean squared errors for different tidal periods for the Notelaer – longitudinal profile

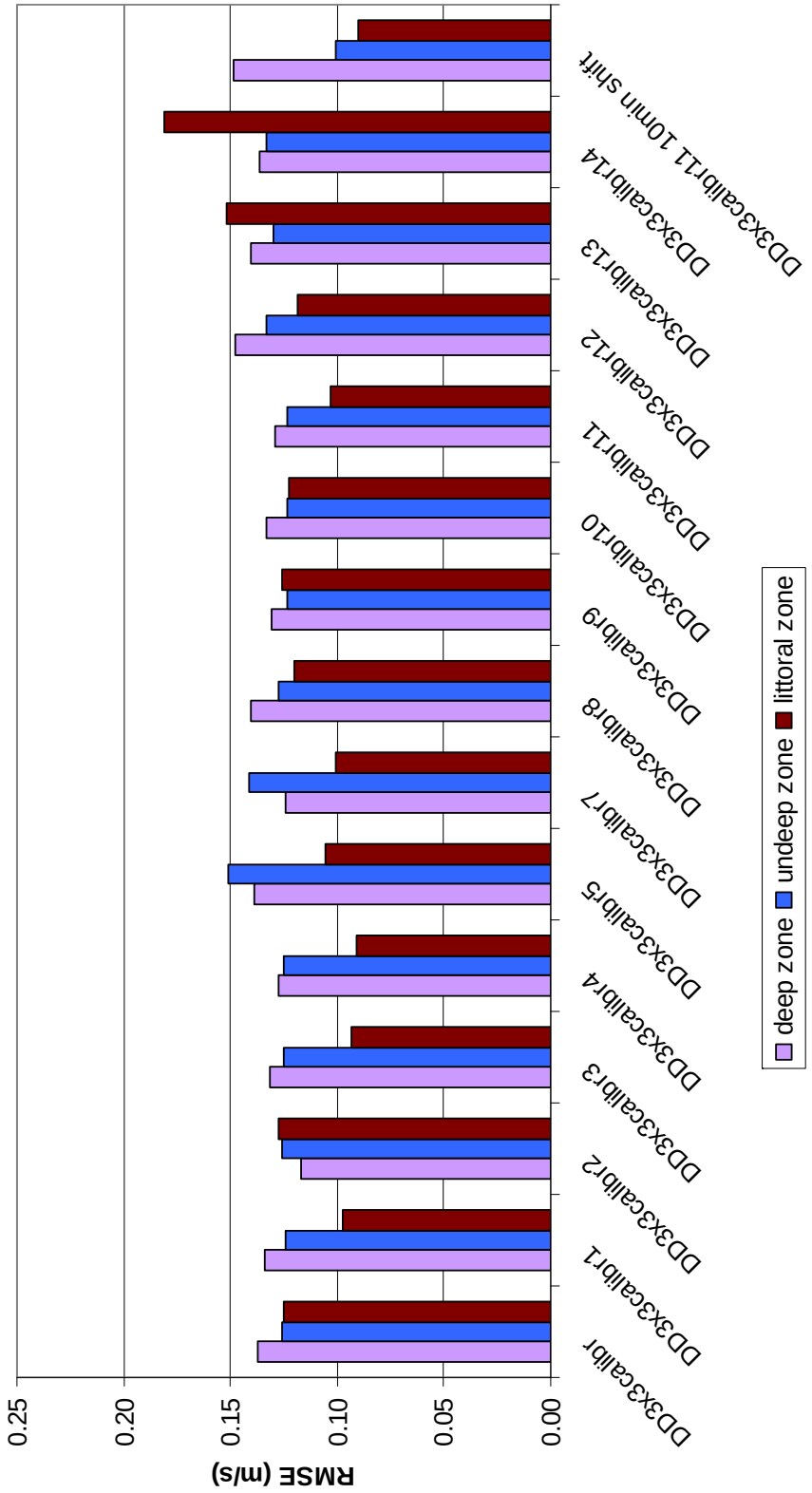

Figure 106 - Root mean squared errors for different depth zones for the Notelaer – longitudinal profile

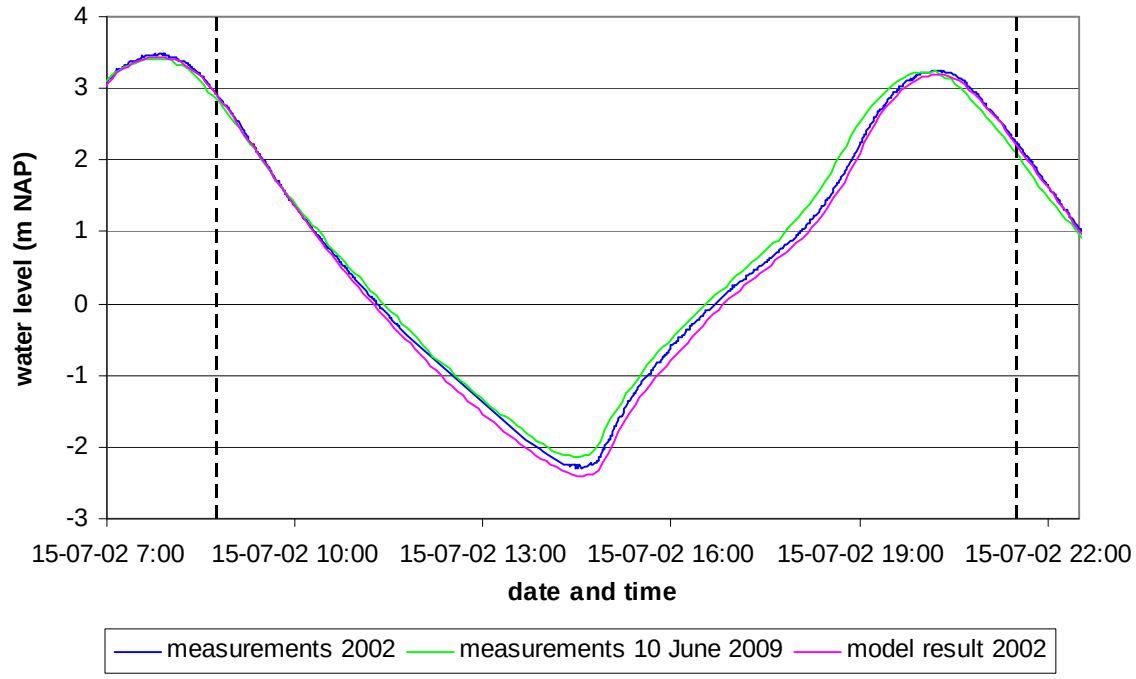

Figure 107 - Comparison of the water levels at Schelle in 2002 and 2009 for the calibration period

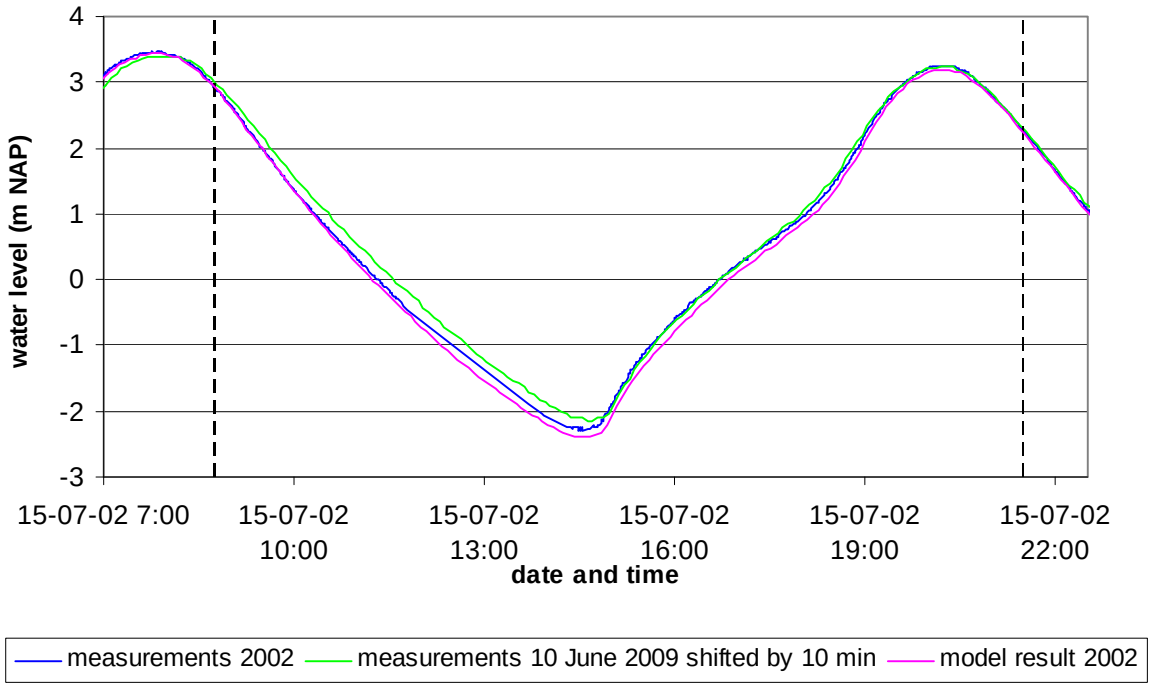

Figure 108 - Comparison of the water levels at Schelle in 2002 and 2009 for the calibration period (measurements are shifted by 10 min)

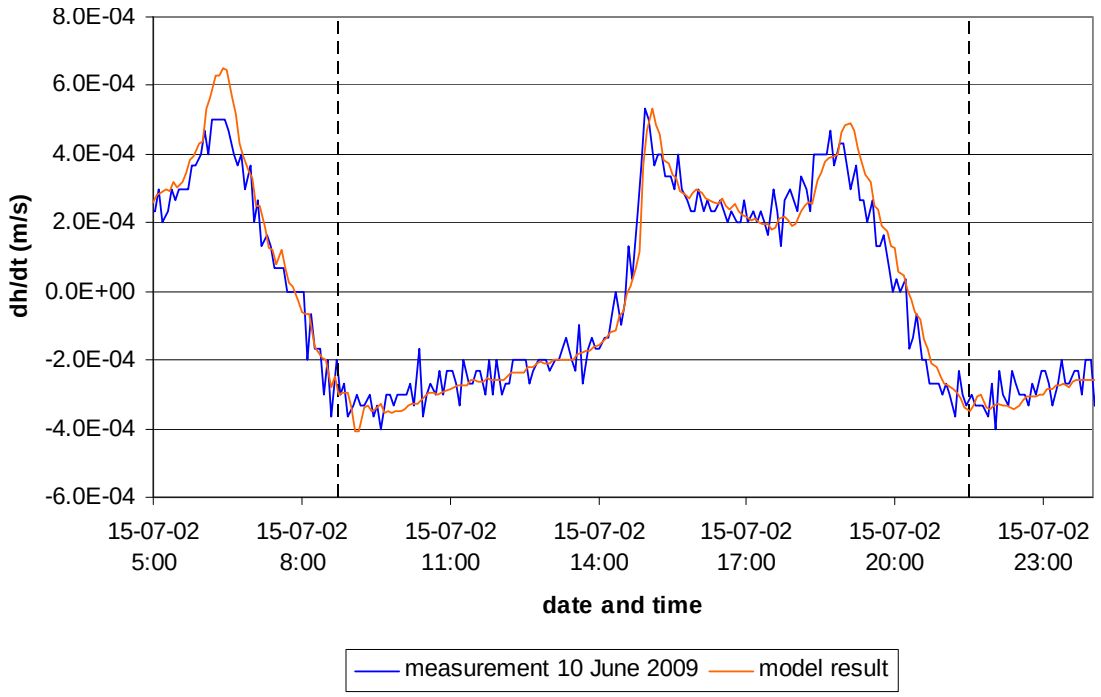

Figure 109 - Time series of the rate of the water level change dh/dt for the calibration period

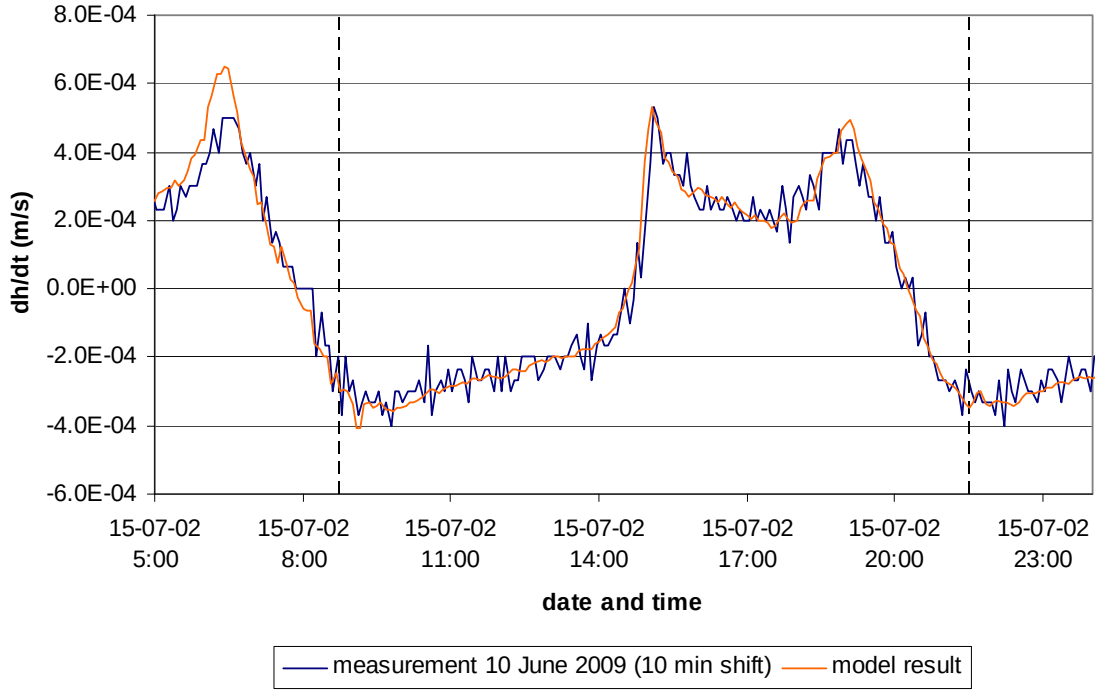

Figure 110 - Time series of the rate of the water level change dh/dt for the calibration period (measurements are shifted by 10 min)

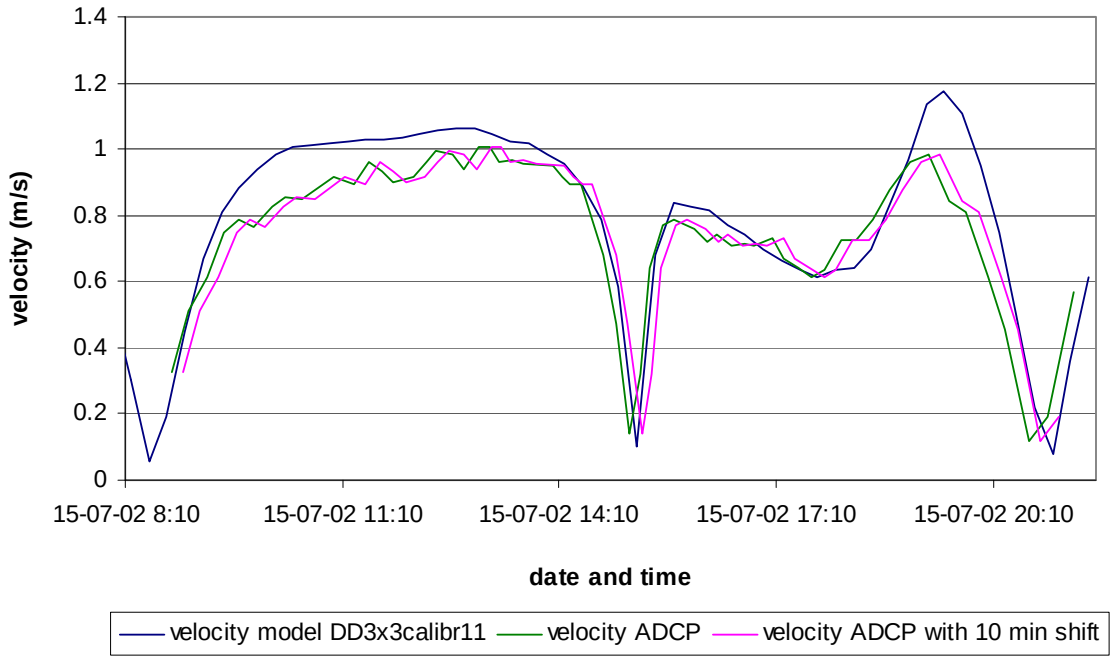

Figure 111 - Calculated and measured velocities in deep zone of the Ballooi – transverse profile (point 1)

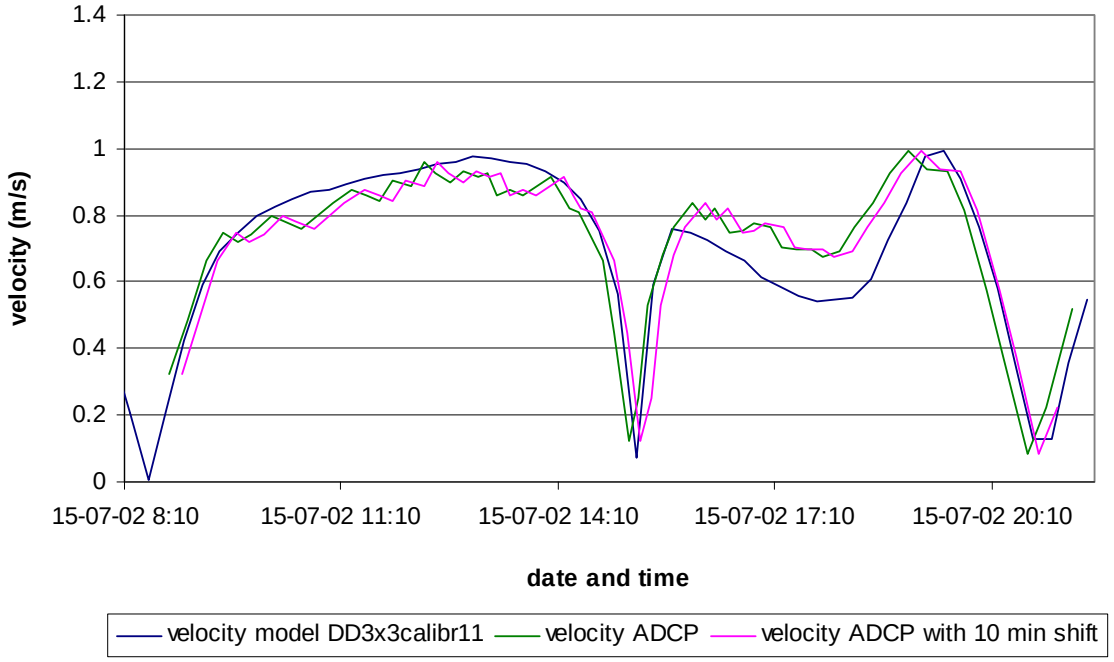

Figure 112 - Calculated and measured velocities in deep zone of the Ballooi – transverse profile (point 2)

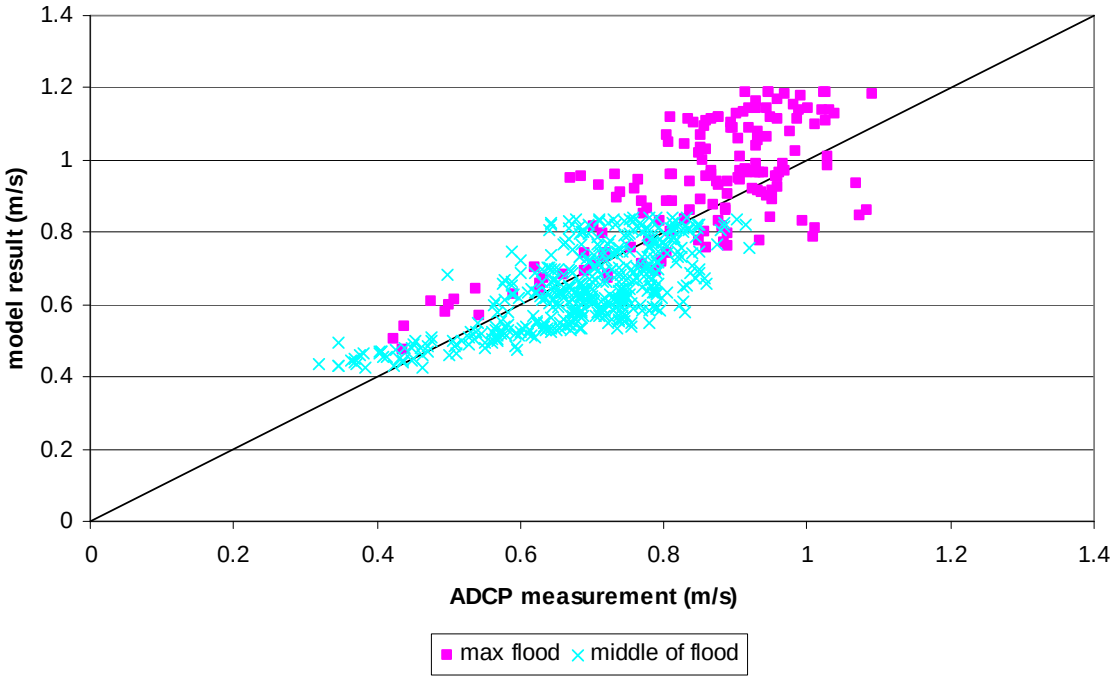

Figure 113 - Velocity magnitude for Ballooi – transverse profile in deep zone for flood
(model result DD3x3calibr11 shift 10min vs ADCP measurement)

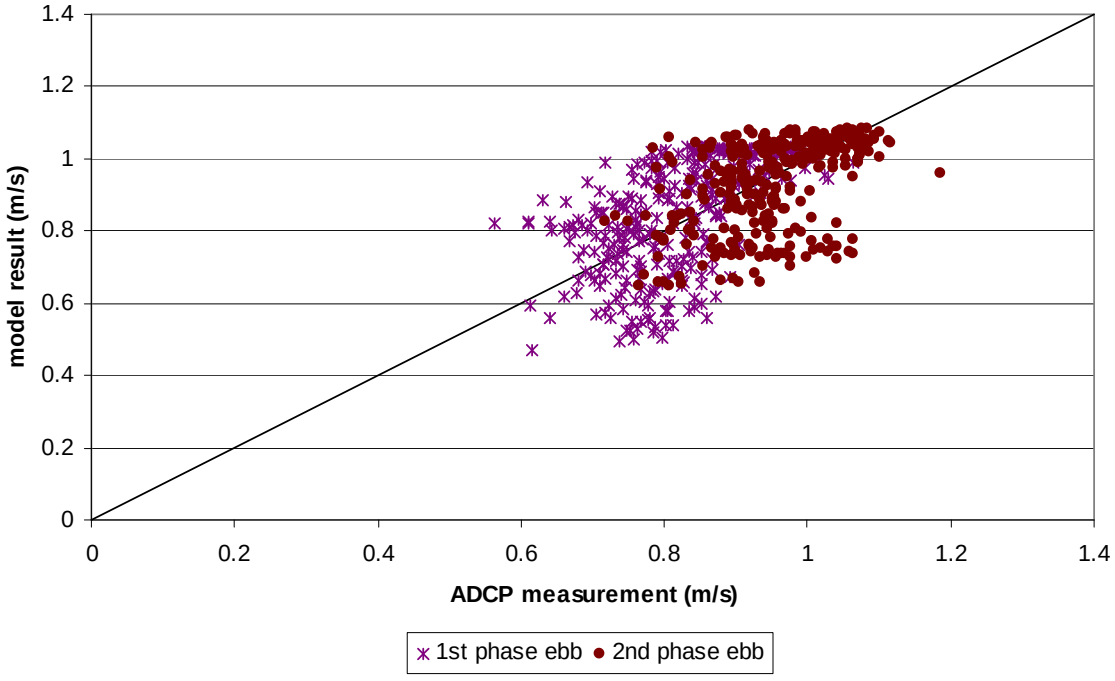

Figure 114 - Velocity magnitude for Ballooi – transverse profile in deep zone for ebb
(model result DD3x3calibr11 shift 10min vs ADCP measurement)

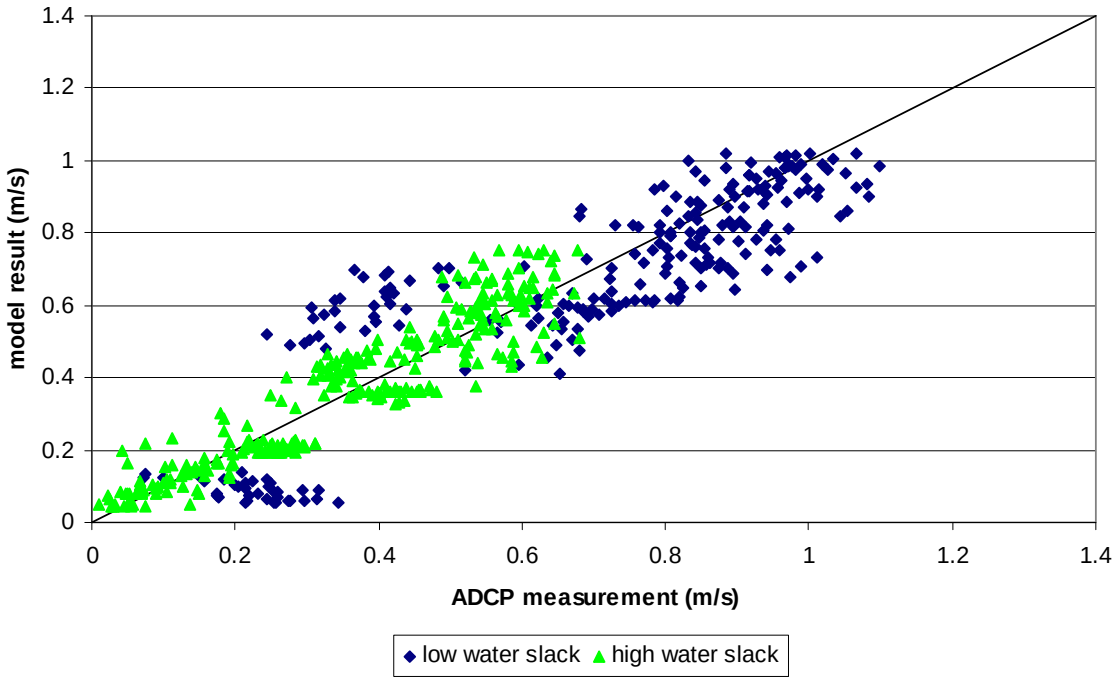

Figure 115 - Velocity magnitude for Ballooi – transverse profile in deep zone for slack
(model result DD3x3calibr11 shift 10min vs ADCP measurement)

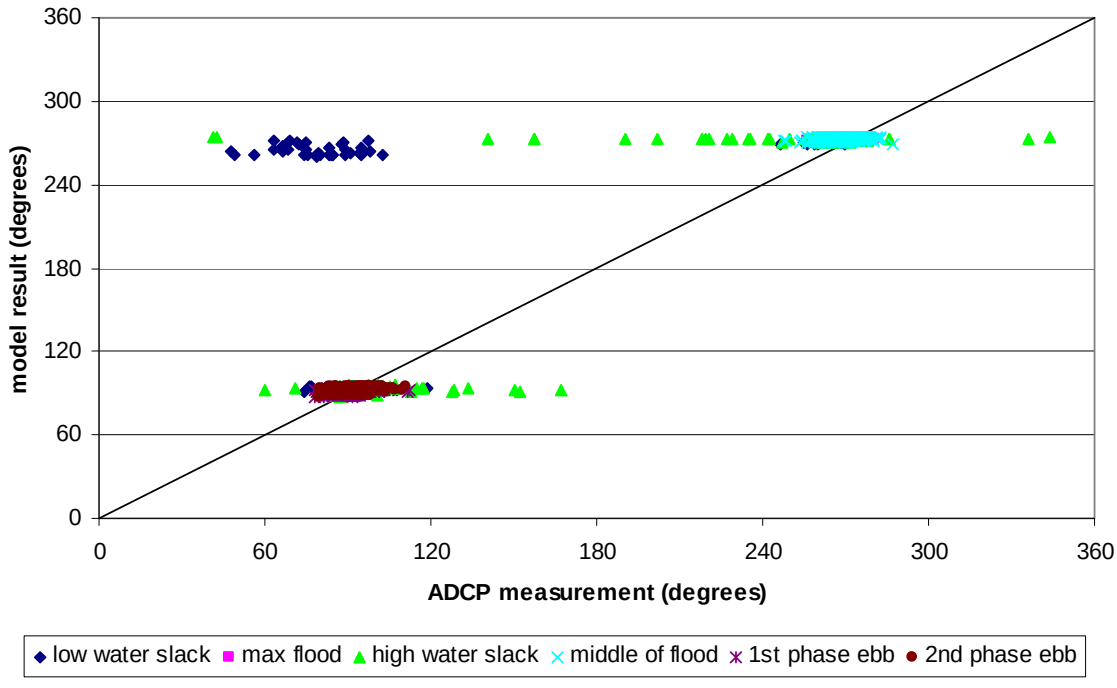

Figure 116 - Velocity direction for Ballooi – transverse profile in deep zone
(model result DD3x3calibr11 shift 10min vs ADCP measurement)

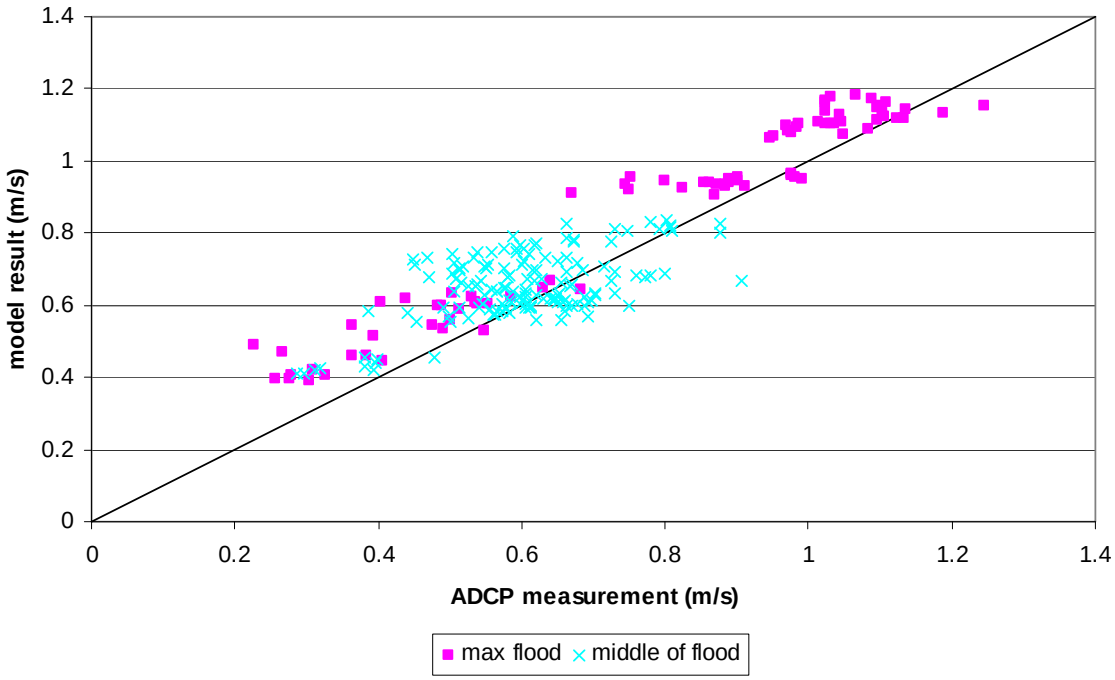

Figure 117 - Velocity magnitude for Ballooi – transverse profile in undeep zone for flood
(model result DD3x3calibr11 shift 10min vs ADCP measurement)

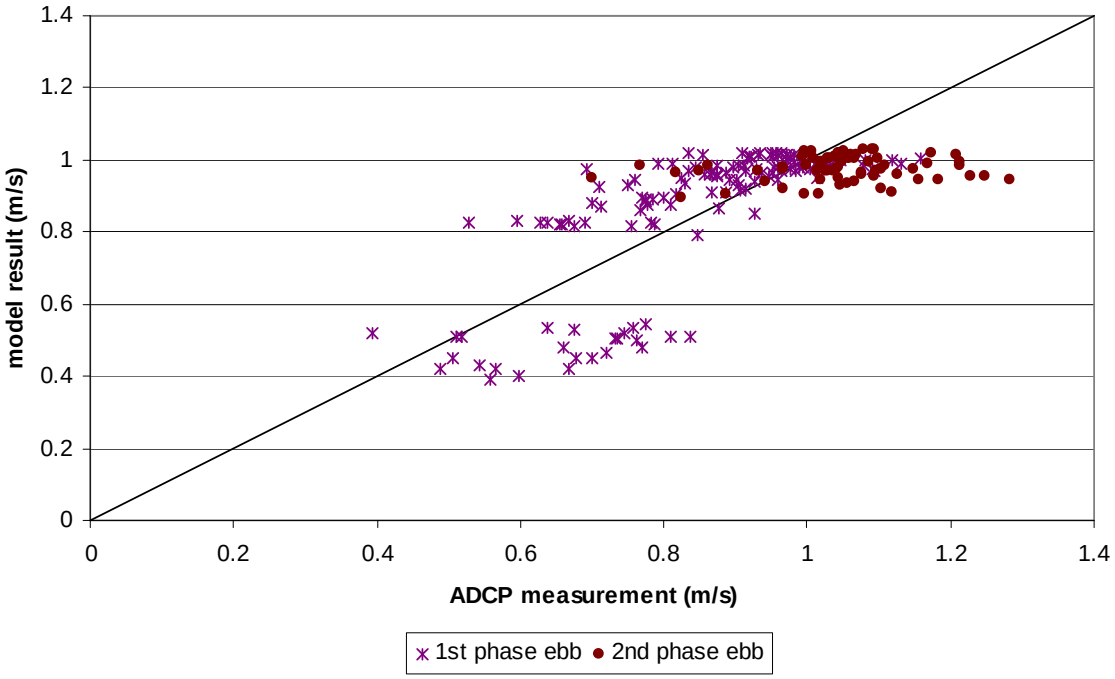

Figure 118 - Velocity magnitude for Ballooi – transverse profile in undeep zone for ebb
(model result DD3x3calibr11 shift 10min vs ADCP measurement)

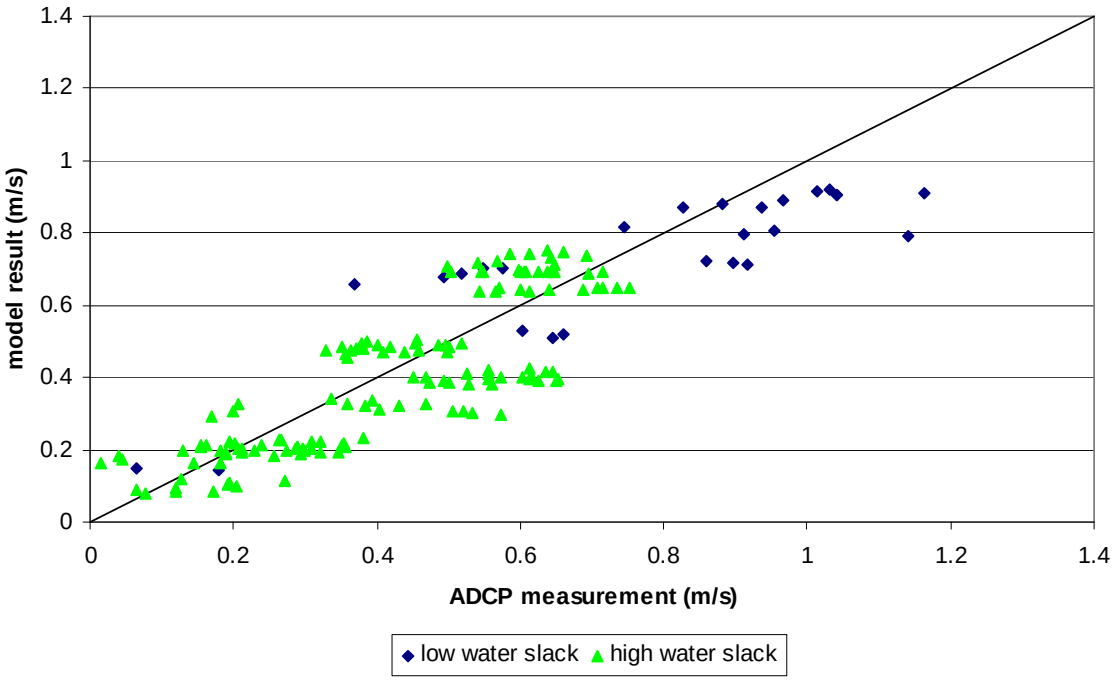

Figure 119 - Velocity magnitude for Ballooi – transverse profile in undeep zone for slack
(model result DD3x3calibr11 shift 10min vs ADCP measurement)

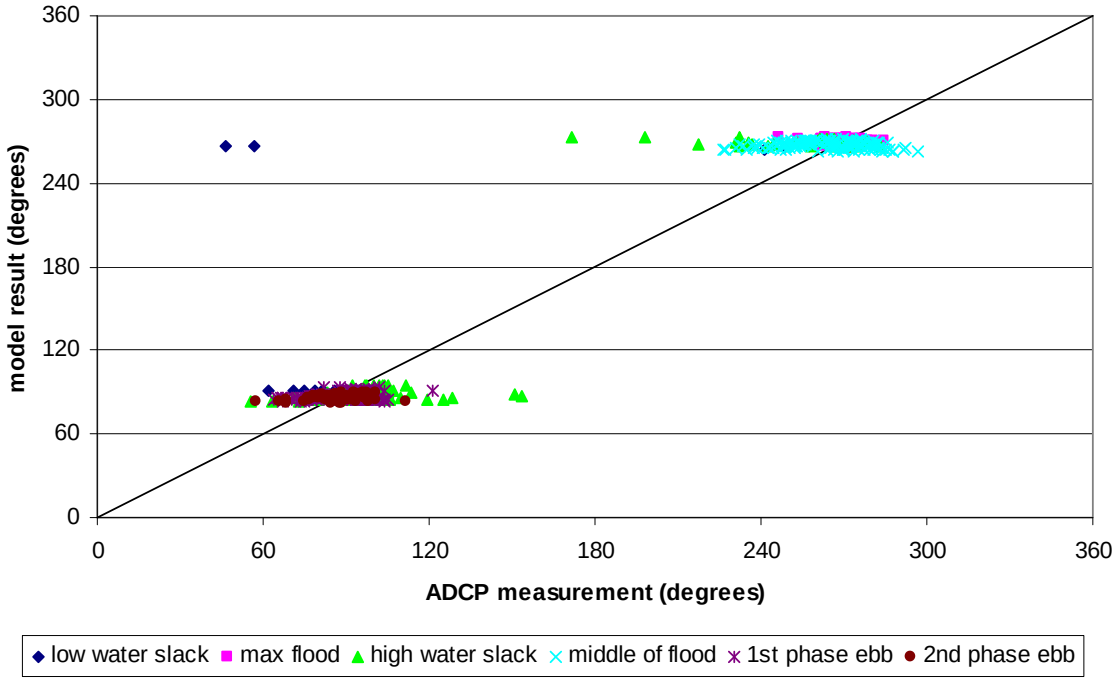

Figure 120 - Velocity direction for Ballooi – transverse profile in undeep zone
(model result DD3x3calibr11 shift 10min vs ADCP measurement)

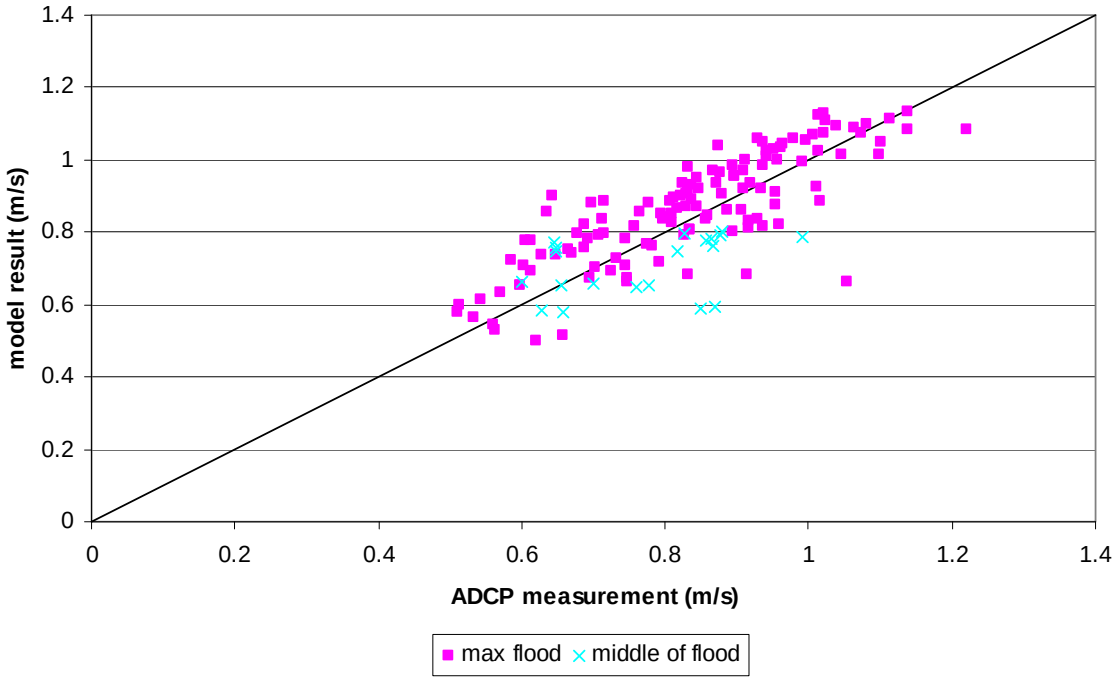

Figure 121 - Velocity magnitude for Ballooi – transverse profile in littoral zone for flood
(model result DD3x3calibr11 shift 10min vs ADCP measurement)

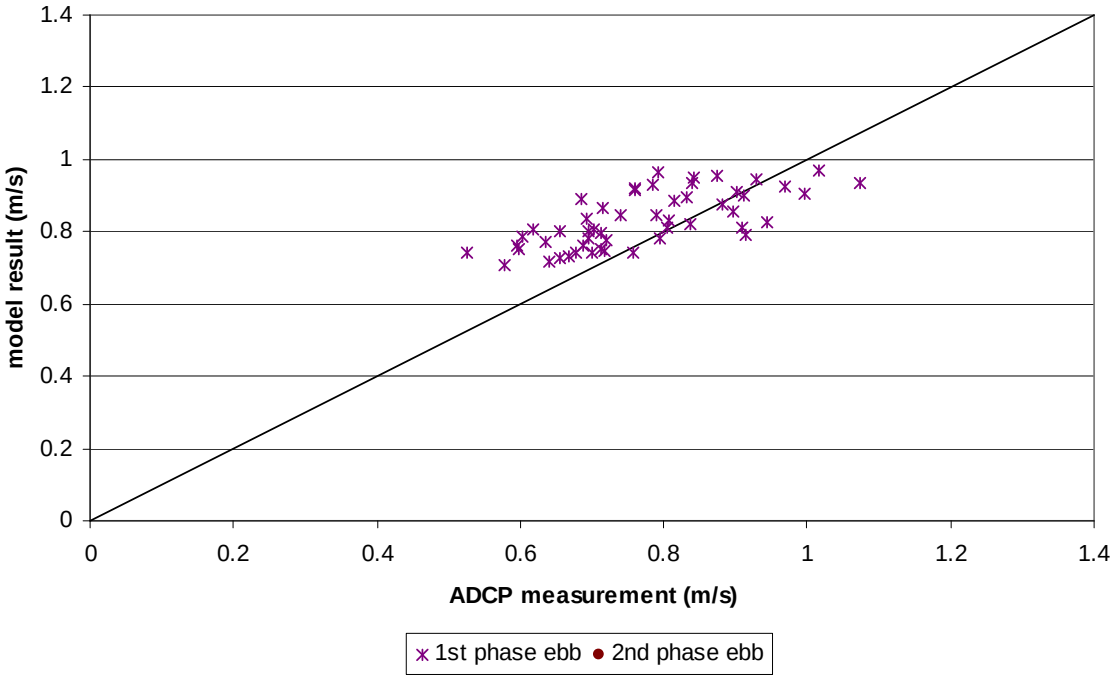

Figure 122 - Velocity magnitude for Ballooi – transverse profile in littoral zone for ebb
(model result DD3x3calibr11 shift 10min vs ADCP measurement)

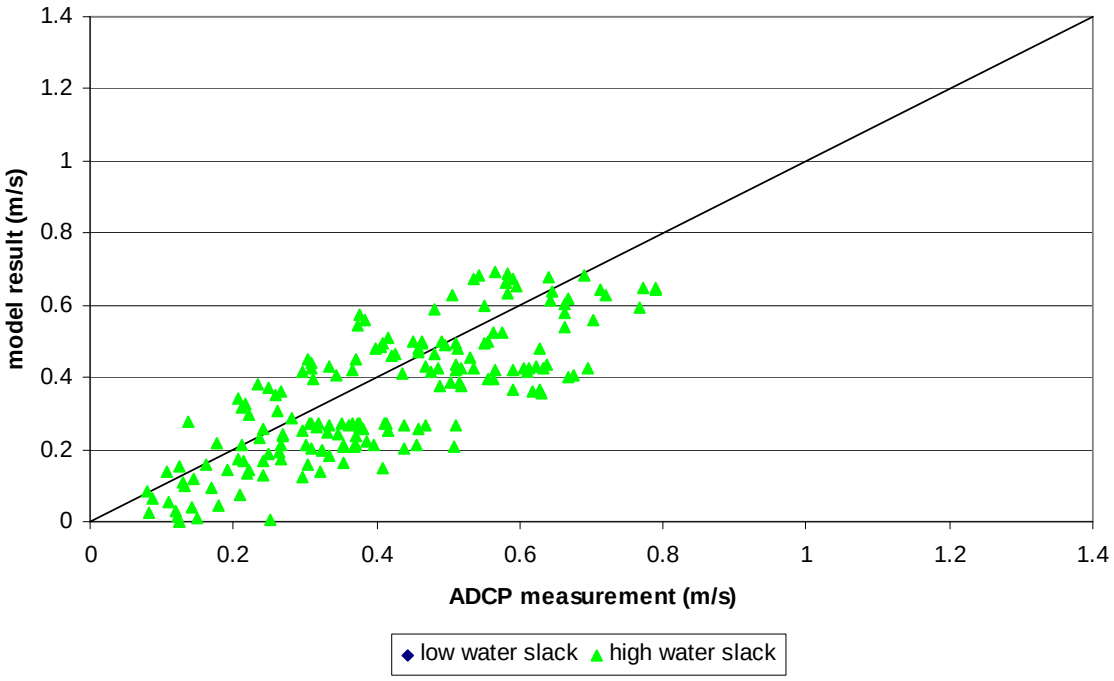

Figure 123 - Velocity magnitude for Ballooi – transverse profile in littoral zone for slack
(model result DD3x3calibr11 shift 10min vs ADCP measurement)

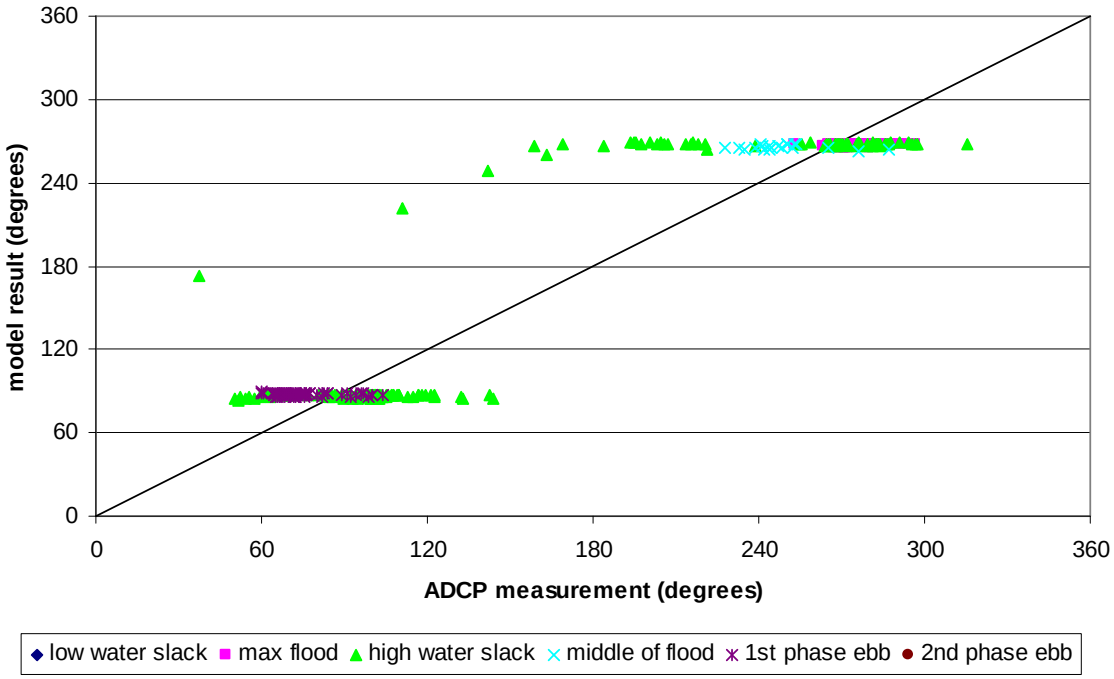

Figure 124 - Velocity direction for Ballooi – transverse profile in littoral zone
(model result DD3x3calibr11 shift 10min vs ADCP measurement)

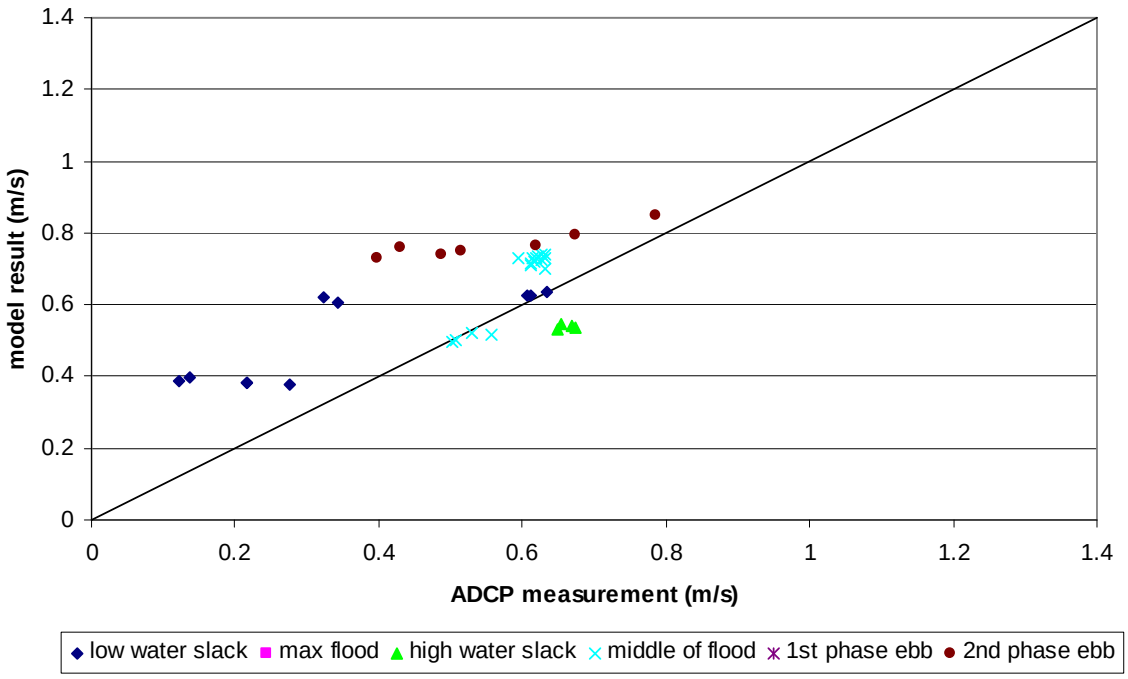

Figure 125 - Velocity magnitude for Notelaer – longitudinal profile in deep zone
(model result DD3x3calibr11 shift 10min vs ADCP measurement)

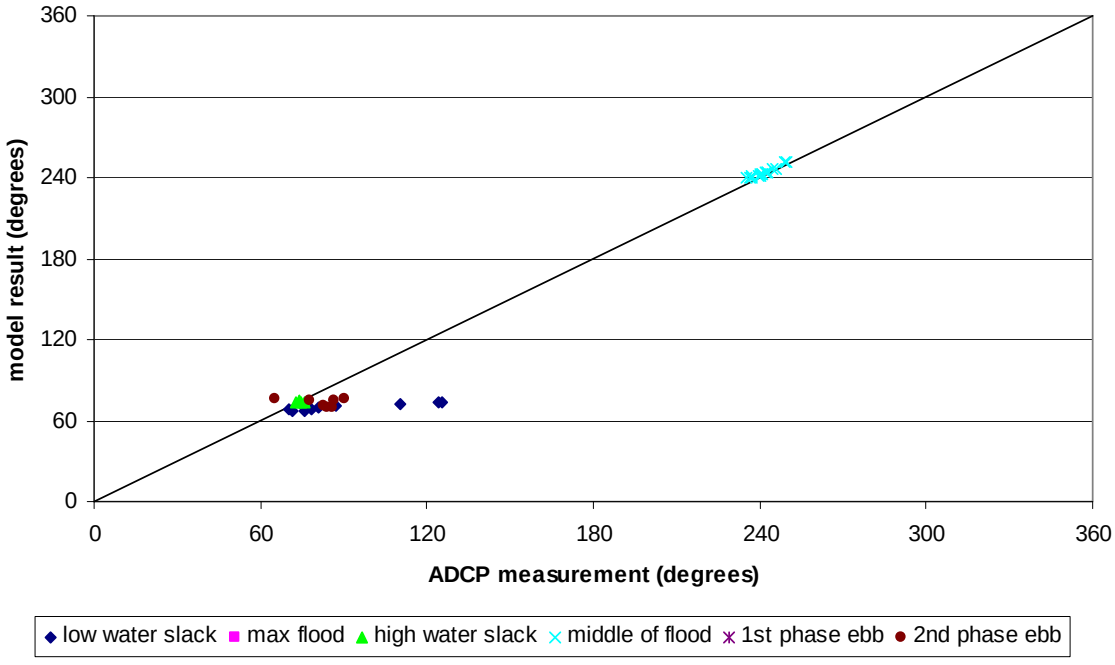

Figure 126 - Velocity direction for Notelaer – longitudinal profile in deep zone
(model result DD3x3calibr11 shift 10min vs ADCP measurement)

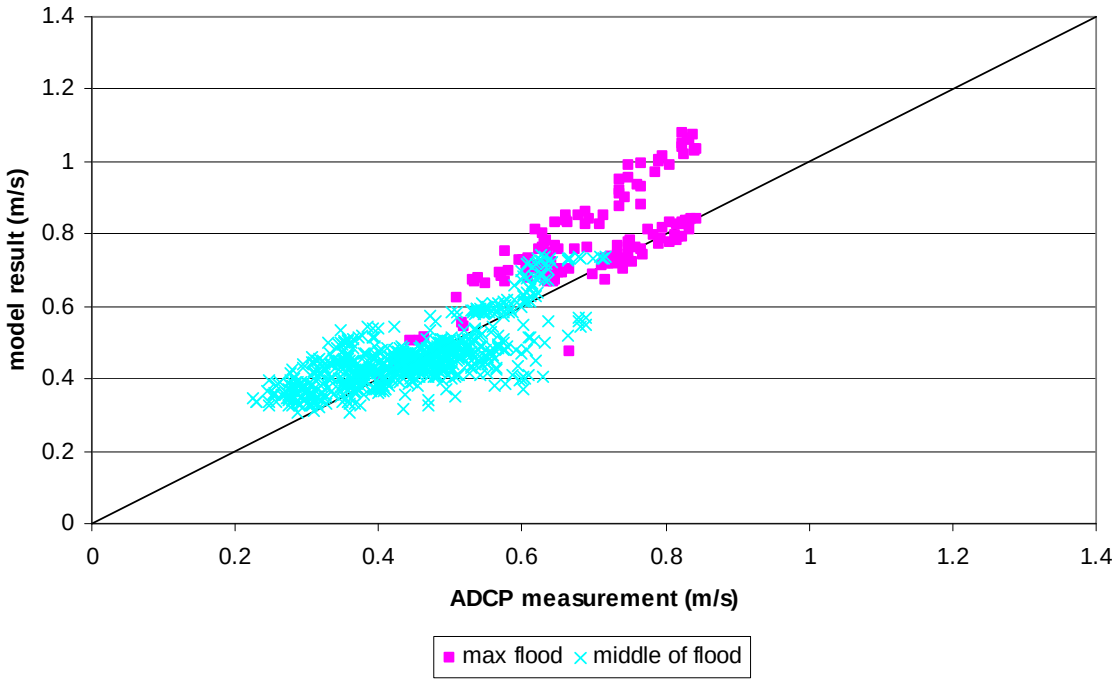

Figure 127 - Velocity magnitude for Notelaer – longitudinal profile in undeep zone for flood (model result DD3x3calibr11 shift 10min vs ADCP measurement)

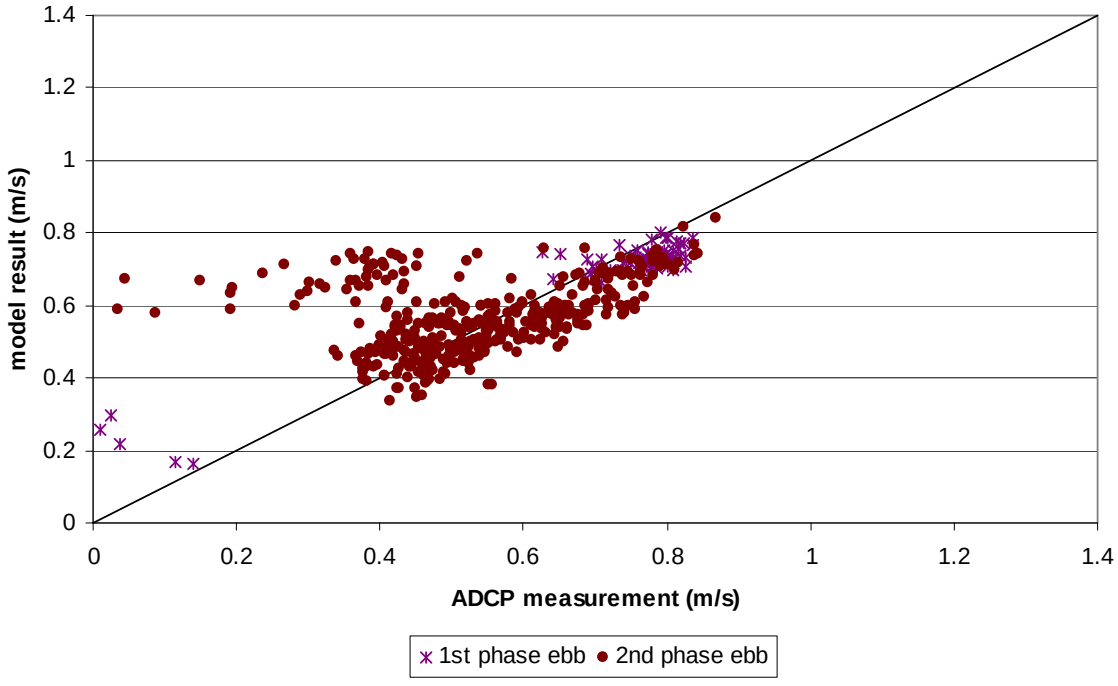

Figure 128 - Velocity magnitude for Notelaer – longitudinal profile in undeep zone for ebb (model result DD3x3calibr11 shift 10min vs ADCP measurement)

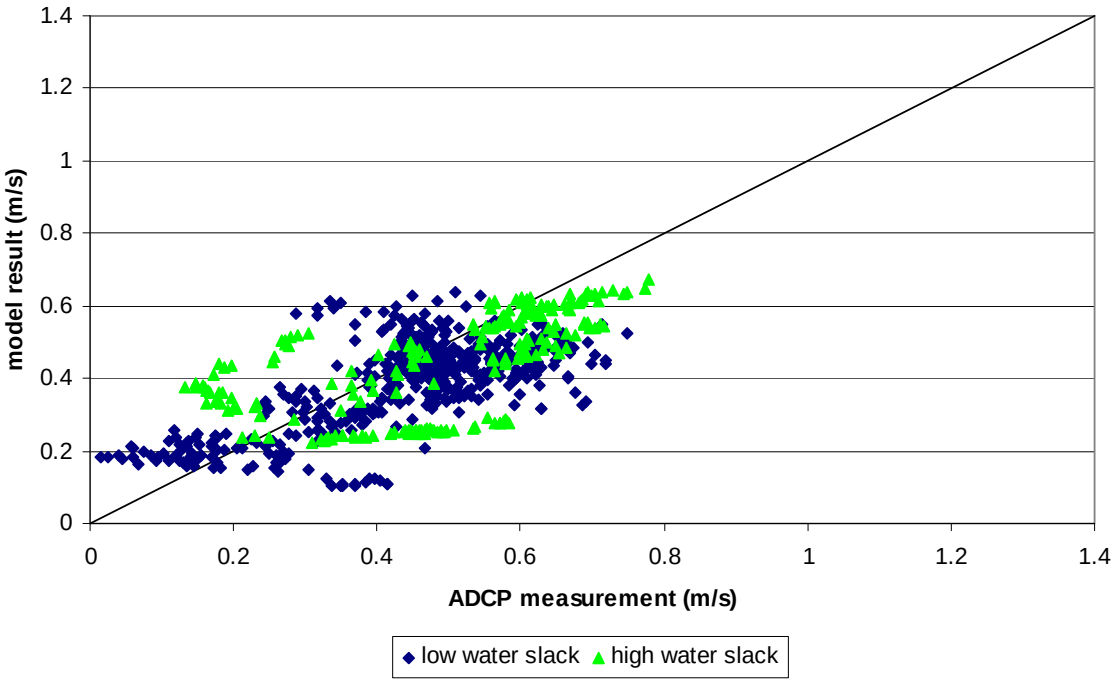

Figure 129 - Velocity magnitude for Notelaer – longitudinal profile in undeep zone for slack
(model result DD3x3calibr11 shift 10min vs ADCP measurement)

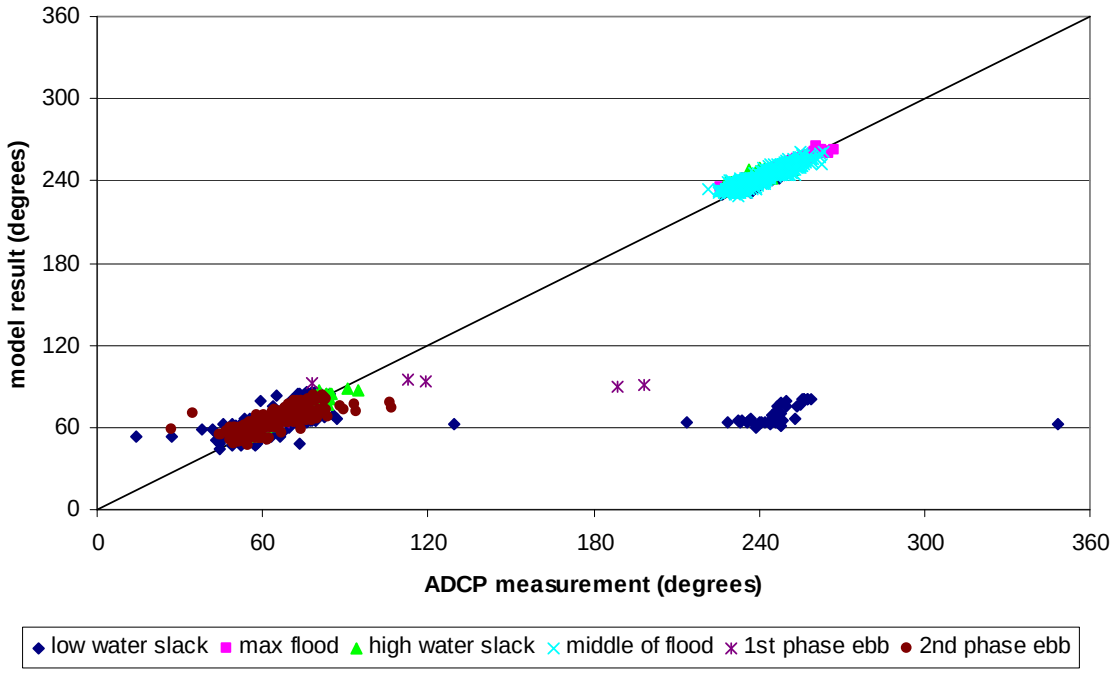

Figure 130 - Velocity direction for Notelaer – longitudinal profile in undeep zone
(model result DD3x3calibr11 shift 10min vs ADCP measurement)

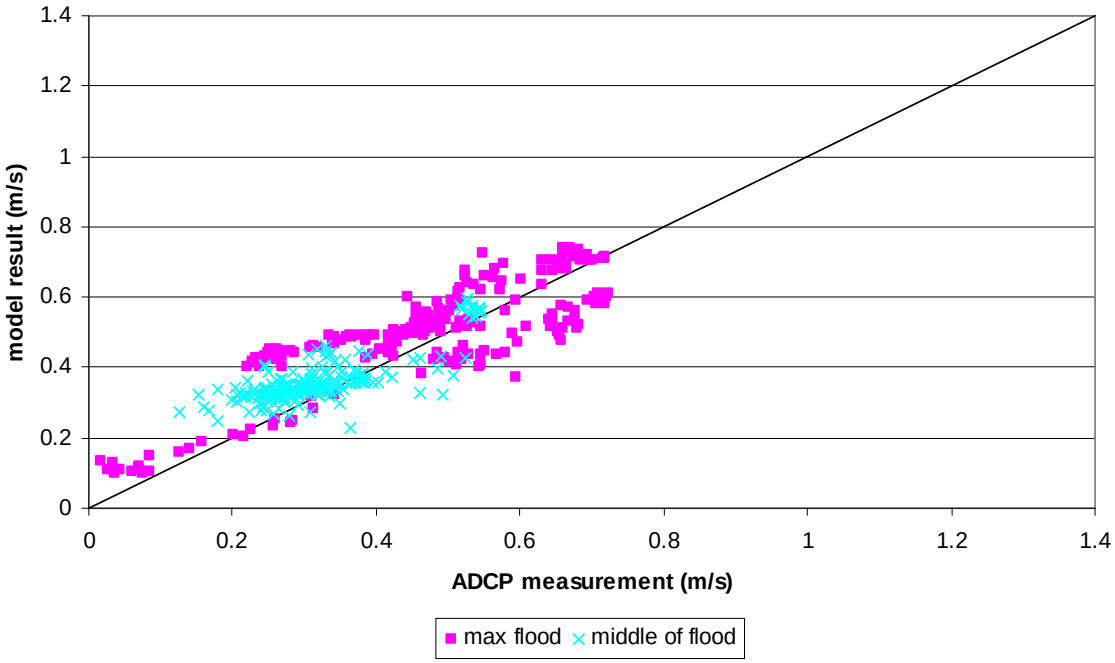

Figure 131 - Velocity magnitude for Notelaer – longitudinal profile in littoral zone for flood (model result DD3x3calibr11 shift 10min vs ADCP measurement)

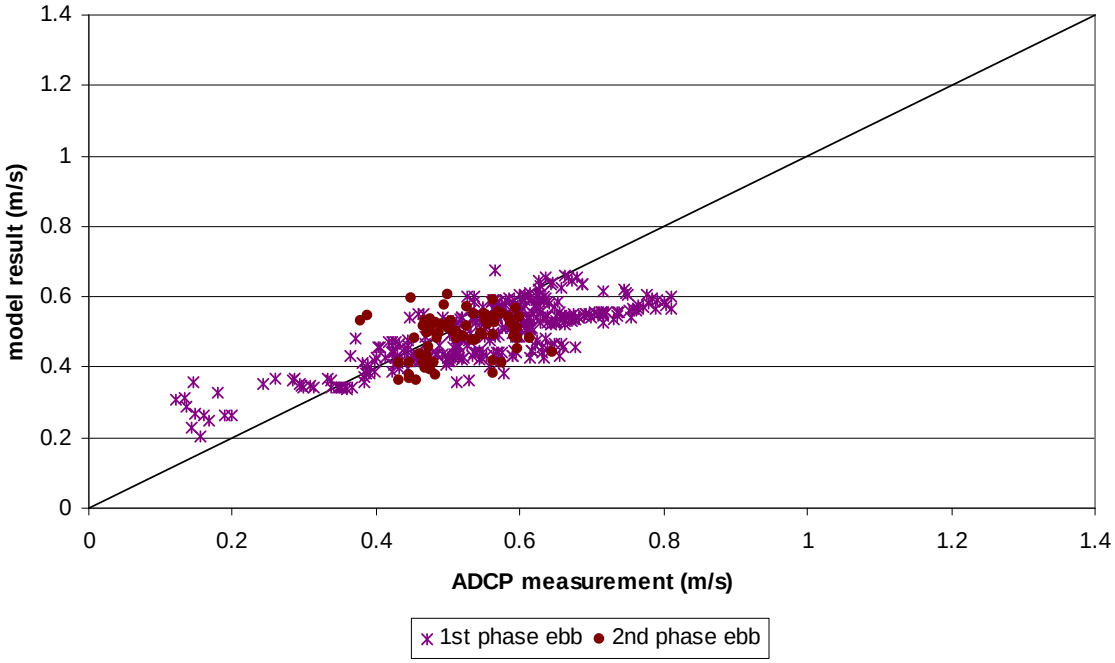

Figure 132 - Velocity magnitude for Notelaer – longitudinal profile in littoral zone for ebb (model result DD3x3calibr11 shift 10min vs ADCP measurement)

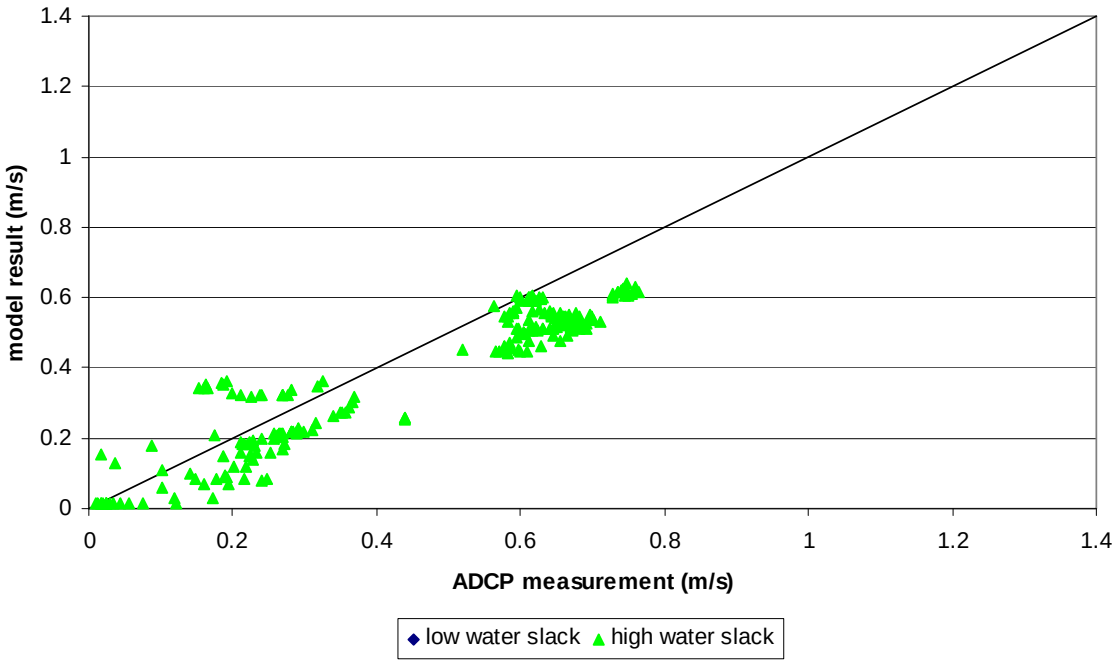

Figure 133 - Velocity magnitude for Notelaer – longitudinal profile in littoral zone for slack
(model result DD3x3calibr11 shift 10min vs ADCP measurement)

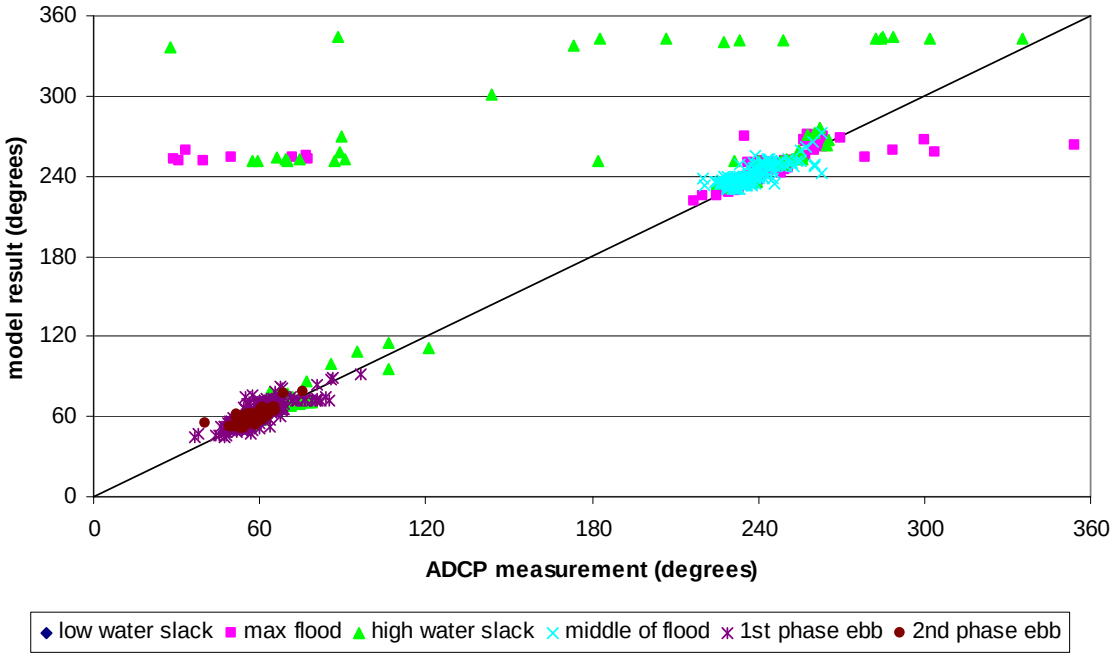

Figure 134 - Velocity direction for Notelaer – longitudinal profile in littoral zone
(model result DD3x3calibr11 shift 10min vs ADCP measurement)

Figure 135 - Bias for model run DD3x3calibr11 shift 10min for Ballooi – transverse profile

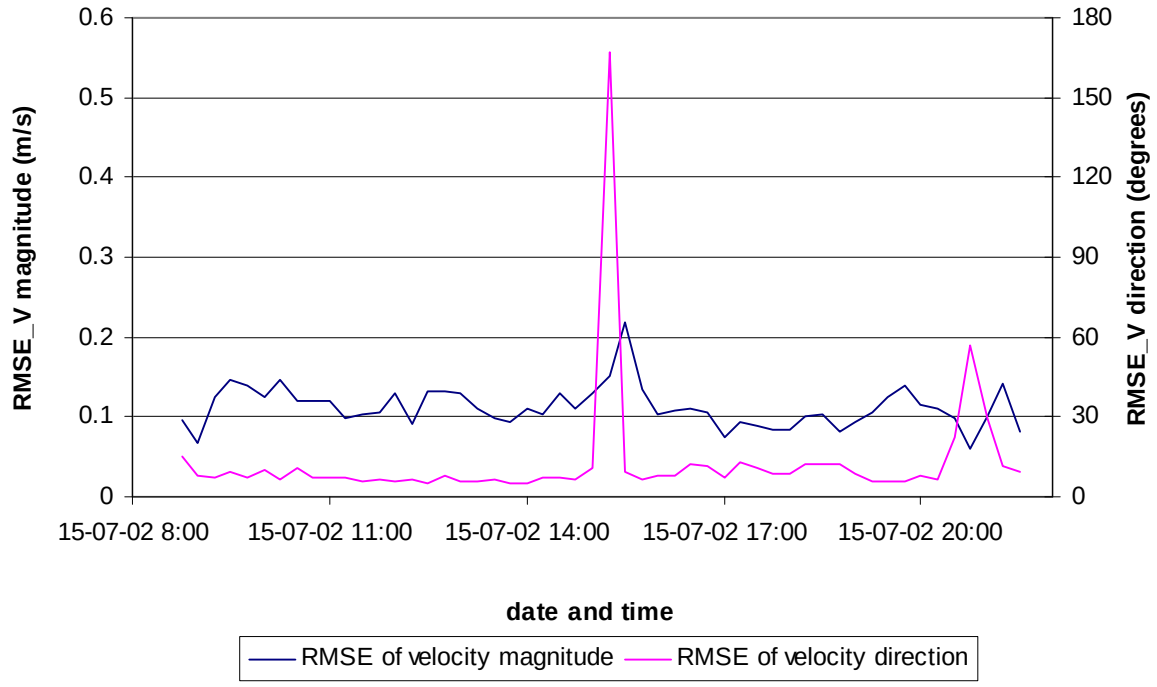

Figure 136 - Root mean squared error for model run DD3x3calibr11 shift 10min for Ballooi – transverse profile

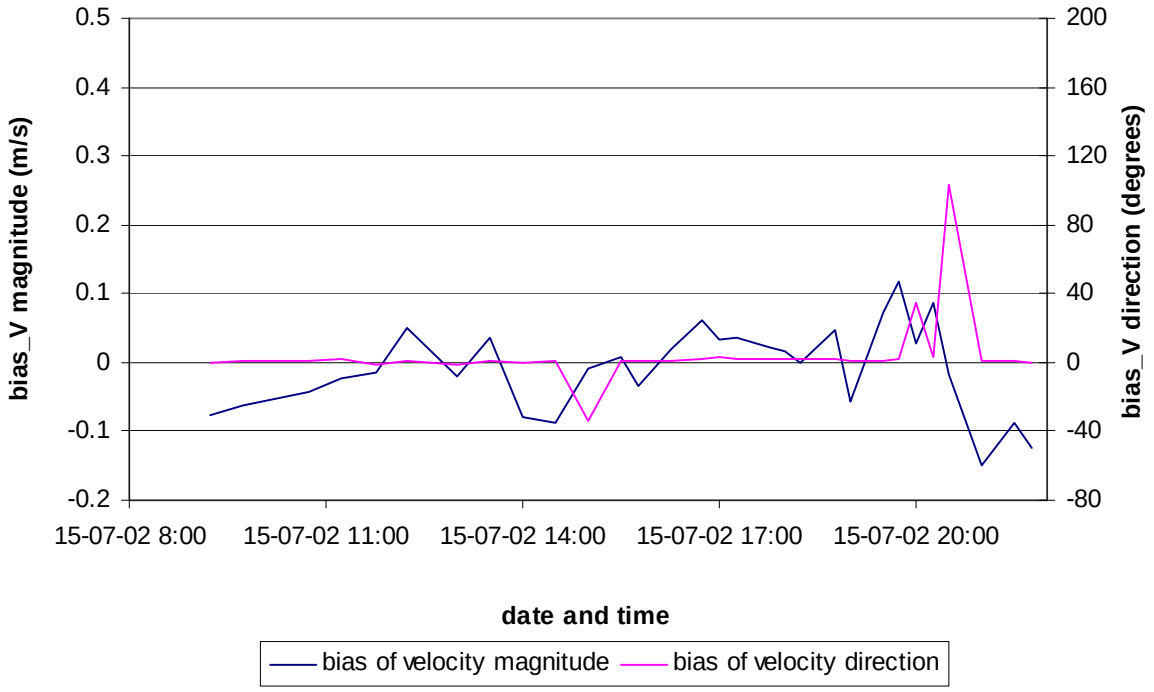

Figure 137 - Bias for model run DD3x3calibr11 shift 10min for Notelaer – longitudinal profile

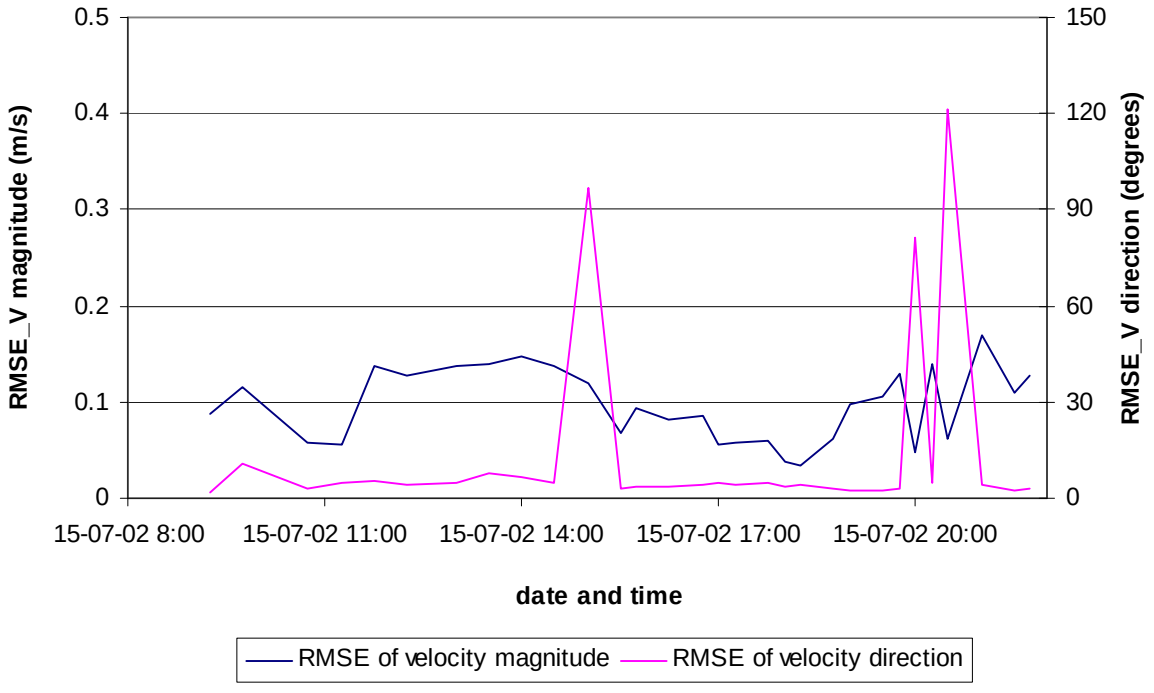

Figure 138 - Root mean squared error for model run DD3x3calibr11 shift 10min for Notelaer – longitudinal profile

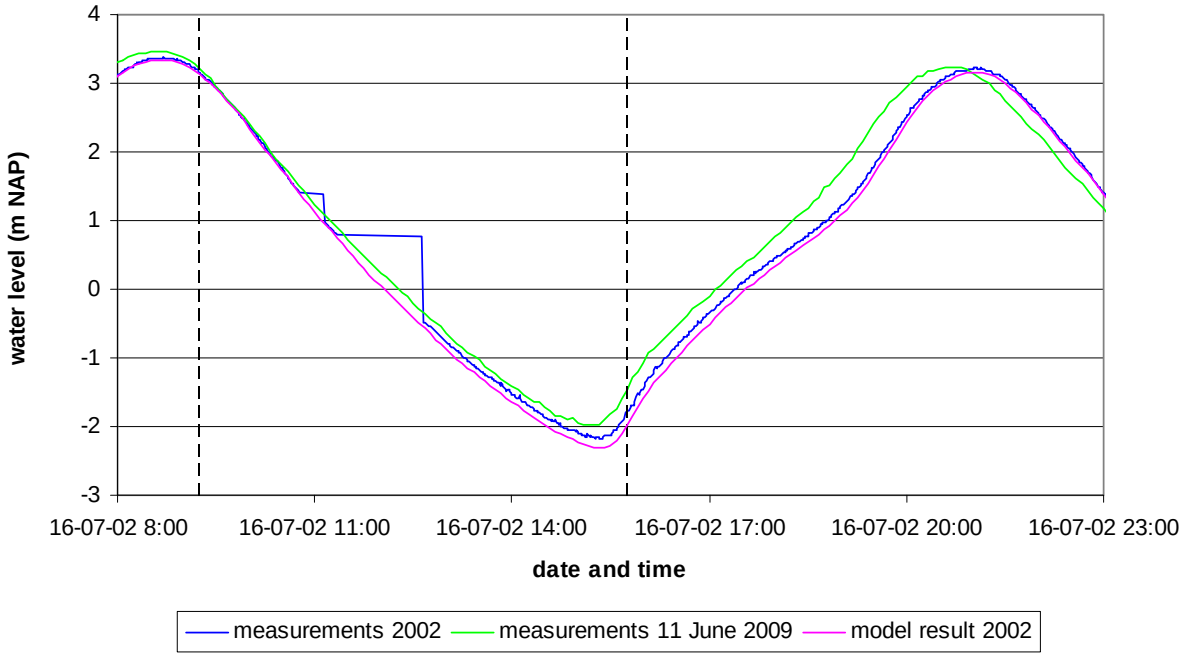

Figure 139 - Comparison of the water levels at Schelle in 2002 and 2009 for the validation (ebb period)

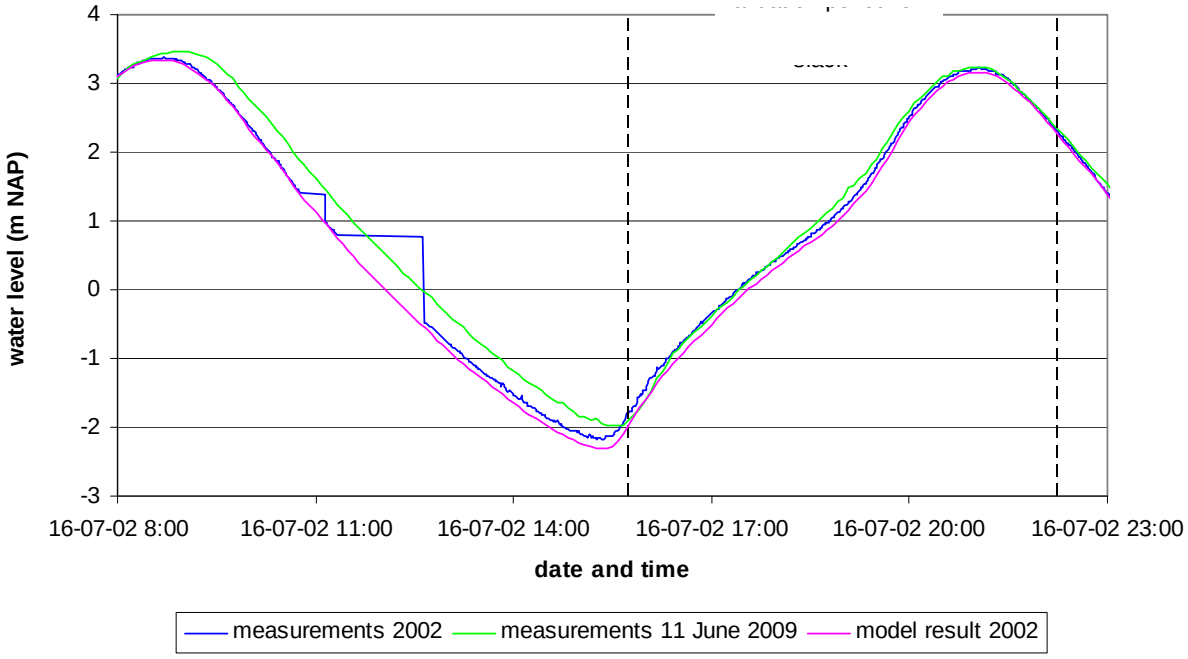

Figure 140 - Comparison of the water levels at Schelle in 2002 and 2009 for the validation (flood period)

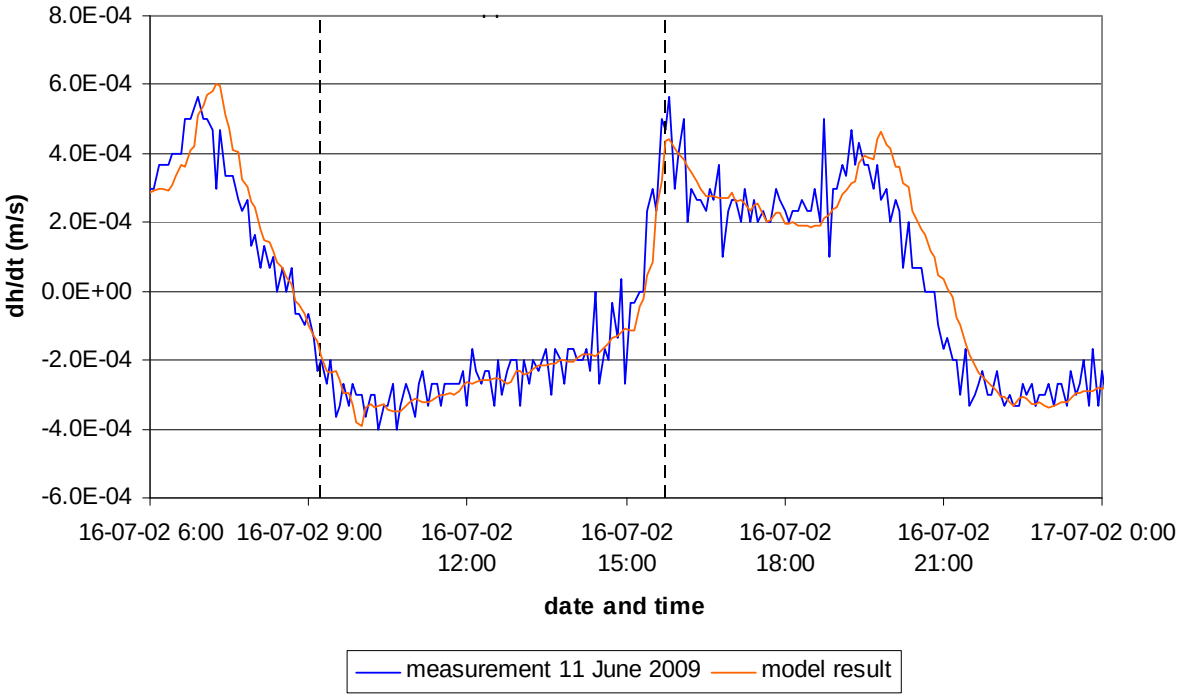

Figure 141 - Time series of the rate of the water level change dh/dt for the validation (ebb period)

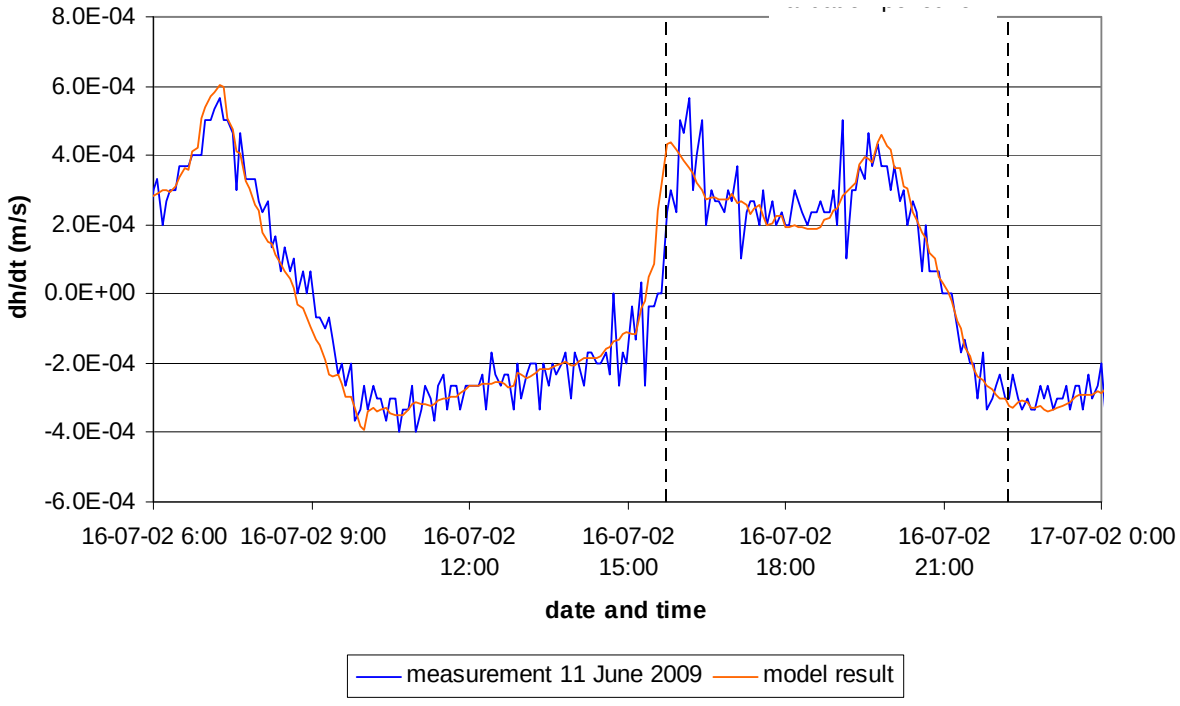

Figure 142 - Time series of the rate of the water level change dh/dt for the validation (flood period)

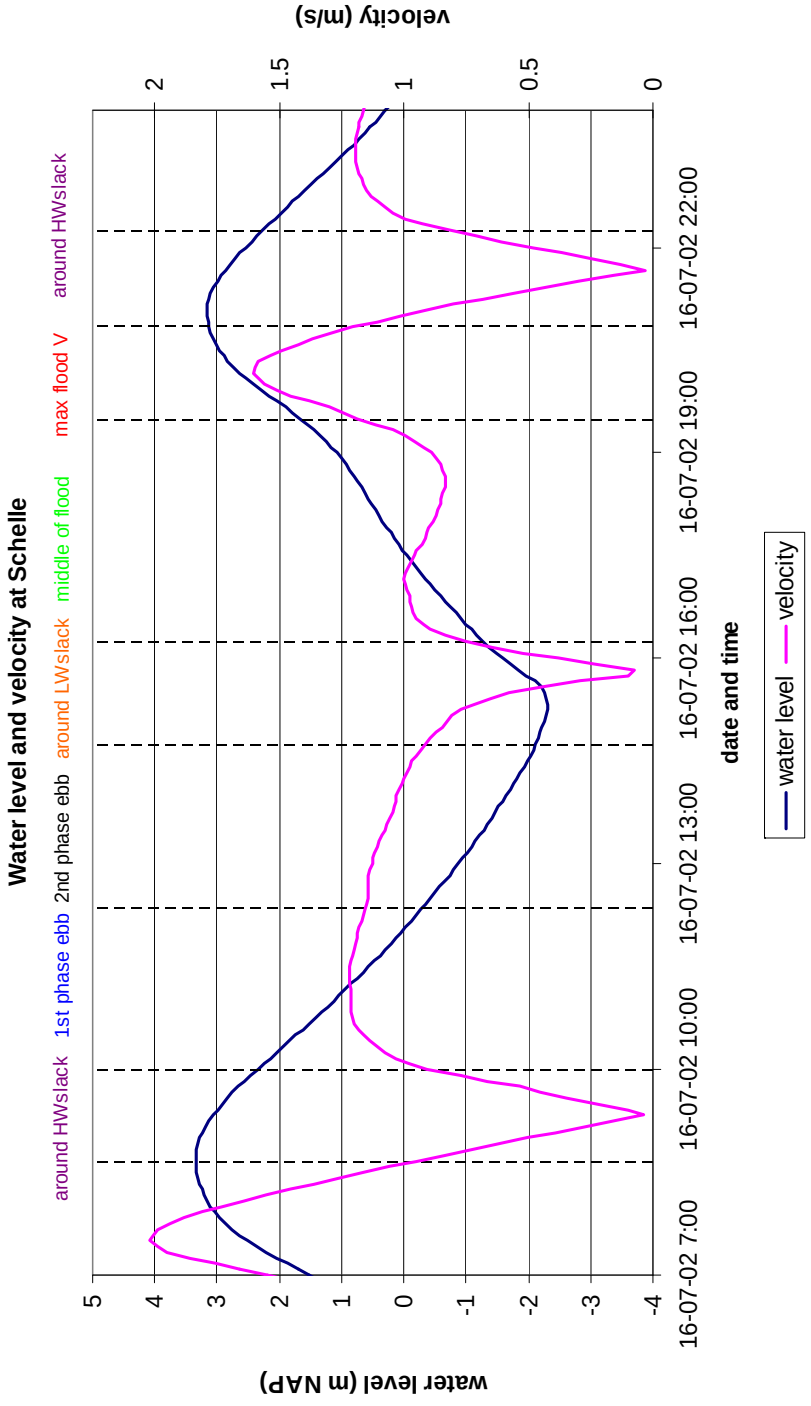

Figure 143 - Time periods for the comparison of the model results and measurements for the model validation

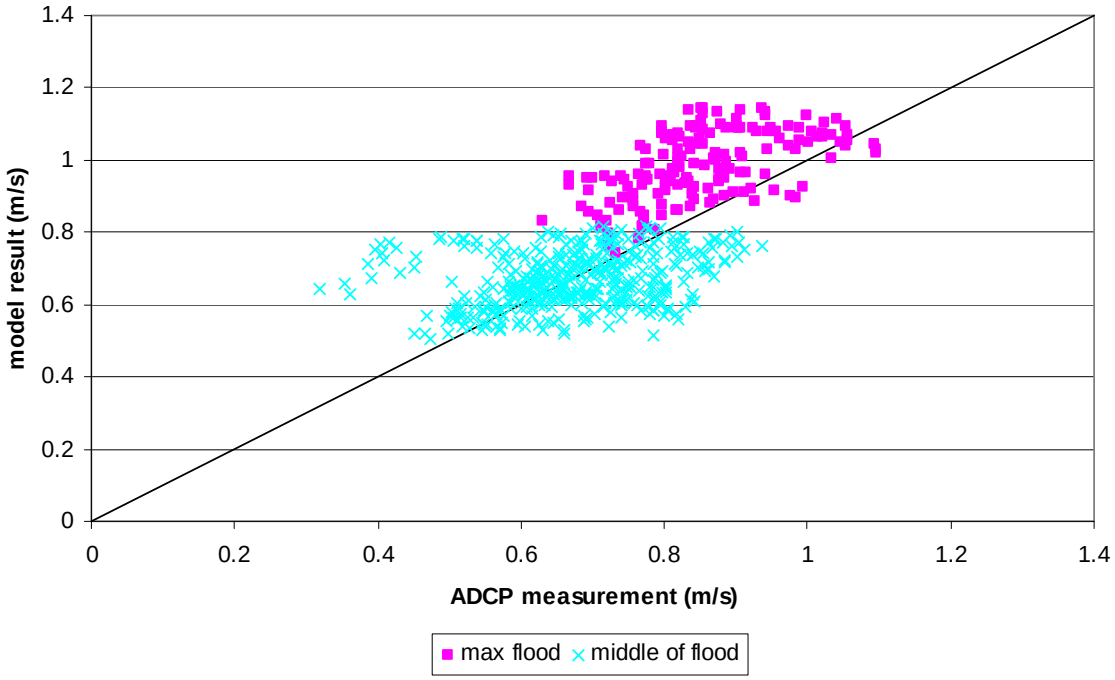

Figure 144 - Velocity magnitude for Notelaer – transverse profile in deep zone for flood
(model result DD3x3validation vs ADCP measurement)

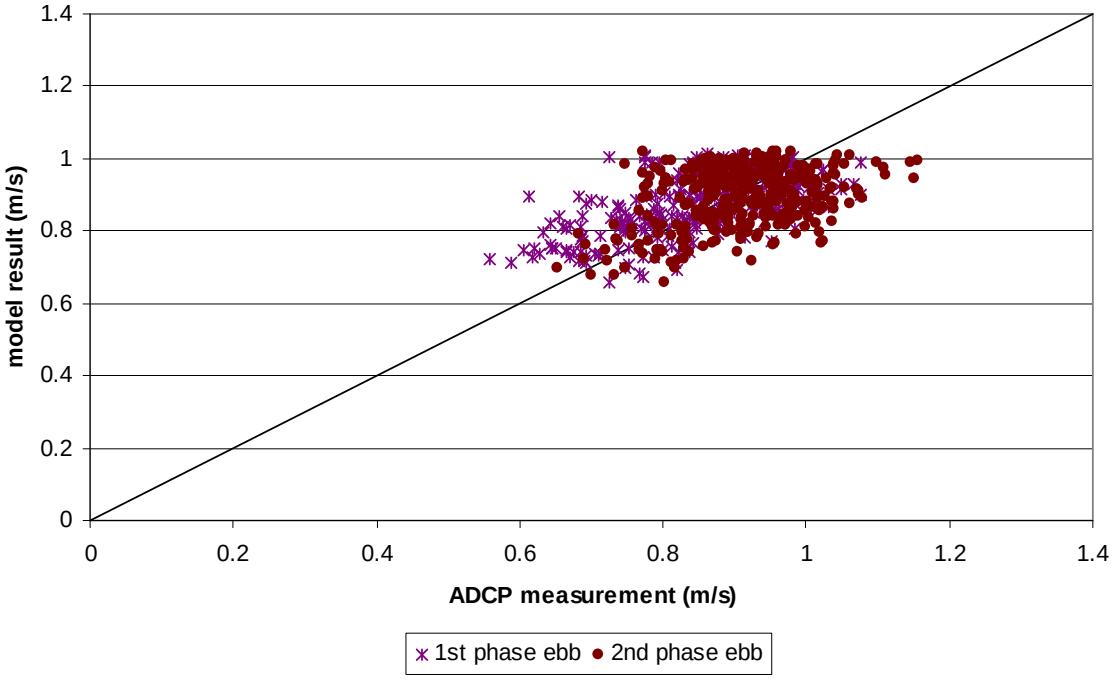

Figure 145 - Velocity magnitude for Notelaer – transverse profile in deep zone for ebb
(model result DD3x3validation vs ADCP measurement)

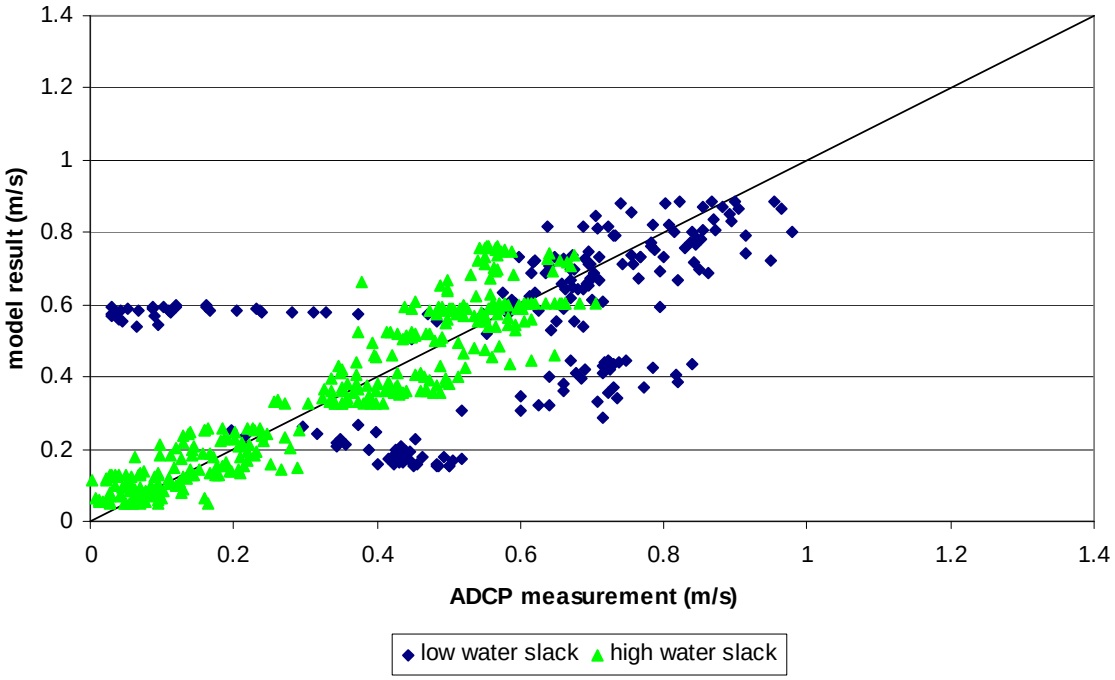

Figure 146 - Velocity magnitude for Notelaer – transverse profile in deep zone for slack
(model result DD3x3validation vs ADCP measurement)

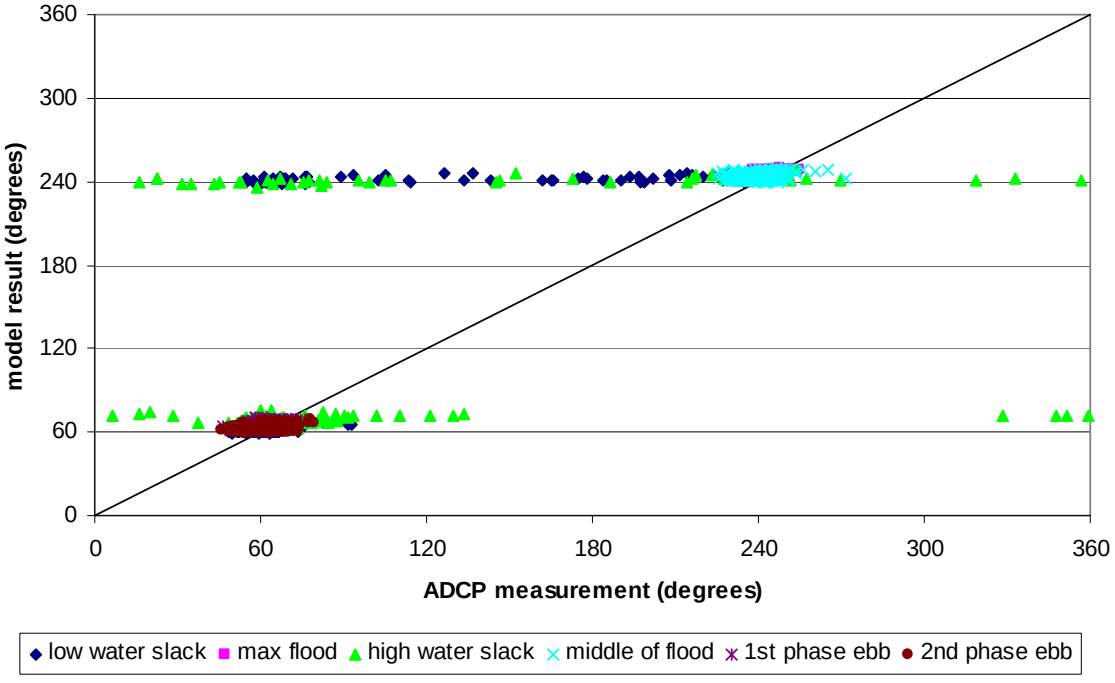

Figure 147 - Velocity direction for Notelaer – transverse profile in deep zone
(model result DD3x3validation vs ADCP measurement)

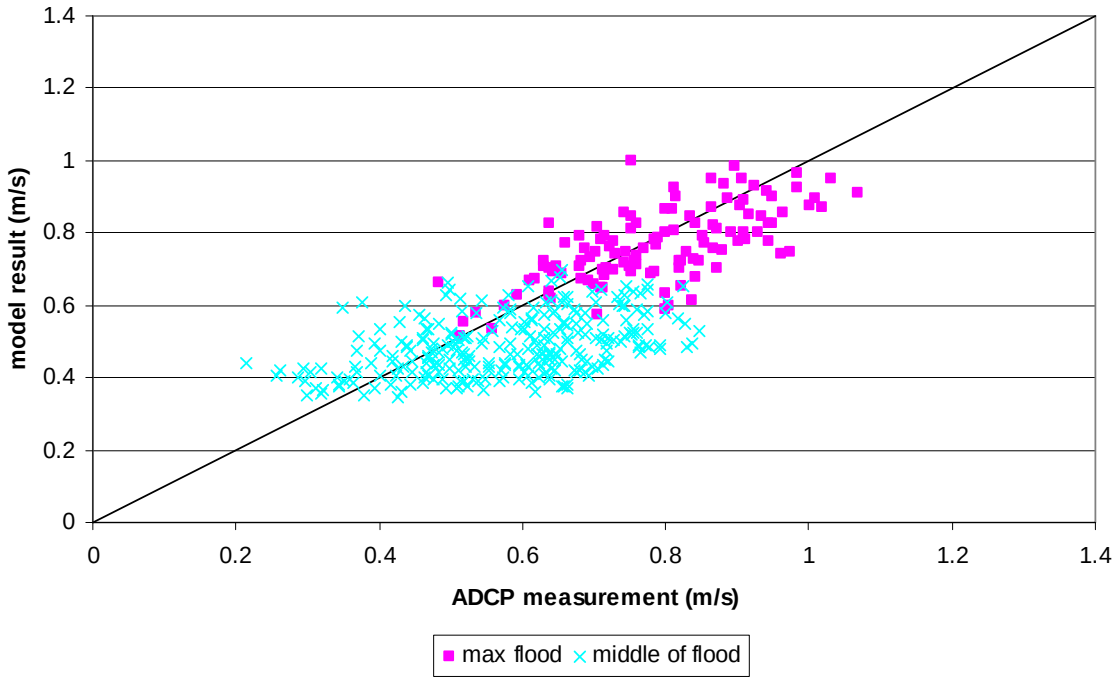

Figure 148 - Velocity magnitude for Notelaer – transverse profile in undeep zone for flood
(model result DD3x3validation vs ADCP measurement)

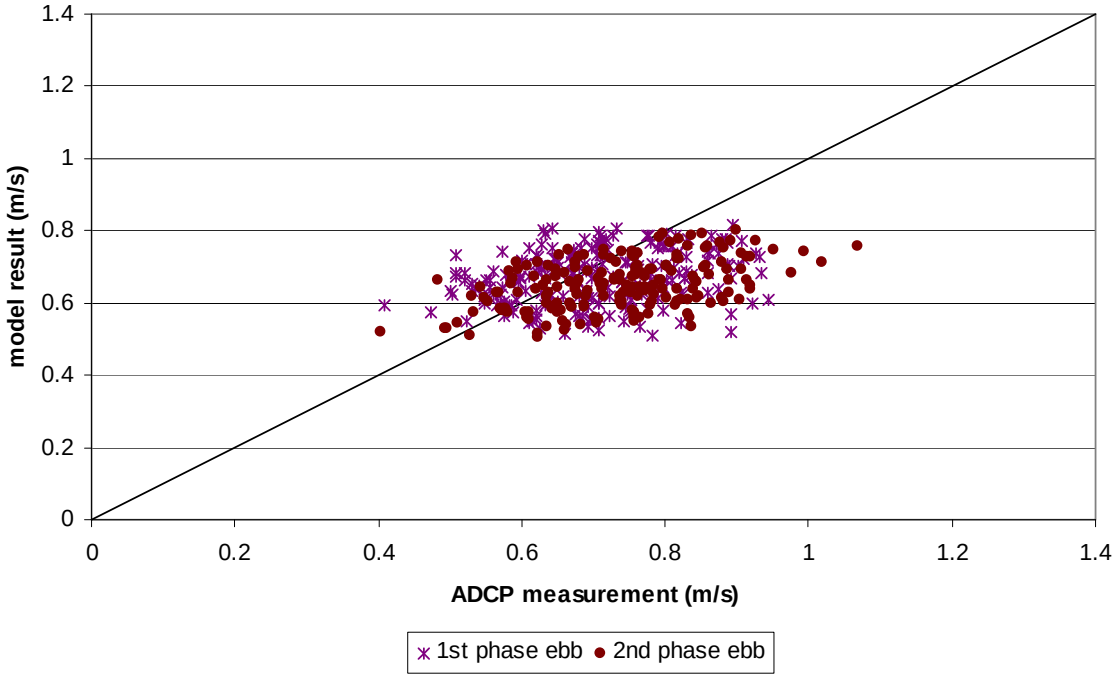

Figure 149 - Velocity magnitude for Notelaer – transverse profile in undeep zone for ebb
(model result DD3x3validation vs ADCP measurement)

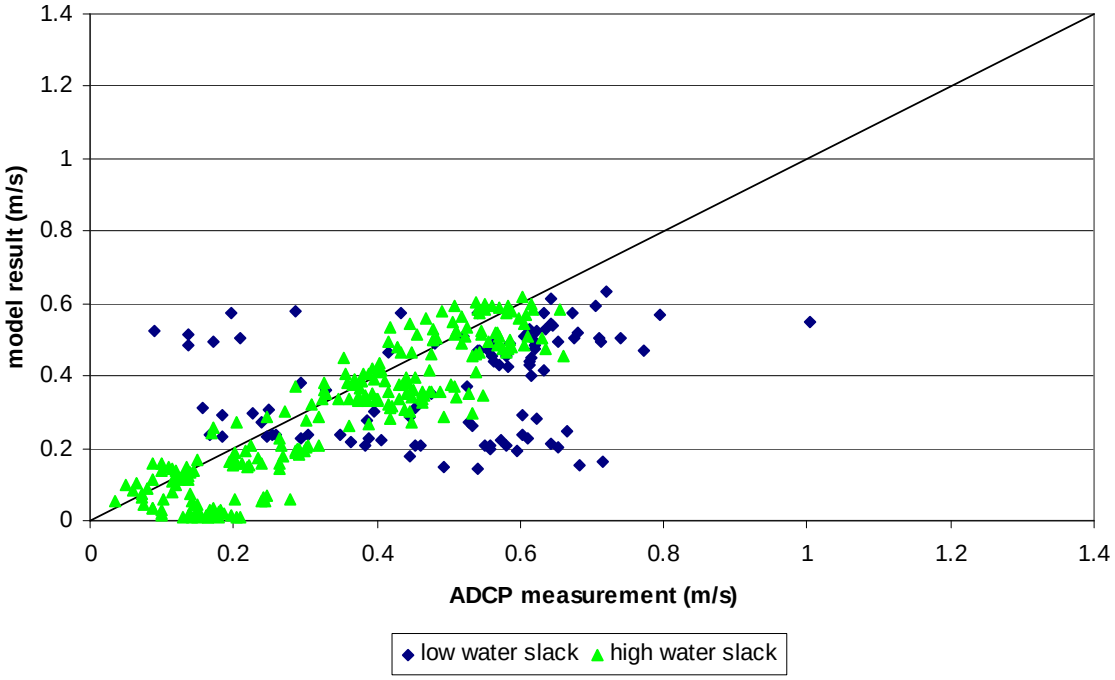

Figure 150 - Velocity magnitude for Notelaer – transverse profile in undeep zone for slack
(model result DD3x3validation vs ADCP measurement)

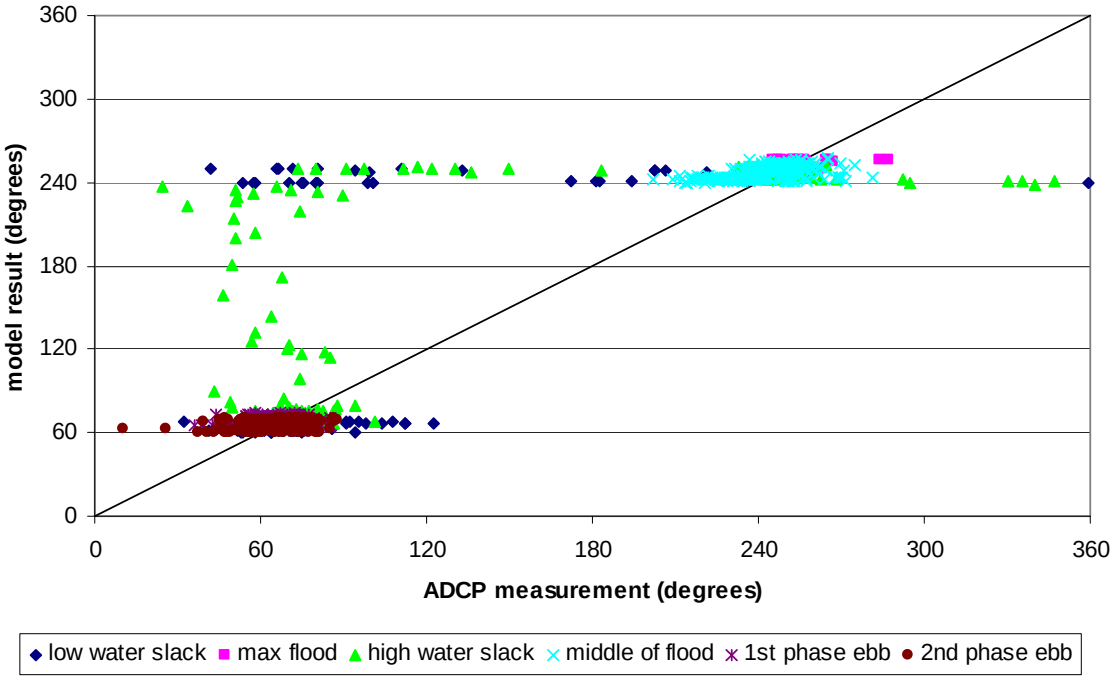

Figure 151 - Velocity direction for Notelaer – transverse profile in undeep zone
(model result DD3x3validation vs ADCP measurement)

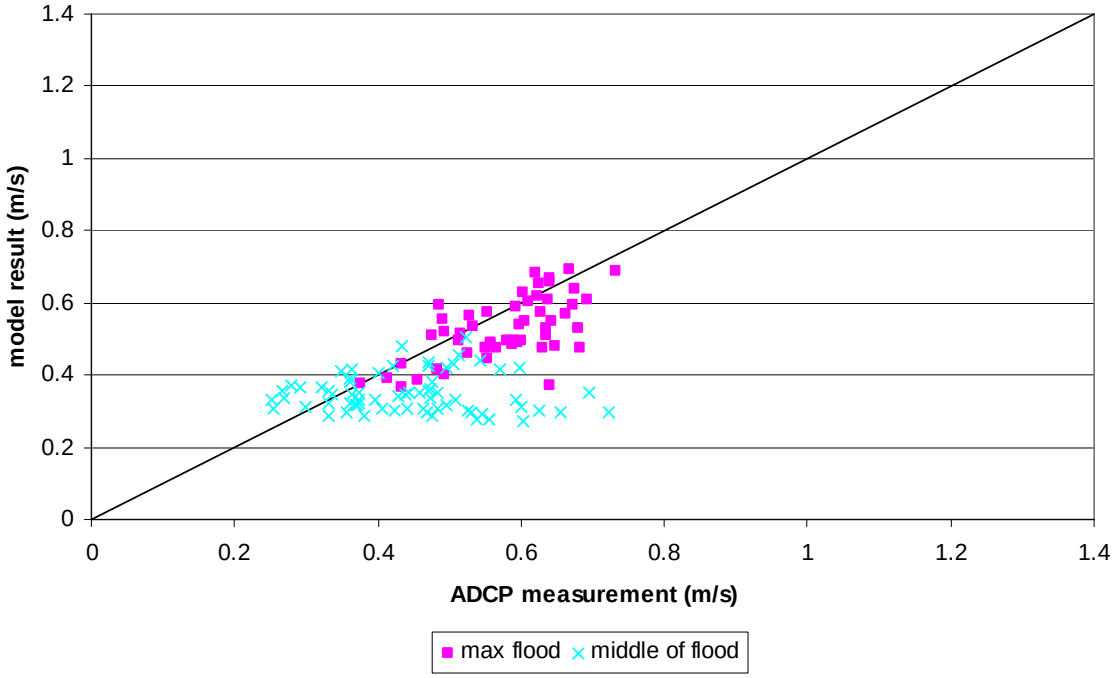

Figure 152 - Velocity magnitude for Notelaer – transverse profile in littoral zone for flood
(model result DD3x3validation vs ADCP measurement)

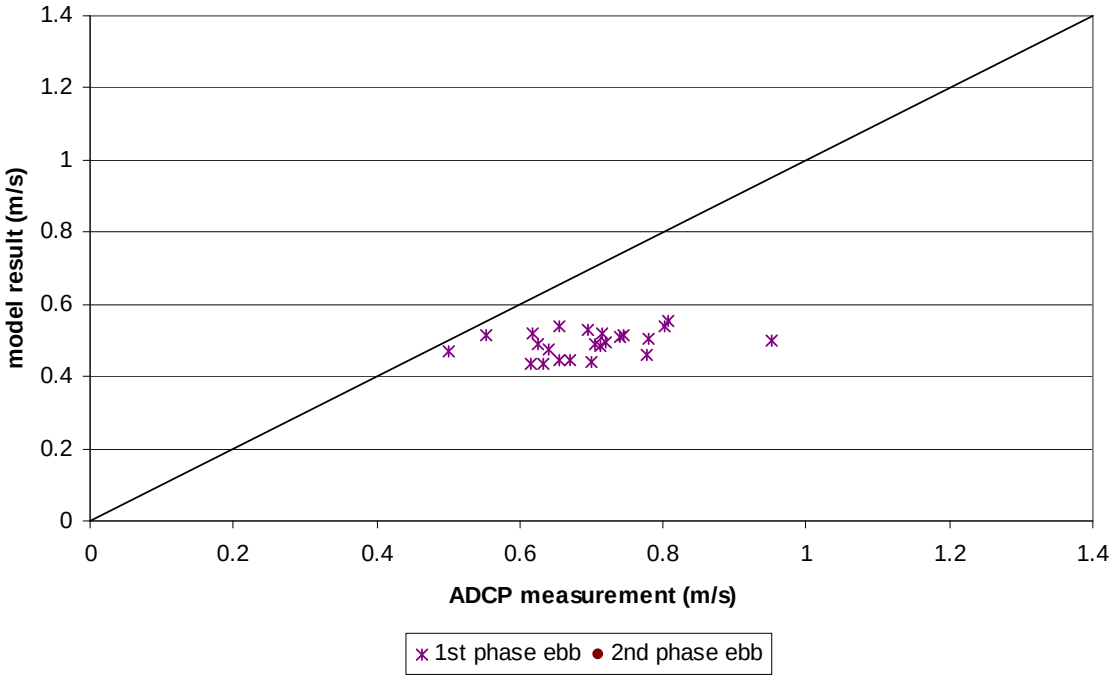

Figure 153 - Velocity magnitude for Notelaer – transverse profile in littoral zone for ebb
(model result DD3x3validation vs ADCP measurement)

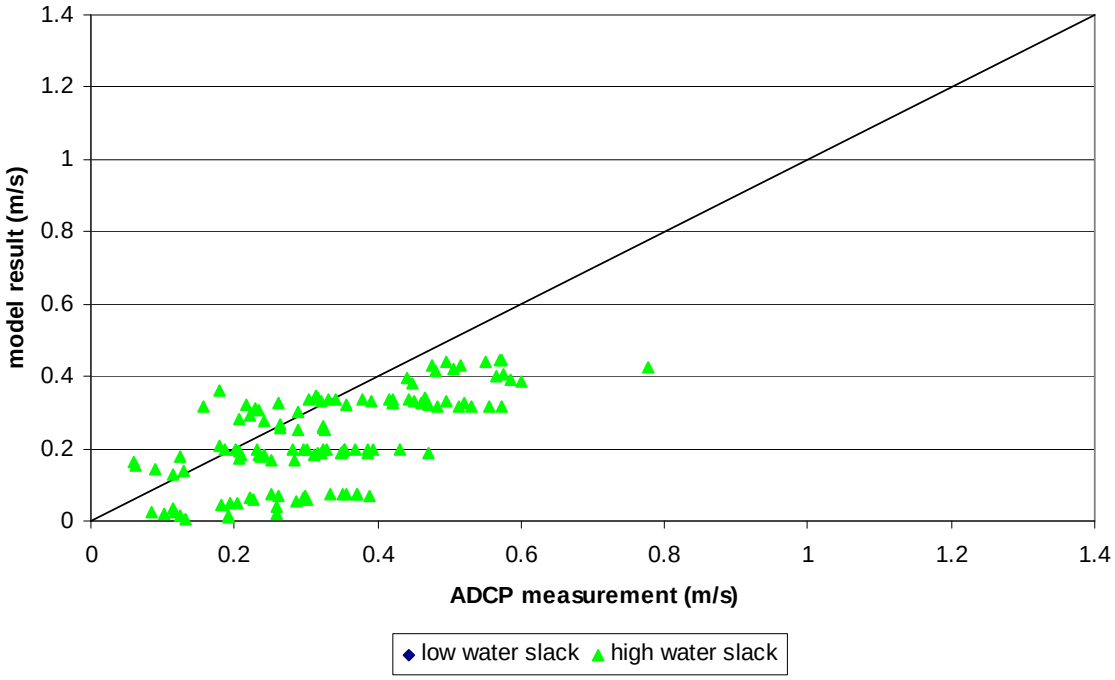

Figure 154 - Velocity magnitude for Notelaer – transverse profile in littoral zone for slack
(model result DD3x3validation vs ADCP measurement)

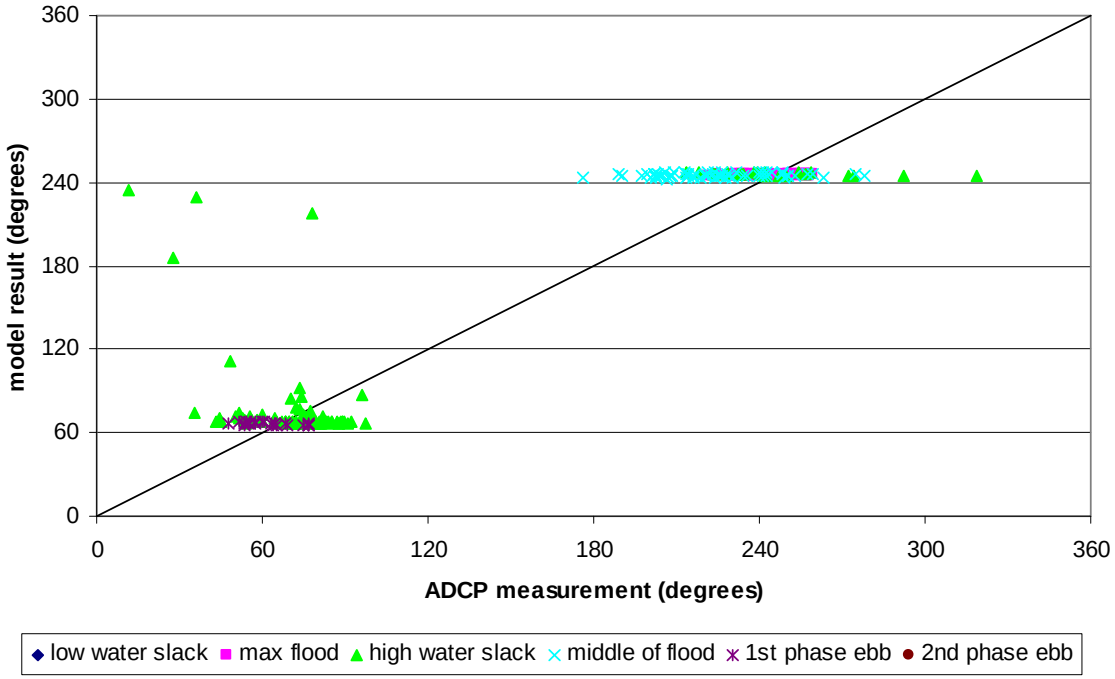

Figure 155 - Velocity direction for Notelaer – transverse profile in littoral zone
(model result DD3x3validation vs ADCP measurement)

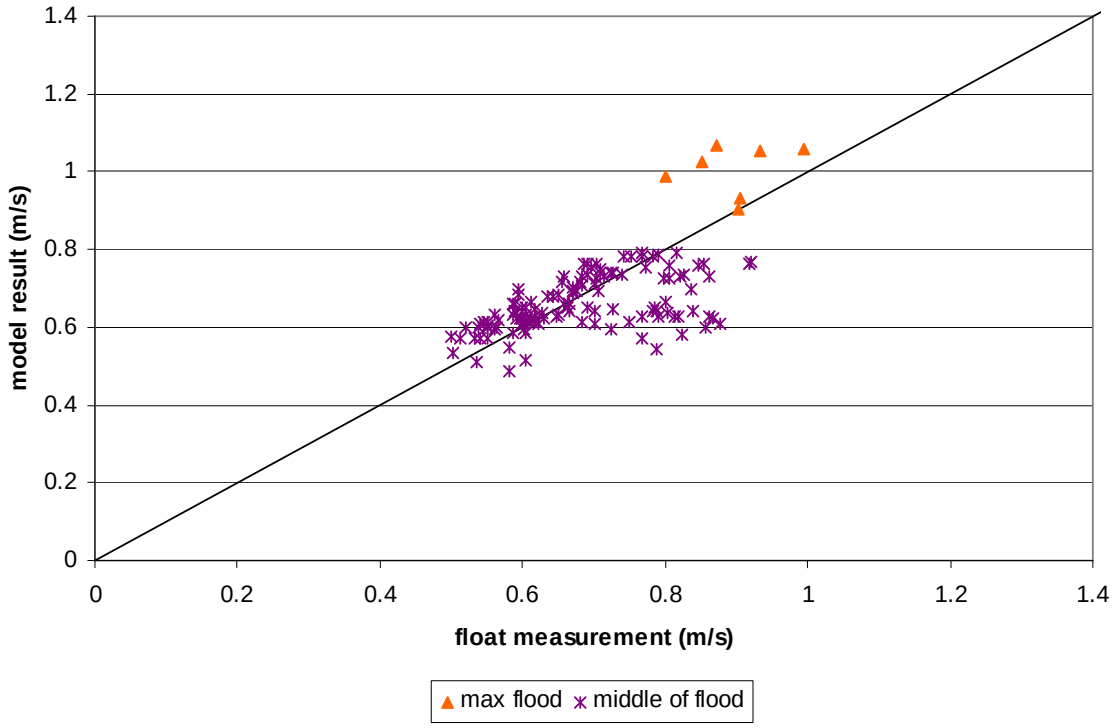

Figure 156 - Velocity in deep zone for flood (model result DD3x3validation vs float measurement)

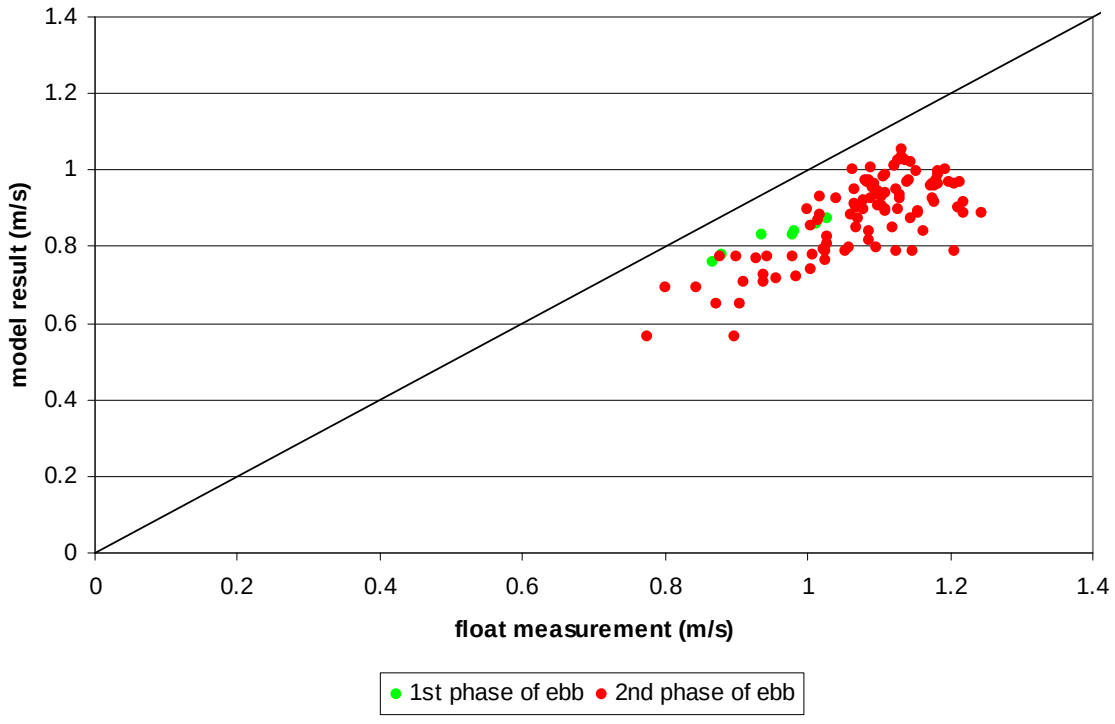

Figure 157 - Velocity in deep zone for ebb (model result DD3x3validation vs float measurement)

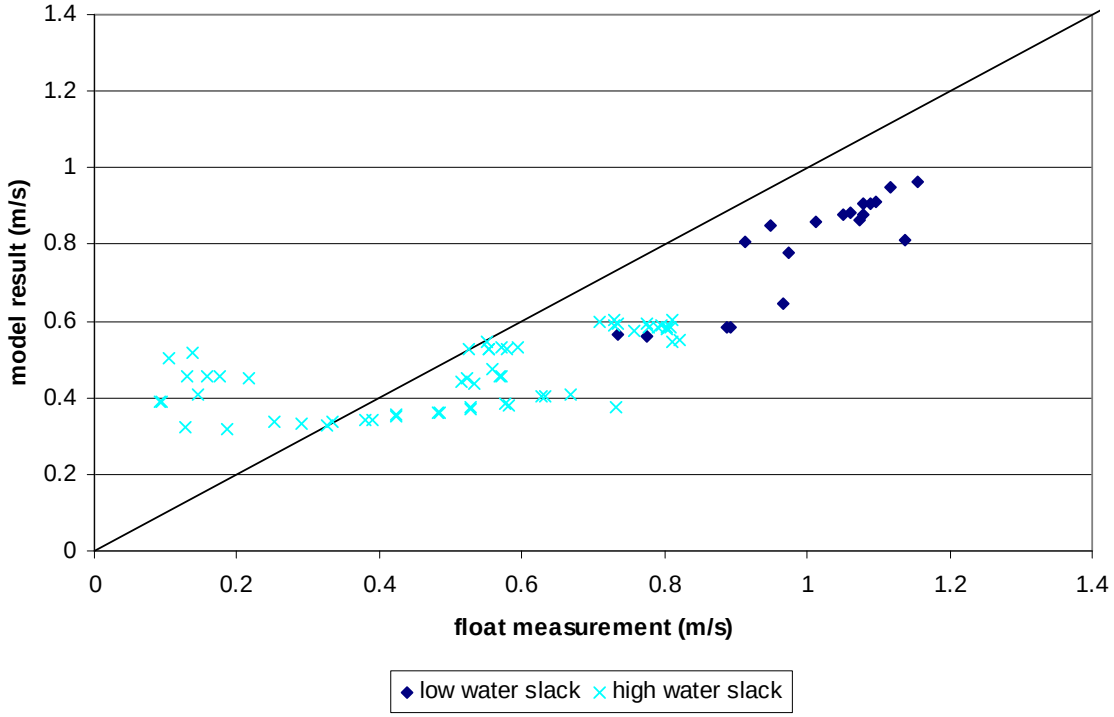

Figure 158 - Velocity in deep zone for slack (model result DD3x3validation vs float measurement)

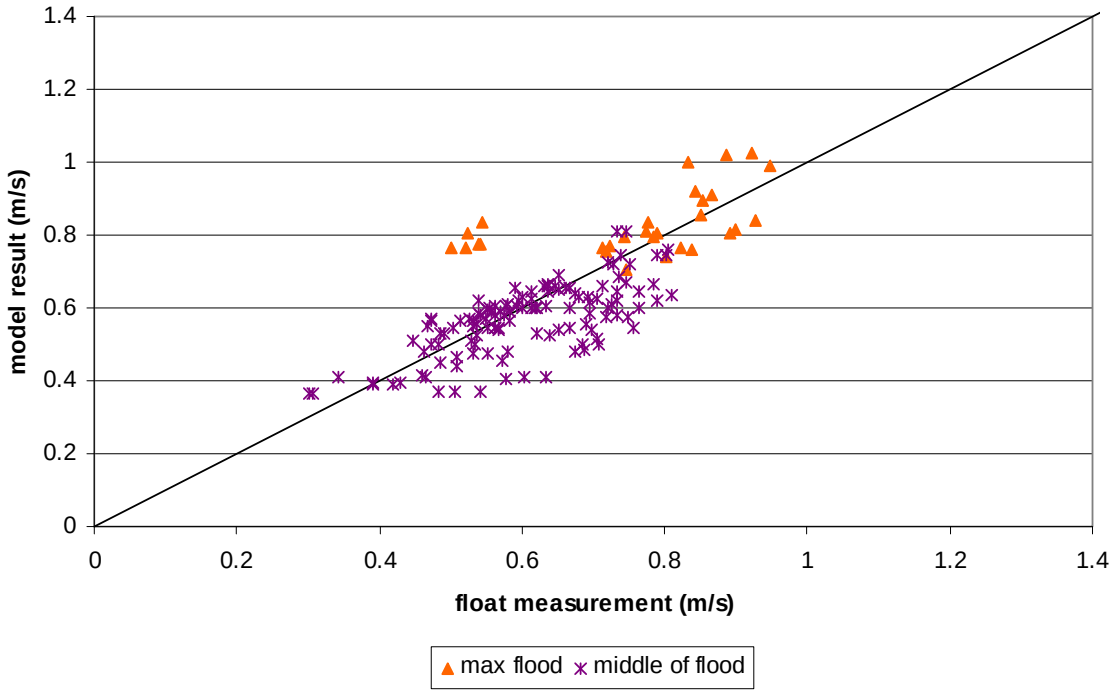

Figure 159 - Velocity in undeep zone for flood (model result DD3x3validation vs float measurement)

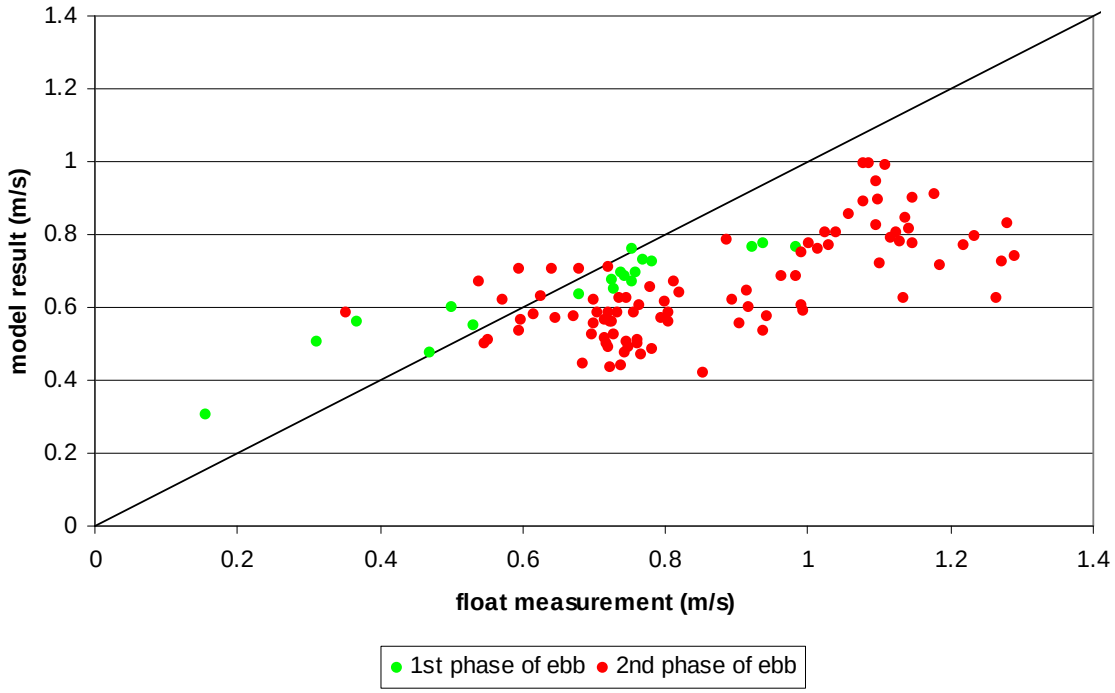

Figure 160 - Velocity in undeep zone for ebb (model result DD3x3validation vs float measurement)

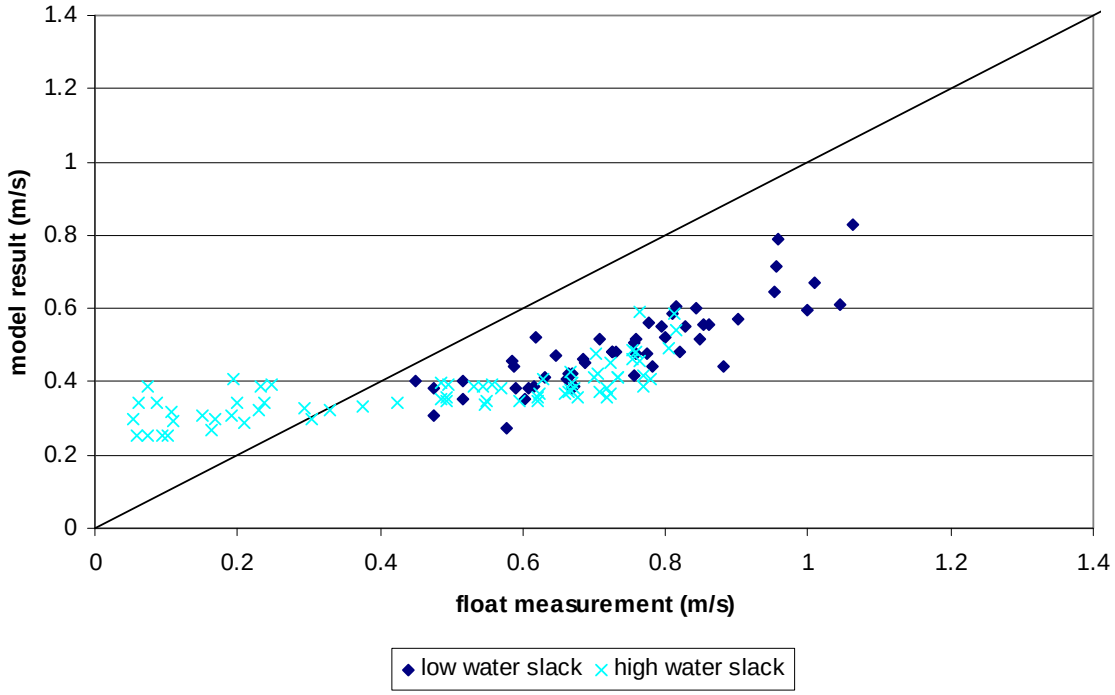

Figure 161 - Velocity in undeep zone for slack (model result DD3x3validation vs float measurement)

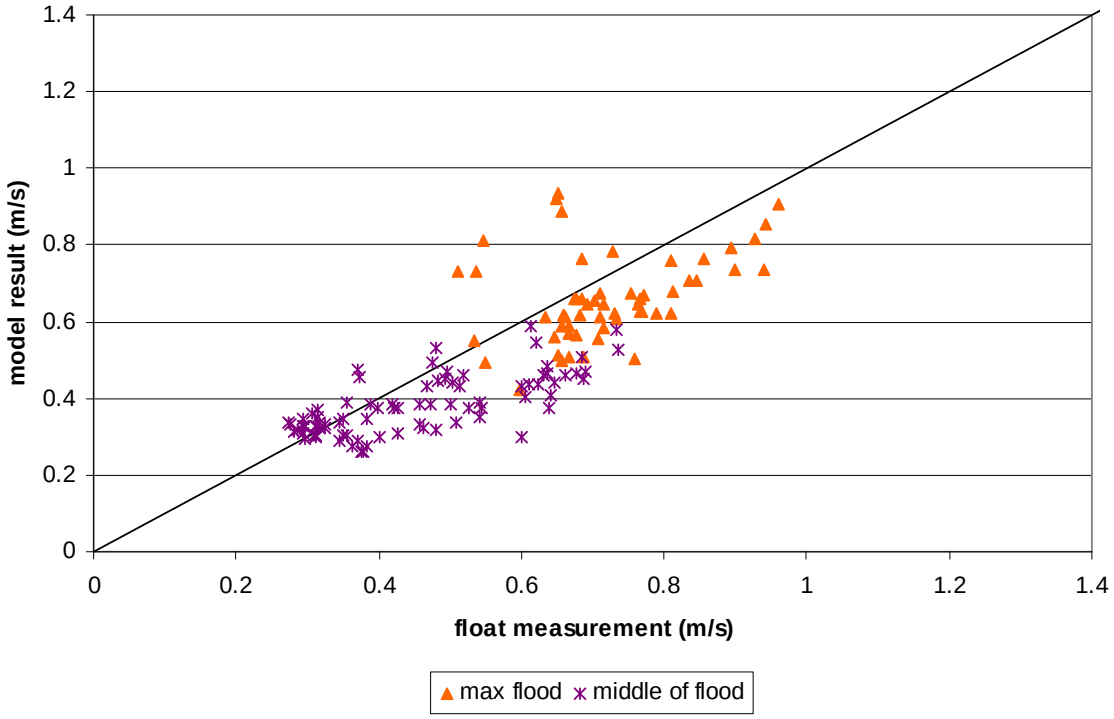

Figure 162 - Velocity in littoral zone for flood (model result DD3x3validation vs float measurement)

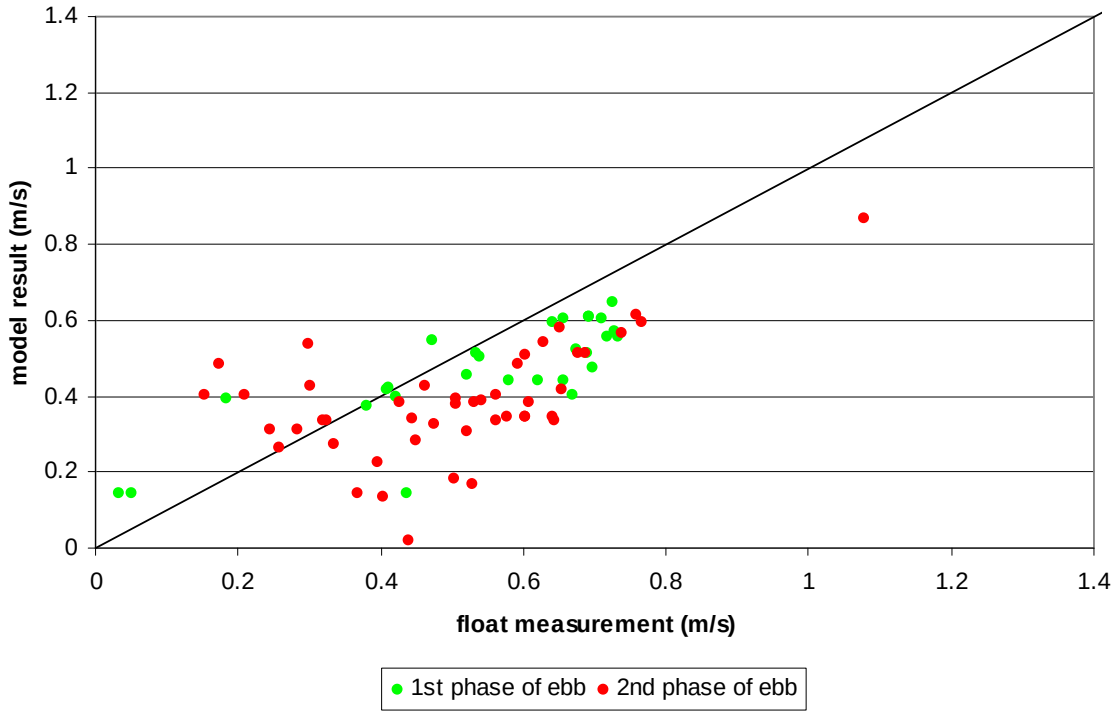

Figure 163 - Velocity in littoral zone for ebb (model result DD3x3validation vs float measurement)

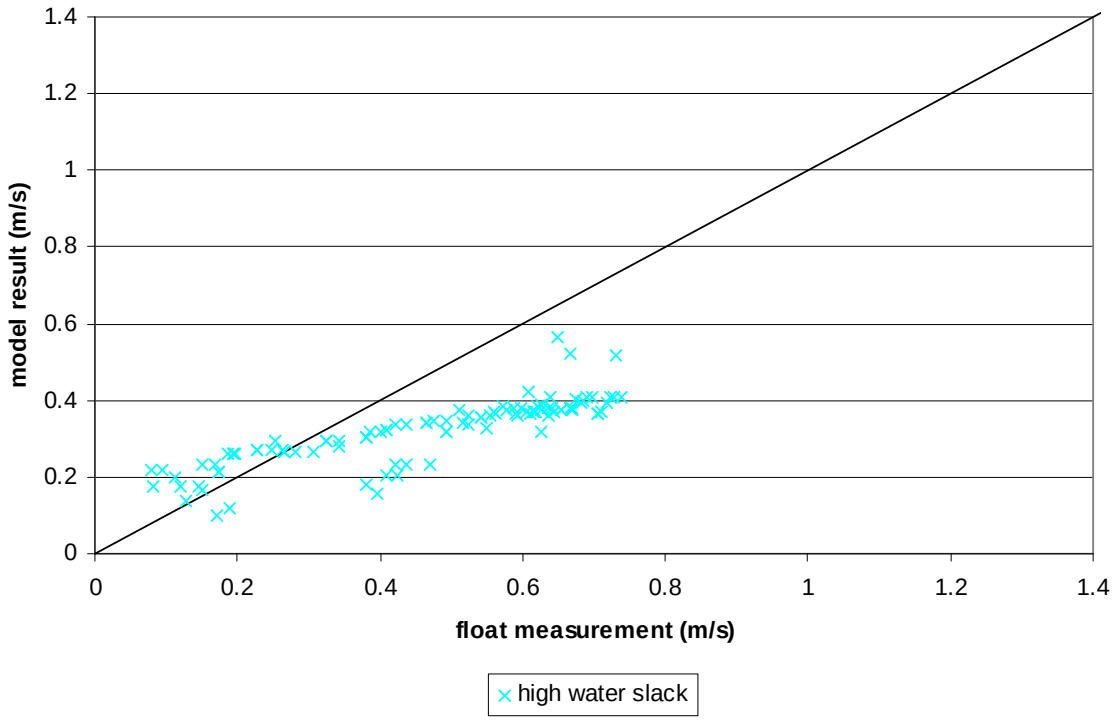

Figure 164 - Velocity in littoral zone for slack (model result DD3x3validation vs float measurement)

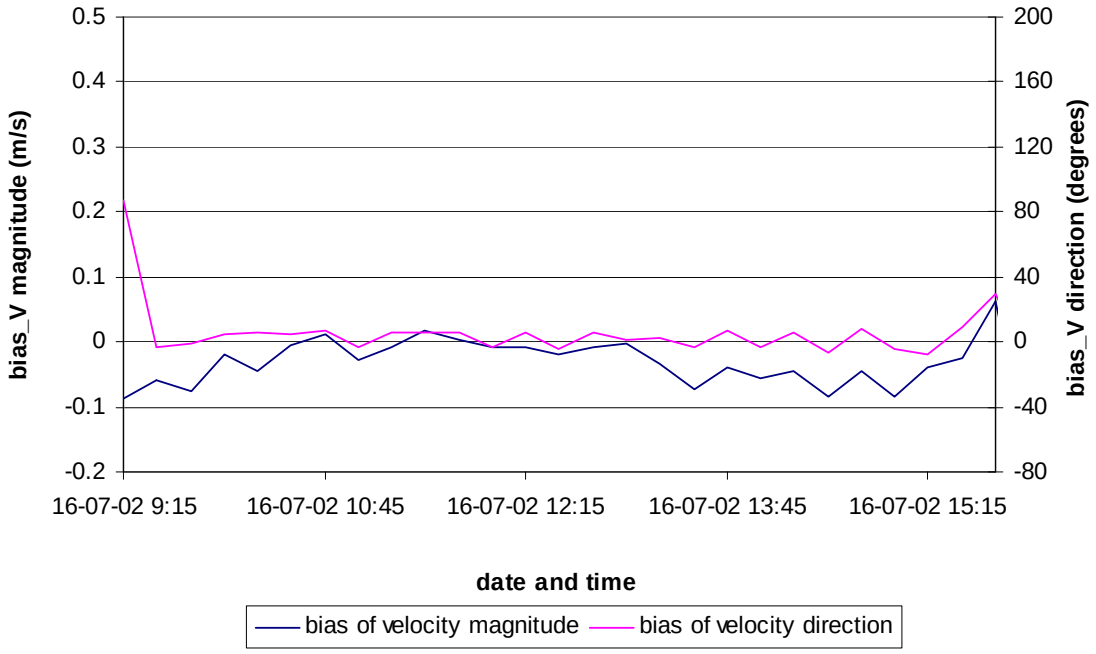

Figure 165 - Bias for model run DD3x3validation for Notelaer – transverse profile for the ebb period

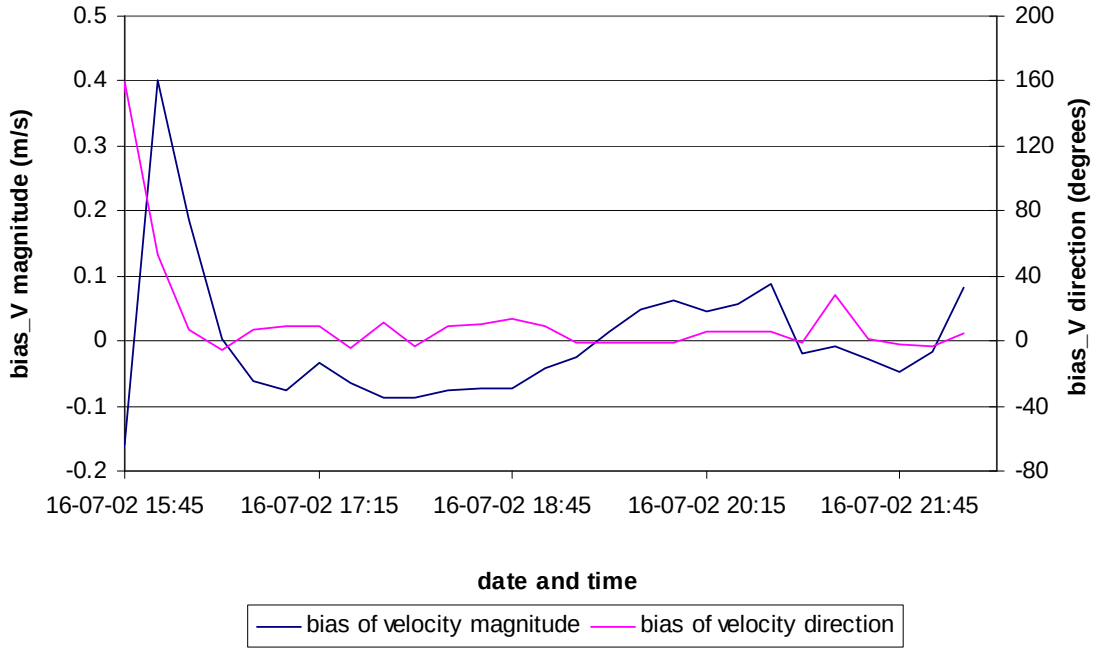

Figure 166 - Bias for model run DD3x3validation for Notelaer – transverse profile for the flood period

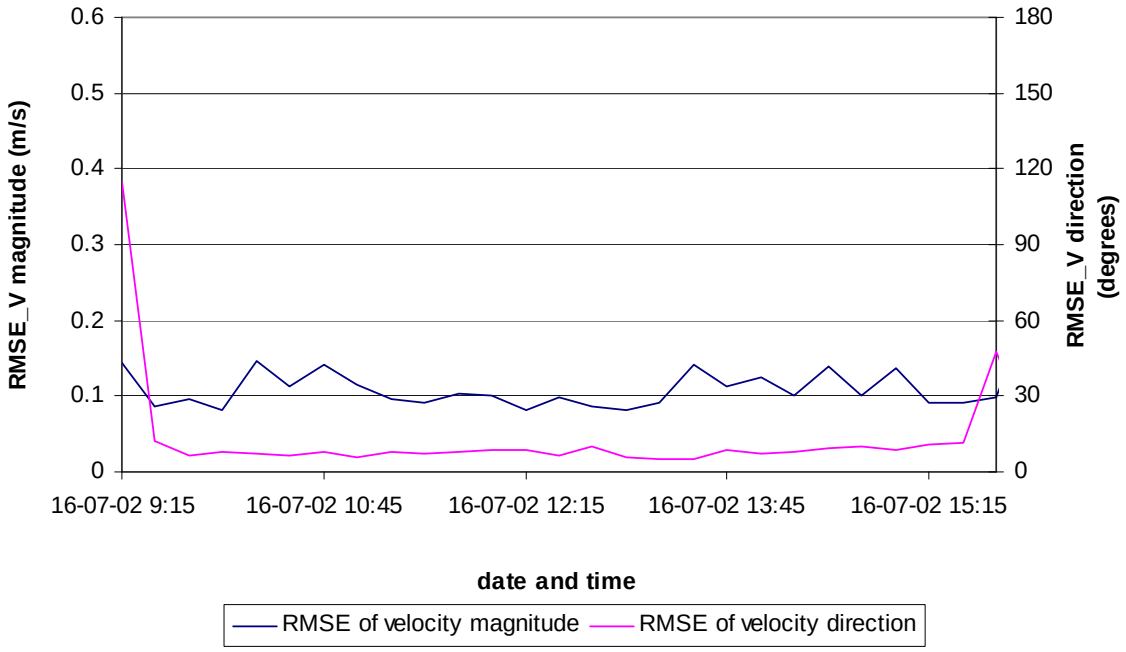

Figure 167 - Root mean squared error for model run DD3x3validation for Notelaer – transverse profile for the ebb period

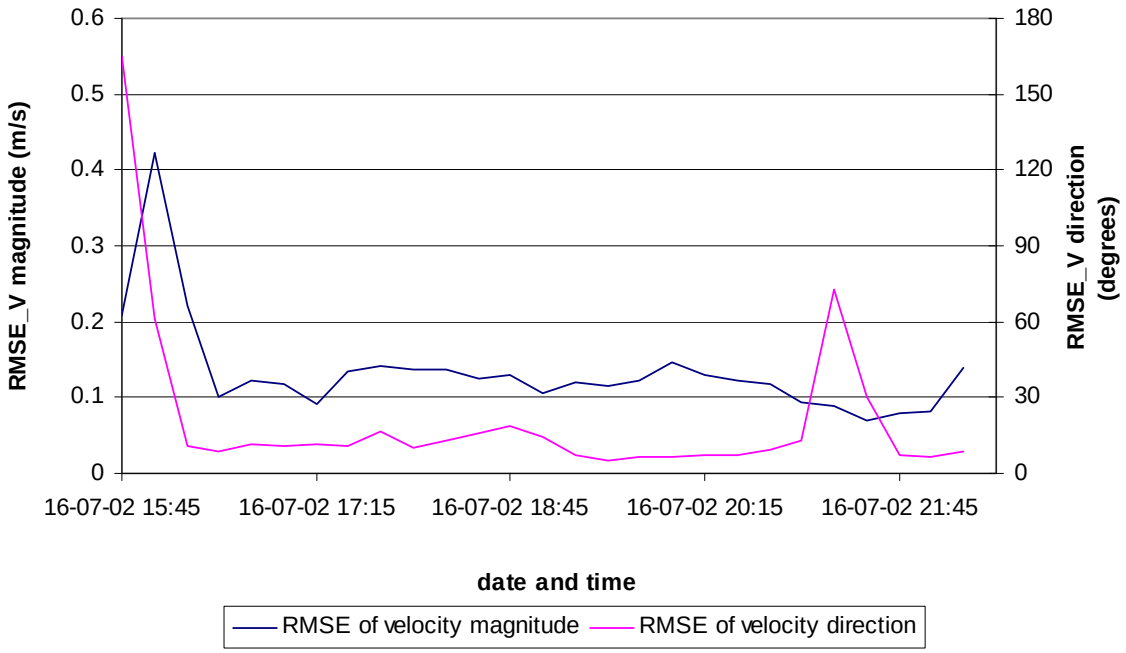

Figure 168 - Root mean squared error for model run DD3x3validation for Notelaer – transverse profile for the flood period

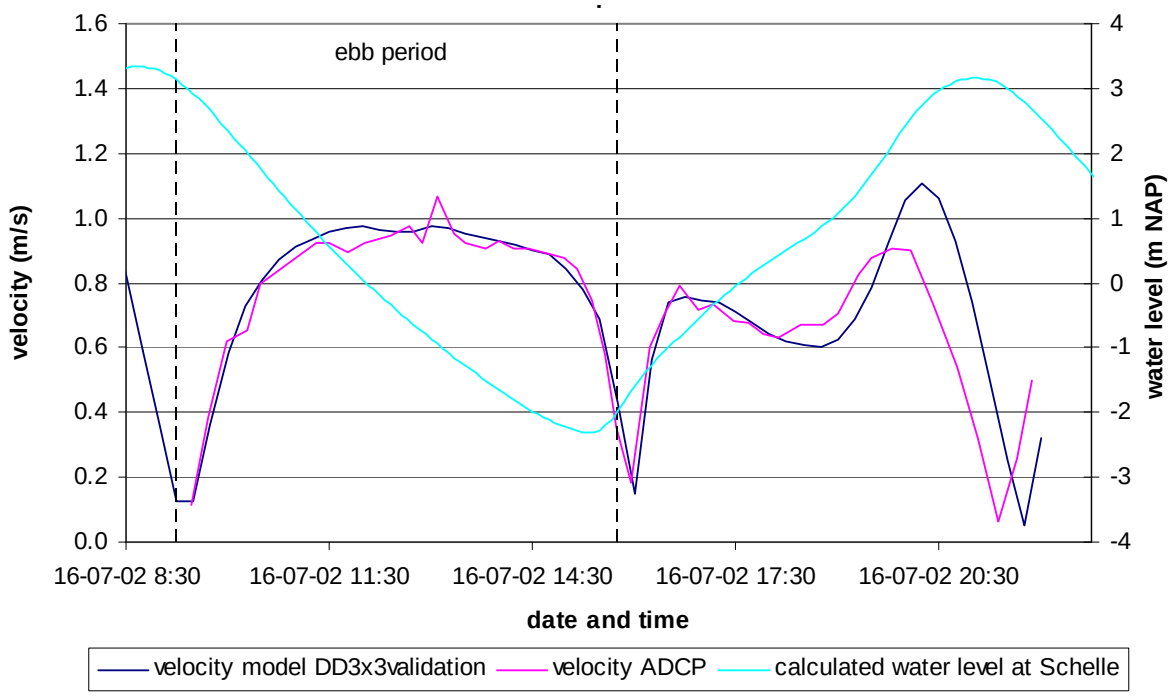

Figure 169 - Comparison of the calculated and measured velocity in deep zone of Notelaer – transverse profile for ebb period

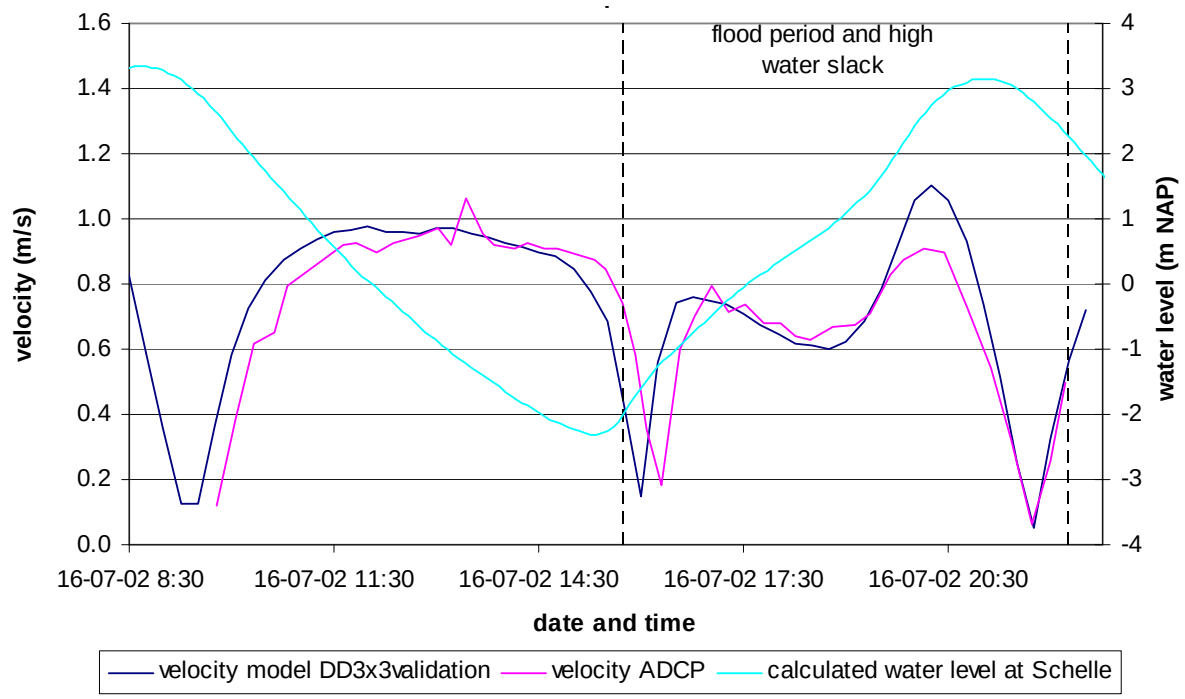

Figure 170 - Comparison of the calculated and measured velocity in deep zone of Notelaer – transverse profile for flood period

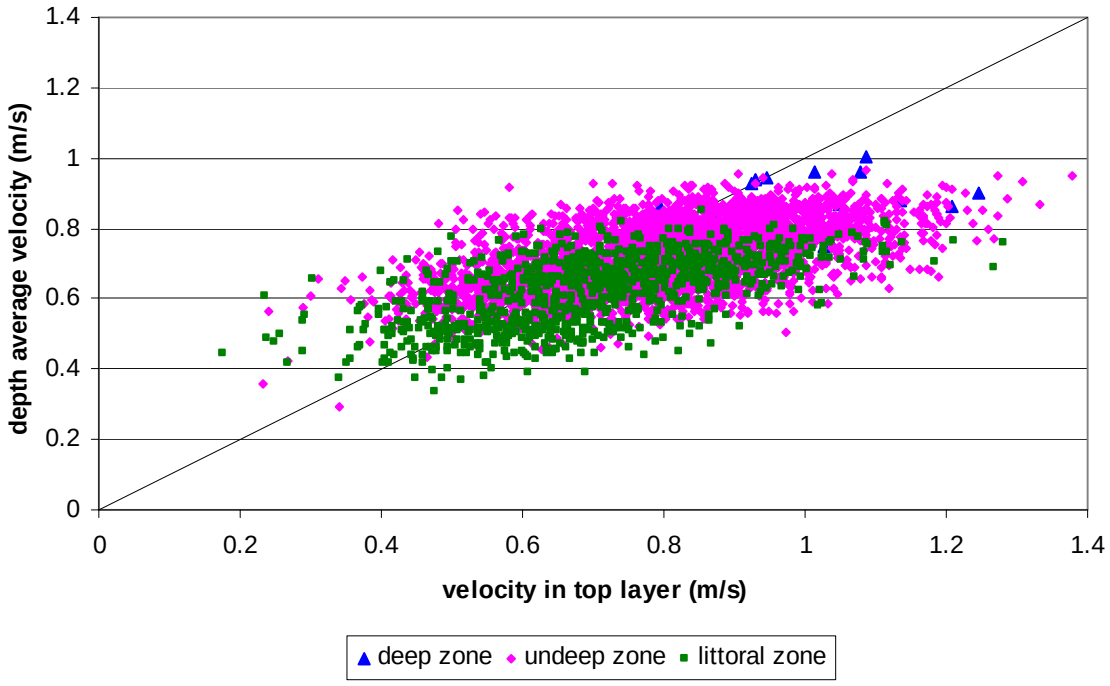

Figure 171 - Comparison of surface and depth average velocity for one of the measured profiles (period of maximal flood velocity)

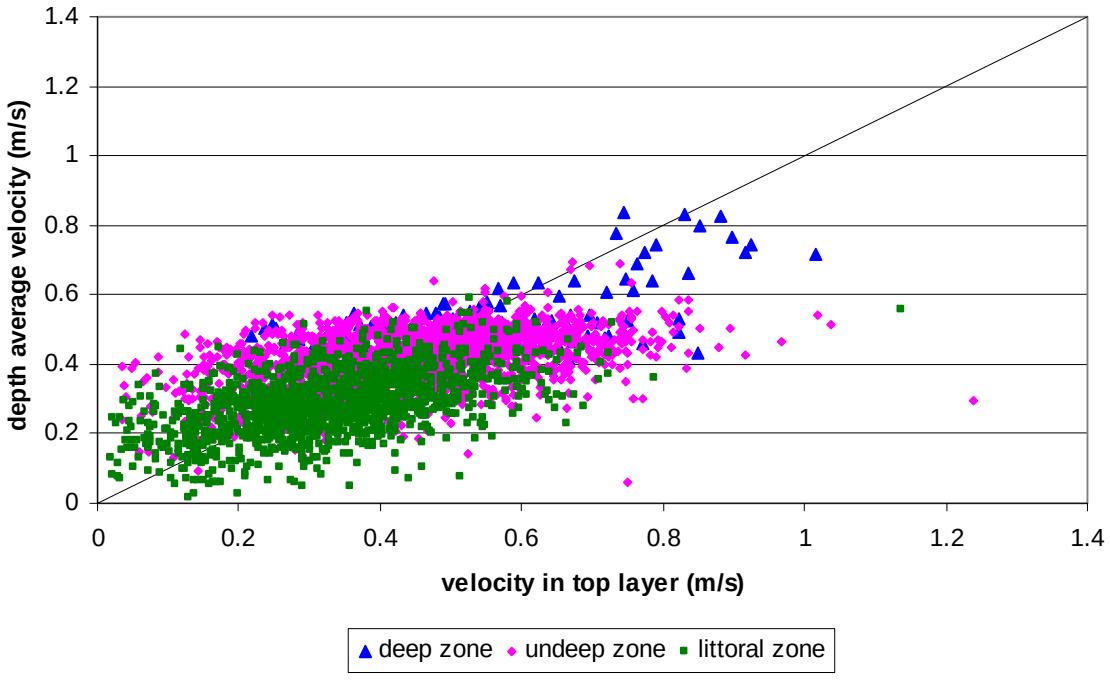

Figure 172 - Comparison of surface and depth average velocity for one of the measured profiles (middle of flood)

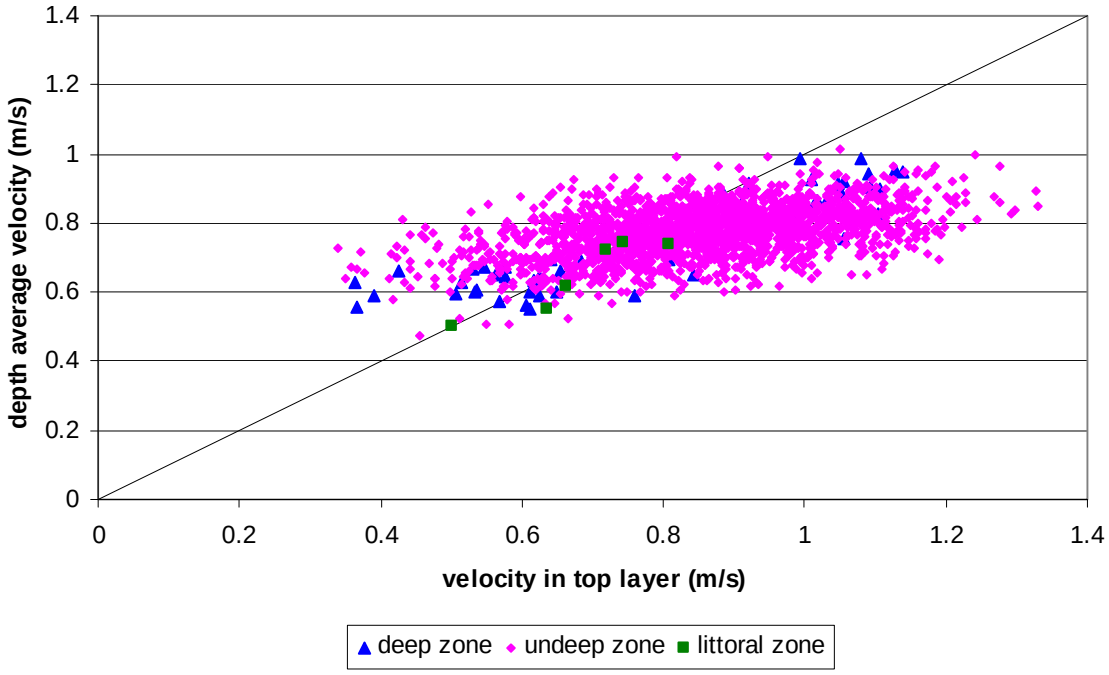

Figure 173 - Comparison of surface and depth average velocity for one of the measured profiles (first phase of ebb)

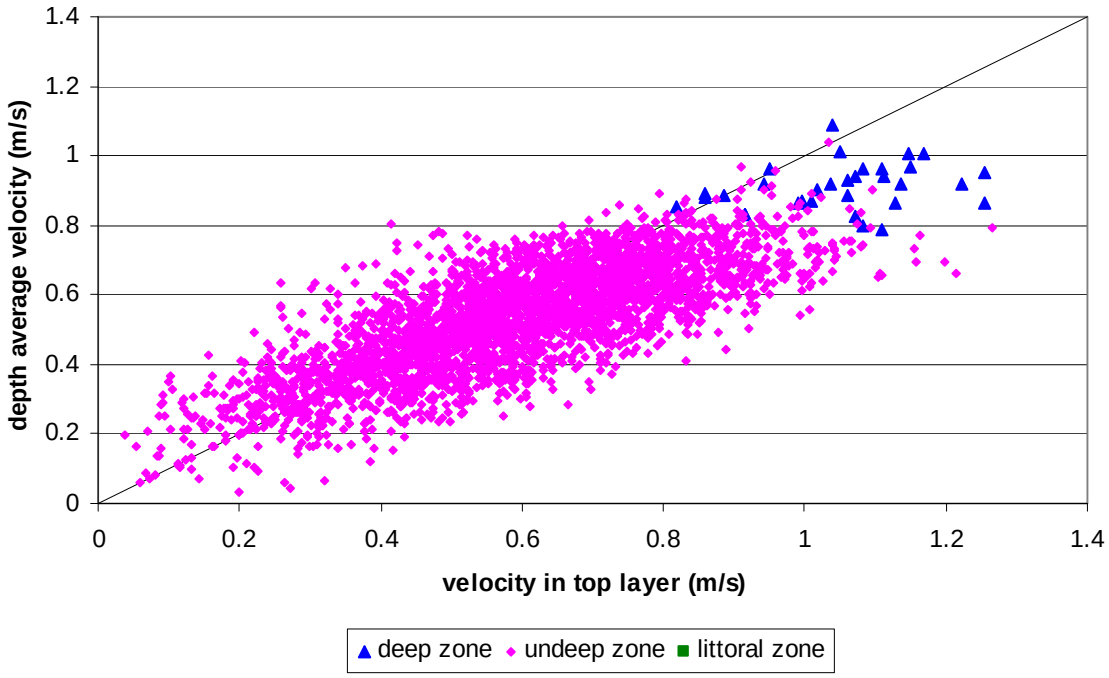

Figure 174 - Comparison of surface and depth average velocity for one of the measured profiles (second phase of ebb)

Appendix 1: Statistical parameters

The following statistical parameters are calculated in this study: mean bias, root mean squared error and standard deviation.

The mean values of the modelled (x) and measured (y) timeseries are calculated as follows (N is the length of the timeseries):

$$\bar{x} = \frac{1}{N}\sum_{i=1}^{N} x_i$$

$$\bar{y} = \frac{1}{N}\sum_{i=1}^{N} y_i$$

Mean bias is a difference between the mean values of the modeled and measured timeseries.

$$\Delta = \bar{x} - \bar{y}$$

Root mean squared error helps to quantify the difference between the model results and measurements. RMSE is the square root of the average of the square of the bias.

$$RMSE = \sqrt{\frac{1}{N}\sum_{i=1}^{N}(x_i - y_i)^2}$$

Standard deviation characterizes the difference between the bias of each model result and the mean bias. It shows how close the points of the scatter plot are to each other. A large standard deviation indicates that the points on the scatter plot are far from each other and a small standard deviation indicates that they are clustered closely together.

$$\sigma = \sqrt{\frac{1}{N}\sum_{i=1}^{N}\left[(x_i - y_i) - (\bar{x} - \bar{y})\right]^2}$$

Waterbouwkundig Laboratorium

Flanders Hydraulics Research

Berchemlei 115
B-2140 Antwerpen
Tel. +32 (0)3 224 60 35
Fax +32 (0)3 224 60 36
E-mail: waterbouwkundiglabo@vlaanderen.be
www.watlab.be